The role of nitric oxide in myocardial ischaemia/reperfusion injury

Thesis submitted by

Robert Midgley Bell, MBBS, Bsc (Hons)

BHF Clinical Research Fellow

For the degree of

Doctor of Philosophy

in the

Faculty of Medicine

University of London

The Hatter Institute and Centre for Cardiology

(Division of Medicine)

University College London Medical School

Department of Cardiology

University College London Hospitals

Grafton Way

London WC1E 6DB

March 2001

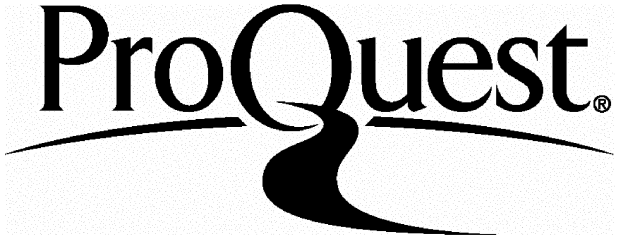

Abstract

The management of acute myocardial infarction requires rapid restoration of blood flow to attenuate cell death. In recent years, the possibility of fortifying the myocardium against ischaemia/reperfusion injury has emerged with the identification of signalling pathways that promote cellular survival, modalities that include preconditioning and ischaemia/reperfusion injury salvage (IRIS). Preconditioning and IRIS are defined as the protection triggered by a stimulus either before the insult or upon reperfusion respectively. Nitric oxide has been implicated as a potential mediator of cell survival and cell death; whether the cell lives or dies may be critically dependent upon the synthesis of this second messenger. Therefore to determine the role of nitric oxide in the mediation/ protection from ischaemia/reperfusion injury, the aim of this thesis is to elucidate the role of nitric oxide in preconditioning and IRIS paradigms.

In early ischaemic preconditioning, an immediate onset phase of protection after the preconditioning stimulus, nitric oxide was found to lower the preconditioning threshold significantly; in eNOS knockout animals, the ischaemic preconditioning threshold is at least twice that in eNOS wild type animals. Delayed *pharmacological* preconditioning, whereby transient adenosine A_1 receptor activation with 2-chloro N6 cyclopentyl adenosine results in robust protection 24 hours later, was found to be dependent upon the synthesis of nitric oxide. Interestingly, whilst previous studies indicated that delayed *ischaemic* preconditioning was dependent upon the induction of the *inducible* isoform of nitric oxide synthase, this study implicates the *endothelial* nitric oxide synthase (eNOS) as having an important role in mediating the protection observed.

IRIS is a novel form of myocardial protection that we have hypothesised is dependent upon the activation of a reperfusion injury salvage kinase (RISK) pathway to attenuate necrotic injury. To activate the RISK pathway we used bradykinin, which was found to trigger protection that was reliant upon the activity of eNOS.

Exogenous nitric oxide was administered to hearts subjected to ischaemia/reperfusion injury. In this study, a clear dose-response relationship was found between the concentration of nitric oxide and myocardial protection that peaks at 2 μM. At higher concentrations, protection against ischaemic injury was lost. The protection mediated by nitric oxide was found to be closely linked to the opening of the mitochondrial ATP sensitive potassium channel (K_{ATP}), as indicated by studies in isolated mitochondria and in the whole heart subjected to ischaemia/reperfusion injury.

Thus, this thesis provides evidence that (*i*) nitric oxide is involved in all facets of myocardial resistance to injury, (*ii*) eNOS is a far more important source of nitric oxide than previously thought, and (*iii*) nitric oxide has a concentration dependent influence upon infarct size, possibly via a direct action upon mitochondrial K_{ATP} channels.

TABLE OF CONTENTS

TABLE OF FIGURES

LIST OF TABLES.

Acknowledgements.

I am grateful to a number of individuals who have provided help and assistance during the period of research that encompasses the writing of this thesis. In particular, I am grateful for the close support and supervision provided by Professor Derek Yellon, and the unfettered succour and advice of Dr. Gary Baxter.

I am indebted to the kind help in the use of HPLC in the assessment of nitric oxide synthesis by Dr. Chris Smith, based in the laboratories of the Jules Thorne Institute, Middlesex Hospital, UCL.

I am grateful to Dr. Andrej Loesch for his kind collaboration in performing the electron immunocytochemistry in the Department of Anatomy, UCL.

I would also like to extend my thanks to Professor Michael Marber and Harold Raat in the Rayne Institute, St. Thomas' Hospital, for their demonstration of isolated mouse perfusion in the early days of setting up the model used in the studies incorporated in this thesis.

Further acknowledgement and gratitude is made towards the British Heart Foundation for the financial support provided over the 3 years of research to the submission of this PhD thesis.

Finally, I would like to thank my mother and father, my brother and especially my fiancé, Yimmy, for all their boundless support in the goods times and the bad.

List of Abbreviations.

The following abbreviations are used in this thesis:

5-HD	5 hydroxy decanoate
ACE	Angiotensin converting enzyme
ADMA	Asymmetric dimethylarginine
ADP	Adenosine diphosphate
Akt	Cellular Akt/ Protein kinase B
AMP	Adenosine monophosphate
ANOVA	Analysis of variance
AP-1	Activator protein-1
Apaf-1	Apoptotic protease activating factor-1
ATP	Adenosine triphosphate
B2	Bradykinin type 2 receptor
Bad	$Bcl\text{-}2_{XL}$/ Bcl-2 - associated death promoter
Bax	Bcl- associated X protein
BCA	Bicinchoninic acid
Bcl	B-cell leukaemia (oncogene)
Bcl	B-cell lymphoma oncogene
BH_4	5,6,7,8- tetrahydro-L-biopterin
Bid	BH3 Interacting domain Death agonist
BMK-1	Big mitogen activated protein kinase 1
BSA	Bovine serum albumin
Caspase	Cystein aspartate specific proteases
CCCP	carbonyl cyanide m-chlorophenylhydrazone
CCPA	2-chloro N6 cyclopentyl adenosine
cGMP	cyclic guanosine-5'-monophosphate
CHE	Chelerythrine chloride
Chel	Chelerythrine
CREB	c-Fos and cAMP-response element-binding protein
DAB	diaminobenzidine
DAG	Diacylglycerol
DDAH	Dimethylarginine dimethylaminohydrolase
DDTC	Diethyldithiocarbamate
DNA	De-oxyribonucleic acid
$\Delta\psi_m$	mitochondrial membrane potential
ECSOD	Extracellular superoxide dismutase

ECSOD	Extracellular superoxide dismutase
eNOS	endothelial nitric oxide synthase
ERK	Extracellular signal-regulated kinase
ETA	Endothelin-1 type A
ETB	Endothelin-1 type B
εV1-2	PKCε selective activating peptide
FAD	Flavin adenine dinucleotide
FADD	Fas associated death domain
FasL	Fas ligand
FGF	Fibroblast growth factor
FMN	Flavin mononucleotide
G- protein	Guanine nucleotide- binding regulatory protein
G-protein	GTP-binding regulatory protein
GDP	guanosine diphosphate
GTN	Glyceryl trinitrate
GTP	guanosine triphosphate
H9c2	Rat myoblast derived cell line
HPLC	High performance liquid chromatography
HSP	Heat shock protein
ICE	Interleukin converting enzyme (caspase-1)
IGF	Insulin-like growth factor
IκB	Inhibitor of NF-κB
iNOS	inducible nitric oxide synthase
IP_3	inositol 3,4,5 triphosphate
IRIS	Ischaemia/reperfusion injury salvage
JNK	c-jun N-terminal kinase
K_{ATP}	ATP sensitive potassium channel
kD	kilo Daltons
KO	Knockout
L-NAME	Nw-nitro-L-arginine methyl ester
L-NMMA	Nomega-monomethyl-L-arginine
MAPK	Mitogen activated protein kinase
MAPKAPK2	Mitogen activated protein kinase activating protein kinase 2
MEF2A	Myocyte enhancer factor 2A
MEF2C	Myocyte enhancer factor 2C
MEK	MAPK/ERK kinase
MEK	MAPK/ERK kinase
MKKK	Mitogen activated protein kinase kinase kinase

MnSOD	Manganese Superoxide dismutase
mRNA	Messenger ribonucleic acid
NADPH	Nicotinamide adenine dinucleotide phosphate
NEP	Neutral endopeptidase
NF-κB	Nuclear factor κB
NHE	Na/H ion exchanger
NIH	National Institutes of health
nNOS	neuronal nitric oxide synthase
NO	Nitric oxide
NOS	Nitric oxide synthase
NO_X	Nitrogen oxides (NO2 and NO3)
p70 S6K	70 kDa ribosomal S6 kinase
$p90^{rsk}$	p90 ribosomal S6 kinase
PARP	Poly (ADP ribose) polymerase
PD98059	2'-amino-3'-methoxyflavone
PI3 kinase	Phoshatidylinositol-3'-OH kinase
PIP	Phosphatidyl inositol phosphate
PKB	Protein kinase B
PKC	Protein kinase C
PLA	Phospho lipase A
PLC	Phospholipase C
PLSD	Protected least significant difference
PTP	Permeability transition pore
RACK	Receptor for activated protein kinase C
Raf	MAP kinase kinase kinase
RISK	Reperfusion injury salvage kinases
ROI	Region of Interest
SAPK	Stress activated protein kinase
SB203580	4-(4-fluorophenyl)-2-(4-methylsulphinylphenyl)-5-(4-pyridyl)1H-imidazole
SDMA	Symmetric dimethylarginine
SEM	Standard error of the mean
SNAP	S-nitroso N-acetyl penicillamine
SR	Sarcoplasmic reticulum
STAT-1	Signal transducer and activator of transcription
SWOP	Second window of protection
Thr	Threonine
TK	Protein tyrosine kinase
TKCR	Tyrosine kinase coupled receptors

TKLR	Tyrosine kinase linked receptor
TMRM	tetramethylrhodamine methyl ester
TNF	Tumour necrosis factor
TTC	Triphenyl tetrazolium chloide
TUNEL	terminal dUTP deoxynucleotidyl-transferase nick end-labelling
Tyr	Tyrosine
UTP	Uracil triphosphate
UVB	Ultra violet light (B) ~360 nm
VEGF	Vascular endothelial growth factor
WT	Wild type

Chapter 1. Introduction.

Coronary artery disease is a major cause of mortality and morbidity in the western world, with acute myocardial infarction accounting for a third of all deaths in the UK, and over 6 million deaths world wide per annum[1]. Loss of myocardial viability leads to death or significant morbidity. Therefore, myocardial preservation is the primary objective of the clinician managing a patient presenting with acute myocardial infarction. Until the advent of rapid thrombolysis, no clinical management could be demonstrated to significantly reduce myocardial damage resulting from acute myocardial ischaemic injury. With the introduction of effective thrombolytic modalities, it is proposed that further myocardial salvage may be achieved by harnessing the cell's own protective mechanisms. One potential avenue of research for achieving this goal is to harness the phenomenon known as preconditioning.

1.1 Cell death and lethal myocardial ischaemia

The mechanisms of cell death precipitated by lethal ischaemic injury and subsequent reperfusion remain poorly understood. Until recently, cell death following lethal myocardial ischaemia was presumed to be primarily through a process of irreversible oncosis (necrosis). Oncotic injury associated with ischaemia/reperfusion is characterised by a sequence of histological and metabolic events that can lead to irreversible damage and necrosis. Histological changes appear early during ischaemia. Mitochondria swell and undergo ultrastructural disruption typified by cristae amorphism and loss, and there is a diminution of matrix volume.[2-6] Cells undergo glycogen depletion[7] consistent with the conversion of metabolic process from aerobic to anaerobic respiration, and the utilisation of glucose and glycogen stores. With depletion of high energy phosphates (ATP is rapidly depleted to ~10% of the pre-ischaemic levels after 40 minutes of ischaemia[8]), ionic gradients across the sarcolemmal membranes start to run down with the consequence of reduced pH (occurring as a consequence of anaerobic metabolism and lactic acid generation, and reduced antiporting of Na^+ and H^+ due to reduced Na^+ gradient) increased intracellular sodium (as a result of Na^+/H^+ exchange secondary to the proton load and reduced activity of the Na^+/K^+ ATPase) and depletion of cellular potassium (due to increased intracellular Na^+, and reduced activity of the Na^+/K^+ ATPase and opening of sarcolemmal K_{ATP} channels); the sarcolemmal membrane depolarises, and the cells undergo osmotic swelling. After 10 minutes of ischaemia, intracellular free calcium also starts to increase,[9] associated with the depletion of intracellular ATP. Initially, the primary source of this Ca^{2+} is the sarcoplasmic reticulum, but later, secondary to increased Na^+ influx, the Na/Ca antiporter starts to import more Ca^{2+} which is not compensated by the Ca^{2+}-ATPase.

The consequence is Ca^{2+} overload, which may be exacerbated upon reperfusion. Reduced ATP, exacerbated by the accumulation of lactate, H^+ and inorganic phosphate results in contractile dysfunction[10] and ultimately, functional quiescence. If reperfusion does not intervene, cells develop terminal membrane disintegration, myofibrillar proteolysis occurs and the mitochondria become vacuolated and contain flocculent densities characteristic of cellular necrosis.[11, 12] Reperfusion following a reversible ischaemic insult results in the resolution of these ultrastructural abnormalities of the myocytes, so long as the sarcolemma remains intact.[5] Irreversible ischaemic injury is associated with a less benign sequence of events following reperfusion. Reperfusion is thus characterised by contraction band necrosis (condensation of the myofibrillar contractile elements into bands[13]), intracellular oedema,[8] calcium overload of the mitochondria,[14-17] increasing contractile dysfunction, osmotic stress associated with calcium, sodium, phosphate and chloride overload, and cellular disruption.[18]

Recently however, it has been realised that necrosis may not be the sole mode of myocardial damage. Apoptosis, the mechanism of programmed cell death (or cell 'suicide') is now thought to play a role in ischaemia/reperfusion injury. The precise trigger(s), role and prognostic implications of apoptosis within the development of myocardial injury remain to be determined. Some investigators have speculated whether the apoptotic cells are salvageable; at the present time this remains unclear. The relative contribution of each form of cell death in mediating the injury resulting from an ischaemia reperfusion insult remains controversial however. In studies examining the number of myocytes demonstrating evidence of apoptosis following ischaemia/reperfusion injury with terminal dUTP deoxynucleotidyl-transferase nick end-labelling (TUNEL)-positive nuclei in the region at risk, the percentage of cells that appear to have apoptosed are dwarfed by the number of cells that have apparently undergone necrotic cell death, as determined by triphenyl tetrazolium chloride (TTC) staining or electron microscopy.[19, 20] These data suggest that apoptosis may play a comparatively small role in the evolution of ischaemia/reperfusion injury. Indeed, there appears to be very little evidence of apoptosis until the onset of reperfusion.[20] Whilst these data suggest that necrosis is the overwhelming form of death in ischaemia/reperfusion injury, there may be significant overlap in these two forms of cellular death. In studies in which the apoptotic signalling cascade is blocked either before or at reperfusion, necrotic injury, as measured by TTC staining, is 30% less than that observed in control animals.[19, 21] Therefore, the cardioprotection observed resulting from inhibition of apoptotic pathways is over 10 times greater than could be explained by inhibition of apoptosis alone. These observations suggest that both necrotic and apoptotic cell death share similar signalling pathways, and thus to the hypothesis that apoptosis is the common pathway for cell death where necrosis supervenes when high energy phosphates are depleted to the extent that the apoptotic programme cannot be

successfully completed.[22] Similarly, reperfusion salvage agents such as the growth factor, insulin,[23, 24] and phosphatidylinositide 3'-OH kinase (PI3 kinase) activators such as adenosine,[25] reduce both necrotic cell death and apoptosis via putative anti apoptotic pathways. These data have lead some observers to consider myocardial damage not as necrosis and/or apoptosis, but as reversible or irreversible injury.[26]

The mechanisms of myocyte cell death remain poorly understood. Given the circumstantial evidence implying that necrotic and apoptotic cell death share common pathways, the apoptotic pathway may provide more insight into the mechanisms of both preconditioning and reperfusion salvage modalities in attenuating reversible cell death.

The triggers and mediators of the apoptotic cascade are summarised in figure 1.1. Apoptosis may be triggered by both cell membrane receptors and mitochondrial damage in this paradigm. Cell membrane receptors, CD95/ Fas/ APO-1 are found to be activated in reperfusion,[27] leading to the induction of the caspase proteolytic cascade via the cleavage of pro-caspase-8 to the active large (p20) and small (p10) subunits of caspase-8.[28] Ischaemia/reperfusion also appears to cause significant damage of the mitochondria and opening of the mitochondrial permeability transition pore (PTP). The opening of this non-specific outer membrane channel leads to the release of cytochrome-c, the subsequent activation of caspase-9 and ultimately, caspase-3.[29] The release of cytochrome-c is regulated by the ratio of Bcl to Bax: Bcl inhibits cytochrome release whereas Bax appears to promote it.[30] Caspase-3 appears to be the final common pathway to cell death, leading to poly (ADP-ribose) polymerase (PARP) activation, laminin proteolysis and endonuclease DNA degradation.[31]

Inhibition of specific targets in this signalling cascade may provide clinically useful therapies in the management of ischaemia reperfusion injury. However, at the current time, it is unknown whether once the death cascade is activated, apoptotic cell death is an inevitable consequence, or indeed if apoptosis is inhibited, whether the damaged cell will instead revert to necrosis.

FIGURE 1.1. THE APOPTOTIC CASCADE.

Apoptosis may be triggered as a result of a number of disparate stimuli, from the action of killer lymphocytes rupturing cells as occurs as a result of allograft rejection through the action of Fas ligand receptor occupation and activation of caspase-8 to the release of cytochrome-c from mitochondria with the subsequent activation of caspase-9.

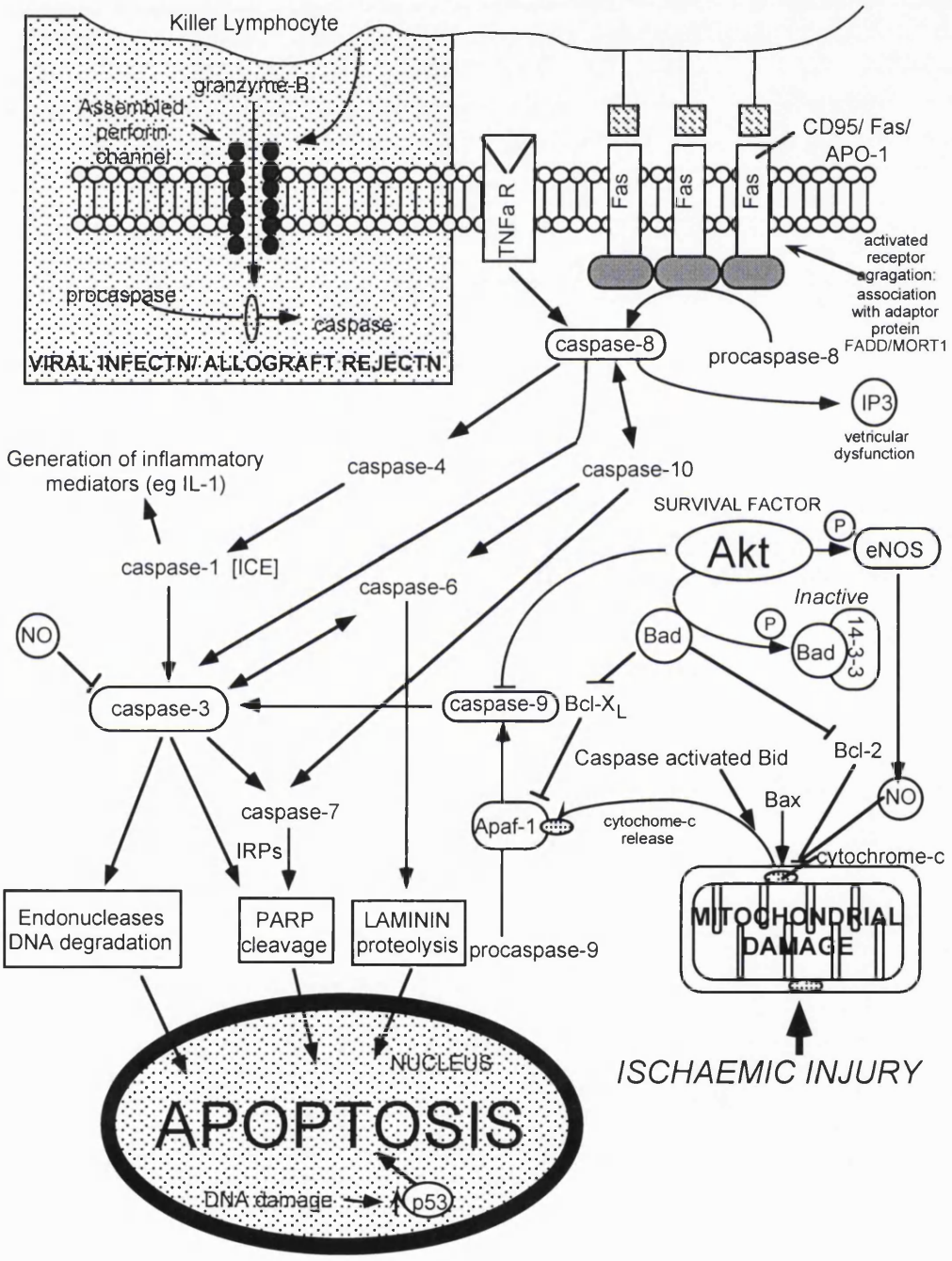

1.2. Preconditioning

1.2.1. Introduction.

Ischaemic preconditioning is the phenomenon whereby brief periods of non-lethal ischaemia confer protection against subsequent, prolonged injurious ischaemia and reperfusion. Preconditioning has two temporally distinct phases of myocardial protection. The first, which is analogous to the initial observations of Reimer et al.[32], has immediate onset, lasting for up to three hours. This early phase of preconditioning has been termed 'classical' or 'early' preconditioning. The second phase of preconditioning, known as delayed preconditioning or second window of protection (SWOP), occurs 24 hours after the initial preconditioning stimulus and has duration of up to 48-72 hours.[33] This is summarised in figure 1.2.

Preconditioning results in resistance to the many facets of ischaemia/reperfusion mediated injury. It results in the delay of onset of reversible and irreversible injury in terms of ultrastructural damage, preservation of myocardial ATP content and attenuation of lactic acid accumulation.[8] Thus, there is attenuation of necrotic cell death, observed as a result of both phases of preconditioning, as can be seen in figure 1.3. Figure 1.3.A shows slices from a naive mouse heart subjected to 35 minutes global ischaemia and 30 minutes reperfusion. As a result, over 30% of the ventricular myocardium has necrosed (pale stained tissue on this triphenyl tetrazolium stained preparation, the viable tissue stains a dark brick red). In contrast, figure 1.3.B shows slices from a heart that has been ischaemically preconditioned. As a result, there is significantly less infarcted tissue evident: less than 20% of the risk zone. Preconditioning also results in the attenuation of post-ischaemic contractile dysfunction ("stunning") in both phases of preconditioning in *regional* models of ischaemia/reperfusion injury,[34, 35] and protects coronary vasculature resulting in attenuated endothelial dysfunction; the coronary arteries of preconditioned hearts are shown have a near-normal vasodilatory response to acetylcholine.[36] Moreover, endothelial cells demonstrate a biphasic response to preconditioning stimuli, consistent with the induction of HSP27, preserving function and structural integrity.[37] In addition preconditioning results in significant reduction of arrhythmias in both early[38] and delayed[39] phases and thus, preconditioning is potentially a potent tool in the management of and the diminution of the sequelae of an acute coronary occlusion.

FIGURE 1.2. THE TWO PHASES OF PRECONDITIONING: EARLY AND DELAYED.

This cartoon depicts the time course of myocardial resistance to injury following a preconditioning stimulus. Early preconditioning has immediate onset, resulting in significant attenuation of infarction, but only has a limited duration of protection of 2 to 3 hours. Delayed preconditioning becomes evident after a 24-hour delay after the initial preconditioning stimulus. Whilst in some models not as robust as early preconditioning, this phase nonetheless results in significant attenuation of necrosis resulting from lethal ischaemia/reperfusion injury. This phase however, has a much longer duration of protection: 48-72 hours.

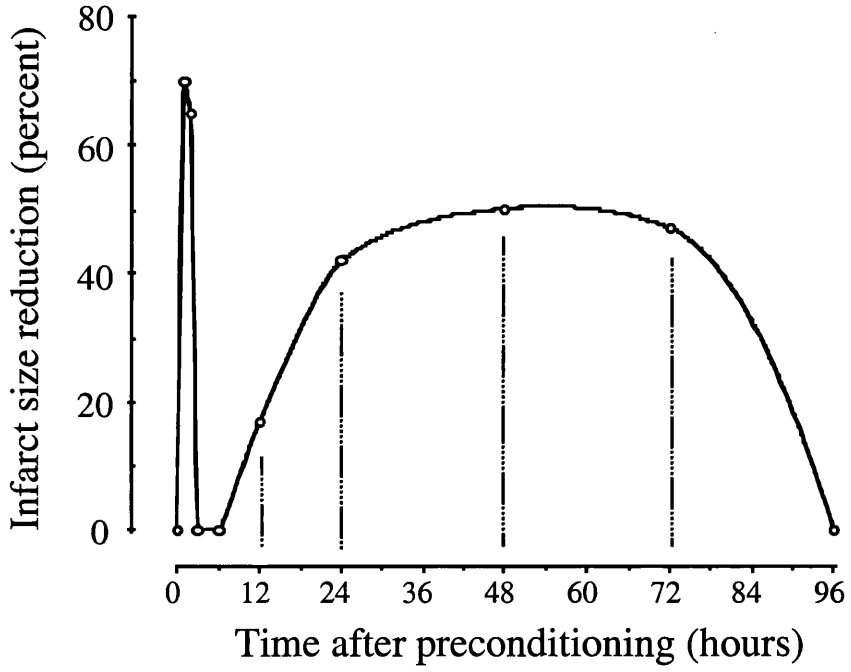

FIGURE 1.3. TTC STAINED MOUSE HEART SLICES.

This figure demonstrates the result of global ischaemia/reperfusion injury in mouse heart that has been stained with the dye, triphenyl tetrazolium chloride (TTC). This dye stains viable tissue a dark brick red, whilst tissue that has undergone irreversible injury fails to hold the stain, and appears pale.

A. Slices from a control heart. As can be seen from the extent of the pale staining, a significant proportion of tissue has undergone necrosis, destroying over 30% of the ventricular myocardium.

B. The preconditioned heart has greater infarct resistance, with an infarct to risk zone ratio of less than 20%.

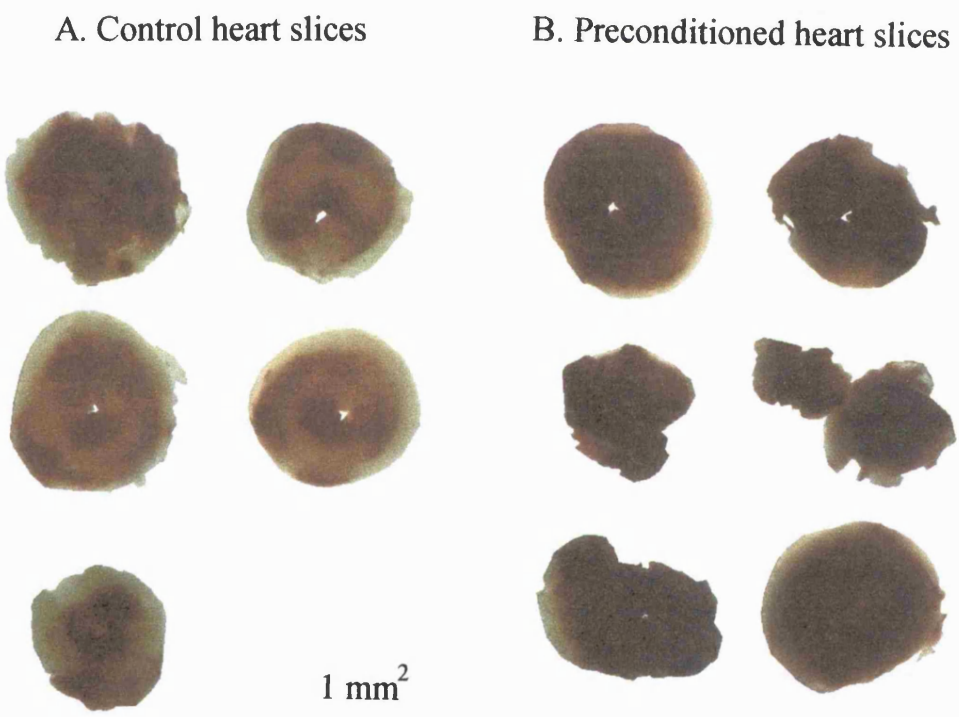

1.2.2. Triggering the preconditioning response.

Transient ischaemia is not the sole trigger of preconditioning against lethal ischaemia/reperfusion injury. Ischaemic preconditioning is associated with the release of a number of mediators, including adenosine, bradykinin, opioids and angiotensin that act upon cell sarcolemmal receptors to trigger the preconditioning response. Furthermore, blockade of these receptors is capable of attenuating preconditioning protection (references [40], [41], [42], and [43] respectively). Interestingly, receptor agonists to these known mediators of ischaemic preconditioning may trigger preconditioning pharmacologically, and this is described in greater depth below in section 1.4.1. Furthermore, preconditioning is induced by various cellular stresses, such as bacterial endotoxic shock and heat stress.

In characterising these 'preconditioning-mimetics', it has been noted that the dose response relationship between agonist and myocardial infarct sparing is not linear. In fact, triggering of preconditioning demonstrates a dose-response threshold. If the duration of transient ischaemia or the concentration of the preconditioning-mimetic is inadequate, no resistance to lethal ischaemic injury is observed. By progressive incrementation of the preconditioning stimulus, a threshold is breached and the preconditioning response triggered. Interestingly the summation of two disparate sub-threshold stimuli may trigger the full preconditioning response (figure 1.4). This "*preconditioning threshold*" hypothesis is supported by observations in both rabbit[44, 45] and human myocardium[46]. These studies demonstrate that sub-threshold transient ischaemia prior to the index ischaemic insult may be augmented by the addition of an angiotensin converting enzyme (ACE) inhibitor. ACE inhibitors attenuate bradykinin metabolism and breakdown by ACE present in the extra cellular milieu. Bradykinin, via bradykinin B2 receptors, is capable of triggering the preconditioning response when administered exogenously.[47] Endogenously, bradykinin is released by the endothelium under conditions of ischaemia,[47] therefore adding to the preconditioning stimulus following transient ischaemia.[48] Whilst the administration of an ACE inhibitor is in itself inadequate to provide a sufficient increment to the basal bradykinin concentration to trigger myocardial protection, the addition of a sub-threshold ischaemic preconditioning stimulus and therefore increased total bradykinin in the extra cellular milieu, is adequate to trigger preconditioning and reduce both myocardial death[44, 45] and dysfunction.[46]

Therefore preconditioning appears to consist of a number of triggers that can be pharmacologically manipulated individually or collectively to induce protection against subsequent lethal ischaemia/reperfusion injury.

FIGURE 1.4. THE THRESHOLD HYPOTHESIS OF PRECONDITIONING INDUCTION.

As described in the text, transient ischaemia results in the release of a number of signalling moieties that result in the triggering of the preconditioning response (**A**). Morris et al. reported that in isolated human papillary muscle, 1 cycle of 5 minutes ischaemia was sufficient to trigger the preconditioning response (**A**), whilst 1 cycle of 3 minutes ischaemia was not (**B**). The addition of an ACE inhibitor to the subthreshold preconditioning stimulus was sufficient to trigger preconditioning (**C**), presumably through a mechanism of augmented extracellular bradykinin as the effect of the ACE inhibitor could be blocked with the bradykinin B2 receptor selective antagonist, HOE 140.

Abbreviations used in figure:

Ado: adenosine;
Bk: bradykinin;
AgT: angiotensin

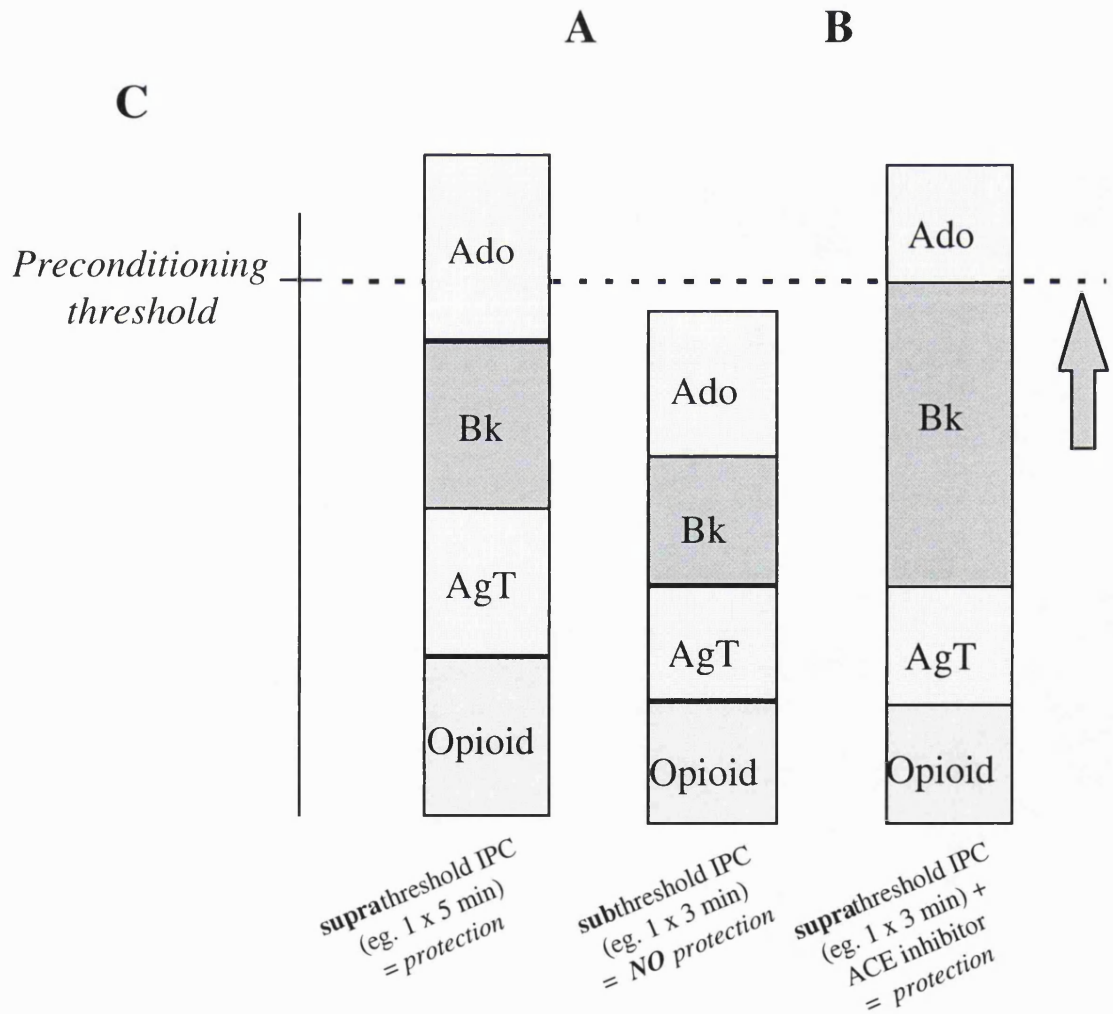

1.3. Growth factor signalling and reperfusion injury salvage

As an alternative modality to preconditioning for the attenuation of ischaemia/reperfusion injury, the administration of agents at reperfusion that inhibit the apoptotic cascade have emerged, based on evidence that apoptosis appears to predominantly occur at reperfusion. In this respect, growth factors have recently been demonstrated to function as "survival factors", both during normal embryonic development,[49] and during pathological processes such as reperfusion injury.[23, 50] These survival factors have been shown to signal through a reperfusion injury salvage kinase (RISK) pathway involving the activation of phosphatidyl inositide 3'-OH kinase (PI3 kinase) and the serine/threonine kinase Akt/PKB. Activation of these kinases is adequate to prevent cellular apoptosis in a number of cell types, including myocytes. By administering insulin or insulin related growth factor-1 (IGF-1) either before[51] or at reperfusion,[23] it has been shown that growth factors are effective in reducing cell death resulting from lethal ischaemia reperfusion injury. The nature of the down stream signalling cascades, and the manner in which this protection is effected remain to be determined. However, a number of candidate pathways are emerging. We have recently demonstrated the involvement of a ribosomal kinase, the 70-kDa S6 kinase (p70 S6 kinase), as a necessary component for the limitation of reperfusion injury (Jonassen et al, unpublished data). The p70 S6 kinase phosphorylates the S40 ribosomal subunit, thus regulating the translation of mRNA. The inhibition of this kinase abrogates the protective effects of insulin administration at reperfusion (unpublished data). Further targets of Akt include the Bcl-2 family member, Bad (figure 1.1). Bcl-2 related proteins comprise a family that are closely involved in the initiation and regulation of the apoptotic programme.[52] Pro-apoptotic family members, Bax and Bid, promote the release from mitochondria of both cytochrome-c[53] and, in neurones and myocytes, the precursor protease, pro-caspase-9.[54] Cytochrome-c binds with the adapter protein, Apaf-1 to activate caspase-9 and bind to form the apoptosome.[55] Anti-apoptotic family members, Bcl-2 and Bcl-X_L, inhibit the release of cytochrome-c and the activation of caspase-9 by Apaf-1 respectively.[56] Bad plays an important regulatory role. Constitutively active, it dimerises and inactivates both Bcl-2 and Bcl-X_L.[52] However, Akt dual phosphorylates Bad, inactivating the protein, and enabling Bad to bind to a chaperone protein 14-3-3.[57] Therefore, with Bad inactivated, Bcl-2 and Bcl-X_L are enabled to exert their anti-apoptotic function. There are further targets of Akt including caspase-9[58] and the Forkhead family of pro-apoptotic gene transcription factors[52] that reinforce the anti-apoptotic credentials of the PI3 kinase-Akt pathway.

1.4. Cellular Mechanisms of Preconditioning

1.4.1. Triggers of preconditioning

Despite the temporal distinction between the two phases of preconditioning and the apparent differences in signalling pathways and adaptive processes (discussed in section 1.5), both early and delayed preconditioning appear to have similar triggers (including adenosine[59, 60] and δ opioid stimulation[42, 61]). Furthermore, there appears to be a significant level of intra-species homogeneity with respect to preconditioning; the same triggers are found to ubiquitously trigger preconditioning in the majority of species studied (reviewed in reference [62]).

1.4.2. Receptor mediated triggers

During ischaemia, products of metabolism and cytokines are released into the intercellular milieu. These substances may act in either an autocrine or endocrine fashion, occupying specific sarcolemmal receptors which will, with adequate receptor occupancy, trigger preconditioning (figure 1.5). These triggers of preconditioning, known as "preconditioning-mimetics," exert their biological affect via specific receptors: adenosine via A_1/A_3 receptors[63, 64]; acetyl choline via muscarinic M-2 receptors[65]; catecholamines via α-1 receptors[66]; angiotensin II via AT-1 receptors[67]; bradykinin via B-2 receptors[68], and the opioids via δ–1 opioid receptors[69]. These are all examples of G-protein linked receptors that have each been demonstrated to evoke the early preconditioning response and maybe released during transient ischaemia, contributing to the preconditioning stimulus (section 1.2.2).

A well-described example of the autocrine/paracrine stimulation model is adenosine. Adenosine is released as a result of high-energy phosphate degradation during myocardial ischaemia, a process that involves the 5-nucleotidase dephosphorylation of adenosine triphosphate (ATP) via adenosine diphosphate (ADP) to adenosine. Released by the ischaemic myocyte, adenosine is subsequently able to bind to purine receptors on the sarcolemmal membrane, initiating signalling cascades as summarised in figure 1.5. Thus transient ischaemia results in the release of a number of mediators (autocoids and "paracoids", figure 1.5) that summate to activate the preconditioning cytoprotective cascades.

1.4.3. Non-receptor mediated triggers

The generation of oxygen free radicals as part of the oxidative stress of the ischaemic preconditioning stimulus is thought to be an important trigger for triggering the preconditioning response. In early preconditioning, free radical generation appears to

contribute to the milieu of preconditioning-mimetics to reach the threshold for preconditioning. Where supra-threshold preconditioning stimuli are used, the free radical contribution is no longer essential to trigger the early preconditioning response.[70] Free radicals are however thought to play an important role in the induction of delayed preconditioning[71]. The introduction of reactive oxidative species is adequate to result in myocardial resistance to injury 24 hours later, in the absence of other potential triggers. In a similar paradigm, nitric oxide, through the generation of peroxinitrite radicals, can also be found to trigger delayed preconditioning[72]. (The role of nitric oxide in preconditioning is discussed in more detail in section 1.7.) The downstream signalling path may follow that seen in with receptor mediated preconditioning, via PKC[73]. In addition to these signalling roles, reactive oxygen species are found to increase DNA binding of heat shock factor-1, a transcription factor regulating the expression of heat shock proteins, proteins implicated in the evolution of the second window of protection[74]. Free radical generation is therefore implicated as an important trigger of the preconditioning phenomena.

FIGURE 1.5. AUTO- AND PARACRINE STIMULATION MODEL OF PRECONDITIONING INDUCTION:

A. Autocrine model of preconditioning. Exposure of the myocyte to ischaemia (1) leads to the release of adenosine (2)- autocrine substances such as adenosine have been termed 'autocoids'. Autocoids interact with dedicated receptors on the sarcolemmal membrane of the cardiac myocyte (3) to trigger an intracellular signalling cascade (4) that leads to myocardial adaption to subsequent cellular stress.

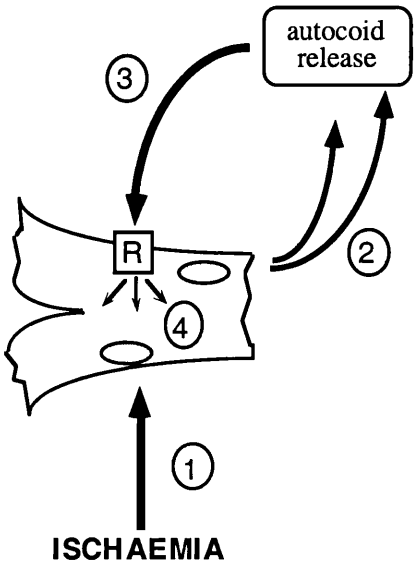

B. Paracrine model of preconditioning. As in (A), ischaemia (1) leads to the release of preconditioning-mimetics from the endothelium (e.g. bradykinin), that can either precondition the endothelium in an autocrine fashion, or precondition myocytes, acting as a paracrine agent (3), triggering adaptive cellular processes.

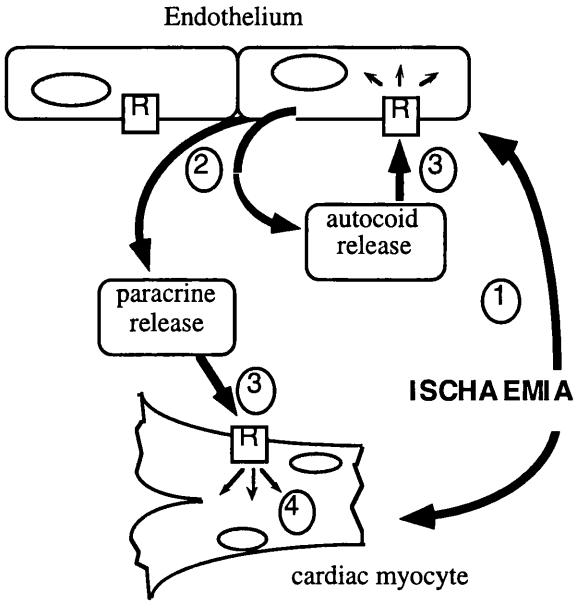

FIGURE 1.6. PKC ACTIVATION FOLLOWING RECEPTOR ACTIVATION.

Adenosine, bradykinin and δ opioids are mediated via G-protein linked 7 transmembrane-domain receptors. Receptor activation leads to the activation and binding of PKC to its receptor for activated C-kinase (RACK) with translocation from cytosolic to sub cellular compartment- review see[75]

Abbreviations used in figure:

DAG: diacylglycerol
GDP: guanosine diphosphate
GTP: guanosine triphosphate
IP_3: inositol triphosphate
PIP: phosphatidyl inositol phosphate
PKC: protein kinase C
PLC: phospholipase C
RACK: receptor of activated protein kinase C

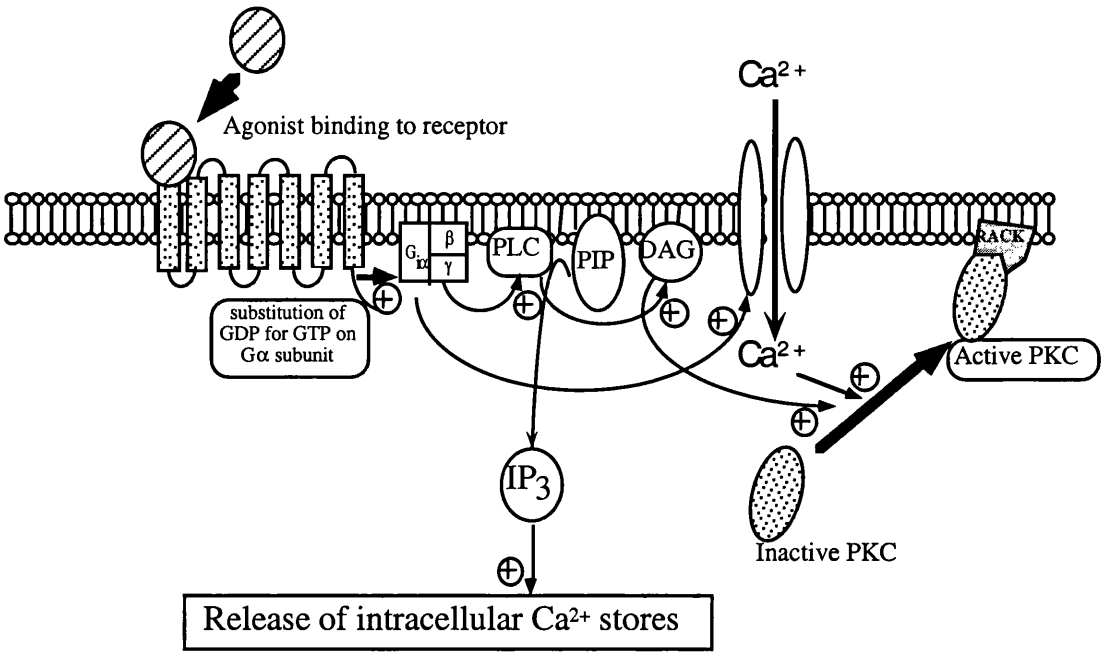

1.5. The mediators of preconditioning and the signalling cascade

1.5.1. Receptor linked pathways

There are two main categories of cellular membrane receptors known to be involved in preconditioning: Guanine nucleotide-binding regulatory protein (G protein) coupled receptors and tyrosine kinase receptors.

1.5.1.1. G-protein coupled receptors

Many of the triggers mentioned (adenosine, bradykinin, opioids, angiotensin and noradrenaline) precondition via GTP-binding regulatory protein (G-protein) coupled receptors. The hetero-trimeric G- protein consisting of three polypeptide sub units (α, β and γ), function as 'molecular switches', existing in two alternate conformations according to GTP binding to Gα: an active GTP bound form and inactive GDP bound form. Mammalian α-subunits are divided into four subfamilies: Gs, Gi, Gq and Go. Stimulatory (Gs) or inhibitory (Gi), G-proteins are defined upon the ability to active adenylate cyclase. Gq receptors activate phospholipase Cβ, which hydrolyses phosphatidylinositol 1,4,5 trisphosphate and diacylglycerol.[76] Go is the main G-protein of the brain, and is thought to directly regulate ion channels.

Early ischaemic preconditioning is reliant upon the activation of G-proteins; inhibition of receptor-linked Gi activation with pertussis toxin abolishes preconditioning.[77] Adenosine A_1 and A_3 receptors and δ opioid receptors are linked via Gi proteins; the α subunit inhibits the activity of adenylate cyclase and thus the production of the second messenger, cyclic adenosine mono phosphate (cAMP). Giα subunits are additionally able to open voltage independent Ca^{2+} channels, activate phosphatidyl inositol-3 kinase (PI3 kinase),[78] and lead to the generation of inositol 3,4,5 triphosphate (IP_3)- an important intracellular messenger capable of mobilising intracellular calcium stores. Bradykinin and noradrenaline signal via the Gs protein. The Gsα subunit stimulates the adenylate cyclase, and thus function via cAMP second messenger mediated signalling. cAMP, which activates AMP-linked protein kinase, has been associated with activation of the endothelial isoform of nitric oxide synthase (eNOS), phosphorylating the enzyme at serine 1177[79, 80]. This signalling step may be of some importance in triggering the preconditioning response, and is discussed later (section 1.7.4). Gβγ have multifarious signalling properties, including activation of PI3 kinase, phospholipase-Cβ (PLCβ), ion currents (I_K and I_{ca}), tyrosine kinases and G- protein-coupled receptor kinases. This is briefly summarised in part in figure 1.6. For review see reference [81]. PLC, and its

product diacylglycerol (DAG) have been demonstrated to activate protein kinase C (PKC).[82] This is supported by evidence that both phorbol myristate and diacylglycerol analogues can independently activate PKC, and precondition the heart.[83, 84] Thus, second messengers are critical in the induction of the signalling cascade, pivotal with the activation of PKC.

PI3 kinase, like AMP linked protein kinase, phosphorylates eNOS through the action of Akt.[85, 86] The role of the Akt/AMP-kinase activated protein kinase eNOS pathways in preconditioning have not yet been explored.

Preconditioning-mimetics that signal via G-protein linked receptors have been demonstrated in all the mammalian species studied, although some controversy surrounds the involvement of adenosine in the rat. However, as myocardial ischaemia in rat releases three times the concentration of adenosine into the microcirculation compared to that found in rabbit under the same conditions,[87] it is possible that this species has fewer adenosine receptor and/or is a less efficacious signal for preconditioning. Thus, failure to account for this difference in efficacy of adensoine may have lead to a number of negative studies in the rat.[88-93] As direct infusion of adenosine into the microcirculation of the rat does result in cardioprotection[94] and moreover the recent demonstration of adenosine A_1 receptor agonists induce both the early[95] and delayed preconditioning in this species,[96] it would appear that adenosine indeed does induce preconditioning in rat (although its contribution to the 'preconditioning stimulus' - section 1.2.2 - may be less) and thus adenosine receptor activation has been shown to induce preconditioning in the majority of mammalian species, including man.[97]

1.5.1.2. Tyrosine kinase coupled receptors

A number of trophic/mitogenic factors signal via tyrosine kinase linked receptors (TKLRs). However, cardiac myocytes are terminally differentiated. As such, myocytes cannot therefore undergo mitosis in response to a mitogenic signal. However, these mitogenic signals have been shown to posses cardioprotective properties in the context of injurious ischaemia, eliciting an early preconditioning- like response,[98, 99] and thus appear to act as "cell-survival' factors. Two examples of cell survival factors that signal via this pathway are fibroblast growth factor (FGF)[98] and insulin-like growth factor-II (IGF-II)[99]. FGF causes receptor dimerisation and translocation to the perinuclear area. The activation of the receptor/ tyrosine kinase complex is then thought to cause direct activation of the Ras/ mitogen activated protein kinases (MAPK) pathway, possibly independently of PKC (although TKLRs have been shown to lead to activation of PLCγ and PKC activation, this may be outweighed by MAPK activation[100]). Therefore G-protein receptor and tyrosine receptor linked pathways appear converge and integrate

with the activation of MAP kinases. At present however, tyrosine kinase receptor agonists have not been investigated with respect to the second window of protection.

1.5.2. Post receptor signalling

1.5.2.1. Protein Kinase C

The pivotal role of PKC in preconditioning appears to be confirmed by the attenuation of preconditioning by the PKC inhibitors staurosporine[83], polymyxin B[83, 101], and chelerythrine,[84, 102] with the possible exception of pig, where PKC inhibition alone may be insufficient in itself to abrogate preconditioning,[103] and may require the co-inhibition of tyrosine kinase[104] (discussed in section 1.5.2.2).

Interestingly, whilst total PKC activity may not markedly increase in response to stress, two isoforms of PKC, PKC-ε[105-107] and PKC-η[106], significantly translocate from the cytosolic to the particulate fraction in response to preconditioning, and demonstrate specific increases in enzymatic activity (PKCε). Furthermore, the particulate fraction of PKCε increases in a dose-dependent fashion to the ischaemic stimuli administered. In contrast, maximal translocation of PKCη occurs immediately after the preconditioning trigger[106].

Pharmacological stimulation of the novel ε/δ isoforms with ingenol 3, 20-dibenzoate (an ε, δ-PKC isoform selective activator) protects incubated isolated rabbit myocytes against ischaemia, whereas stimulation of calcium dependant α/β/γ PKC isoforms with thymeleatoxin had no protective effect[108]. Furthermore, using a PKCε-selective antagonist, εV1-2 peptide, preconditioning can be ablated[109], suggesting that whilst PKCη may be involved in preconditioning in an as yet undetermined way, PKCε activation and translocation is pivotal to the preconditioning signal cascade.

1.5.2.2. Tyrosine Kinases.

Recent work has implicated protein kinases other than PKC in preconditioning; that maybe either in parallel and/or downstream to this enzyme group. Experiments with the tyrosine kinase inhibitor, genistein, have demonstrated that tyrosine kinase (TK) activation is a crucial step in the preconditioning cascade[110]; the delayed preconditioning effect of stimulation via the adenosine A_1 receptor can be attenuated both by chelerythrine (PKC inhibitor) and lavendustin-A (TK inhibitor)[111]. With respect to the relationship of TK with PKC in the activation of the preconditioning signalling cascade, it is thought that TK is downstream of PKC[112], although to block preconditioning in pigs requires the combined blockade of both TK and PKC[104], implicating parallel and independent signal transduction in this species.

1.5.2.3. Mitogen activated protein kinases

Mitogen activated protein kinases (MAPK) are highly conserved serine/threonine protein kinases that are activated by dual phosphorylation on a Thr-X-Tyr motif[113]

during ischaemia and/or reperfusion, possibly contributing to structural and functional changes after myocardial ischaemia. They are activated in response to a wide variety of stimuli including growth factors (via G-protein coupled receptors) and environmental stresses. Three major MAP kinases have been studied in the heart with respect to ischaemia/reperfusion injury: p38- mitogen activated protein kinase (of which α and β isoforms have been identified in the heart[114]), p42/p44 extra cellular signal-regulated kinase (ERK), and the stress activated c-jun N- terminal kinase, p46/p54 JNK/SAPK. Within these classifications, there are a number of identified isoforms characterised: there are currently 10 p46-p54 JNK isoforms and 6 p38-MAPK isoforms (α_1, α_2, β_1, β_2, γ and δ) (JNK and p38 MAPK are reviewed in depth in reference[113] and ERK reviewed in reference [115]). In addition to the increasing complexity of MAP kinase isoforms, another MAP kinase has been identified which is closely related to ERKs- BMK-1 (ERK-5). [116, 117] Comparatively little is known about BMK-1 with regard to preconditioning and ischaemia/reperfusion injury, so the summary below concentrates upon the better-characterised p38 MAPK, p42/p44 ERK and p46/p54 JNK families.

1.5.2.4 Activation of the MAP kinases

Growth factors, and other G-protein coupled receptor agonists rapidly signal via pathways that include the activation of the various isoforms of PKC. Activated PKC phosphorylates the mitogen activated protein kinase kinase kinase (MKKK), raf-1,[118] directly activating p42/p44 ERK and indirectly p38 MAPK and p46/p54 JNK. Over expression of PKCε results in the dual phosphorylation of p42/p44 ERK and imbues protection against lethal simulated ischaemia/reperfusion in isolated rabbit myocytes.[119] This pathway has been shown to be triggered following ischaemic preconditioning, whereby transient ischaemia leads to rapid activation of Raf-1.[120]

Ischaemia or reactive oxygen species has been shown to rapidly activate p38 kinase and JNK SAPK[121, 122] without the obligatory requirement of receptor activation. However, G-protein coupled receptors can modulate activity of these MAP kinases. In kidney 293 cells, Gq/G11 muscarinic m1, Gi coupled m2, Gs β-adrenergic receptors activate p38 MAPK, which is completely inhibited by the expression of Gαo. This activation of p38 MAPK is mimicked by the over expression of Gβγ,[123] indicating the G-protein mechanisms of signalling of p38 MAPK in this cell line.

Therefore, the patterns of MAP kinase activation are complex, and appear to involve significant cross talk between the small G-protein Ras and the MKKK, Raf-1 to lead to the patterns of MAP kinase activation observed in ischaemia and reperfusion, and as a result of preconditioning.

1.5.3. MAP kinases in ischaemia/reperfusion injury and early and delayed preconditioning.

The three MAP kinase signalling pathways (summarised in figure 1.7) are activated remarkably rapidly, concomitant with the time course of the early preconditioning phenomena, and even during the period of the ischaemia/reperfusion insult.[124, 125] Therefore, these signalling pathways have been investigated to determine whether they have a role in myocardial ischaemia/reperfusion injury and resistance to injury.

1.5.3.1 Ischaemia/reperfusion injury

p38 MAPK phosphorylation and activity is rapidly upregulated by cellular stress, including both ischaemia[122] and oxidative stress.[114] Unlike p42/p44 ERK and p46/p54 JNK, p38 MAPK is activated solely during ischaemia, not requiring subsequent reperfusion for maximal activation. Recent studies have indicated that p38 MAPK activation in this paradigm is significantly deleterious in terms of necrotic cell death resulting from an injurious ischaemia/reperfusion insult.[126] Further evidence for this deleterious role comes from studies where p38 MAPK is inhibited with the specific inhibitor 4-(4-fluorophenyl)-2-(4-methylsulphinylphenyl)-5-(4-pyridyl)1H-imidazole (SB203580) during the ischaemia/reperfusion insult: inhibition reduces injury in cardiac tissue both in terms of measured necrosis[127-130] and apoptosis.[127, 131] Furthermore, the abrogation of p38 MAPK dephosphorylation further augments ischaemia/reperfusion injury.[128]

During ischaemia/reperfusion, p38 MAPK is not the only deleterious MAP kinase. Recent studies have indicated an injurious role for p46/p54 JNK. Phosphorylation and in-gel kinase assays have shown that ischaemia increases p46/p54 JNK activity, which is further augmented by reperfusion.[132] The injurious role is supported by evidence demonstrating that the inhibition of JNK by curcumin attenuates ischaemia/reperfusion necrotic injury,[130] whilst transfection with a dominant negative mutant into the H9c2 cell line markedly attenuates apoptotic cell death.[133]

The role of p42/p44 ERK in ischaemia/reperfusion is less well determined. It has been shown that ischaemia/reperfusion triggers p42/p44 ERK activity via a mechanism dependant upon the activity of PKCε.[119] Activation appears dependent upon reperfusion[132, 134] but this activity appears to be unrelated to cellular resistance to or exacerbation of necrosis following ischaemia/reperfusion injury, although a recent report has suggested that ischaemia/reperfusion triggered apoptotic injury may be exacerbated by inhibition of the activation of p42/p44 ERK by 2'-amino-3'-methoxyflavone (PD98059, a MEK1/2 inhibitor).[131]

There is, therefore, strong evidence for the activity of MAP kinases during ischaemia/reperfusion. These signalling pathways, in their own right, could be used as

pharmacological targets to reduce myocardial injury. Furthermore, these pathways may be modulated following preconditioning stimuli.

1.5.3.2. Early Preconditioning

Whilst p38 MAPK has been demonstrated to be deleterious during ischaemia/reperfusion injury, paradoxically perhaps, ischaemic preconditioning increases p38 MAPK phosphorylation following the preconditioning stimulus. The increase of p38 MAP kinase activity is associated with increased cytoskeletal translocation of HSP27,[135] an αB crystalline small heat shock protein thought to have a cytoskeletal protective role against cellular stress. Ischaemic and pharmacological preconditioning in rabbit (via A_1 receptor activation) increases p38 MAPK phosphorylation, concomitantly increasing MAPKAPK2 activity and is associated with significant attenuation of infarction.[136] The cardioprotection resultant from ischaemic preconditioning can be mimicked by the pre-treatment of the myocytes with a stimulator of p38 MAP kinase activity, anisomycin, to significantly reduce infarct size.[125, 130, 136] Furthermore, early ischaemic preconditioning has been shown to be attenuated with inhibitors of p38 MAPK, SB203580, [125, 129, 130, 136-139] PKC[129] (demonstrated to reduce the activation of p38 MAPK) and tyrosine kinase,[137] but not with inhibitors of the other MAP kinases. The conundrum of increased p38 MAP kinase activity following preconditioning being paradoxically protective rather than deleterious may be explained by observations in neonatal rat myocytes. Ischaemic preconditioning appears to attenuate p38α activation during index simulated ischaemia, without effect upon p38β activity.[126, 129] Therefore, the initial increase of p38 MAP kinase during the preconditioning stimulus, appears to abrogate later, deleterious p38α activation in myocytes.

Whilst p42/p44 ERKs are phosphorylated and active during the time frame of early preconditioning, the role of these kinases remain controversial. There is conflicting evidence regarding the role of p42/p44 ERK in early preconditioning, in which activition has been shown to be either protective (pig[140]) or to have no role in this phase in myocardial resistance to injury (rabbit[141] and H9c2 cells[129]). The cause of this dichotomy in the literature is unclear, but may relate to the species of study, as other investigators, using the pig model of preconditioning, have failed to demonstrate any clear correlation between MAP kinase activation and myocardial tissue injury.[142]

Where the role of p46/p54 JNK has been studied in relation to ischaemia/reperfusion and preconditioning, p46/p54 JNKs are demonstrated to be activated. However, inhibition of JNKs has no effect upon infarct sparing in the rat,[130] suggesting that the upregulation of p46/p54 may be an epiphenomenon following early ischaemic preconditioning.

1.5.3.4. Delayed preconditioning

In early preconditioning, p38 MAPK has been shown to be efficacious in reducing injury through a pathway that involves MAPKAPK2 and HSP27 phosphorylation. In delayed preconditioning, a similar protective pathway has been postulated, using an adenosine A_1 receptor agonist in rat as a trigger of delayed pharmacological preconditioning. In this paradigm, recent work suggests that p38 leads to a late phase phosphorylation of HSP27 via MAPKAPK2, which is associated with attenuation of infarct size.[143, 144] This pathway is sensitive to both PKC and tyrosine kinase inhibition, although the necessity of p38 MAPK activity was not tested directly. These results appear to be supported in a human cell line model, whereby SB203580 attenuates both ischaemic and pharmacological delayed preconditioning.[145] In rat neonatal myocytes however, SB203580 failed to attenuate protection triggered by ischaemic preconditioning.[134] Therefore, at the present time, the weight of evidence would support a role for p38 MAPK in delayed preconditioning, although the definitive answer remains to be determined.

Evidence for a role of p42/44 ERKs in delayed preconditioning is more robust. Delayed ischaemic preconditioning in rat ventricular myocytes results in the activation and phosphorylation of p42/p44 MAPK,[146, 147] which is associated with protection against simulated lethal ischaemia. This protection is attenuated by the administration of PD98059, but not by SB203580 or wortmannin.[134] The activation of p42/p44 ERK would appear to be an essential component of a signalling cascade involving PKCε upstream, and the activation of gene transcription factors such as NF-κB and AP-1 downstream.[147]

Limited data are available regarding the role of p46/p54 JNKs in delayed preconditioning. Whilst p46/p54 has been shown to be pro-apoptotic in some models, the expression of a dominant negative mutant of MAPK kinase-4, inhibiting p46/p54 JNK, prevented the upregulation of the down stream gene transcription factors, NF-κB and AP- 1, that are thought to play an important role in mediating delayed protection against lethal ischaemic injury.[147]

1.5.4 Downstream targets of MAPKs

1.5.4.1 Cell death pathways

One potential target for the beneficial/detrimental actions of MAP kinase activation is the cell death cascades classically associated with apoptosis (as discussed in section 1.1).

In H9c2 cultured myoblasts, inhibition of p42/p44 ERK with PD98059 exacerbates ischaemia/reperfusion induced apoptosis.[131] The p42/p44 ERK pathway appears to be a potent mechanism for cell survival, capable of arresting apoptosis even after release of

cytochrome-c from mitochondria.[148] One potential anti-apoptotic target is the p90 ribosomal S6 kinase ($p90^{rsk}$). Activated as a result of ischaemia/reperfusion,[120] $p90^{rsk}$ is an ERK substrate and ubiquitous and versatile mediator of ERK signal transduction.[149] Essential functions include (1) regulation of gene transcription via phosphorylation of transcription factors including c-Fos and camp-response element-binding (CREB) protein,[150] (2) regulation of protein synthesis by phosphorylation of poly ribosomal proteins and glycogen synthase kinase-3; and (3) stimulation of the Na/H exchanger (NHE) by phosphorylating serine 703 of the NHE-1.[151] p90rsk has recently been shown to phosphorylate serine 112 the pro-apoptotic Bcl-2 family member, Bad, and thus inactivate it. [150, 152, 153] Therefore, p42/44 ERKs have been demonstrated to promote survival both via inhibition of cell death machinery and the increased transcription of pro-survival genes. Similarly, the related BMK-1 has also been shown to have a potentially anti-apoptotic role in ischaemia/reperfusion injury.[154] BMK-1 activation results in phosphorylation and activation of MEF2A and MEF2C myocyte enhancer factor-2 transcription factors[155] that are important regulators of cardiac gene expression. As PD98059 has been shown to attenuate BMK-1 activity at the same concentrations required to block Mek 1/2, some caution therefore needs to be applied into the interpretation of the results using this drug.

In a number of studies, p38 MAPK appears to have a pro-apoptotic role. In myocyte models of ischaemia/reperfusion, inhibition of p38 MAPK with SB203580 reduces apoptosis.[127, 131] In the HaCaT cell line, where ultraviolet radiation appears to be a potent stimulator of p38 MAPK, the ensuing apoptotic injury appears to be mediated via the release of cytochrome-c from the mitochondria.[156] In T-cells, p38 MAPK activation is associated with Fas ligand (FasL) expression:[157] ligand/receptor interaction leads to the activation of caspase-8 and thus lead into cell death. In the cardiac myocyte, the cause of cell death remains to be clearly determined. However, it has been suggested that there is isoform specificity of apoptotic function: the p38α MAPK isoform may be pro-apoptotic, whilst p38β MAPK may have an anti-apoptotic role. [158] Indeed, in other models, p38β has been shown to attenuate FasL and UVB induced cell death, whereas p38α has been shown to mildly exacerbate injury.[159] Thus, the specific roles of the p38 isoforms in apoptotic signalling potentially provide a mechanism by which differential regulation of p38 MAPK isoforms may be beneficial following ischaemic preconditioning regimen.

The role of p46/p54 JNK is thought to be deleterious to cell survival. Indeed, inhibition of JNK reduces apoptotic cell death,[131] and dominant negative JNK transfection in this cell line reduces DNA fragmentation associated with apoptosis following oxidative stress.[133] JNK-mediated apoptosis in some cell lines has been shown to involve ubiquination and degradation of p53, which may be regulated by the JNK-mediated phosphorylation of p53. [160] However, p53 does not appear important for hypoxia

induced apoptosis in cardiac myocytes; cell death triggered by hypoxia with acidosis is independent of p53, with no significant difference in cell death observable between hearts from wild type and p53 knockout mice.[161] Therefore, the mechanism for JNK-induced apoptosis remains unexplained.

1.5.4.2. Gene transcription factors

Preconditioning stimuli, through the induction of reactive oxygen species, PKC or tyrosine kinase activation, each linked to MAPK activation, leads to the rapid dissociation of nuclear factor (NF)- κB from inhibitory IκB proteins[162], and subsequent translocation of the active NF-κB subunits to the nucleus[162, 163]. Indeed, activation of this nuclear transcription factor occurs rapidly as a result of ischaemia/reperfusion,[162] and can be found to be induced in the myocardium of patients suffering from acute coronary syndromes, such as unstable angina.[164] Blockade of NF-κB with the inhibitor diethyldithiocarbamate (DDTC) leads to the complete loss of protection associated with the second window of protection[163]. The loss of cytoprotection resultant from attenuation of NF-κB activity is likely to be associated with the loss of availability of the gene products that are regulated. Candidate genes include inducible nitric oxide synthase (iNOS/NOS-2) and guanosine triphosphate cyclohydralase-1,[165] and adenosine A_1 receptor expression.[166] Regulation of NF-κB appears to be both via p38 MAPK and p42/p44 ERK. MKK6 activates NF-κB in a p38 MAPK dependent manner[167, 168] Cytokines appear to preferentially signal via the p42/p44 ERK pathway to upregulate gene products such as inducible isoforms of nitric oxide synthase[169, 170] and cyclooxygenase.[171] Unfortunately, there are insufficient data to draw definitive conclusions as to the significance of these apparently separate triggers of NF-κB activation, but may hint at differences between pharmacological and ischaemic preconditioning that need to be considered when comparing results of various investigations. Equally, there are comparatively little data on the roles of other transcription factors following preconditioning, such as MEF2s (discussed in section 1.5.4.1 in relation to p38 MAPK activation, and reviewed in [172]) and activator protein (AP)-1 (associated with p46/p54 JNK[173] and/or p42/p44 ERK[132, 174, 175] activation and encodes a number of genes associated with cardiac hypertrophy[176, 177]).

1.5.5. MAP kinases and cellular adaption to injury: Summary

The patterns of MAP kinase activation are complex, and remain poorly understood. From data currently available, it appears that whilst p38 MAPK activation during ischaemia/reperfusion injury is deleterious, it is nonetheless an essential signalling component of both early and delayed preconditioning. The role of p42/44ERKs remain controversial in early preconditioning, although in the context of delayed preconditioning, its activation appears to be an essential signalling step in the mediation

of protein upregulation required for this phase of protection. P46/54 JNKs are the least understood of the MAP kinases: deleterious during ischaemia/reperfusion, their role as a result of preconditioning remains unclear.

FIGURE 1.7. MITOGEN ACTIVATED PROTEIN KINASE SIGNALLING CASCADE.

The mitogen activated protein kinase cascade is summarised below.

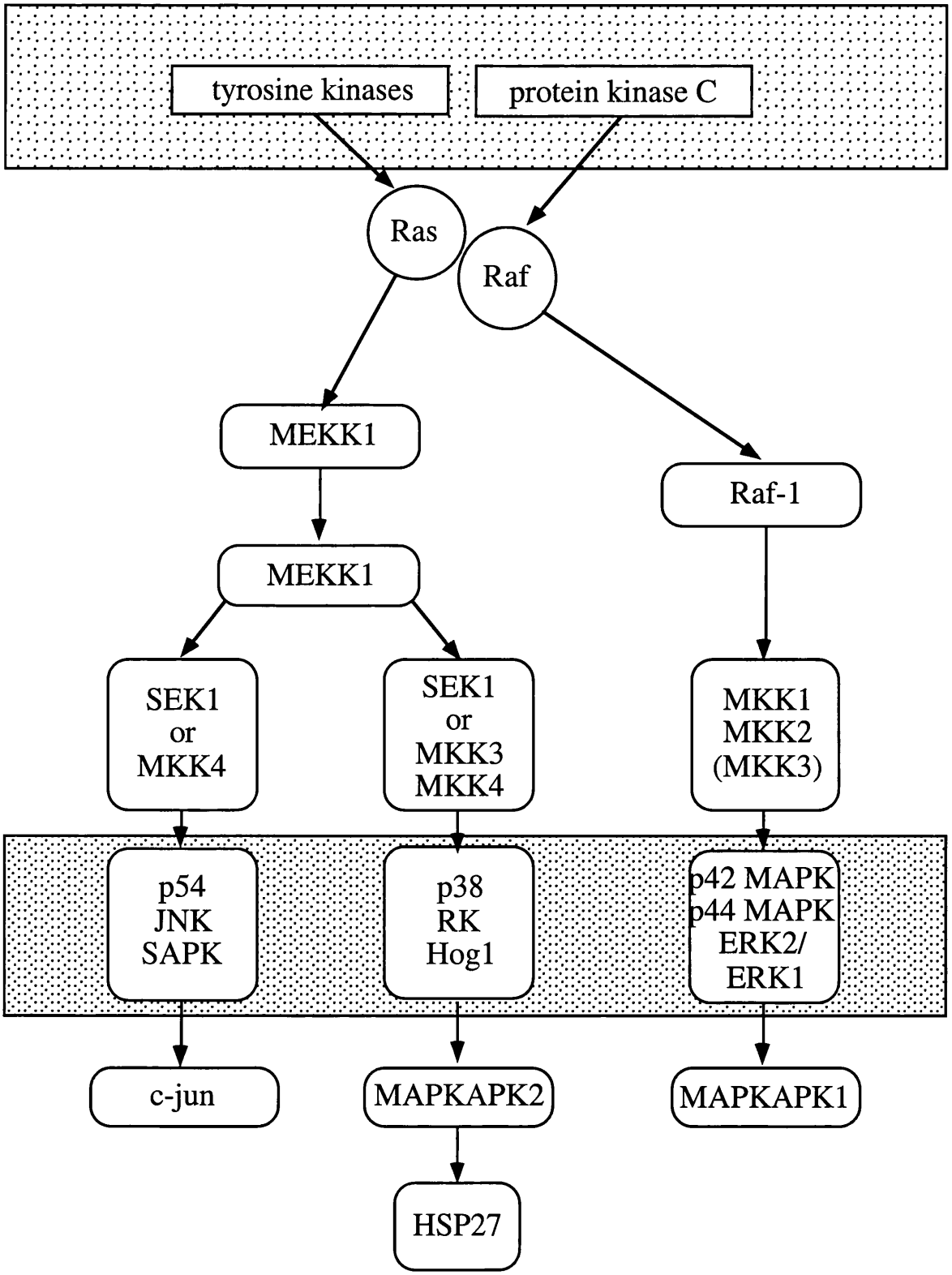

1.6. The effectors of preconditioning.

1.6.1. Effectors of preconditioning

Downstream of the signalling cascades are the end-effector mechanisms that mediate cell death and survival. Amongst the candidate proteins and channels, there appears to be some similarity between both early and delayed preconditioning. The interesting parallels between these phases of preconditioning suggest that these pathways are significant in myocyte survival, however, there is a significant difference between early and delayed preconditioning: protein synthesis. Whilst early preconditioning can be elicited in the presence of protein synthase inhibitors,[178] it is perhaps significant that delayed preconditioning can not.[179]

1.6.2. Effectors of early preconditioning

1.6.2.1. The K_{ATP} channel.

During early preconditioning, PKC is thought to translocate from the cytosol to the cellular membrane to activate the K_{ATP} channel; application of purified constitutively active PKC to the intracellular surface of patch clamped isolated rabbit myocytes produces an approximately threefold increase in the channel open probability.[180] Ischaemic preconditioning mediated via PKC is lost with the blockade of K_{ATP} by the sulphonylurea, glibenclamide.[181] Numerous studies have been performed, both with K_{ATP} channel openers[182], and K_{ATP} channel blockers (rats[42, 183], rabbits[184, 185], dogs[186], pigs[187, 188] and man[181]), to demonstrate either preconditioning-mimetic behaviour or preconditioning attenuation respectively.

Activated sarcolemmal K_{ATP} channels shorten the duration of the action potential[188]. Shortened action potential duration is potentially pro-arrhythmogenic, yet the opening of K_{ATP} is thought to be protective by accelerated ion flux through the channel, reducing calcium overload.

However, the assumption that myocardial protection is mediated by sarcolemmal K_{ATP} channels has been recently challenged by the observation that low dose bimakalim (a K_{ATP} channel opener) confers cardioprotection without attenuation of the action potential duration[189]. Thus the involvement of K_{ATP} channels in other cellular compartments has been suggested, and specifically in the mitochondria (see review [190]). Diazoxide has been demonstrated to be relatively selective for the mitochondrial K_{ATP} channel.[191] Even at doses required to induce the preconditioning-like myocardial protection, mitochondrial channel opening (as assayed through the oxidation of mitochondrial

flavoproteins) can be demonstrated in the absence of sarcolemmal potassium current (I_{KATP}). Furthermore, selectively blocking the sarcolemmal K_{ATP} with HMR-1883 fails to attenuate the infarct sparing effect of ischaemic preconditioning,[192] providing further evidence for the mitochondrial rather than the sarcolemmal K_{ATP} channel being essential for preconditioning.

1.6.2.2. Small heat shock proteins: αB crystallin and HSP27

Recently, Baines et al. have demonstrated that preconditioning can abrogated by depolymerisation of actin cytoskeleton, possibly interfering with the regulation of the mitochondrial K_{ATP} channel.[193] Therefore, it has been proposed that small heat shock proteins, such as αB crystallin and HSP27, may mediate early cytoprotection against lethal ischaemia/reperfusion injury.

1.6.2.2.1 αB Crystallin

αB crystallin is highly constitutively expressed, composing 1-2% of rat and pig soluble protein.[194] In unstimulated myocytes the majority of the protein is in the cytosolic pool. However, following transient ischaemia, αB crystallin has been demonstrated to rapidly translocate to the myocyte's intercalated discs and Z-lines.[194, 195] Interestingly, translocation is in itself inadequate to convey protection in isolated perfused rats hearts. Michael Shattock's group[196] demonstrated that whilst transient hypercapnia was efficient in promoting αB crystallin to the cytoskeleton, functional recovery was equivalent to controls. Ischaemic preconditioning however was demonstrated to phosphorylate αB crystallin via a pathway sensitive to inhibition by tyrosine kinase inhibitor, genistein, and the p38 MAPK inhibitor, SB203580. Thus modified, the αB translocation was associated with functional preservation from a 35-minute lethal ischaemic insult.[196]

1.6.2.2.2. HSP27

A similar pattern of activation and translocation has been observed following ischaemic preconditioning with αB crystallin's homologue, HSP27. HSP27, in its non-phosphorylated form, acts as an F-actin cap binding protein, inhibiting polymerisation of F-actin filaments. Phosphorylation of HSP27 promotes polymerisation, opposing actin filament disruption that occurs as a result of ischaemic injury.[197] This phosphorylation step is mediated by MAPKAPK2,[198] a kinase activated following transient ischaemia and p38 MAPK activation.[136] Ischaemic preconditioning has been associated with significant translocation of HSP27 from cytosolic to membranous/nucleic fractions in the H9c2 cell line[199] and significant phosphorylation (which can be mimicked by adenosine pre-administration)[129]. The cell work has

recently been replicated in isolated perfused rat heart, again demonstrating significant translocation of HSP27 occurring as a result of preconditioning,[135] although in this study, phosphorylation of HSP27 was not quantified. Phosphorylation appears to be an essential component of HSP27 activity. Mutation of the phosphorylation site of HSP27 abrogates the benefits observed from over expressing this protein; ischaemic protection is lost.[200, 201] Therefore, presumed phosphorylation is not adequate to assume HSP27 activity, although the p38 MAPK/ MAPKAPK2 is almost certain to have been activated by preconditioning. Armstrong et al., in a primary ventricular rabbit myocyte model,[202] failed to demonstrate a significant alteration of HSP27 cellular compartmentalisation, or a significant change in baseline HSP27 phosphorylation. This result appears to be contrary to the studies previously described. It must be noted that there was surprisingly high level of phosphorylation of HSP27 in seen in control samples compared to that reported by Nagarkatti et al.[129] Given the method of cellular extraction used by Armstrong et al., it is conceivable that the cells were pre-stressed (myocytes are extracted in calcium free buffer, to which calcium is added; the myocytes that survived and used in their study may well have been subjected to a calcium paradox stress) thus leading to pre-activation of HSP27. If this is the case, then the lack of preconditioning regulation of compartmentalisation or phosphorylation is to be expected.

Therefore, both small heat shock proteins (αB crystallin and HSP27) are subject to phosphorylation and activation by p38 MAPK mediated pathways in myocardial ischaemia. These proteins may, therefore, be an essential component of the early preconditioning response.

1.6.3. The mediators and effectors of delayed preconditioning

Infarct sparing triggered by delayed preconditioning is thought to have a number of important differences from that of early preconditioning, and this is inferred from the varying patterns of MAP kinase activation described in section 1.5.3. Amongst downstream targets of delayed preconditioning are protein synthesis induction and post-transcriptional protein modification. The identities of many of the protective proteins and associated mechanisms/pathways remain to be elucidated. There are, however, a number of candidates.

1.6.3.1. The putative mitochondrial K_{ATP} channel

As with early preconditioning, the mitochondrial K_{ATP} channel has been associated with cardioprotection against cell death. Evidence of the channel's involvement is derived from a number of models: following antecedent ischaemic stimuli in rabbit[203] and human derived cell lines;[145] pharmacological stimuli with opioids,[61] bacterial endotoxin derived monophosolipid A (MLA),[204] and A_1 receptor activation;[205] and preceeding heat stress in rabbit.[206, 207] In each case, protection against cellular necrosis could be

abrogated by the administration of K_{ATP} channel blockers prior to the lethal ischaemic injury.

Whilst the mechanisms of delayed phase mitochondrial K_{ATP} channel opening remain unclear, nitric oxide has been implicated in enhancing K_{ATP} channel open probability.[208] Therefore, it may be hypothesised that through nitric oxide generation from the inducible isoform of nitric oxide synthase,[209] K_{ATP} channel opening is mediated. However, the mechanism by which nitric oxide increases the open probability of the K_{ATP} channel are unknown.

1.6.3.2. Inducible proteins:

1.6.3.2.1. Manganese superoxide dismutase (MnSOD)

The role of endogenous anti-oxidants has been suggested as one potential mechanism of cellular adaption to ischaemic stress and the free radical induction associated with reperfusion. Interestingly, it has been shown that the mitochondrial free radical scavenger, MnSOD, has a biphasic pattern of temporal activity following a preconditioning stimulus, consistent with early and delayed preconditioning.[210]. This observation provides circumstantial evidence for MnSOD's involvement with cardioprotection. Further evidence has been provided by two recent studies in rat cultured myocytes and in-vivo, where the administration of an anti-sense oligonucleotide abrogated both MnSOD protein expression and the cardioprotection observed resulting from either ischaemic or pharmacological preconditioning.[96, 211]

MnSOD may therefore have an important role in protecting the heart in times of free radical generation and oxidant stress.

1.6.3.2.2. Chaperone heat shock proteins: HSP70 and HSP90

Heat shock proteins (HSP) are expressed in the cell following a number of stressful stimuli. These molecules are thought to function as molecular chaperones, affecting protein folding assembly and disassembly (review [212]).

1.6.3.2.2.1. HSP70

HSP70 may have direct influence upon cell death cascades. In a number of cell types, apoptotic stimuli are associated with the upregulation of HSP70: in rat 9L tumour cells, HSP70 expression reduced apoptosis triggered by cadmium, in a pathway involving both p42/p44 ERK and/or p38 MAPK;[192] and in astrocytes, hypoxic injury is associated with HSP70 induction by p38 MAPK activation.[213] Furthermore, HSP70 induction is associated with a concomitant inhibition of the putative pro-apoptotic MAP kinase, p46/p54 JNK, associated with TNF-α/ FasL administration in T-cells.[214] (HSP70 regulation of p46/p54 JNK and its implication in apoptosis is reviewed in [215].)

These observations are consistent with a recent study in renal cells whereby in osmotic shock, HSP70 induction was associated with p38MAPK activity, and where p38 MAPK activity was blocked with SB203580, the activity of p46/p54 JNK was potentiated.[216] In rat heart[217] and isolated myocytes,[218] over transfection has been shown to reduce apoptotic injury against hypoxic stress. Therefore, HSP70 may have cytoprotective roles in cardiac myocytes beyond the pure role as molecular chaperone.
In delayed preconditioning, HSP70 expression has been shown to be elevated 24 hours after the preconditioning stimulus, consistent with the time course of delayed protection.[219] Furthermore, gene transfected cells[220] and transgenic mice with constitutively over expressed rat HSP70[221] are imbued with cellular protection against ischaemia/reperfusion injury. However, in a recent time course study, Cornelussen et al. demonstrated that HSP70 expression is significantly elevated prior to the onset of delayed protection.[222] Therefore, it would appear that cytoprotection from ischaemia/reperfusion injury requires more than expression of HSP70; other signalling processes may be required.

1.6.3.2.2.2. HSP90

HSP90 is the most abundant molecular chaperone in eukaryotic cells, of which there are two isoforms: the constitutively expressed HSP90α and the inducible HSP90β. The induction pattern of HSP90β following a preconditioning stimulus is consistent with the delayed phase of myocardial protection. HSP90 appears to be essential to MAP kinase signalling. HSP90 binds to the MKKK, Raf-1, facilitating the formation of multiprotein complexes essential in the MAP kinase signalling cascade; inhibition of HSP90/Raf-1 association with the specific HSP90 inhibitor, the antibiotic geldanamycin, attenuates p42/p44 ERK activation.[223, 224] Other chaperone roles of HSP90 include the interaction with and up-regulation of the constitutive nitric oxide proteins, and thus the expression of nitric oxide second messenger.[225] Up-regulation of HSP90 may also have impact upon the cell death cascade, with recent evidence suggesting that HSP90 is capable of binding to Apaf-1, disabling the ability of cytochrome-c release to bind and form an active complex with Apaf-1 and caspase-9.[226] Whilst HSP90 induction has been demonstrated following heat and metabolic stress in cultured rat myocytes,[227] the potentially protective roles of HSP90 have yet to be fully elucidated in the heart.

1.6.3.2.2.3. HSP27

αB-crystallin family of heat shock proteins unique for being under both transcriptional and post translational control, and are described in greater detail in section 1.6.2.2.1. Unphosphorylated, it is associated with actin to prevent polymerisation or as aggregates.[201] Phosphorylation of HSP27 dissociates the aggregates and facilitates actin polymerisation and stress fibre formation.[197] HSP27 is phosphorylated by

MAPKAPK2, part of the p38 MAPK signalling cascade which is initiated as a result of preconditioning[124]. Thus activated, HSP27 binds to cytoskeletal actin, possibly imbuing the increased osmotic strength observed in preconditioned isolated rabbit myocytes, cells with concomitantly increased p38 MAPK activation[125].In delayed phase preconditioning, Dana et al.[143] have demonstrated that adenosine A_1 receptor activation and delayed phase protection is linked to p38 MAPK and HSP27 tri-phosphorylation on 2D gel electrophoresis.[143] As previously described, this post-translational modification of the HSP27 can convey protection to the cytoskeleton, and conceivably maintain function of the putative mitochondrial channel.[193]

1.7. The Role of nitric oxide and the nitric oxide synthases in preconditioning.

Nitric oxide (NO) is associated with many aspects of cellular biology, involved in neuronal signalling, maintenance of vasodilatory tone in numerous vascular beds, cell growth, regulation of platelet aggregation and leukocyte binding to endothelium[228, 229]. NO has also been linked to both myocyte survival[209, 230] and death[231, 232] following ischaemia/reperfusion injury. Therefore, with conflicting reports in the literature regarding NO in ischaemia reperfusion injury, and yet showing great potential as a mediator of myocyte preservation in the face of cellular stress, NO has become the subject of significant cardiovascular research.

1.7.1. Biology of nitric oxide synthases

NO is synthesised by one of the major three isoforms of NO synthase in the myocardium: NOS-I or neuronal NOS (nNOS), NOS-II or inducible NOS (iNOS) and NOS-III or endothelial NOS (eNOS). All three, in their active form, exist as homodimers, with the approximate subunit molecular weights of 130, 135 and 160 kD for iNOS, eNOS and nNOS respectively. Each isoform catalyses the conversion of L-arginine to L-citrulline and NO, a process requiring O_2 and NADPH derived electrons. NOS requires several cofactors and prosthetic groups for activity: thiolate-bound heme, FAD and FMN, calmodulin and Ca^{2+} (for the constitutive eNOS and nNOS isoforms only) and tetrahydrobiopterin (BH_4).[233]

NOS is a modular enzyme in which the heterodimer consists of a number of discrete domains. From the C-terminus, these consist of: a reductase domain sharing extensive homology with the cytochrome p-450 reductase; a calmodulin binding domain; an oxygenase domain; and a N-terminal, isoform-specific sequence.

The most significant catalytic distinction between NOS isoforms is the affinity for calmodulin binding at the calmodulin binding domain. Calmodulin is thought to convey a conformational change that is necessary for internal electron transfer; it is absolutely required for electron transfer from the reductase to the oxidase domain (i.e. from FMN to the heme complex- see figure 1.8 [234]), and furthermore, calmodulin is found to increase and stimulate electron transfer within the reductase domain (i.e. FAD to

FIGURE 1.8. THE ACTIVE NITRIC OXIDE SYNTHASE HOMODIMER.

Nitric oxide catalyses the conversion of L-arginine to L-citrulline and nitric oxide, a process that requires the donation of two electrons from NADPH and the reduction of molecular oxygen. Calmodulin binding is essential for nitric oxide synthase activity; in the constitutive isoforms (eNOS and iNOS) the binding of calmodulin is facilitated by the presence of Ca^{2+}. The binding of calmodulin to the inducible isoform of nitric oxide synthase is so strong that Ca^{2+} is no longer essential.

Abbreviations used in figure:

Arg:	L-arginine
BH_4:	tetrahydrobiopterin
e^-:	electron
CaM:	calcium calmodulin
Fe:	iron centre of heme complex

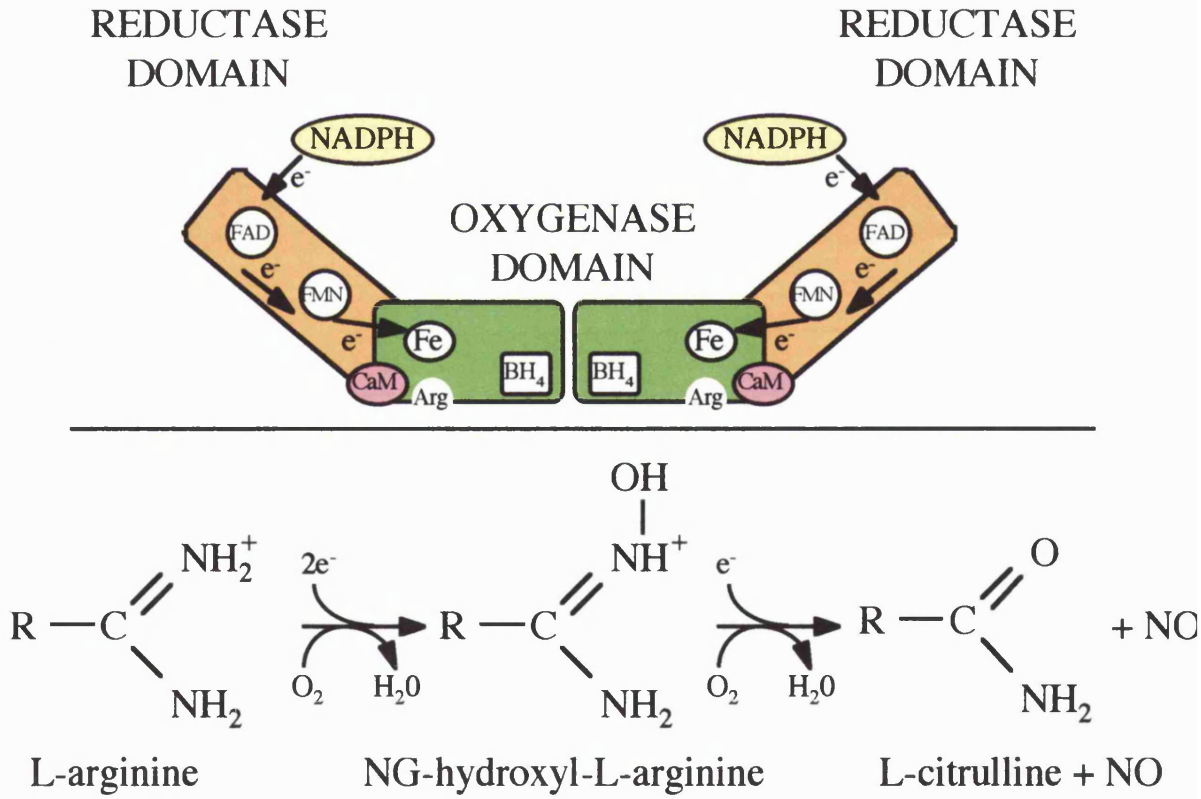

FMN[235]). The constitutively expressed isoforms, eNOS and nNOS, require Ca^{2+} for calmodulin binding and therefore for enzymatic activity. The iNOS calmodulin binding domain has such a high affinity for calmodulin, and the binding so great, that Ca^{2+} is not required for iNOS catalytic activity. Therefore, regulation of iNOS activity appears primarily dependent upon transcriptional and translational modulation.[236]

The heme pocket in the oxygenase domain is the site where L-arginine and O_2 are bound and catalysed to generate NO. The co-factor, BH_4 also binds to the oxygenase domain, probably in the immediate vicinity of the heme pocket, stimulating dimerisation of the NOS homodimer,[237] inducing a low-to-high spin shift in the heme complex,[237] and enhancing the binding affinity of the catalytic region of NOS for L-arginine.[238] Thus BH_4 acts as an essential co-factor for NOS activity.

The N-terminal sequence is isoform specific, and determines sub cellular localisation. nNOS has a 300 amino acid N-terminus region that determines its location in the cell by interaction of its PDZ/GLGF-domain to membrane associated proteins such as the dystrophin-associated protein syntrophin.[239] eNOS has a smaller N-terminus sequence, consisting of three fatty acetylation sites required for binding to membrane caveoli and anchoring into the membrane itself.[240] Further modifications, including myristoylation and palmitoylation,[241] occur to promote membrane binding of this constitutive enzyme. The inducible NOS, iNOS, does not have the N-terminus extensions found on the constitutive isoforms of NOS, and thus is soluble and free in the cytosol.

The neuronal form of NOS exists in a number of different isoforms because of alternative splicing of the nNOS mRNA. The principle isoform in the brain is nNOSα, accounting for 95% of activity, the remainder consisting of minor isoforms, nNOSβ and nNOSγ. One further isoform of nNOSμ, has recently been isolated in skeletal muscle. This isoform is slightly larger than the brain nNOSα isoform because the alternate slicing inserts an additional 34 amino acids in-between the protein sequence of the calmodulin and FMN-binding domains.[242] The relative importance of these splice variants in ischaemia/reperfusion injury in the heart have not been explored, although one report suggests that infarct size resulting from injurious ischaemia/reperfusion in a nNOS knockout was no greater than that seen in the control wild type animals.[243]

1.7.2. Regulation of nitric oxide synthases

In addition to the regulation of NOS via the modulation of co-factors and prosthetic groups described above in section 1.7.1, and post-transcriptional modifications described below in section 1.7.3.2 and elaborated upon in section 1.7.4, there are at least two further mechanisms of nitric oxide synthase activity regulation: modulation of mRNA stability and endogenous inhibition by asymmetric dimethylarginine (ADMA).

1.7.2.1. Regulation of cellular eNOS activity through mRNA stability

Recently, a novel mechanism for the modulation of eNOS has been identified in a number of cell types, through the regulation of messenger mRNA stability. Protein tyrosine kinases have been demonstrated to increase eNOS gene transcription,[244, 245] a signalling cascade also implicated in the upregulation of iNOS following lipopolysaccharide administration.[246] In a number of recent papers, the mRNA half-life was found to be augmented by the activation of tyrosine kinase and PKC dependent pathways by the prior administration of endothelin (mediated through ETA receptors) and exogenous vascular endothelial growth factor (VEGF). Both systems are activated following *transient* hypoxia,[247, 248] and thus may play a role in ischaemia/reperfusion injury. Of equal interest are stimuli that reduce eNOS mRNA stability, which include *prolonged* hypoxia[249] and pro-inflammatory cytokines.[250] The balance between factors that promote versus factors that denigrate mRNA stability therefore may warrant further investigation.

1.7.2.2. Endogenous inhibition of NOS activity

A number of chemical agents have been used in study the role of nitric oxide by inhibiting NO synthesis, and these include L-arginine derivatives that are methylated at their terminal guanidino nitrogen group. One such example is N^{ω}-monomethyl-L-arginine (L-NMMA). However, L-NMMA and other methylated L-arginine analogues are also endogenously synthesised. Amongst these, asymmetric dimethylarginine (ADMA) and symmetric dimethylarginine (SDMA) are the most common.[251] Like L-NMMA, ADMA is a NOS inhibitor, whilst SDMA is inert with regard to NOS activity. ADMA is synthesised by N-methyl transferases that methylate L-arginine residues within specific proteins; free ADMA is released during the proteolytic cleavage of these methylated proteins. In the cell, the concentration of free ADMA is regulated by their metabolism by the enzyme, dimethylarginine dimethyl aminohydrolase (DDAH); inhibition of DDAH activity can increase intracellular ADMA concentrations, and inhibit NOS activity.[252] In a number of pathological states, ADMA can be demonstrated to be found at increased concentration in cells, including cardiovascular diseases atherosclerosis, hypercholesterolaemia, hypertension and heart failure.[251] Possible involvement of ADMA in ischaemia/reperfusion injury has not yet been investigated although cytokines such as TNF-α, increase the cellular content of ADMA[253] raises the intriguing possibility of ischaemia/reperfusion mediated regulation of DDAH.

1.7.3. Localisation of the NOS isoforms

1.7.3.1. Gross localisation

Recent immunohistochemical studies have sought to determine the sub-localisation of the three isoforms of NOS in the myocardium. Consistent with Western blot results of resting myocardium,[230] Brahmajothi and Campbell were able to demonstrate low level iNOS antibody binding throughout the myocardial wall.[254] Patterns of both nNOS and iNOS were not homogenous in their distribution; both isoforms were found to be comparatively more highly expressed in endocardial regions. However, both nNOS and iNOS were weakly expressed compared to eNOS expression. In direct contrast to the other isoforms of NOS, the distribution of eNOS in the left ventricle was significantly greater in the epicardial than endocardial ventricle;[254] a distribution matched by the expression of extracellular membrane bound superoxide dismutase (ECSOD). These observations were confirmed in both ferret and human myocardium. Although not discussed by the authors, it is interesting to note an inverse correlation between eNOS and ECSOD distribution in ventricular myocardium to the radial pattern of extension of infarction found in evolving subendocardial (non-Q wave) myocardial infarction: infarction extends from the endocardium towards the epicardium.[255-257] It is, therefore tempting to speculate a role for eNOS and ECSOD in resistance to ischaemia/reperfusion injury.

1.7.3.2. Sub-cellular localisation

As discussed in section 1.7.1, the N-terminus domain determines to a significant extent the sub-cellular localisation of the three NOS isoforms. iNOS, with its truncated N-terminus domain is a water soluble, and therefore found, when expressed in the cytosolic fraction of the cell. In contrast, the eNOS isoform is found in the caveoli of the cellular membranes thanks to the acetylation sites on the N-terminus domain, and other membrane binding promoting post translational modifications through myristoylation and palmitoylation (discussed further in section 1.7.1). The nNOS isoform however possesses a 300 amino acid N-terminus domain that enables the protein to be targeted and fixed into cellular membranes. Possibly through this mechanism, as in skeletal muscle with a PDZ protein targeting domain, nNOS in myocytes can be found localised in the membranes of the sarcoplasmic reticulum (SR).[258] As in skeletal muscle, the isoform found located in the cardiac SR is nNOSμ. In nNOS knockout mice, or by the use of anti-nNOSμ antibody, determined that calcium uptake by the SR is modified by the activity of nNOSμ, as NO generated inhibited the calcium SR uptake transporter, Ca^{2+}-ATPase,[258] potentially influencing myocyte contractility.

Although the full significance of the localisation of NOS in the normal physiology and in pathophysiology of the heart remain to be fully elucidated, macro and microscopic localisation may provide new insights into disease states such as ischaemia/reperfusion injury.

1.7.4. The involvement of NO synthesis in early preconditioning

Triggers of preconditioning are also associated with mechanisms that upregulate the activity of the constitutively expressed NOS isoform, eNOS. In the unstimulated cell, eNOS is largely inactive, bound to sarcolemmal components such as caveoli promoted by post-transcriptional modifications to eNOS including myristoylation and palmitoylation.[241] Additionally, a number of receptors have been identified that possess a binding domain for eNOS,[259] which include bradykinin B2, the angiotensin II, AT1 and endothelin-1 ETB receptors. Whilst the eNOS regulatory roles of AT1 and ETB have yet to be established, the receptor binding site on the B2 receptor inhibits eNOS catalytic activity.[259] These receptors have been demonstrated to be involved in ischaemic preconditioning (see section 1.4.2; B2[41]; AT1[43]; and ETB[247]). Therefore, following an ischaemic preconditioning stimulus, receptor activation leads to transient phosphorylation of the binding site by receptor activation and thus to the disassociation of eNOS into the cytosol. Furthermore, eNOS dissociates from sarcolemmal caveoli with the activation of bradykinin B2 receptors,[260] providing a further mechanism of receptor mediated activation of eNOS. Thus eNOS released into the cytosol becomes susceptible to activation by calcium/calmodulin.

Interaction of eNOS with inhibitory binding sites is not the sole method of regulation of eNOS activity; further post-transcriptional modifications occur to regulate the enzyme. Two separate pathways exist to increase the catalytic activity of eNOS by phosphorylation ('unstimulated' eNOS is typically about 8 times slower than either the nNOS or iNOS isoforms[236]). The PI3 kinase and cAMP linked protein kinase pathways, both activated by G-protein linked receptors (described in section 1.5.1.1) can lead to significant upregulation of eNOS activity. Recent work has shown that eNOS may be phosphorylated at serine 1177, which significantly increases eNOS catalytic activity in a calcium independent fashion. The serine phosphorylation is catalysed by both protein kinase B (PKB or Akt, a downstream target of PI3 kinase)[85, 86, 229, 261, 262] and by AMP linked protein kinase.[79, 80] Both of these signalling pathways will be active following ischaemic preconditioning; it is therefore attractive to speculate that NO may be involved in the preconditioning signalling cascade.

Therefore, in preconditioning the heart, eNOS activity may be increased, raising the possibility of this enzyme's involvement in early preconditioning. At present however, the role of eNOS in early preconditioning remains unclear. With pharmacological

inhibitors of NOS activity, investigators have demonstrated that early preconditioning is either not abrogated[263-265] or partially attenuated.[266, 267] However, in no previous study has NO release been measured and therefore, no direct evidence that NO synthesis was completely inhibited. Furthermore, the pharmacological inhibitors used in these studies may have non-specific properties that promote protection. For example, N^{ω}-nitro-L-arginine methyl ester (L-NAME) used in each of these investigations has been purported to possess anti-muscarinic properties[268]). It therefore remains equivocal as to whether NO has a part to play in the triggering and mediation of early preconditioning.

1.7.5. The role of NO in delayed preconditioning

Whilst delayed preconditioning has been shown to be efficacious in reducing infarct size resulting from lethal ischaemic insults, the mechanisms triggering and mediating this cardioprotection remain unclear. Recent work by Bolli and colleagues has implicated the synthesis of nitric oxide (NO) as being both an important trigger[72, 269, 270] and mediator of delayed ischaemic preconditioning.[230, 271] In support of this hypothesis, pharmacological inhibition of NO synthesis prior and during the index ischaemia abrogates the protection of delayed preconditioning.[209, 271] Furthermore, recent work in transgenic mice with targeted disruption of the iNOS gene have demonstrated similar results.[230, 272]

As a trigger of delayed preconditioning, the mechanisms necessary for increased NO synthesis have not been fully elucidated, but may occur in a similar paradigm to that proposed above (section 1.7.4) for early preconditioning. However, increased NO bioavailability has been demonstrated to cause isoform specific translocation and activation of PKC in a fashion similar to that observed following ischaemic preconditioning, and furthermore to result in equivalent delayed protection.[273]

The mechanisms leading to increased NO synthesis that mediates delayed protection are better understood, and thought to involve the induction of iNOS. Whilst the iNOS protein is detectable at low levels in naive myocardium[230, 274] this observation is of unknown biological significance, and is not thought to play a role in triggering preconditioning[230]. However, iNOS is markedly induced following ischaemic stress by signalling cascades resulting in the activation of transcription factors such as NF-κB[163, 169]. Given that the triggers of delayed preconditioning result in significant transcriptional upregulation of iNOS (and thus to concomitant increased NO synthesis[236]), and that NO generation appears essential for the mediation of protection in this phase of protection, has lead to the hypothesis that iNOS is pivotal to the mediation of delayed preconditioning. However, recent work by Vallance and colleagues, in a cytokine model of shock and vascular response in man[275], has demonstrated that eNOS activity can be markedly up-regulated by increased BH_4

availability. The investigators found no evidence of iNOS induction, yet there was clear evidence of NO generation, therefore they hypothesise that eNOS is capable of "masquerading" as iNOS. The potential importance of this observation in context of preconditioning has not as yet been determined, but is explored in more detail in this thesis.

Preconditioning may be triggered both by ischaemia, and by pharmacological targeting of specific receptors involved in the transduction of the preconditioning signal. It is not known whether the mechanisms for delayed *pharmacological* preconditioning differs from the protection observed following delayed *ischaemic* preconditioning. Ischaemic preconditioning involves the release of multiple signalling moieties whilst pharmacological triggers can specifically select a single signalling pathway. Pharmacological manipulation of the triggers of preconditioning may be of benefit to the study of the signalling pathways, and to elucidate the roles of the various isoforms of NOS.

1.7.6. The role of NO in ischaemia reperfusion injury salvage

It has been recently demonstrated that insulin is capable of imbuing significant protection against myocardial infarction when administered at reperfusion following a lethal ischaemic insult.[23] Insulin signals via a tyrosine kinase linked receptor, and has been demonstrated to signal via PI3 kinase.[276] Indeed, the administration of the selective PI3 kinase inhibitor, wortmannin, abrogates the protective properties of insulin administered at reperfusion.[23] Similarly, by administering insulin related growth factor-1 (IGF-1) before reperfusion,[51] this growth factor is effective in reducing cell death resulting from lethal ischaemia reperfusion injury. Furthermore, the protection is also dependent upon the activation of PKB/Akt[51]. The role of eNOS in this form of cardioprotection has not been elucidated, but given that PKB is associated with the phosphorylation and regulation of eNOS activity[85, 86, 229, 261, 262] there is biological plausibility for its involvement. Indeed, it has been recently be demonstrated that insulin does increase NO production via this pathway.[277, 278]. It is therefore attractive to speculate that eNOS and NO may play a role in the evolution of cardioprotection in this paradigm of reperfusion salvage.

1.7.7. Mechanisms of NO mediated protection

The end effectors of NO mediated cardioprotection remain unclear, although a number of potential mechanisms have been identified.

1.7.7.1. NO inhibition of death cascades

NO may interact and regulate numerous targets of the apoptotic death cascade described above (section 1.1, summarised in figure 1.1 and reference [26]). One of the initiating

events in the apoptotic cascade is the release of cytochrome-c through the mitochondrial permeability transition pore (PTP),[279] opened under conditions of prolonged ischaemia and mitochondrial calcium overload. Exogenously administered NO has been shown to inhibit both calcium accumulation by mitochondria and impede the opening of the PTP.[280] In this process, NO can be demonstrated to inhibit the release of cytochrome-c in a dose dependent manner.[280] In the intact cell, Bcl, antagonised by Bax, inhibits the release of cytochrome-c from mitochondria,[30] and therefore preventing the cleavage and activation of pro-caspase-9. NO generation appears to have a favourable effect upon Bcl stability, by preventing the de-phosphorylation of p42/p44 ERK,[281] which is beneficial for cellular survival in the face of an ischaemic insult.

Downstream of cytochrome-c release and caspase 9 regulation, NO has been demonstrated to nitrosylate and inhibit a number of downstream caspases, including, significantly, caspase 3.[282] The antiapoptotic influence upon cell death in ischaemia-reperfused myocytes has yet to be explored, but given multiple sites of action, it is possible that NO may have a significant cardioprotective effect, reducing cell death possibly by attenuating apoptosis.

1.7.7.2. NO and the mitochondrial K_{ATP} channel

Opening of mitochondrial K_{ATP} channels prior to index ischaemia will elicit significant cardioprotection following preconditioning.[283, 284] The mechanisms by which K_{ATP} mediates this protection remain unclear however, although it has been suggested that opening of the mitochondrial K_{ATP} leads attenuation of mitochondrial calcium overload, thus preventing the opening of PTP.[285] The potential role of the mitochondrial K_{ATP} is discussed further in sections 1.6.2.1 and 1.6.3.1. The mitochondrial K_{ATP} channel may be a potential target for NO. NO has been demonstrated to increase the open probability of both sarcolemmal K_{ATP},[208] and more recently, mitochondrial K_{ATP} channels.[286] Therefore, cardioprotection resulting from either endogenous or exogenous NO would be expected to be mediated by opening of K_{ATP} channels, and the protection abrogated by mitochondrial selective K_{ATP} channel inhibitors, such as 5 hydroxy decanoate. This hypothesis appears to be supported by recent work by Csont et al with glyceryl trinitrate (GTN), the cardioprotection from which was inhibited by the non-selective K_{ATP} channel inhibitor, glibenclamide.[287]

1.7.8. NO in ischaemia/reperfusion: summary

The role of nitric oxide in ischaemia/reperfusion therefore remains controversial. Potential roles of nitric oxide in early preconditioning and in reperfusion injury salvage have not been fully explored. Furthermore, the role of nitric oxide in delayed pharmacological preconditioning needs further investigation. Based on these tenants, and the lack of a full understanding of the role of nitric oxide in ischaemia/reperfusion

injury, the studies in this thesis were designed to investigate the role of nitric oxide in mediating ischaemia/reperfusion injury, early and delayed preconditioning and ischaemia/reperfusion injury salvage pathways.

Chapter 2. Hypotheses and Aims.

As discussed in chapter 1, nitric oxide has been shown to posses both beneficial and detrimental effects in respect to cardiac myocyte survival. Preconditioning, associated with modest nitric oxide synthesis has been shown to reduce infarct size,[230] whereas the significant induction of nitric oxide synthesis in conditions such as myocarditis[288] and allograft failure[289] is deleterious to myocyte survival. Whilst nitric oxide is reasonably well characterised with respect to delayed *ischaemic* preconditioning, its role in (*i*) early ischaemic preconditioning, (*ii*) delayed *pharmacological* preconditioning (*iii*) reperfusion injury salvage and (*iv*) the cardioprotective dose/response relationship of exogenous nitric oxide has not been completely characterised. Therefore the aim of the investigations contained in this thesis is to characterise the role of nitric oxide and the isoforms of its synthase in all forms of cardioprotection.

2.1 Hypotheses.

The following hypotheses are investigated in this report:

2.1.1. Early ischaemic preconditioning is dependent on the synthesis of nitric oxide derived from eNOS.

Pharmacological investigations to date have failed to reveal a role for nitric oxide in early ischaemic preconditioning. However, as discussed in section 1.7.4, these results are surprising given that the triggers associated with ischaemic preconditioning are highly likely to lead to the increased activity of the endothelial isoform of nitric oxide synthase (eNOS). That eNOS is upregulated is circumstantially supported from work from Roberto Bolli's laboratory demonstrating that the trigger for delayed preconditioning appears to be reliant upon the synthesis of nitric oxide from a constitutive isoform of nitric oxide synthase.[72] Therefore to remove potential confounding non-specific pharmacological effects of nitric oxide synthase inhibitors, the aim was to examine the role of nitric oxide in early ischaemic preconditioning using eNOS knockout mice (chapter 5).

2.1.2. Delayed *pharmacological* preconditioning requires the synthesis of nitric oxide derived from iNOS.

Considerable evidence exists regarding the role of the inducible nitric oxide synthase (iNOS) in delayed *ischaemic* preconditioning (section 1.7.5.), however, comparatively little is known with regard to the role of nitric oxide and delayed *pharmacological* preconditioning. At the inception of this study, it was unclear as to whether pharmacological triggers, such as adenosine A_1 receptor agonists mediate delayed

protection by mechanisms that may be completely independent of nitric oxide synthesis. Therefore, the aim was to characterise the role of nitric oxide in delayed pharmacological preconditioning, and to test the hypothesis that this form of protection is dependent upon the synthase activity of iNOS (chapter 6).

2.1.3. Exogenous nitric oxide mediates cardioprotection in naive hearts in a dose responsive fashion.

Evidence accrued from examining the role of nitric oxide in delayed preconditioning clearly implicates nitric oxide as a mediator of infarct resistance against lethal ischaemia/reperfusion injury. However, with data also implicating nitric oxide in triggering cell death, the aim of this study was to characterise, through the construction of a dose/response curve, the role of nitric oxide and cardioprotection. Thus the aim was to examine the hypothesis that nitric oxide could reduce infarct size in a dose dependent fashion up to an optimal nitric oxide concentration beyond which deleterious effects of nitric oxide would be observed (chapter 5).

2.1.4. Reperfusion salvage is dependent upon the synthesis of nitric oxide from eNOS.

Comparatively little is known with respect to the protective mechanisms of ischaemia/reperfusion injury salvage pathways (discussed in sections 1.3 and 1.7.6). However, as the signalling pathways associated with this form of protection are also associated with the up regulation of eNOS synthase activity (section 1.7.6), it is attractive to speculate that nitric oxide synthesis may be associated with this form of cardioprotection. Thus the aim of this study was to a determine whether there is a role for nitric oxide in ischaemia/reperfusion injury salvage, and whether this protection is dependent upon the synthase activity of eNOS (chapter 7).

2.1.5. Nitric oxide mediated cardioprotection occurs via a direct action upon mitochondria, possibly via the mitochondrial K_{ATP} channel.

Mitochondria are sensitive to ischaemic injury, showing morphological changes during ischaemia, and evidence of calcium overload at reperfusion (section 1.1). The mitochondrial K_{ATP} has been implicated as a potential mediator of both early and delayed preconditioning (sections 1.6.2.1 and 1.6.3.1). Nitric oxide has been demonstrated to interact with mitochondria, and also with the K_{ATP} channel (section 1.7.7.2). Therefore to establish whether there is a direct link between mitochondria and the cardioprotective effects of nitric oxide, the aim was to characterise preconditioning induced subcellular localisation of the nitric oxide synthases, whether nitric oxide has a direct effect upon isolated mitochondria and the K_{ATP} channel, and whether mitochondrial K_{ATP} channel

blockers could attenuate the protection associated with exogenous nitric oxide administration (chapter 8).

Chapter 3. Methods.

3.1 General

All experiments contained within this report, unless stated otherwise, were performed in the Laboratory of the Hatter Institute, University College London Medical School, University College London Hospitals, and performed in accordance with the Home Office *Guidance on the Operation of the Animals (Scientific Procedures) Act* 1986.

3.2 Choice of animal model

With the advent of molecular biological methodologies that are capable of identifying and cloning specific genes, techniques have been developed to enable the selective targeting of specific genes to create transgenic cell lines. The adoption of these techniques to modify the genome of stem cells has thus led to the creation of whole transgenic animals. The most common animal chosen for the development of specific gene mutants is the mouse by virtue of cost and ease of breeding. Once the initial transgenic genotype has been created, rapid breeding enables the swift establishment of a heterozygote colony, whilst the comparatively modest maintenance associated with mouse husbandry helps keep the unit cost low. The ability to manipulate genes such that they are either suppressed or over-expressed is a potentially powerful tool in the investigation of disease states and specific signalling pathways. Unsurprisingly, interest in the mouse model for cardiovascular study has exponentially increased in recent years.

Myocardial preconditioning recruits a number of signalling pathways. By deleting or over-expressing specific components of these cascades, considerable insight can be made in regard to the relative importance of a specific gene product. This approach has particular advantages over pharmacological techniques, most notably regarding specificity of action and the elimination of pharmacokinetic and pharmacodynamic considerations. Hence, with the availability of a variety of transgenic mice, the adaptive mechanisms associated with ischaemia/reperfusion injury can be investigated in new ways. However, as with any model, some caution must be exercised in interpreting the data from transgenic models. With the genotype altered from the wild type animal, it is hypothetically possible that other genes may either be silenced or upregulated in compensation. It is with this caveat that the studies contained within this thesis are presented.

3.3 Mouse strains

The nitric oxide synthase knockout mice used in these experiments were generated as described by Laubach et al[290] and Huang et al[291] for the inducible nitric oxide synthase (iNOS) knockout (KO) and endothelial nitric oxide synthase (eNOS) KO respectively. Both are created in similar fashion. In brief, the NOS gene is mapped and cloned prior to disrupting the gene in 129-derived ES cells with a targeting vector carrying the neomycin resistance gene. The recombinant cells are cultured and passaged in neomycin containing culture, and subsequently injected into C57BL/6J (B6) blastocysts. These are then implanted into pseudo-pregnant females for development. The chimeric males from the litter of these mice were then mated with B6 females, resulting in B6,129 F1 heterozygote mutant (+/-) mice which were inbred to generate F2 homozygote mutant (-/-) mice for the NOS disruption. Their progeny are genotyped by Southern blot analysis to confirm the knockout status.

iNOS and eNOS mice are indistinguishable from wild type mice in appearance, growth rate or reproduction. Adult eNOS KO mice are found to become spontaneously hypertensive,[291] and have a higher incidence of bicuspid aortic valve abnormalities.[292] The evolution of cardiac hypertrophy secondary to hypertension does not inhibit preconditioning,[293] therefore the eNOS KO animals remain suitable for study in the context of ischaemia/reperfusion injury resistance, although the eNOS knockout mice in the studies described in this thesis were selected before the onset of any evidence of left ventricular hypertrophy (see chapter 4, section 4.5).

3.4 Chemicals and drugs

Constituents for the Krebs Henseleit buffer were purchased from BDH Laboratory supplies (Merck Eurolab, Dorest, England). 2-chloro N^6 cyclopentyl adenosine (CCPA), carbonyl cyanide m-chlorophenylhydrazone (CCCP), N^{ω} nitro L-arginine methyl ester (L-NAME) and triphenyltetrazolium chloride (TTC) were purchased from Sigma Chemicals Co.(Dorest, England). Chelerythrine chloride and 5 hydroxy decanoate (5-HD) were purchased from RBI (Research Biochemicals International, Dorset, England). Tetramethylrhodamine methyl ester (TMRM) was bought from Molecular Probes Inc. (Leiden, The Netherlands). Pentobarbitone was purchased from Rhone Merieux Ltd (Harlow, England).

3.5 Preparation of hearts for perfusion

3.5.1 Anaesthesia

All animals underwent terminal anaesthesia, induced with an intra-peritoneal (*ip*) injection of pentobarbitone, 60 mg/kg, prior to euthanasia. Heparin, 100 IU, was administered concomitantly to prophylactically prevent thrombus formation in the coronary vasculature or ventricular chambers. Consciousness was usually lost within 120 seconds, and the animal weighed. The animal was then transferred to an operating board, and the forelimbs and one hind limb secured with small strips of masking tape. The depth of anaesthesia was confirmed by the loss of hind limb withdrawal reflex to pain prior to securing the remaining limb with masking tape.

3.5.2 Dissection

Upon the confirmation of adequate depth of anaesthesia, the animal underwent parasternotomy. The anterior chest wall was reflected and removed to optimise the field of view. The heart and lungs were removed, en-bloc, by transecting the descending aorta, inferior vena cava, plus the superior vena cava, common carotids and upper limb vessels. A timer was started with the cessation of corporeal circulation. The heart was then transferred to a dissection dish filled with ice-cold buffer for further dissection of lung and mediastinal tissues. The aorta was then identified and cannulated with a 20 gauge murine cannula (technical design schematic, figure 3.1.A) which was primed with cold buffer to reduce the risk of air embolisation. Great care is taken upon cannulation of the aorta to avoid damage to either the aortic valve or the coronary ostia (apparatus figure 3.1.C). The aorta was fixed to the cannula with a 4/0 silk tie, and transferred to the Langendorff perfusion apparatus. Upon the onset of crystalloid perfusion, the timer was stopped and the time to perfusion recorded. After considerable practice, the time to the onset of Langendorff perfusion never exceeded three minutes, essential to reduce the potential risk of ischaemic preconditioning due to perfusion delay.[294, 295]

FIGURE 3.1. TECHNICAL DESIGN SCHEMATIC FOR THE MURINE PERFUSION CANNULA.

The component parts of the perfusion cannula and their application in mouse heart Langendorff perfusion is detailed below. In **A**, the technical drawing of the cannula pictured in **B**. In **C**, the ice-cooled cannulation apparatus with lower half of cannula in situ.

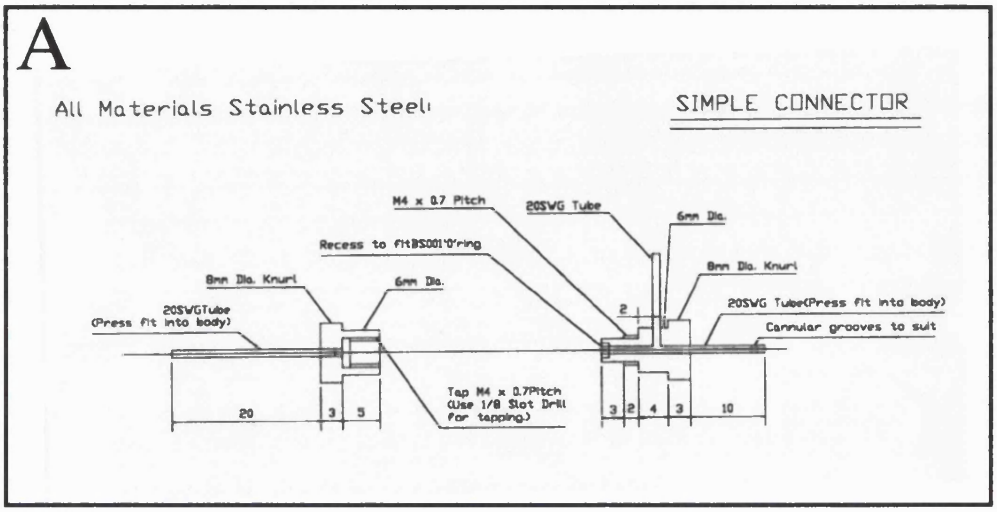

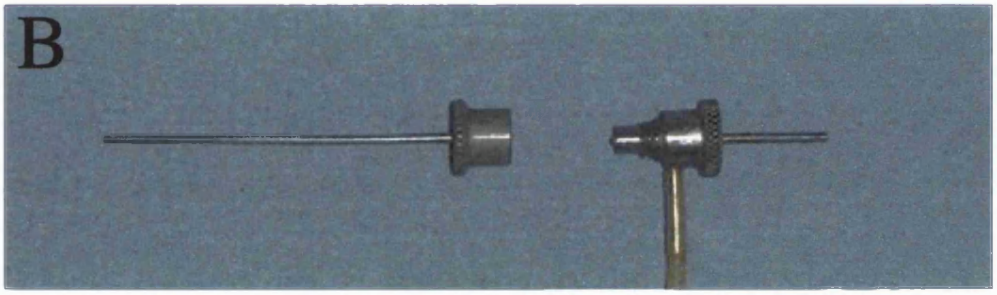

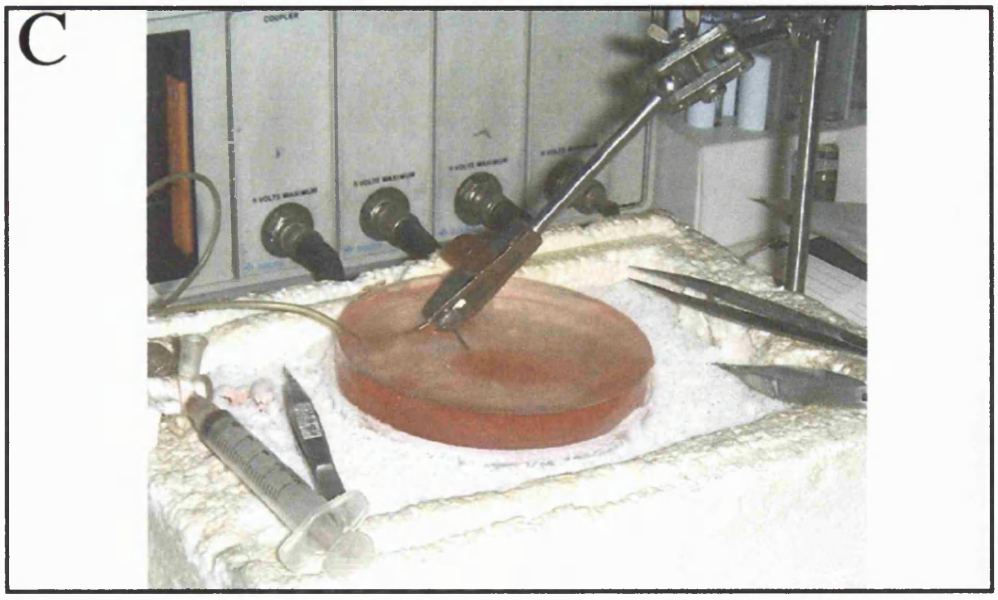

3.6 Langendorff perfusion

The principles of Langendorff perfusion have remained unaltered since the method's original description.[296] An aortic cannula is inserted into the aorta, above the sinuses of Valsalva. The heart is then perfused retrogradely, via the aorta. In this mode, the aortic valves are forced closed as they are in diastole by the weight of the perfusate column. Thus the buffer flows directly into the coronary vasculature, and drains via the coronary sinus of the right atria. Perfusate pressure is maintained either by a gravity feed system from a fixed height reservoir (constant pressure), or by a peristaltic pump (constant flow). In this way, a heart may be maintained with oxygenated substrate containing buffer for many hours.

In the case of murine heart perfusion, there are technical difficulties associated with the size of the preparation (mouse hearts typically weigh between 120 to 180 mg, 10% of the weight of a typical rat heart), and the rate of myocardial contractions (mouse hearts spontaneously beat at a rate of between 310 to 840 beats per minute, compared to rat hearts with rates of 250 to 450 beats per minute[297]).

To account for the smaller scale, a special 20 gauge cannula was designed to enable cannulation of the mouse aorta (technical schematic, figure 3.1.A). It is in two halves; the top half is permanently mounted into the bubble trap of the perfusion apparatus (figure 3.2.B), whilst the lower half is removable to allow cannulation of the aorta away from the Langendorff apparatus (as described in section 3.5.2, and pictured in figure 3.2.C). Once cannulated, the cannula is transferred to the Langendorff rig, and the two halves of the cannula reunited by a screw thread. The seal is maintained by the compression of a rubber 'O' ring between the two halves of the cannula. The design enables both halves of the cannula be pre-flushed with buffer to reduce the risk of air embolisation.

The mouse heart can then be perfused, with a modified Krebs Henseleit buffer (NaCl 118 mM, $NaHCO_3$ 24 mM, d-Glucose 10 mM, KCl 4 mM, NaH_2PO_4 1.0, Na_2EDTA 0.5 mM, $MgCl_2$ 1.2 mM, $CaCl_2$ 2.5 mM) as described by Marber et al,[221] and perfused retrogradely at constant pressure (110 mm Hg, the mean arterial pressure of an awake active mouse). The perfusate was oxygenated with 95% O_2/ 5% CO_2 gas mixture perfusate pH 7.4, measured on an AVL model 993 Automatic blood gas system at 37°C).

A temperature probe (a fine thermocouple wire, 'IT-18' Physiotemp, NJ, USA) is inserted into the right ventricle to enable the close continuous monitoring of normothermia (37°C) throughout the experiment, via a digital thermometer (Physiotemp Bat-12; Sensortek, Clifton, NJ, USA). Given the high surface area to volume of the

isolated mouse heart, radiated heat loss is a particular problem of mouse heart perfusion and therefore maintenance of temperature homeostasis becomes critically important.
In order to maintain a reproducible and consistent heart rate, the mouse hearts are paced whilst perfused in Langendorff mode. The pacing rate is 600 beats per minute, equivalent to the heart rate of an awake and active mouse.[297] Spontaneous heart rates are slower, typically around 480 beats per minute, the equivalent of a resting or sleeping mouse. The positive electrode (a round, non cutting needle attached to a pacing wire) is placed into the left ventricle near the atrio ventricular junction. The earth electrode is the aortic cannula. The hearts are paced with a square 20 msecond pulse, with the voltage set at, or close to, the pacing threshold (typically approximately 1.0 volts). The optimal pacing voltage and current range, pace signal duration and waveform were determined in a short series of experiments which enabled the setting of specifications for the construction of integrated and isolated battery powered pacing boxes (constructed by Mr William Potter, Physiology Electrical workshop, UCL).
Global ischaemia was achieved with the cessation of coronary flow by switching off the perfusion circuit. Normothermia was maintained by submerging the hearts in pre-warmed (37°C) non-oxygenated Krebs Henseleit buffer.

3.6.1. Inclusion/ exclusion criteria.

From observation in initial validation experiments, it was found that prolonged time to Langendorff perfusion, and very high or very low coronary flow rates were associated with grossly enlarged infarcts. Therefore, for purposes of experimental reproducibility, a set of experimental exclusion criteria were drawn up and are listed below:

- Prolonged time to perfusion* $\geq$ 3 minutes
- Coronary flow rate at the end of stabilisation $\leq$ 1.0 ml/min or $\geq$ 6.0 ml/min
- Pacing threshold $\geq$1.5 volts
- Stabilisation total arrhythmia duration $\geq$ 3 minutes
- Failure during stabilisation to maintain $\geq$ 80% of initial contractile function.

* defined as the time from the cessation of corporeal circulation to the onset of Langendorff perfusion.

FIGURE 3.2. THE LANGENDORFF PERFUSION APPARATUS.

The Langendorff perfusion apparatus is depicted below (**A**) in schematic form, and a similar apparatus pictured in (**B**).

A

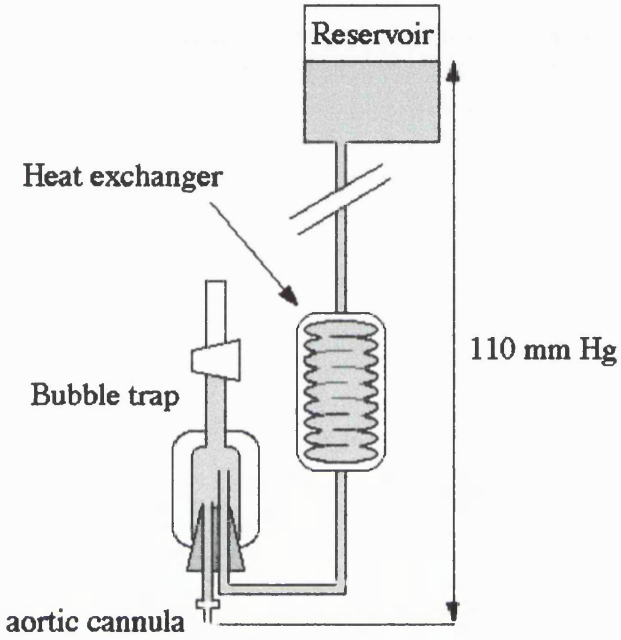

B

3.6.1 Parameters measured

3.6.1.1 Coronary flow rate

As previously detailed, the mouse hearts were perfused at constant pressure (110 mm Hg). Therefore the coronary flow rate will be determined by the vascular resistance of the coronary arterial beds, as determined by heart contraction and arteriolar vascular smooth muscle tone (and hence upon endothelial function). The resistance of each arteriole is inversely proportional to the radius of the vessel raised to the forth power. Thus, coronary endothelial function may be crudely assessed by the measurement of coronary effusate flow, as described below (equations 1 - 5). Coronary flow was simply measured in these experiments, calculated by the collection in a graduated measuring cylinder of coronary effusate, over a set period of time, and expressed as a rate of millilitres per minute (ml/min).

Relationship between coronary flow and arteriolar radii:

Assuming that the Langendorff perfusion apparatus functions as an 'energy circuit':

$\mathbf{p.d. = I.R.}$ where p.d. defines the potential difference, or the perfusion pressure (110 mm Hg), I is the coronary flow rate and R the total vascular resistance.

Thus,

$$\mathbf{I = p.d./R} \quad (1)$$

Resistance to flow through a tube is proportional to the forth power of the radius of the vessel:

$\mathbf{R \propto r^4}$ **(2)** where r is the radius of the tube or vessel.

Given that the resistance of the coronary vasculature is predominantly in the microvasculature, then the radii represents the radii of the myocardial arteriolar beds.
For multiple arteriolar vessels, the total resistance to flow can be determined by the equation:

$\mathbf{1/R_{total} = 1/R_1 + 1/R_2 + \ldots 1/R_n}$ where R_{total} represents the total vascular resistance, n the number arterioles in the vascular bed, and R_x is the resistance of each individual arteriole.

Therefore, from equation (2),

$$1/R_{total} \propto 1/r_1^4 + 1/r_2^4 + \ldots 1/r_n^4$$

Assuming that all the arteriolar radii of the microvasculature are the same,

$$1/R_{total} \propto n/r^4 \quad (3)$$

Therefore, from equations 1, 2 and 3:

$$I \propto n.p.d./r^4 \quad (4)$$

or, to predict the change of arteriolar diameter following an intervention, and assuming that arteriolar number is unchanged and constant perfusion pressure,

$$r \propto (1/I)^{-4} \quad (5)$$

3.6.1.2 Developed force

A 4/0 silk tie, on a circular, non-cutting needle is passed through the apex of the Langendorff perfused heart. The suture is then tied to a transducer arm linked to a calibrated linear force transducer (Scame model GM3). The transducer is mounted on a micro manipulator arm, to enable variable tension to be applied to the suspended heart. The tension is adjusted throughout the stabilisation period to both compensate for stretching of the perfusate saturated silk tie, and to titrate the resting tension to achieve optimal contractile function without excessive loading of diastolic tension. The optimal tension for each heart is recorded.
The contractile function (systolic minus diastolic developed tension) is recorded on a Gould WindoGraf chart recorder.

3.6.1.3 Temperature

Temperature control, by virtue of a large surface to volume ratio resulting in significant radiant heat loss, is critical in the mouse heart. Hypothermia has been shown to attenuate infarction resulting from ischaemia/reperfusion injury,[298] and thus temperature requires continuous monitoring and rigorous maintenance to 37 ± 0.2°C. Methods and apparatus used in the measurement of temperature are documented in the discussion of Langendorff perfusion in section 3.6 above.

3.6.1.4 Heart rate

To confirm that the electrical pacing was correctly functioning, heart rate was calculated regularly from the force trace, by counting the number of contractions within a measured distance. All hearts were paced at a rate of 600 beats per minute during stabilisation, and throughout the preconditioning protocol (where appropriate). Pacing was discontinued after 5 minutes index ischaemia, following the cessation of

measurable function to prevent the precipitation of crystalloid salt around the heart from the buffer contained in the heated organ bath used to main normothermia during preconditioning or index ischaemia.
At reperfusion, the hearts are initially refractory to rapid (≥ 200 beats per minute) pacing rates. Therefore the pacing is titrated incrementally over the initial 20 minutes of reperfusion, at which point the majority of hearts will pace at 600 beats per minute. Pacing in this fashion eliminates inter-experiment heart rate variability that may adversely influence the resultant force-rate product; the linear positive step relationship between heart rate and contractile force appears to be adversely effected following ischaemia reperfusion resulting in an unreliable inter-experimental force-rate product reproducibility.

3.7 Measurement of infarct size

3.7.1 Tetrazolium staining

At the end of the experimental protocol, all hearts were stained with 1% triphenyl tetrazolium chloride (TTC) in phosphate buffer (pH 7.4).
Whilst the heart were still beating on the Langendorff apparatus, the buffer perfusion circuit was switched off, and a 5 ml bolus of pre-warmed (37°C) TTC solution is injected through the side arm port of the perfusion cannula. The heart was then removed from the aortic cannula, transferred and incubated in a 30 ml Falcon tube containing TTC solution for 10 minutes at 37°C.
The hearts were then weighed and frozen at -20°C, a process that allows the hearts to be stored for later analysis, and facilitates processing for photography.
Frozen hearts were thern carefully cut using a sharp scalpel blade perpendicular to the long axis of the heart, into transverse, typically 6 to 8 < 1 mm slices and fixed in 10% formaldehyde for 24 hours (representative sliced hearts, before formaldehyde fixing are shown in figure 3.3).

3.7.1 Digitising TTC stained heart slices

The fixed heart slices were digitised using the techniques previously developed in our Laborartory. Heart slices, prepared as in section 3.7.1 were arranged on a perspex mounting block, with a machined 0.57 mm deep stepped mounting surface. A transparent perspex plate was then screwed down upon the heart slices, fixing their depth to a known 0.57 mm. The slices were then digitally photographed using a specially constructed camera system assembly using a megapixel digital video camera and a high resolution lens with an appropriate focal length. The system uses a S-VHS signal output to a video input card in a Power Macintosh 7500/100 personal computer.

The image, viewed on the screen using Apple's Video Player (version 1.3.1), can be copied and pasted into an open window of the National Institutes of Health freeshare image analysis programme, NIH Image (version 1.6.1, downloaded from http://rsb.info.nih.gov/nih-image/), with the result as shown in figure 3.4.A.

FIGURE 3.3. MOUSE HEART SLICES.

Representative mouse heart slices lain out before fixing in formaldehyde, in (**A**), control heart and (**B**) a preconditioned heart. A ruler is included in these shots to provide scale.

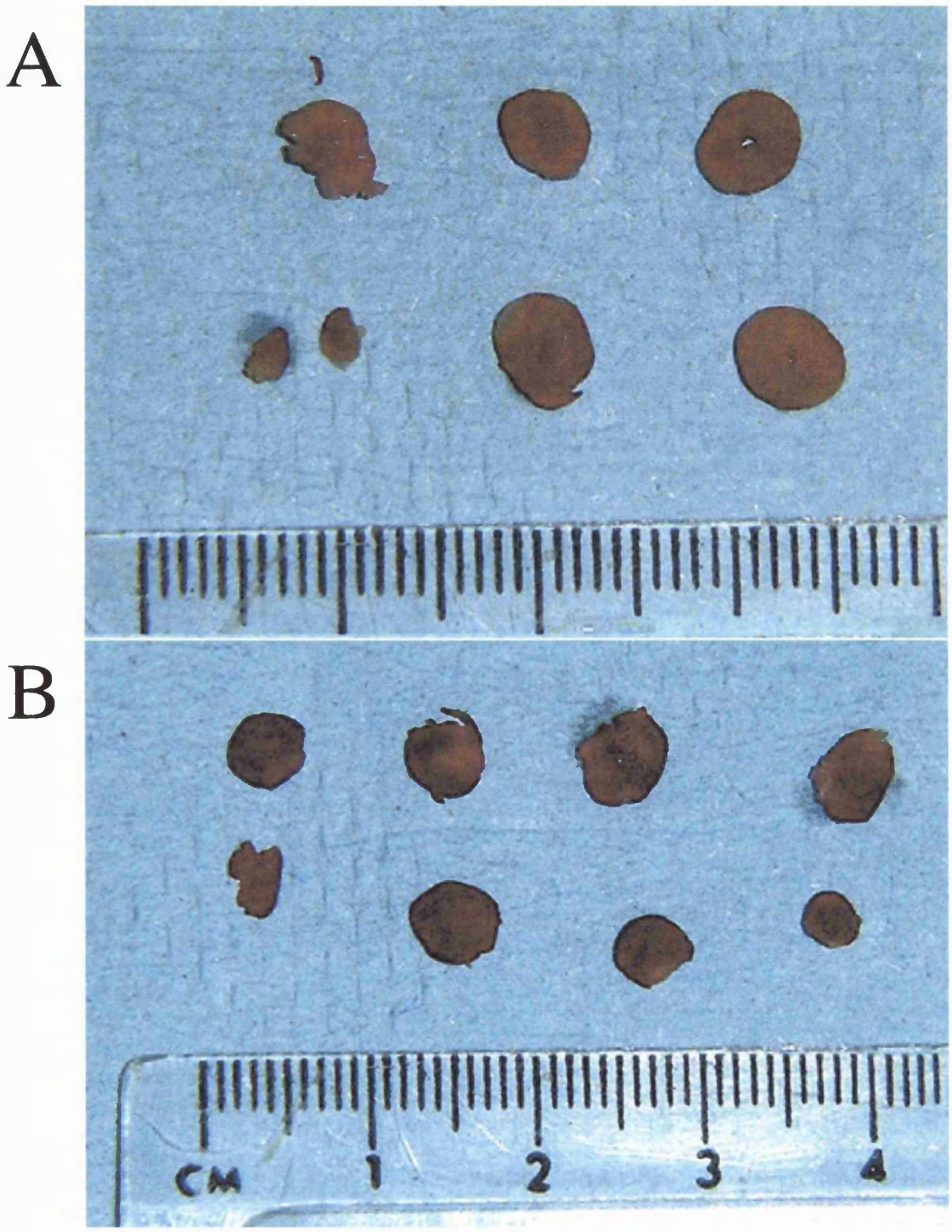

FIGURE 3.4. STAGES OF DIGITAL PLANIMETRY.

The sliced heart is mounted in a perspex mounting block, and processed in the following stages:

A: the slice is digitally photographed;

B: the background is removed from the perimeter and the ventricular aperture;

C: The image converted into a grey-scale image and threshold planimetered as shown. The square in the bottom right hand corner is the calibration square, representing 1 mm^2.

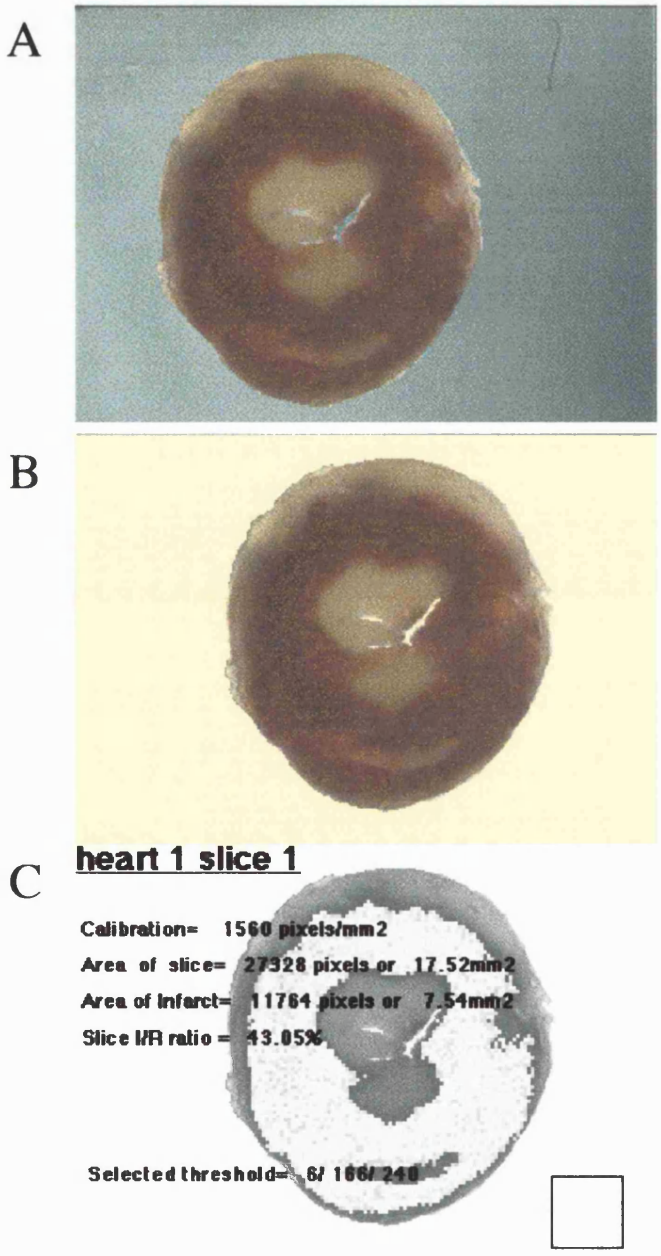

3.7.2 Planimetry of TTC stained heart slices

Following TTC staining and fixing in formaldehyde solution, infarcted myocardial tissue appears pale and viable myocardium brick red. TTC, as characterised by Fishbein et al,[299] is a dye that crosses the cell membrane, and binds to intracellular dehydrogenase enzymes. Viable cells with reducing potential (preserved NADPH) stain dark red. Non viable cells with ruptured sarcolemmal membranes lose the dye and appear pale. The individual slices were placed on a transparent mounting block, under a cover slip 0.57 mm above, and digitally photographed. These images were then transferred to a graphics package (NIH Image v1.61) for planimetry.

Once the slice image is transferred to NIH Image, the raw image was stored onto disc as a permanent record (figure 3.4.A). The image background then needs removing for image analysis. Using the tracing tool, the outline of the heart was traced. This region of interest (ROI) was copied and pasted into a new window with a plain white background, so as to remove spurious shadowing in the image's background. The cavity spaces were also traced and removed so that all that is not myocardium appears white. This second image is saved onto disc as a permanent record (figure 3.4.B).

The image was then be converted into a grey scale image, and an infarct size measuring macro programme then be used to calculate areas of total myocardium and necrosed myocardium (figure 3.4.C). The macro programme works on a grey-scale threshold principle. Thus, total slice area is derived from the contrast from the white background, whereas the viable dark-staining tissue is distinguished from the non-viable pale-staining tissue. The areas of both are calculated, and the proportion of non-viable tissue to viable tissue recorded. Given a calibrated image (figure 3.5), and a known myocardial slice thickness (0.57 mm), the volumes of tissue are readily calculated.

The risk volume is the total ventricular volume, minus the cavity spaces. Infarct size for each heart is expressed as a percentage of risk volume.

FIGURE 3.5. CALIBRATION OF THE PLANIMETRY SOFTWARE.

To calibrate the camera system, a digital picture is taken of a graduated sheet of graph paper, at the same focal length as that used for the image capture of the heart slices. From this image, a single 1 mm^2 'box' can be isolated- as represented below, and its area measured using the planimetry software to determine the equivalent number of square pixels to the square mm, as described in the text in section 3.7.2.

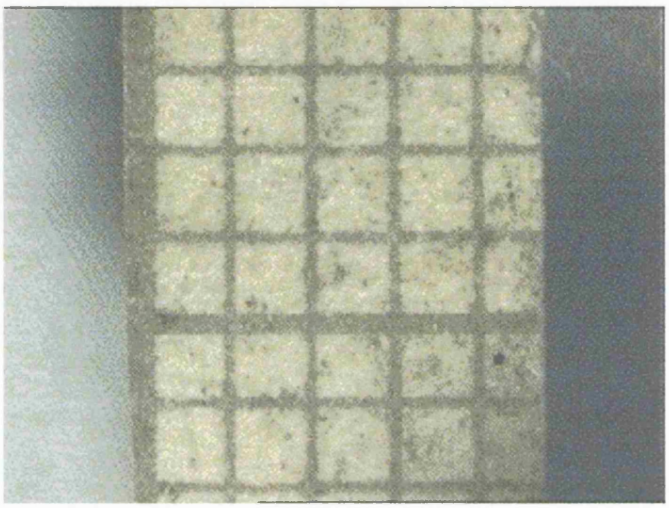

Calibration square = 1 mm^2

3.8 Measurement of oxidised metabolites of nitric oxide

Nitric oxide synthase activity in the Langendorff perfused hearts was determined by measurement of the oxidised products of NO, nitrite and nitrate (NO_2 + NO_3 or NO_X), in the coronary effluent by high pressure liquid chromatography (HPLC) as described by Smith et al [300]. These studies were performed in the laboratories of the Jules Thorne Institute, The Middlesex hospital, London.

Coronary effluent samples were collected at three or four time points throughout the perfusion protocol: the end stabilisation; end of the preconditioning protocol (where appropriate); upon immediate reperfusion and at the end of reperfusion. The effluent was collected in 2 ml Eppendorf tubes that had been thoroughly washed in ultra pure water, and rinsed 12 times before drying. The purpose of the washing regime is to leech NO_X contamination from the plastic walls of the Eppendorf tube, a method previously found effective in removing such contamination. One tube was filled with ultra-pure de-ionised water with each batch of tubes to check for background NO_X contamination and confirm adequate clearance of NO_X contamination. The coronary effluent samples were collected and stored frozen at minus 70°C, and later defrosted for analysis. One further sample, containing buffer run through the Langendorff rig, was also collected to determine background NO_X contamination from the apparatus and chemicals used in the preparation of the perfusion buffer.

Prior to injection into the HLPC column, the effluent samples were cleared of cellular debris and protein by spinning through pre-washed 3k. m. wt. nanosep filters (Nanosep devices, Flowgen, UK. Cat# U3-0144) at 11000 x *g* for 45 minutes. Pre-washing of the nanosep filters with ultrafiltrated distilled water was found to be essential to reduce NO_X contamination that would otherwise reduce the sensitivity of the assay. Other brands of filters were found to be unacceptably contaminated with NO_X, and so were not used for these analyses.

The coronary effluent ultrafiltrate was injected into the HPLC column and NO_2 and NO_3 elution peaks (measured at 214 nm with a Waters Model 441 absorbency detector) were compared to the heights of known standards (run on the same day, and three times in succession to ensure reproducibility) for estimation of coronary NO_X concentration. Typical run time for each assay was approximately 10 minutes, to obtain both elution peaks and avoid interference with the next assay run. The sum of the NO_2 and NO_3 concentrations derived from the elution peaks, minus the background contamination NO_X from same day's Krebs Henseleit buffer blank, was assumed to be equivalent to the amount of NO generated by the isolated heart. A typical trace is illustrated in figure 3.6.

FIGURE 3.6. TYPICAL NITRIC OXIDE ELUTION PEAK TRACES FROM HPLC.

Purified coronary effluent sampled and various time points and compared to known standards of NO2 and NO3. (A) NO2 and NO3 standard peaks, (B) coronary effluent sampled during heart stabilisation and (C) sample collected immediately upon reperfusion following a 35 minute ischaemic insult.

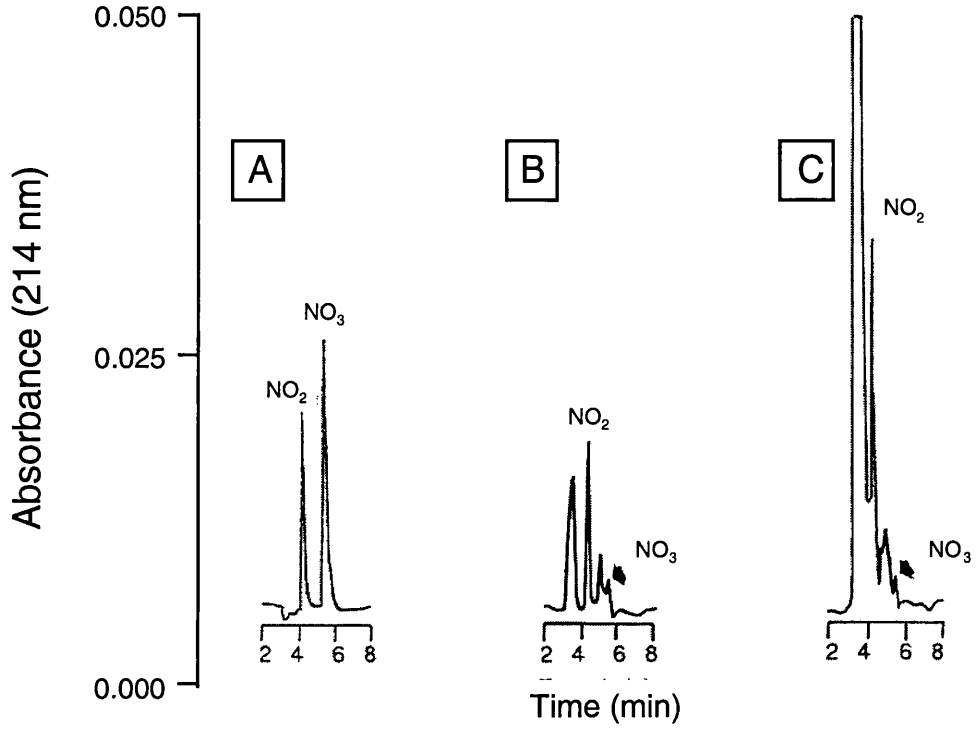

3.9 Molecular biological techniques

3.9.1 Reverse transcriptase polymerase chain reaction (rt-PCR)

The rt-PCR was performed according to the methods described by Saiki et al,[301] using a proprietary kit (GeneAmp® EZ rTth RNA PCR kit; Perkin Elmer Applied Biosystems, Warrington, UK) that enables the reverse transcriptase reaction in the same vial as the polymerase chain reaction without interruption. This process is catalysed by the *rTth* DNA polymerase, a recombinant thermostable enzyme derived from a modified strain of *Thermus thermphilus*, and as such is capable of transcribing RNA in the presence of Mn^{2+} and high temperatures required for DNA strand separation.

3.9.1.1 Tissue preparation

Mice were anaesthetised as previously described and the hearts isolated and Langendorff perfused. After 20 minutes perfusion, an equivalent time to the stabilisation period of the ischaemia/reperfusion protocol, coronary flow was stopped, and the hearts immediately snap frozen with a pair of snap-freeze tongs pre-cooled in liquid nitrogen. The heart was broken into small pieces and stored at minus 70°C for later analysis.

For genotyping of mice whose hearts were subjected to ischaemia/reperfusion, liver tissue was extracted from the cadaver, snap frozen as described above, and stored at minus 70°C for later analysis.

3.9.1.2 mRNA extraction and preparation

Stored tissue samples (of approximately 50 mg weight) were placed directly into a pre-cooled vial containing RNAzol, and placed on ice to defrost for 5 minutes. The samples were then homogenised with a Polytron homogeniser (model T25, IKA Labortechnick, Janke & Kunkel GmbH & co, Germany) taking care not to over-heat samples. 200 µl of 0.1% pre-cooled chloroform was then added to the homogenate, which was then vortexed for 15 seconds, and allowed to stand in ice for 15 minutes. The samples are then spun in a refrigerated centrifuge (Eppendorf centrifuge, model 5417R, Netheler-Hinz GmbH, Hamburg, Germany) at 10,500 rpm for 15 minutes at 4°C. The supernatant was then decanted into a fresh, pre-cooled Eppendorf, to which was added an equal volume of chloroform (usually approximately 1 ml). The sample was then vortexed (15 seconds), and allowed to stand in ice for 5 minutes, before centrifugation at 10,500 rpm for 15 minutes at 4°C. The top layer was again extracted, decanted into a fresh pre-cooled Eppendorf, and an equal volume of isopropanol (approximately 1 ml) added. The sample was then vortexed for 15 seconds, and stored overnight at minus 20°C.

RNA preparations were then spun again at 10,500 rpm for 15 minutes at 4°C, and the supernatant removed. The pellet was resuspended in 1 ml of 75% ethanol (in 0.1% DEPC H_2O), and spun at 10,500 rpm for 5 minutes at 4°C. The ethanol was then poured off from the pellet, and the Eppendorf allowed to dry for 2 minutes. The pellet was then resuspended in 40 µl 0.1% DEPC H_2O, from which 2 µl was removed and added to 1 ml H_20 for RNA quantification.

Quantification of extracted RNA was performed by determining the optical density at 260 nm using a spectrophotometer (Jenway model 6405 UV/Vis, Dunmow, UK). Cuvettes (1 ml) were rigorously washed in 0.1% DEPC H_20 prior to use. An optical density of 1.000 is equivalent to 40 µg/ml.

3.9.1.3. PCR reaction

3.9.1.3.1. Primer design

The mouse iNOS gene sequence was obtained from the GenBank library available at http://www.ncbi.nlm.nih.gov:80/entrez/query.fcgi?CMD = &DB = Nucleotide. This was imported to a sequence processor programme (Gene Jockey II, Biosoft, Cambridge, UK), which provided potential 5' and 3' prime promoter sequences. The custom oligonucleotide were ordered after checking the specificity of the sequences to the iNOS gene from Gibco Life Technologies (Paisley, UK). The sequences used for iNOS were:

5' to 3': AAGAGGAGCAACTACTGC

3' to 5': TCATCCAGAACCTCCAGG

3.9.1.3.2. rt PCR

A master solution of rt-PCR reagents were prepared, on ice, allowing 50 µl per sample. For a reaction vial of 50 µl, the following quantities were used: 23 µl sterile distilled water, 10 µl 5x EZ buffer (250 µM bicine, 575 µM potassium acetate, 40% glycerol; pH 8.2), 6 µl dNTP mix (1:1:1:1 10 µM dATP, 10 µM dCTP, 10 µM dGTP and 10 µM dTTP), 1 µl of nitric oxide synthase (iNOS) primer mix (1:4 dilution of a 1:1 mix of 100 pmol/µl each of 5' and 3' iNOS primers), and 2 µl *r*T*th* DNA polymerase (2.5 U/µl). The equivalent of 300 ng of total RNA was pipetted into each PCR reaction tube. Master solution (46 µl) was added to each test sample and a blank tube. The rt-PCR was undertaken with a programmable PCR heating block (Progene; Techne Ltd, Cambridge, UK), using the optimised protocol shown in figure 3.7.

FIGURE 3.7. RT-PCR PROTOCOL FOR iNOS cDNA AMPLIFICATION.

Samples were prepared as described in the text. Sample vials were loaded into the PCR machine and the following sequence programmed.

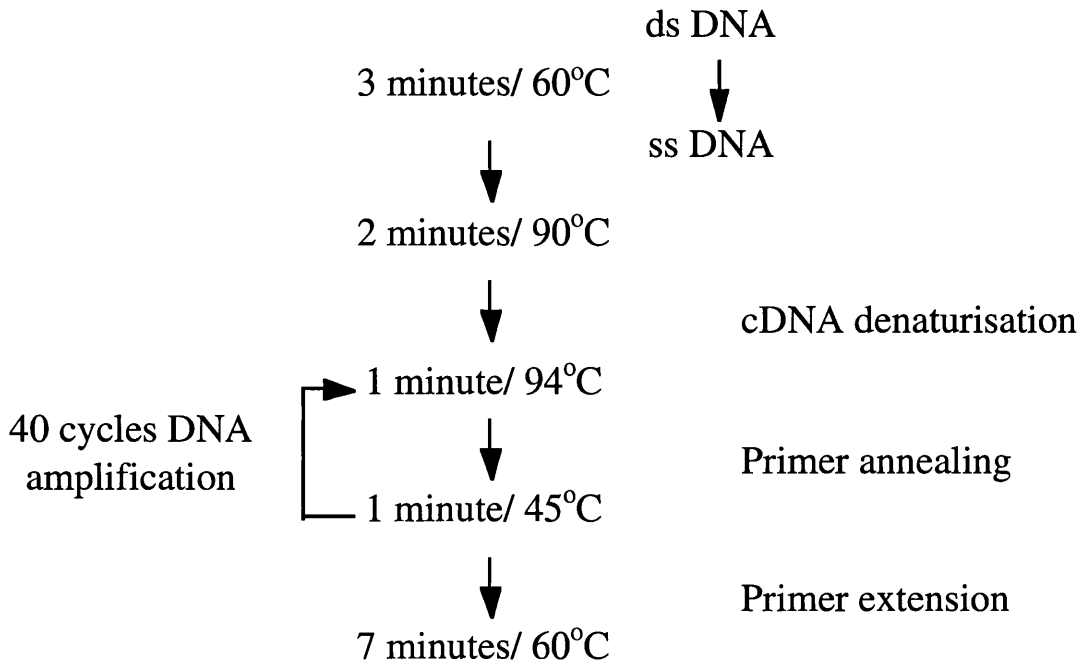

3.9.1.4 Formaldehyde agarose gel electrophoresis

3.9.1.4.1. Gel preparation

3.0 ml 10x MOPS solution was warmed to 55°C, to which was added 4.9 ml of 37% formaldehyde and agarose solution made by melting 0.6 g agarose in 22.1 ml H_20. The gel was then cast into the running bath, using 1x MOPS solution as the running buffer.

3.9.1.4.2. Sample preparation

6 µl of RNA sample + 0.1% DPEC H_20 was added to 12.5 µl de-ionised formaldehyde, 4 µl 37% formaldehyde solution, 2.5 µl 10x MOPS and 0.3 µl 0.5 mg/µl ethidium bromide. The sample mixtures were then heated to 60°C for 15 minutes before being cooled on ice for 2 minutes. Thereafter, 2 µl blue tracking dye was added to the samples and the samples briefly spun.

3.9.1.4.3. Electrophoresis

The samples were loaded onto the gel, which are then run for four hours at 85 volts. The gel was then removed from the tank, and trans-illuminated with UVB light (360 nm) and photographed with an SLR Polaroid film camera. The gel was then blotted against a nylon high bond membrane pre-soaked in de-ionised water/ 10x SSC, avoiding bubbles, which was then placed under a Whatman paper stack and a heavy weight, over night (16-24 hours).

3.9.1.5. Quantification

Gels and membranes were scanned on a flat-bed picture/document scanner and the digital image saved to disc. The image was imported into a NIH freeshare programme, NIH Image (version 1.61). The relative densitometry was determined using the grey scale technique, using the supplied macro 'Gel plotting macro.' Images may be calibrated against absolute densitometer values if one of the lanes has been so measured. Results are expressed as a percentage proportion of wild-type control expression (± SEM).

3.9.2 Western blotting

3.9.2.1 Tissue preparation

Mouse hearts were isolated from anaesthetised mice, and Langendorff perfused for 20 minutes (equivalent to the stabilisation period of the ischaemia/reperfusion protocol, and to remove blood elements from the preparation). The coronary flow was terminated, and the heart immediately snap frozen with liquid-nitrogen pre-cooled tongs. The hearts were then broken up and stored at minus 70°C for later analysis.

3.9.2.2 Protein extraction

Approximately 50 mg of frozen ventricular tissue was used for each protein extraction sample. Tissue was homogenised on ice in 250 ml suspension buffer (NaCl 100 mM, TRIS 10 mM (pH 7.6), EDTA 1 mM (pH 8.0), Sodium pyrophosphate 2 mM, Sodium fluoride 2 mM, β-Glycerophosphate 2 mM; PMSF 0.1 μg/ml; and 1 μg/ml each of aprotinin, leupeptin, trypsin inhibitor and protease inhibitor), using a IKA Labortechnik T25 basic homogeniser. Samples were subsequently centrifuged and supernatant divided for protein quantification (duplicate 2 μl samples) and electrophoresis (the remaining sample). The purified protein was then further diluted in 2x sample buffer (TRIS 100 mM (pH 6.8), DTT 200 mM; and SDS 2%, bromophenol blue 0.2% and glycerol 20%) and subsequently boiled for 10 min at 100^0C, and stored at minus 20^0C for later analysis.

3.9.2.3 Protein estimation

Protein concentrations were estimated using a Bicinchoninic acid based (BCA™) protein assay reagent system (Pierce, Rockford, USA). The assay relies on the reduction of ionised copper, and the formation of a BCA-Cu^+ complex as described below:

1. protein (peptide bonds) + Cu^{2+} -- > tetradentate-Cu^+ complex
2. Cu^+ + 2 bicinchoninic acid (BCA) -- > BCA-Cu^+ complex

The BCA-Cu^+ complex is purple coloured, and can be measured by optical densitometry at 562 nm. The relationship between the absorbance at 562 nm and protein content is linear over a wide concentration range (20 - 2000 μg/ml), and thus the protein content of the samples can be estimated through comparison with a standard curve.

Thus, in brief, duplicate samples of increasing concentration bovine serum albumin (BSA) in suspension buffer (contents as described in 3.9.2.2) were quantified to generate a standard curve derived from the results of the optical density using a photospectrometer (Janway model 6405 UV/Vis, Dunmow, UK). The protein in the samples was then quantified using this method, and the protein content compared against the standard curve to provide an estimate of the protein concentration (μg/μl) to enable equal loading of the polyacrylamide gel.

3.9.2.4 Polyacrylamide gel electrophoresis.

3.9.2.4.1 Gel preparation.

For eNOS and iNOS electrophoresis, 8% acrylamide gels were made (34.8 ml de-ionised H_2O, 19.2 ml acrylamide, 18 ml running gel base (1.5 M TRIS and 0.4% SDS in de-ionised H_2O, pH 8.8), 30 μl TEMED and 400 μl 10% ammonium sulphate). The

gel was made between two glass plates separated by spacers, with the edges sealed with agarose. Protein loading wells were made in the stacking gel (14 ml H_2O, 6 ml stacking gel base (0.5 M TRIS, 0.4% SDS in de-ionised H_20, pH 6.8), 4 ml 30% acrylamide, 40 µl 8% bromophenol blue, 20 µl TEMED and 200 µl 10% APS).

3.9.2.4.2. Electrophoresis.

A total of 60 µg of protein for each sample was loaded into the gel. A high molecular weight rainbow marker (covering the molecular weights of eNOS and iNOS- 130-140 kDaltons) was also loaded (7 µl). The gel was then allowed to run over night at 75 mV.

3.9.2.4.3. Transfer and immunoblotting.

Following electrophoresis, the gel was mounted in a transfer tank containing transfer buffer (200 ml methanol, 700 ml distilled H2O and 100 ml blot buffer (containing glycine, TRIS)). The gel was careful opposed to an equivalently sized Hybond ECL nitro-cellulose membrane (Amersham). The gel and membrane were then sandwiched between sheets of Whatman paper, with care taken to avoid air bubbles. The gel was then allowed to transfer over night (12-16 hours) at 125 mA. Membranes were then removed, and equal protein loading was confirmed by Ponceau red staining (Sigma Chemicals Co, Poole, UK) of membrane which were then digitally scanned at this stage so that any inequalities in protein loading may be compensated for as described by Ping et al.[106]

3.9.2.5 Immunoblotting

The membranes were then washed, and blocked in blocking buffer (0.1% milk) for 2 hours. Subsequently, the membranes were incubated with 1 in 250 primary antibody (eNOS and iNOS rabbit primaries, New England Biolabs) in 0.1% milk for two hours, prior to washing and incubation with secondary anti-rabbit antibody (cat #P0217, DAKO A/S, Denmark) at a dilution of 1 in 2000 for 1 hour. Proteins were detected using enhanced chemiluminescence ECL Western blotting detection reagent and bands were visualised by autoradiography onto Kodac AR film.

3.9.2.5 Quantification

Autoradiography films and Ponceau stained membranes were scanned on a flat-bed picture/document scanner and the digital image saved to disc. The image was imported into a NIH freeshare programme, NIH Image (version 1.61). The relative densitometry was determined using the grey scale technique, using the supplied macro 'Gel plotting macro.' Images may be calibrated against absolute densitometer values if one of the lanes has been so measured. Results are expressed as a percentage proportion of wild-type control expression (± SEM), and corrected for Ponceau determined protein loading.

3.10 Mitochondrial assessment by Flow cytometry

3.10.1. Isolation of mitochondria

Mitochondria were isolated from hearts of male Sprague-Dawley rats (body weight 200-250 grams) using a method previously described.[302] In brief, hearts were removed from terminally anaesthetised rats and briefly infused with cold MSTEB buffer (containing mannitol 210 mM, sucrose 70 mM, TRIS 10 mM (pH 7.2 with hydrochloric acid), EGTA 1 mM and BSA 0.5 mg/ml). The heart was then homogenised (Polytron model T25, IKA Labortechnick, Janke & Kunkel GmbH & co, Germany) in MSTEB buffer. After centrifugation (450 *g*, 5 minutes), two thirds of the supernatant was decanted into fresh, pre-chilled tubes. Mitochondria were isolated by further centrifugation (5800 *g*, 10 minutes). The mitochondrial pellet was resuspended in cold MST (containing mannitol 210 mM, sucrose 70 mM and TRIS 10 mM) and the previous centrifugation step repeated. The mitochondrial isolate was found to be stable on ice for several hours, enabling a number of experiments to be performed on the same day under equivalent conditions.

Mitochondrial concentration was determined by protein assay using a similar technique to that described in section 3.9.2.3. In brief, a bovine serum albumin standard curve was generated using the BCA™ protein assay kit, measuring absorbance on a photospectrometer at 562 nm (Janway model 6405 UV/Vis). Duplicate samples of 5 µl mitochondria were made up to 50 µl by adding de-ionised water. To the resuspended mitochondria was added 1 ml of BCA working reagent, and then incubated for 30 minutes. The mitochondrial protein was then quantified using the photospectrometer absorbance at 562 nm.

3.10.2. Cytometry.

Mitochondria were assessed using the fluorometric probe, tetramethyl rhodamine methyl ester (TMRM, Molecular Probes Inc., Leiden, The Netherlands), a non-toxic, mono-valent cation, that reversibly accumulates according to membrane potential with a Nernstian distribution.[303] (Structure of TMRM is shown in figure 3.8.A.) Thus, by using these membrane potential-sensing properties, TMRM may be used as a membrane potential probe, and has been employed previously to determine mitochondrial membrane potential.[304]

By using the Nernst equation, mitochondrial membrane potential may be estimated based upon the determination of TMRM fluorescence inside the mitochondria compared to the fluorescence of unbound fluorescence in the suspension media.

From the Nernst equation:

$$\Delta G = (2.303*R*T/F)*\text{Log}([TMRM_m]/[TMRM_o]) \quad (1)$$

Where:

R = gas constant = 8.314 joules/Mol/degree

F = Faraday = 96500 joules/volt

T = Temperature = 298 Kelvin

$[TMRM_m]$ = concentration of TMRM in mitochondria (proportional to fluorescence).

$[TMRM_o]$ = concentration of TMRM outside mitochondria in supernatant.

Thus, in mitochondria,

$$\Delta\psi_m \approx 59*\text{Log}([TMRM_m]/[TMRM_o]) \quad (2)$$

The absorbence and emission spectra are shown graphically in figure 3.8.B. TMRM peak light absorbence (and therefore, optimal excitation wavelength) is 549 nm. Following excitation, TMRM fluoresces in the green spectra, with peak fluorescent light emission occurring at 573 nm. Of note however, significant overlap exists between absorbance and fluorescence spectra between approximately 520 and 580 nm (illustrated, figure 3.8.B), and thus where emission and detection wavelengths are similar, significant attenuation of the signal to noise ratio may occur. However, emission and absorbance wavelengths were limited by the availability of commercially available lasers and filter/detectors. Thus for the current studies an argon ion-laser with an emission wavelength of 488 nm in conjunction with a fluorescence detector fitted with a 560 nm ± 20 nm filter. These figures were within the necessary absorption/emission spectra of the probe to provide adequate recording of mitochondrial membrane potentials.

3.10.2.1. Measurement of $[TMRM]_M$

The measurement of $[TMRM]_M$ is based upon the measured fluorescence of the mitochondria as detected by the flow cytometer. The basic principles of the device are shown in figure 3.9. The excitation of the mitochondria by the argon laser causes the mitochondria to emit light. On the detection of forward scatter of the laser light by a mitochondrion passing though the laser beam, the fluorescence intensity of the mitochondria as it is illuminated by the 488 nm argon laser is measured by a photodetector equipped with a 560 nm filter, and recorded as an individual event. As a number of events are recorded, the data can then be displayed as a frequency/ fluorescence intensity histogram (as shown in figure 8.7). The data is non-parametric, which precludes the interpretation of mean fluorescence data, thus the median of the

data were used for estimation of membrane potential of the population and statistical analysis.

3.10.2.2. Measurement of $[TMRM]_O$

As the cytometer only records the fluorescence of mitochondria and not of the surrounding media, $[TMRM]_O$ needs to be determined separately. This is achieved by spinning down the mitochondrial sample (10,500 rpm) to pellet out the mitochondria leaving the suspension buffer as the supernatant. The supernatant's florescence can then be measured using a fluorometer (as described by Scaduto and Grotyohann[305]) using the same excitation and detection settings as that used by the flow cytometer (488/560 nm for emission/detection respectively).

3.10.2.3. Calibration and limitations of measurements

As tetraphenyl phosphonium (TPP), a compound used extensively in the estimation of $\Delta\Psi_M$, and TMRM have a linear relationship with respect to membrane potential,[305] the use of a TPP electrode (in Michael Duchenne's laboratory, Dept of Physiology, UCL) was used to (*i*) confirm mitochondrial membrane potential under resting conditions (measured at 150 mV), (*ii*) to confirm that the mitochondrial membrane potentials of the populations investigated were correctly polarised and (*iii*) that the Nernst equation, using the values of TMRM fluorescence measured as described above, correctly estimated the resting membrane potential. As Garlid and colleagues[306] had predicted small membrane potential changes with the opening of the mitochondrial K_{ATP} channel, for the purposes of membrane potential shifts measured resulting from the drug treatments used in this study, the $[TMRM]_O$ was assumed to be unaltered (as $[TMRM]_M >> [TMRM]_O$). As TMRM does bind independently of membrane potential to the inner and outer mitochondrial membranes, a further correction to the Nernst equation needs to be applied to accurately estimate membrane potential (K_o and K_i at 28° Celsius are 88 and 33 respectively[305]). However, for the purposes of this study where the delta change of membrane potential was of primary interest, these corrections were assumed to be the same in the conditions used for all samples tested.

Thus, the calculated mitochondrial membrane potentials recorded in this study are estimates used to determine membrane potential changes based upon median TMRM fluorescence shifts rather than absolute membrane potentials. Efforts to further characterise the membrane potential shifts with TMRM fluorescence, as measured by flow cytometry, is the subject of on-going work in the laboratory, and were unavailable at the time of the submission of this thesis.

FIGURE 3.8. MOLECULAR STRUCTURE AND PROPERTIES OF TMRM.

A. Structure of Tetramethylrhodium methyl ester (TMRM). Molecular weight 500.93. (Xanthylium, 3,6-bis(dimethylamino)-9-(2- (methoxycarbonyl)phenyl)-, perchlorate)

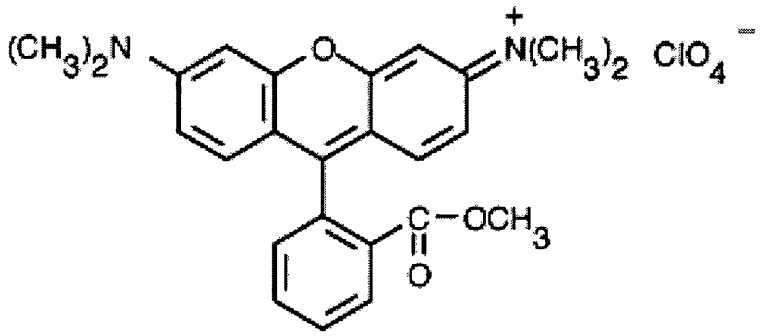

Molecular formula: $C_{25}H_{25}ClN_2O_7$

B. Fluorescence properties of TMRM. Peak excitation wavelength is 549 nm; peak fluorescence wavelength is 573 nm.

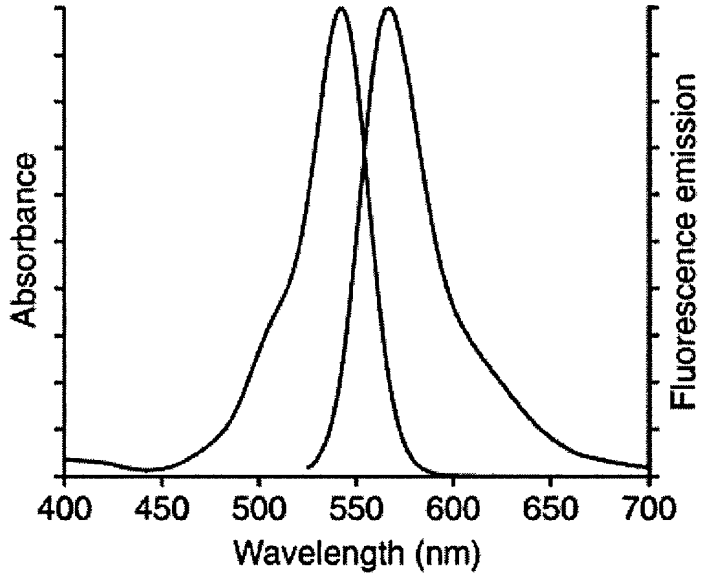

FIGURE 3.9. BASIC PRINCIPLES OF THE FLOW CYTOMETER.

Below is a cartoon depicting how the flow cytometer functions. On insertion of a sample solution containing mitochondria (M), the sample is pumped through the laser chamber in a fluid stream encased by a linear air flow sheath. Thus only one mitochondrial particle passes through the laser light at any given time. The passage of the mitochondria through the laser light is detected by forward scatter. The excitation of the mitochondria at 488 nm causes light emission which is then detected by a detector with a 520 nm filter. The fluorescence intensity is then recorded for each particle that is detected in the sample. On a typical run, 15 to 20 thousand mitochondria are subjected to laser excitation and the fluorescence of each is recorded and the data summarised on a frequency/ fluorescence histogram- typical histograms are shown in figure 8.7.

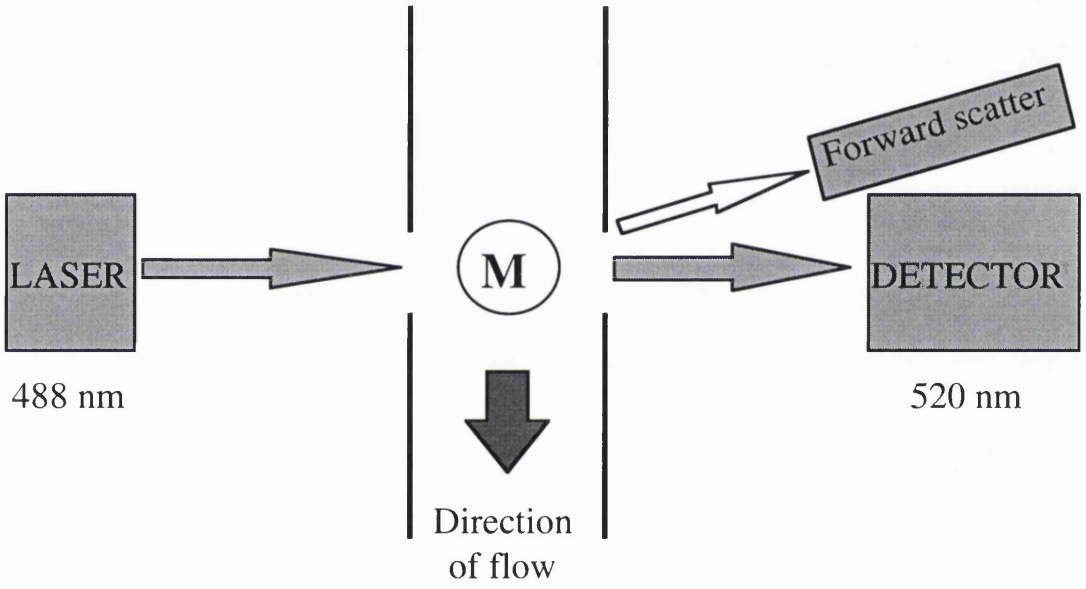

3.10.2.4. Sample preparation

For each experiment a mitochondrial aliquot of 100 µl was re-suspended in a KCl buffer (containing KCl 45 mM, potassium acetate 25.4 mM, TES 5 mM, EGTA 0.1 mM, pH 7.4 and $MgCl_2$ 1 mM). Each sample was incubated with substrates for respiration (glutamate 5 mM and malate 2 mM) and the mitochondrial membrane potential ($\Delta\psi_m$) sensitive dye tetramethylrhodamine methyl ester (TMRM, 200 nM[305]) at room temperature (22°C) for 2 minutes. Where the experiment required the administration of a drug, this was added immediately prior to cytometry.

3.10.2.5. Demonstration of healthy mitochondrial respiration.

To demonstrate normal functioning of the mitochondrial K_{ATP} channel, guanosine triphosphate (GTP, 50 µM), an endogenous K_{ATP} channel opener, was added to the TMRM-stained mitochondria 2 min before measurements of fluorescence in the absence or presence of 5-Hydroxydecanoate (mitochondrial K_{ATP} channel inhibitor, 5-HD, 100 µM). The depolarisation of the mitochondria associated with GTP is blocked by 5-HD. The mitochondrial uncoupler carbonyl cyanide m-chlorophenylhydrazone (CCCP, 1 µM) was used as a positive control, and caused near complete depolarisation of the mitochondria. In the absence of these membrane potential changes, the mitochondria were discarded.

3.10.2.6. Cytofluorometric analysis.

Cytofluorometric analysis was performed using a Partec PAS flow cytometer (Partec, Münster, Germany) equipped with a 488 nm argon ion-laser. The TMRM signal was analysed in the FL2 channel, which was equipped with a bandpass filter at 560 ± 20 nm. Data were acquired on a logarithmic scale. Arithmetic mean values of the median fluorescent intensities were determined for each sample for subsequent graphical representation. Experiments were performed on mitochondria isolated from six individual rats, each experiment representing 15,000 mitochondria.

3.11 Immuno electron microscopy

These studies were performed in collaboration with Andrej Loesch, department of Anatomy and developmental Biology, University College London.

3.11.1 Tissue preparation

Four 3 month old adult female mice (two iNOS knockout and two iNOS wild type) were pre-treated to form a 'control' and a 'preconditioned' group by the administration

of either a saline vehicle or an adenosine A_1 agonist, CCPA (25 μg/kg) 24 hours prior to anaesthesia (60 mg/kg pentobarbitone sodium *ip*) and euthanasia. The anterior chest wall was opened as described in section 3.5.2, and the heart excised. The aorta was then cannulated with a modified 21 gauge needle (bevel removed), which was tied into place by a 3/0 Mersilk tie. The heart was slowly infused (over 3 to 4 minutes) with 5 ml bolus of a fixative consisting of 4% paraformaldehyde and 0.2% glutaraldehyde in 0.1 M phosphate buffer at pH 7.4. The heart was then removed from the cannula, and placed into a labelled vial containing the same fixative for 5 hours at 4°C, and then transferred into another vial containing 4% paraformaldehyde for overnight storage at 4°C. The hearts were then rinsed in phosphate buffer (pH 7.4) for several hours, and then transferred to 0.05 M TRIS-buffered saline at pH 7.6. Coronal sections through the left ventricle were cut at 60-70 μm sections using a vibratome, and collected in TBS. After washing in TBS, the sections were exposed for 45 minutes to 0.3% hydrogen peroxide in 33% methanol for blocking endogenous peroxidases, washed in 0.1 M TBS (pH 7.4) for one hour and processed for the pre-embedding electron-immunocytochemistry of eNOS and iNOS polyclonal antibody using the ExtAvidin peroxidase-conjugate (ABC) method.

3.11.2 Immunocytochemistry

Washed heart slices were incubated for one hour in normal goat serum (Nordic Immunology, Tilburg, The Netherlands) diluted 1:30 in TRIS containing 0.1% sodium azide. The hearts were then washed again in TRIS buffered saline, the sections were incubated for 48 hours at 4°C in either an eNOS or an iNOS polyclonal antibody at a dilution of 1 in 200 in normal goat serum containing TRIS and 0.1% sodium azide, then washed TRIS buffered saline. The sections were then exposed to a biotinulated secondary antibody to the respective primary antibody, diluted 1:40 in TRIS buffered saline. The sections were then rinsed with TRIS buffered saline prior to 4 hour incubation with ExtrAvidin-horseradish peroxidase conjugate (Sigma Chemical Co, Poole, UK) diluted 1:1500 in TBS. After exposure to diaminobenzidine (DAB) and osmication, the sections were dehydrated in a graded series of ethanol and embedded in Aradite. The ultrathin sections were stained with uranyl acetate and lead citrate and examined with a JEM-1010 electron microscope.

3.12 Statistical analysis

Results are presented as group means with the standard error of the mean (SEM). For comparison between two groups, data were compared with Student's unpaired T-test. For comparison between more than two groups, factorial one way analysis of variance

(ANOVA) was used. Where a significant F-value was obtained, Fishers protected least significance difference (PLSD) post hoc test was applied for between group comparisons.

For comparison of data sets recorded over a period of time, ANOVA for repeated measures was used, and where significance was determined, the Fishers PLSD post hoc test was applied. Association between data was tested by Spearman rank correlation and linear regression was used to analyse the association for each group.

Statistical significance was defined as a p value of ≤ 0.05. All statistical analysis was performed on a Power Macintosh (7500/100) computer, using commercially available software (Statview version 4.5, Abacus concepts Inc.).

Chapter 4: Model Characterisation

4.1 Planimetry

4.1.1 Methodology

Infarct size was determined by TTC staining, as described in the methods section 3.7. Because the heart slices are of such small cross sectional area (under 2 mm^2), the hearts have to be magnified to ensure adequate visualisation of infarcted versus viable tissue. To achieve this aim, heart slices are mounted between transparent perspex plates, 0.57 mm apart and photographed with a high resolution megapixel digital camera as described previously (section 3.7). The video image was imported into a Power Macintosh 7500/100 computer, copied and imported into an image analysis software package, available as free share software from the National Institutes of Health web site (http://rsb.info.nih.gov/nih-image/), called NIH Image (version 1.61). The image background was removed, and converted into a grey-scale image as described in 3.7.2, and an example is shown in figure 3.4. A custom macro-program was written by the author of this thesis to enable automatic analysis of infarct size. Based upon the light dark contrast, the macro program (listed in the appendix 1), measures first the total area of the heart slice, and then the total area of viable, dark stained myocardial tissue. The ischaemia/reperfusion models presented in this report consist of a global ischaemic insult, so further image processing to determine risk zone was unnecessary. Therefore, the infarct area of the heart slice could be determined by the difference between measured total and viable areas. For the whole heart, infarct to risk zone area is represented as a percentage of total measured infarct area as a proportion of total measured area of the heart slices. For inter-group comparison, the areas can be readily converted into volumes by the calibration of the camera at a set focal length used to capture the heart slices to set the pixel area of 1 mm^2, multiplied by the known heart slice thickness of 0.57 mm.

4.1.2 Characterisation and validation of planimetry software

4.1.2.1 Calibration of the Planimetry software

Before the camera/planimetry system could be routinely applied to the measurement of infarct size in experimental studies, the system and infarct measuring macro programme required thorough characterisation and validation to confirm that the methods for measurement were accurate and reproducible.

In the first instance, the grey scale recognition of viable versus necrotic myocardium required calibration. To achieve this, twenty mouse hearts subjected to an ischaemia/reperfusion insult were prepared, stained (as described in 3.7.1) and digitised as described in section 4.1.A. These hearts were then planimetered by an independent observer using the tracing methodology then currently used in the laboratory and slice and infarct areas recorded.

Through comparison of measured infarct size by the independent observer, grey scale thresholds could be determined for each slice for each heart analysed such that the measured area of necrosed tissue equalled that made by the initial observer. The grey shade threshold between what was determined to be viable myocardium from that deemed as necrosed was found to be highly variable, necessitating correction for variable TTC stain uptake into the hearts between individual samples and in accordance to ambient light causing automatic lens aperture correction in the digital imaging system. Through repeated observation, a simple formula was determined that could be applied to enable the grey-scale correction to be predicted. The result of the calibration is summarised in figure 4.1.1, with a highly significant ($p < 0.0001$) correlation (r^2) of 0.668 between threshold and darkness threshold for viable myocardium.

Attempts were also made to enable accurate automatic sensing of the region of interest (ROI, the total area of the heart slice, minus cavities and background). However, attempts to automatically delineate background proved unreliable, thus manual methods of determining the ROI were adopted.

4.1.2.2 Validation of the planimetry software

To determine whether the software based automatic planimetry methodology was reproducible, it needed to be compared with a gold standard method already routinely used in the laboratory. To this end, further mouse heart samples were prepared and the heart slices planimetered by an independent observer.

4.1.2.2.1 Determining the region of interest.

Two methods of determining the ROI were compared, using tools provided by the NIH Image software environment used by the infarct calculating macro programme:

1. Erasing the back ground using the eraser tool;
2. Tracing the boundary of the heart slice, copying the ROI from the image and pasting onto a blank white background.

Once the ROI was determined, the macro programme could be used to determine the infarct sizes in the heart slices in a blinded fashion, and the methods compared.

The first ROI determination method was found to be inadequate. Although compared to conventionally planimetered hearts, the total area of the heart slices were insignificantly

different from the computerised planimetry, the p value was 0.072 (Student's paired T-test). Therefore, this method was uncomfortably close to rejecting the desired 'null hypothesis' that there are no significant difference between conventional planimetry and the eraser method of determining ROI.

Using the tracing method of determining the ROI, heart slice areas were compared between conventional planimetry and the tracing method, again in blinded fashion, comparing a different cohort hearts. The correlation of total heart slice areas between manual planimetry and computerised planimetry was markedly improved, with a p value of 0.883.

Therefore, the tracing method for determining ROI was adopted for all further assessments of infarct to risk zone ratios.

4.1.2.2.2 Validation of infarct size measurements

Once a reliable methodology for determining the ROI was adopted, a further 15 hearts were examined, again comparing an independent observer's observation with infarct size data determined from the same heart slices in blinded fashion. The results of the statistical analysis are summarised in figure 4.1.B. Highly significant correlations were achieved between observer and computer based planimetry, both in terms of total slice area size ($r^2 = 0.986$, $p < 0.001$) and total infarct area ($r^2 = 0.995$, $p < 0.001$). On the basis of these results, all further planimetry was performed using the macro-based infarct size assessment.

4.1.3 Planimetry: the adopted method

After establishing a method to predict the grey-scale threshold between viable and necrosed tissue, and validating this against independent observation, the macro-based infarct measurement was the methodology adopted for all further infarct assessment.

Advantages:

- permanent record of heart slices can be kept on a digital media
- good inter-observer reproducibility
- measures infarction even where there are areas of patchy necrosis
- potentially labour saving

Disadvantages

- still requires the region of interest (the heart slice) to be identified
- grey scale correlation between viable tissue and necrosed myocardium, although good ($r^2 = 0.668$), is not perfect. This means that the planimetry is not entirely automatic, and adjustments to the grey-scale threshold adjustments may be required.

FIGURE 4.1.A. CALIBRATION REGRESSION CURVE FOR PLANIMETRY PROGRAMME.

Regression analysis demonstrating the relationship between the estimated grey scale data produced by the macro-programme and the grey scale required to reproduce the infarct sizes estimated by conventional planimetry.

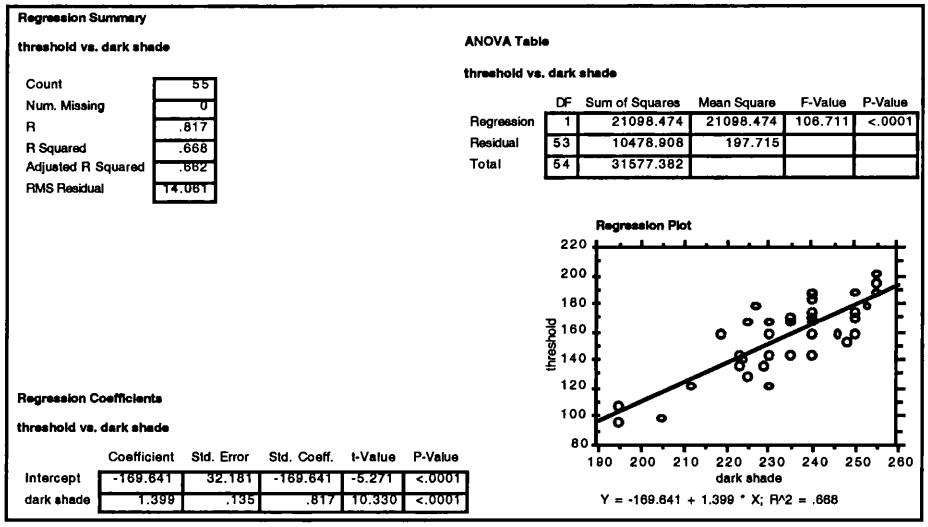

Regression Summary

threshold vs. dark shade

Count	55
Num. Missing	0
R	.817
R Squared	.668
Adjusted R Squared	.662
RMS Residual	14.061

ANOVA Table

threshold vs. dark shade

	DF	Sum of Squares	Mean Square	F-Value	P-Value
Regression	1	21098.474	21098.474	106.711	<.0001
Residual	53	10478.908	197.715		
Total	54	31577.382			

Regression Coefficients

threshold vs. dark shade

	Coefficient	Std. Error	Std. Coeff.	t-Value	P-Value
Intercept	-169.641	32.181	-169.641	-5.271	<.0001
dark shade	1.399	.135	.817	10.330	<.0001

FIGURE 4.1.B. VALIDATION OF COMPUTERISED PLANIMETRY.

As part of the infarct measurement macro programme validation, total myocardial and infarct volumes were measured using both traditional planimetry techniques and the computerised method. Good correlations were found between both measures, enabling the use of this system for future studies. Abbreviations used in figure: **infarct (a)** and **infarct (m)** are the infarct areas measured using the automated and manual planimetry, and similarly for **risk (a)** and **risk (m)** the total myocardial volumes measured by each technique respectively.

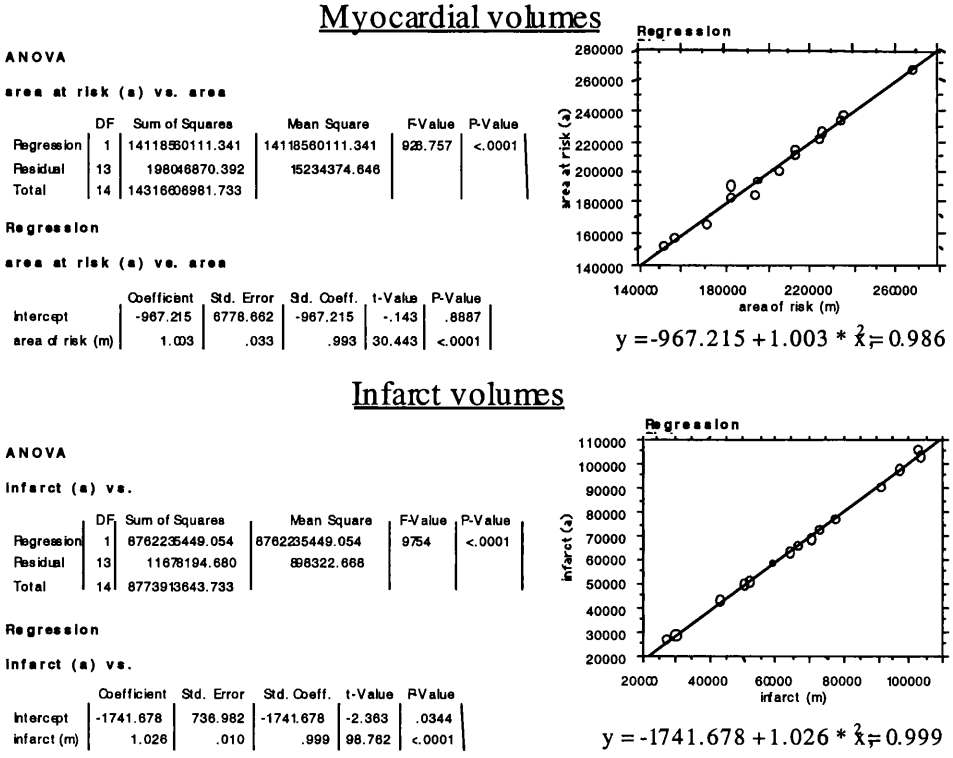

Myocardial volumes

ANOVA

area at risk (a) vs. area

	DF	Sum of Squares	Mean Square	F-Value	P-Value
Regression	1	14118560111.341	14118560111.341	926.757	<.0001
Residual	13	198046870.392	15234374.646		
Total	14	14316606981.733			

Regression

area at risk (a) vs. area

	Coefficient	Std. Error	Std. Coeff.	t-Value	P-Value
Intercept	-967.215	6778.662	-967.215	-.143	.8887
area of risk (m)	1.003	.033	.993	30.443	<.0001

$y = -967.215 + 1.003 * x$, $r^2 = 0.986$

Infarct volumes

ANOVA

infarct (a) vs.

	DF	Sum of Squares	Mean Square	F-Value	P-Value
Regression	1	8762235449.054	8762235449.054	9754	<.0001
Residual	13	11678194.680	898322.668		
Total	14	8773913643.733			

Regression

infarct (a) vs.

	Coefficient	Std. Error	Std. Coeff.	t-Value	P-Value
Intercept	-1741.678	736.982	-1741.678	-2.363	.0344
infarct (m)	1.026	.010	.999	98.762	<.0001

$y = -1741.678 + 1.026 * x$, $r^2 = 0.999$

4.2 Ischaemia/reperfusion protocol

In order to study the ischaemia/reperfusion injury associated with acute myocardial infarction, a reproducible model of injury and measurement is required. The chosen model was mouse, to take advantage of the various transgenic strains developed to investigate specific signalling pathways. To determine the optimal ischaemia/reperfusion protocol in the isolated mouse heart model, a series of experiments were performed to determine the effect of varying durations of global index ischaemia and reperfusion upon infarct size. As infarct size was to be used as the primary end points in all subsequent studies, accurate and reproducible measurement of infarction was essential.

4.2.1 Determining the optimal reperfusion duration

Previous studies in mouse have shown that 30 minutes of reperfusion is adequate for accurate determination of infarct size by TTC following an injurious 30 minute ischaemic insult; prolongation of reperfusion appeared to have minimal influence upon measurable infarction.[221, 307] However, in animal models other than mouse, a minimum period of reperfusion of 2 hours for accurate assessment of infarct size has been deemed as mandatory,[308] probably relating to the necessity of washing out dehydrogenase enzymes from necrotic cells with incompetent sarcolemmal membranes. The apparent discrepancy between the required reperfusion time in mouse compared to other animals models may, in part, be explained by the comparatively high flow rate per unit weight of myocardium (25 ml/g.heart weight/minute in mouse versus 4 ml/g.heart weight/minute in rabbit heart). However, to confirm whether 30 minute reperfusion is adequate in the present model, hearts from adult male B6,129 wild type mice were subjected to 30 minutes of normothermic global ischaemia, followed by three periods of reperfusion: 30, 60 and 120 minutes (protocol, figure 4.2).

The infarct size data are summarised in figure 4.3. Following a 30 minute ischaemic insult, prolonging the period of reperfusion had no significant effect upon infarct size; infarct sizes at 30, 60 and 120 minutes were respectively 33 ± 3%, 34 ± 4% and 34 ± 3% with no statistical difference between groups.

The lack of a measurable difference in infarction between short and long durations of reperfusion would suggest that ischaemia/reperfusion injury is rapidly resolved in this mouse model. Whether extending reperfusion further (> 24 hours) would influence measurable necrosis was not investigated here, as this is impractical in a Langendorff model. However, in *in vivo* models, prolonging reperfusion over a period of days appears not to be associated with larger measured infarcts; in dog, Tanaka et al failed to observe larger infarcts at four days than after 4 hour reperfusion.[309]

Given the current observations (and those of other members of our group, i.e. Marber and Sumeray[221, 307]) demonstrating that 30 minutes reperfusion was adequate for accurate TTC estimation of infarction, this was the reperfusion protocol used for all further experiments outlined in this thesis.

FIGURE 4.2. INCREASING REPERFUSION DURATION AND INFARCTION PROTOCOL.

Isolated, Langendorff perfused hearts were allowed to stabilise for 20 minutes before being subjected to a standardised 30 minute, normothermic global ischaemic insult. Thereafter, the hearts were allowed to recover in reperfusion for 30, 60 or 120 minutes prior to the hearts being stained in TTC for infarct analysis.

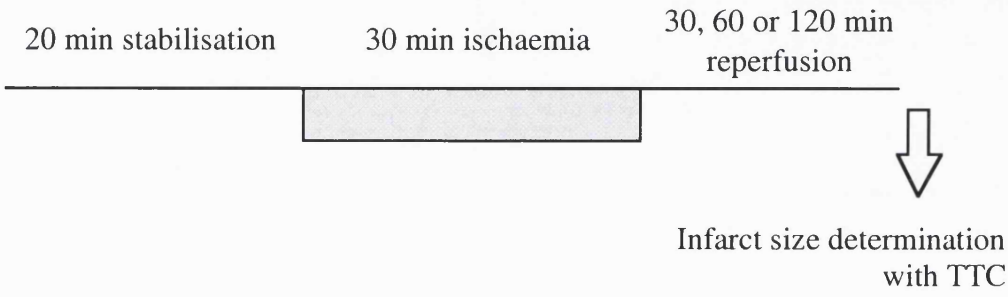

Infarct size determination with TTC

FIGURE 4.3. THE EFFECT OF INCREASING DURATION OF REPERFUSION UPON INFARCT SIZE.

The influence of reperfusion duration upon infarct size determined by TTC staining was examined. All hearts were subjected to a 30 minute normothermic global ischaemic insult. Figures below the bars represent the duration of reperfusion. No significant difference in infarct size was observed between hearts reperfused for 30, 60 or 120 minutes.

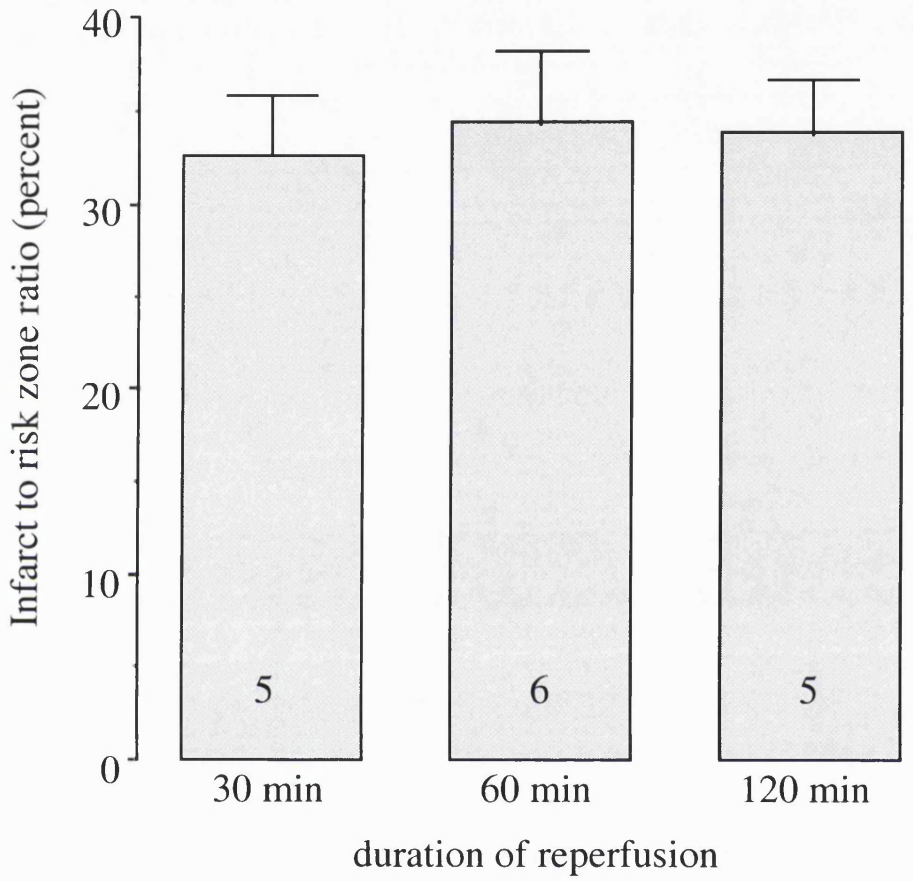

4.2.2 Determining the optimal duration of global ischaemia

Mouse hearts are small. With a typical myocardial weight of 160 mg from an adult male 25-30 gram mouse, the mouse heart weighs a tenth of a typical heart from an adult male 300 gram rat. Given the modest size of the mouse heart, and therefore small cross sectional area of the heart when sliced, there is a potential for a statistical/measurement type 1 error to occur with respect to measurement of infarct size in both control, and in particular with preconditioned hearts where infarct size were predicted to be 30-50% smaller than that found in control hearts. Therefore, it is desirable to obtain a reproducible infarct size of sufficient size from which preconditioning can result in a significant measurable infarct size reduction. Therefore these experiments were divided into two with separate aims:

1. to measure infarct size with increasing ischaemic duration thus determining the relationship between ischaemic period and infarct size, and
2. to determine whether, at these durations of global ischaemia, preconditioning manifests significant infarct size reduction, thus ascertaining the largest control infarct size with efficacious early ischaemic preconditioning.

4.2.2.1 Ischaemic duration and infarct size

To ascertain the effect of prolonging the period ischaemic injury in this model, hearts were subjected to periods of 30, 35, 40, 50 and 60 minutes of global ischaemia.
The experimental protocol (figure 4.4) consisted of 20 minutes of stabilisation prior to the index ischaemia and 30 minutes reperfusion after. Adult male mice were used in this investigation, weighing between 25-30 grams. As summarised in figure 4.5, no significant differences were noted between groups with respect to either body or heart weight.
Experimental results are summarised in figures 4.6-4.8. With increasing duration of ischaemia, there was a concomitant increase in infarct size (figure 4.6). However only ischaemic periods of greater than 40 minutes duration resulted in infarcts of significantly larger size than that seen at 30 minutes ischaemia. Infarct size at 30 minutes index ischaemia was 31 ± 4%, 35 minutes, 33 ± 2%, 40 minutes, 41 ± 9%, 50 minutes 47 ± 3% and 60 minutes, 59 ± 9%. p values for 50 and 60 minutes index ischaemia versus 30 minutes are 0.037 and 0.004 respectively. As would be predicted, increasing necrotic injury was also associated with increasing contractile dysfunction (figure 4.7) and deteriorating reperfusion coronary flow. Shorter ischaemic durations were associated with markedly improved function, with function following 30 minutes global ischaemia being modestly, but significantly greater than that observed after longer ischaemic insults. Prolonged ischaemia (greater than 40 minutes) was associated

with significant attenuation of functional parameters proportional to the degree of myocardial necrosis observed following TTC staining. Both function and coronary flow were significantly lower than that observed following shorter index ischaemic periods. On the basis of these measured parameters, only the three shorter (20, 35 and 40 minute) ischaemic durations were tested in the preconditioning phase of this investigation.

FIGURE 4.4. INCREMENTAL INDEX ISCHAEMIA DURATION PROTOCOL.

All hearts were Langendorff perfused for a 20 minute stabilisation period prior to index ischaemia. Hearts were then randomly ascribed to 30, 35, 40, 50 or 60 minute global ischaemia groups. After index ischaemia, all hearts were allowed to recover for 30 minutes, prior to determination of infarct size by TTC staining.

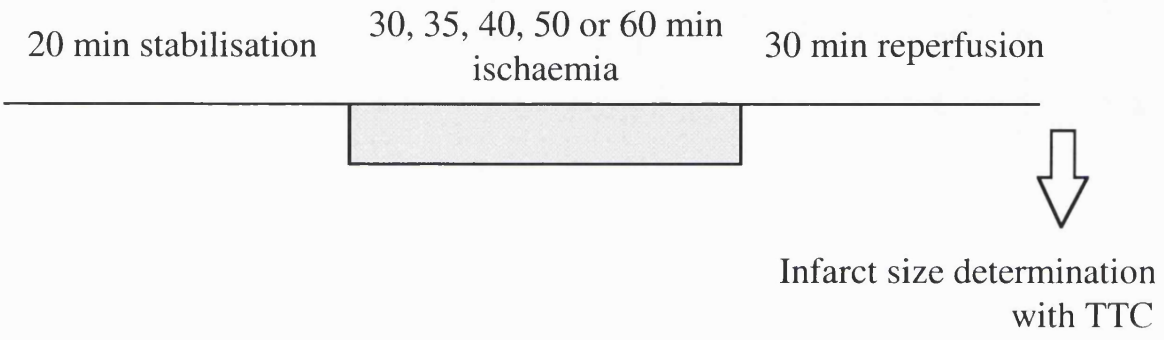

FIGURE 4.5. MORPHOMETRICS

Morphometrics were compared to exclude the potential for confounding influence of either unequal heart (**A**) or body (**B**) weight on later analysis. The number in the bars represents the number of animals in the group. The number under the bars signifies the duration of ischaemia to which the hearts were subjected to. No significant difference in either heart or body weights were measured between groups.

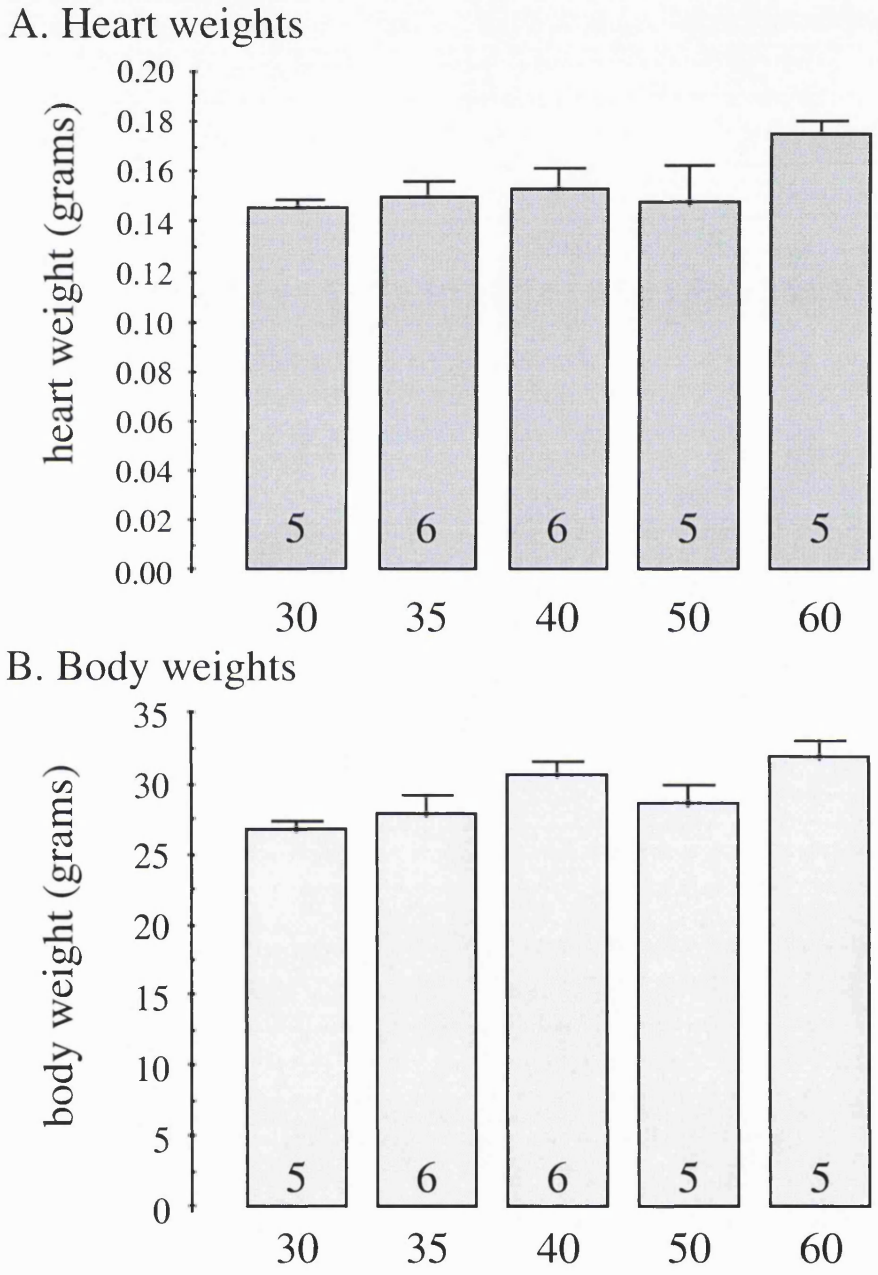

FIGURE 4.6. INDEX ISCHAEMIA DURATION AND INFARCT SIZE.

Increasing the duration of global ischaemia results in an increase in measured infarct size (**A**). By 50 minutes, infarction is significantly greater than that found at 30 minutes. Regression analysis confirms the correlation between ischaemic duration and infarction (**B**).

*, p = 0.037 versus 30 minute index ischaemia.

**, p = 0.004 versus 30 minute index ischaemia.

A. Infarct to risk zone bar-graph with incremental ischaemia.

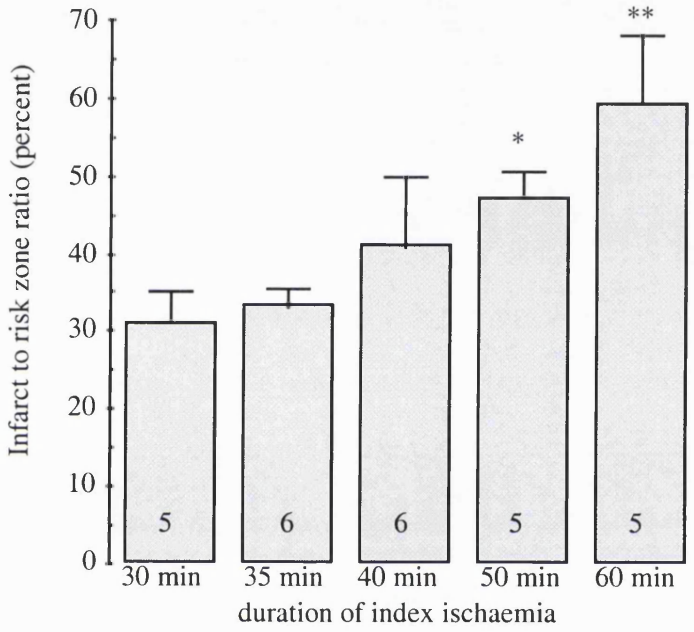

B. Simple regression curve: infarct size is significantly correlated to ischaemia duration.

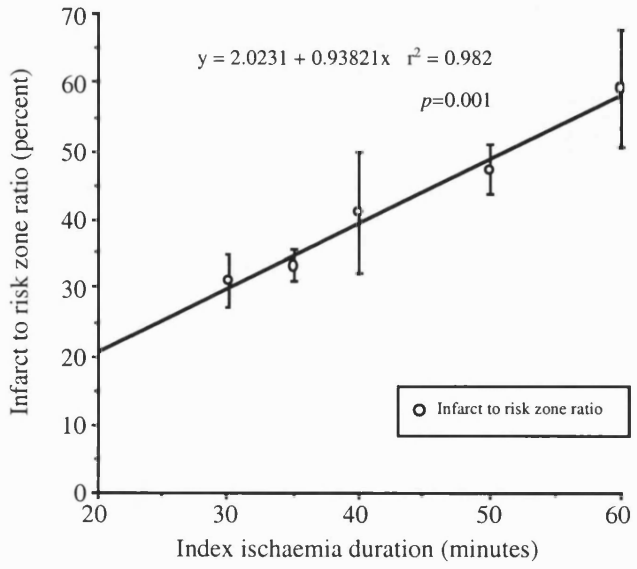

Table 1. Baseline Contractile and coronary flow function.

No sigificant differences were noted between groups with respect to either baseline coronary flow or contractile function.

Group	Contractile function (force-rate product, g.beat.min^{-1})	Coronary flow rate (ml.min^{-1})
30 minute ischaemia (n = 5)	1135 ± 77	3.0 ± 0.5
35 minute ischaemia (n = 6)	1173 ± 126	3.3 ± 0.3
40 minute ischaemia (n = 6)	1168 ± 74	3.6 ± 0.4
50 minute ischaemia (n = 5)	1209 ± 136	3.5 ± 0.3
60 minute ischaemia (n = 5)	1179 ± 181	3.6 ± 0.2

Figure 4.7. Contractile recovery following global ischaemia.
Contractile function following global ischaemia was measured and compared. No significant difference was noted between 30 and 40 minutes of global ischaemia. Longer durations of ischaemia resulted in significant attenuation of function compared to 30 minutes index ischaemia. ($p < 0.001$). Number of hearts per group were 5, 6, 6, 5 and 5 for the 30, 35, 40, 50 and 60 minute ischaemia groups respectively.

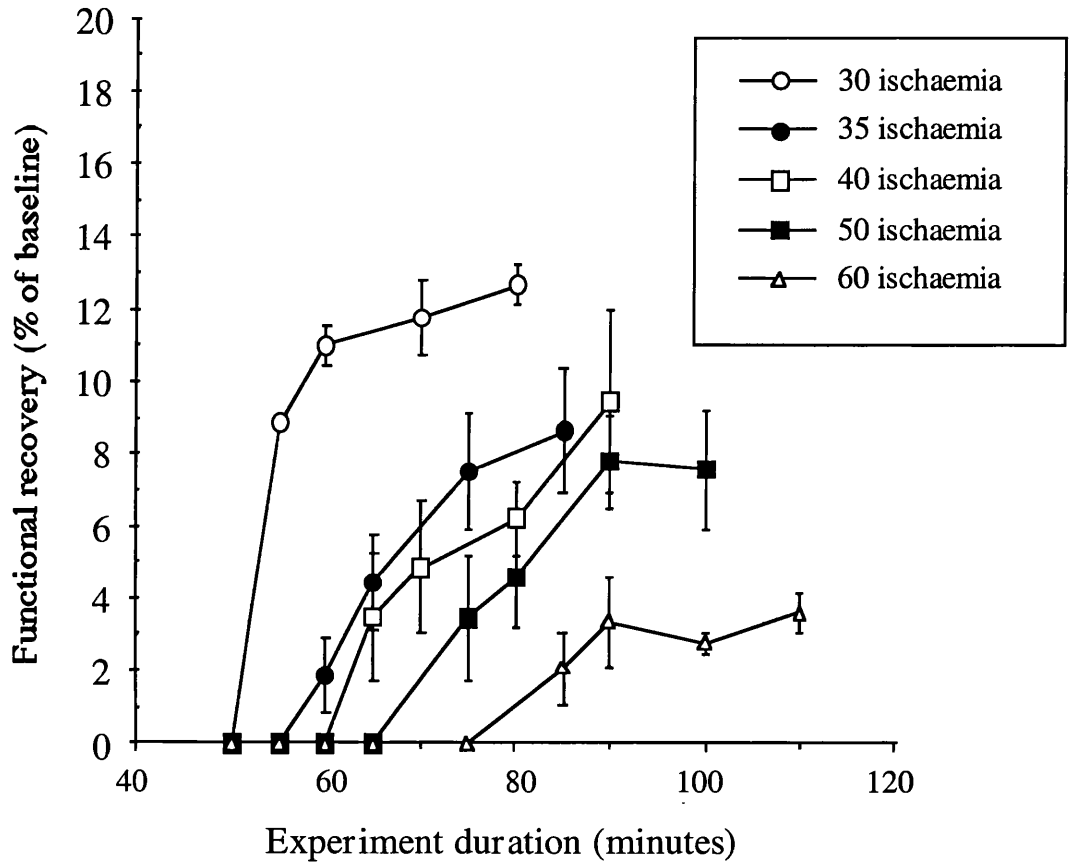

FIGURE 4.8. CORONARY FLOW FOLLOWING INDEX ISCHAEMIA.

Increasing durations of index ischaemia resulted in a significant dose-dependent attenuation of reperfusion coronary flow. Following 60 minutes of index ischaemia, the coronary flow was half of that observed following 30 minutes index ischaemia ($p < 0.0001$). Number of hearts per group were 5, 6, 6, 5 and 5 for the 30, 35, 40, 50 and 60 minute ischaemia groups respectively.

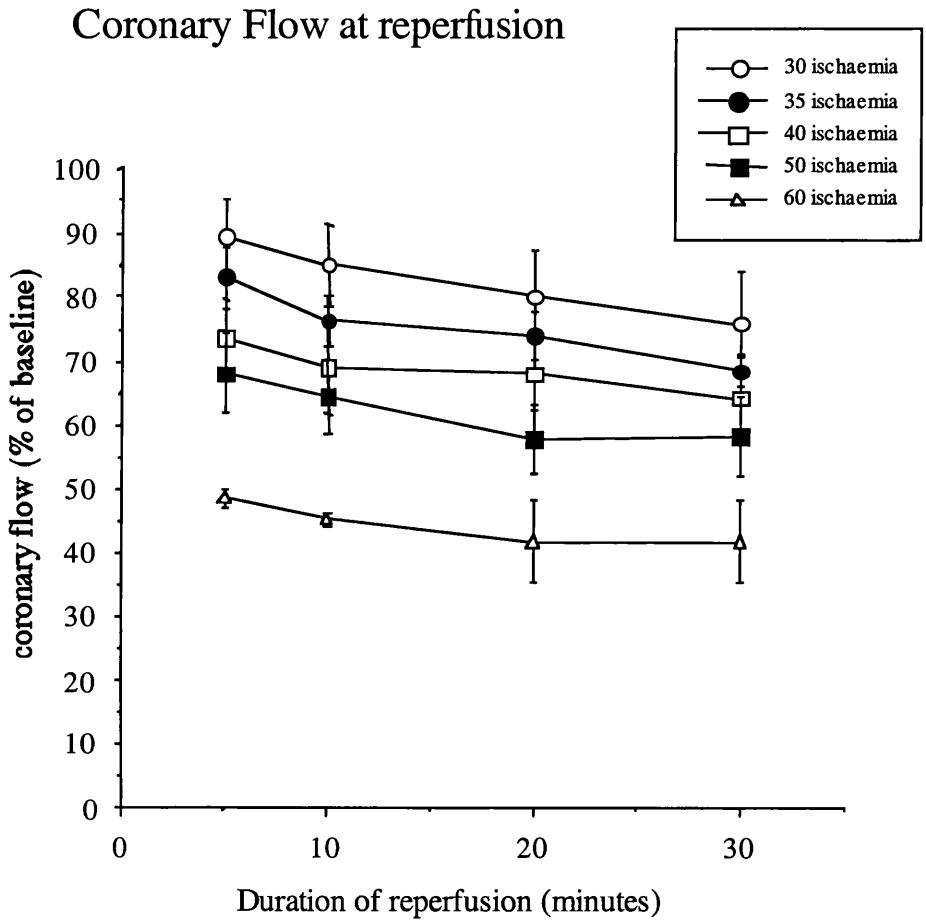

4.2.2.2 Efficacy of preconditioning against increasing injurious ischaemia

Ischaemic preconditioning results in significant attenuation of necrotic cell death in all mammalian species studied.[62] The challenge in the murine heart relates to the measurement of infarction, as discussed in section 4.2. Ideally, there should be as great a difference between control and preconditioned infarct size as possible to aid in accurate delineation of effect. Therefore, in this series of experiments, the efficacy of preconditioning was assessed with ischaemic durations of 30, 35 and 40 minutes of index ischaemia (protocol, figure 4.9). Longer durations of index ischaemia (≥50 minutes) appears too injurious (section 4.2.2.1), and therefore not analysed here.

The ischaemic preconditioning regime used for these experiments, based upon the observations of Sumeray et al,[310] consist of 2 cycles of 10 minutes ischaemia and 10 minutes reperfusion. Control animals were perfused in time matched fashion (figure 4.9). Whilst this represents a robust regime for inducing preconditioning (preconditioning against infarction has been observed against 20 minutes global ischaemia with as little as 2.5 minutes ischaemia in the isolated mouse heart[311]), this regime was thought desirable to elucidate maximal response against prolonged ischaemia.

The results are summarised in figures 4.10 and 4.11(A, B and C).

Significant protection against infarction was observed in all three experimental groups. Preconditioning against 30 minutes ischaemia resulted in a 28.5% reduction of infarct size (36 ± 3% to 25 ± 5% in controls and preconditioning respectively, $p = 0.008$), which was associated in significantly improved functional recovery (figure 4.11.A, $p < 0.001$). Preconditioning against a 35 minute ischaemia resulted in a 31.3% reduction of infarction (33 ± 2% to 23 ± 1%, $p = 0.031$), and again, highly significant improvement in functional recovery (figure 4.11.B, $p < 0.001$). Preconditioning against 40 minutes ischaemia results in a 24.4% reduction of infarction (38 ± 5% to 29 ± 2%, $p = 0.025$) and improvement in post ischaemic function (figure 4.11.C, $p = 0.034$). Whilst preconditioning remained effective against 40 minute ischaemia, the relative reductions of infarct size and improvement in function were comparatively modest, and thus not an ideal ischaemia/reperfusion regime for further study. Preconditioning against 30 and 35 minute ischaemic insults was equally efficacious, therefore, given the marginally greater infarct size reduction resulting from preconditioning in the 35 minute ischaemia group, this was the ischaemia/reperfusion regime adopted for all future experimental studies in this thesis.

FIGURE 4.9. PRECONDITIONING WITH INCREMENTAL INDEX ISCHAEMIA PROTOCOL.

Hearts were randomly assigned to control or ischaemic preconditioning (IPC) groups. Ischaemic preconditioning consisted of 2 cycles of 10 minute ischaemia and 10 minutes reperfusion. In controls, in place of the ischaemia preconditioning protocol, the hearts were instead normally perfused for a further time-matched 40 minutes prior to index ischaemia. Three durations of index ischaemia were examined: 30, 35 and 40 minutes. All hearts were reperfused for 30 minutes prior to determination of infarct size by TTC staining.

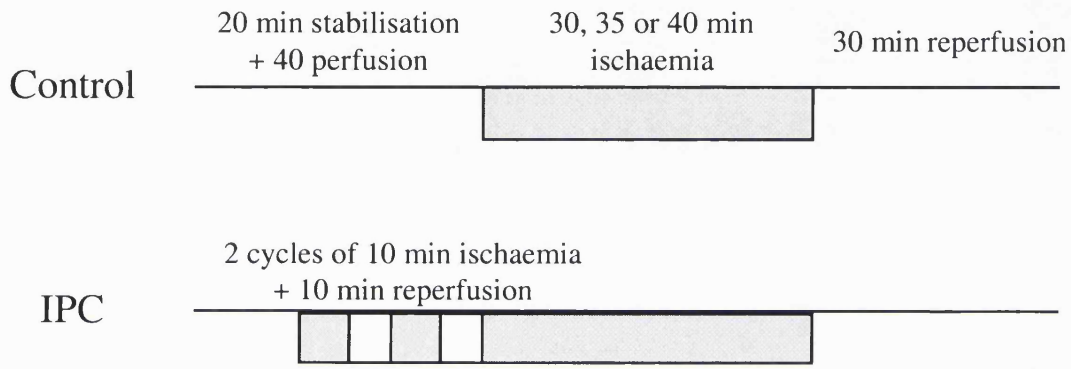

Table 2. Morphometrics and baseline coronary flow and function.

No significant differences were measured between groups in terms of body or heart weight, or in baseline contractle function or coronary flow.

Group	Body weight (grams)	Heart weight (grams)	Contractile function (force-rate product, $g.beat.min^{-1}$)	Coronary flow rate ($ml.min^{-1}$)
30 minute control (n = 5)	28.5 ± 2.0	0.14 ± 0.01	1320 ± 114	3.4 ± 0.1
30 minute preconditioned (n = 5)	27.1 ± 0.4	0.15 ± 0.01	1219 ± 57	3.1 ± 0.1
35 minute control (n = 6)	28.2 ± 1.2	0.15 ± 0.01	1279 ± 66	3.3 ± 0.3
35 minute preconditioned (n = 6)	26.5 ± 0.3	0.14 ± 0.01	1362 ± 150	3.3 ± 0.2
40 minute control (n = 5)	30.0 ± 3.4	0.15 ± 0.02	1200 ± 87	2.3 ± 0.2
40 minute preconditioned (n=5)	27.8 ± 1.0	0.16 ± 0.01	266 ± 119	3.4 ± 0.4

FIGURE 4.10. PRECONDITIONING WITH INCREMENTAL ISCHAEMIA.

Three durations of index ischaemia were tested in this study: 30, 35 and 40 minutes. In each group, hearts were randomly assigned to either time matched control or preconditioning (**pc**). At all three time points, significant attenuation of infarct size was observed, with p-values of 0.0075, 0.0309 and 0.0253 for 30, 35 and 40 minutes index ischaemia respectively. The infarct reduction resulting from preconditioning of 31% in the 35 minute index ischaemia group represented the largest proportional change of the three groups examined.

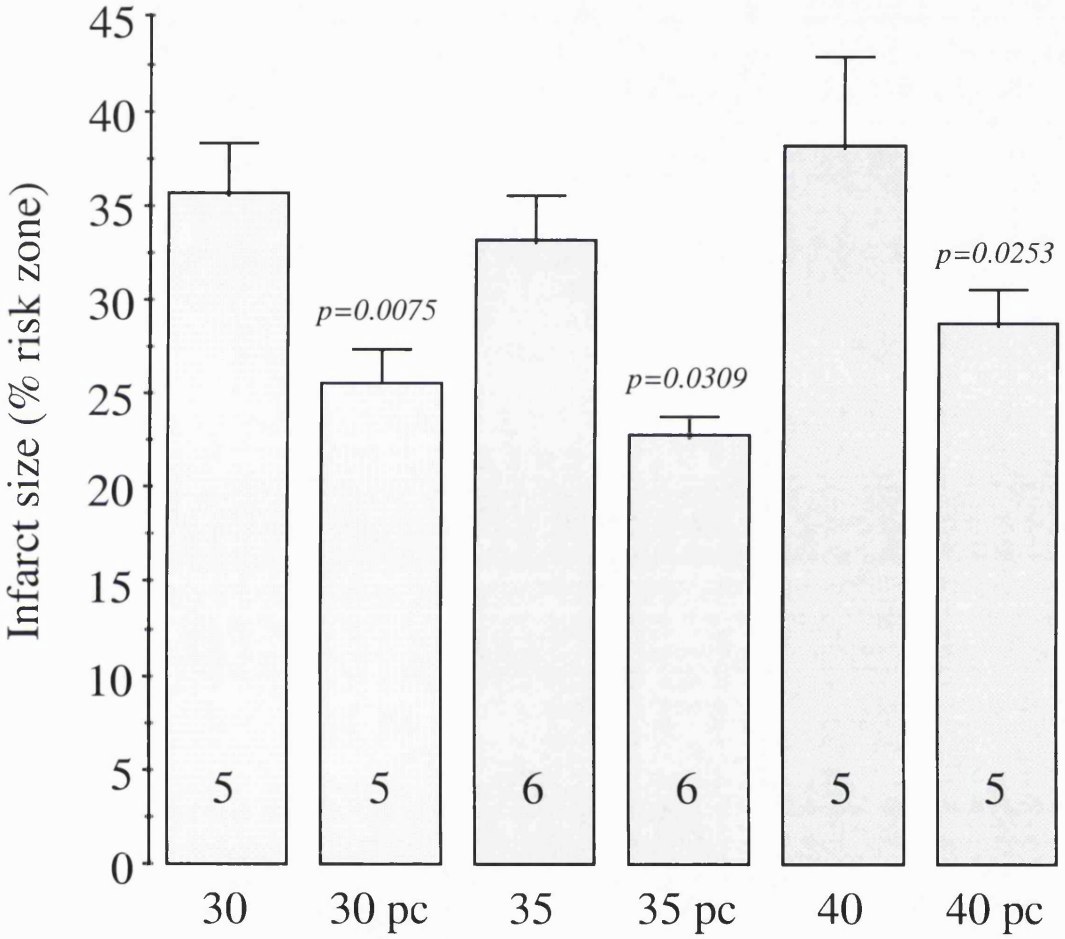

FIGURE 4.11. PRECONDITIONING AND FUNCTIONAL RECOVERY FROM ISCHAEMIA

Contractile recovery represented as a percentage of baseline, end-stabilisation, function. In all three groups preconditioning (**pc**) resulted in modest, yet significant improvement in post-ischaemic function. This is most evident following 30 and 35 minute ischaemia. Comparing control versus preconditioning, **A**: $p < 0.001$; **B**: $p < 0.001$; **C**: $p = 0.0345$. Number of hearts per group were 5, 6 and 5 in both the pc and control arms of the 30, 35 and 40 minute ischaemia groups respectively. Raw data recorded in table 2.

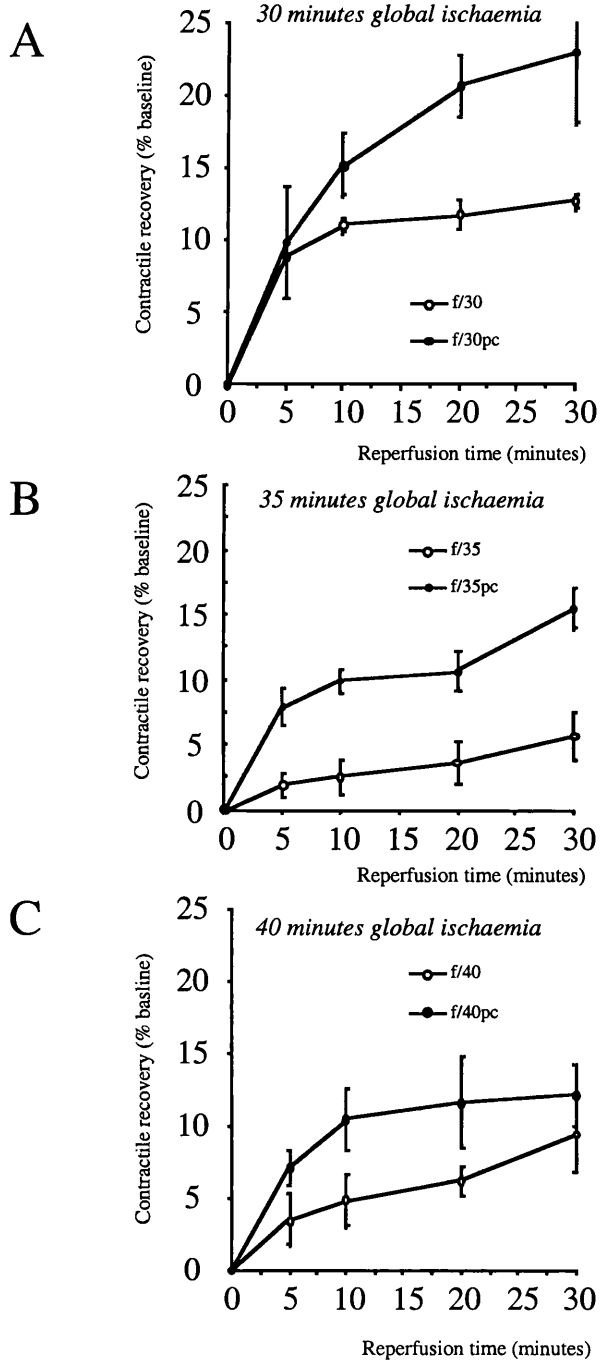

4.3 Harvesting heart does not trigger preconditioning: evidence for a role of PKC in early ischaemic preconditioning in mouse

The preliminary ischaemia/reperfusion studies discussed in section 4.2.2.2 show that ischaemic preconditioning with 2 cycles of 10 minutes ischaemia and 10 minutes reperfusion provides protection against 35 minute ischaemia/ 30 minute reperfusion induced injury (representing an approximately 30% reduction of infarction versus control). Compared to early ischaemic preconditioning in other animal species, such as rabbit, global preconditioning has an infarct sparing effect in *regional* models of lethal ischaemia/reperfusion injury of greater than 65%.[312] Therefore the model used in this thesis appears to have comparatively poor preconditioning induced myocardial protection against ischaemia/reperfusion injury.

There are two potential explanations for the comparatively disappointing protection observed in this *global* ischaemia/reperfusion model of isolated mouse heart injury. First is that this is a model dependent observation: others, using Langendorff perfused mouse heart models of global ischaemia/reperfusion, have found similar control infarct sizes and infarct size limitation following ischaemic preconditioning to that described here in section 4.2.2.2.[310, 311] Interestingly, where hearts are subjected to regional ischaemia, infarct size appears to be concomitantly larger, and preconditioning concomitantly more effective.[313] The second possibility is that the hearts have become ischaemically preconditioned in the process of harvesting the heart from the euthanased mouse. Thus, all hearts are preconditioned, including controls; the preconditioning represents only "super-added" protection, and therefore infarct size reduction is not as great as might be predicted when compared to controls.

To exclude the possibility that the hearts have become preconditioned in the process of mounting the hearts on the perfusion apparatus, the hypothesis that the harvesting procedure causes preconditioning needed to be tested. If the hypothesis were correct, an inhibitor of preconditioning administered prior to euthanasia of the animal would result in larger infarcts resulting from an ischaemia/reperfusion regime compared to hearts from animals that had not received the preconditioning inhibitor. To be administered prior to anaesthetic, the preconditioning would need to have a long half-life and be lipid soluble to remain in the myocardial tissue after the cessation of corporeal circulation. The agent would also have to be an effective inhibitor of the preconditioning cascade. One potential target would be PKC (discussed in section 1.5.2.1). The PKC antagonist, chelerythrine, has the necessary pharmacodynamic and pharmacokinetic properties required, being a lipophillic compound with a long half life and elimination time. Furthermore, PKC has been shown to be an obligatory component of the

preconditioning cascade in a large number of mammalian species.[62] However, PKC's involvement in preconditioning in all species is controversial; some investigators have demonstrated that pig hearts can be ischaemically preconditioned in presence of a PKC inhibitor[103] and that abrogation of protection required the combined inhibition of both PKC and TK.[104] Therefore, because of the relative lack of characterisation of the murine model, it was unknown until recently[314] whether PKC is involved in the mediation of early preconditioning in mouse, and whether the preconditioning signalling cascades were similar to that found in other small rodent species. Thus, in order to test the 'pre-preconditioning' hypothesis, the obligatory role of PKC in ischaemic preconditioning would also require testing.

Mice were pre-treated with the PKC inhibitor, chelerythrine (5 mg/kg, *ip*), 10 minutes ante-mortem, prior to the administration of anaesthesia (protocol, see figure 4.12). To determine whether PKC plays a role in early ischaemic preconditioning in mouse, hearts from chelerythrine treated animals were also ischaemically preconditioned with the two cycle, 10 minute ischaemia and reperfusion preconditioning protocol identical to that used in the previous study (described in section 4.2.2.2). Control animals to the chelerythrine treated group received an equivalent volume of the vehicle (saline) *ip*, 10 minutes ante-mortem, and were randomly assigned to control or ischaemic preconditioning groups.

The infarct size assessment results are summarised in figure 4.13. Pre-treatment of the animals 10 minutes ante-mortem with chelerythrine had no effect upon infarct size of control hearts subjected to 35 minutes normothermic global ischaemia and reperfusion (vehicle control, 33 ± 2% versus chelerythrine control, 33 ± 3%, $p = 0.924$). The lack of modification of infarct size in these control groups suggests that there was no antecedent preconditioning in these hearts. This observation is however reliant upon the assumption that preconditioning in mouse heart is dependant upon the obligatory involvement of PKC.

Preconditioning resulted in a robust reduction of infarct size in hearts from vehicle treated animals. In contrast, hearts from animals that had been treated with chelerythrine 10 minutes ante-mortem, received no benefit from the preconditioning regime: the infarct sparing effect was completely abrogated (vehicle, 22.79 ± 0.99 versus chelerythrine treated group, 33 ± 4%, $p = 0.016$).

The infarct data were mirrored by the functional data (figure 4.14 A and B). Comparing control hearts from animals that had received either chelerythrine or the saline vehicle, the PKC inhibitor had no influence upon contractile recovery. Ischaemic preconditioning resulted in significant improvement in post-ischaemic cardiac function in hearts from vehicle treated animals (figure 4.14 A, $p = 0.001$). Chelerythrine abolished this protective effect of ischaemic preconditioning (figure 4.14 B), consistent with similar observations in the rat.[315]

Therefore, these results demonstrate that ischaemic preconditioning in mouse heart is dependent upon the activation of PKC. Furthermore there is no evidence of any difference between control hearts from animals pre-treated with either chelerythrine or vehicle, implying that the harvesting technique used to isolate the hearts does not trigger a preconditioning response.

In summary therefore, the explanation for the comparatively disappointing infarct size limitation in this model of global ischaemic model of ischaemia/reperfusion injury is not secondary to the heart isolation technique. The comparatively small reductions in infarct size would therefore appear to be a model dependent phenomena, related either to the use of *global* index ischaemia as opposed to *regional* index ischaemia, or to the differences implicit with an *in-vitro* rather than an *in-vivo* procedure.

FIGURE 4.12. PKC IN PRECONDITIONING PROTOCOL.

Animals received either saline (**vehicle**) or 5 mg/kg chelerythrine bolus *ip*, (**Chel**) 10 minutes prior to euthanasia and harvesting of the hearts. Langendorff perfused hearts were randomised to either a time matched perfusion (**control**) group or an ischaemic preconditioning (**IPC**) group, and subjected to an ischaemia reperfusion regime prior to determination of infarct size with TTC.

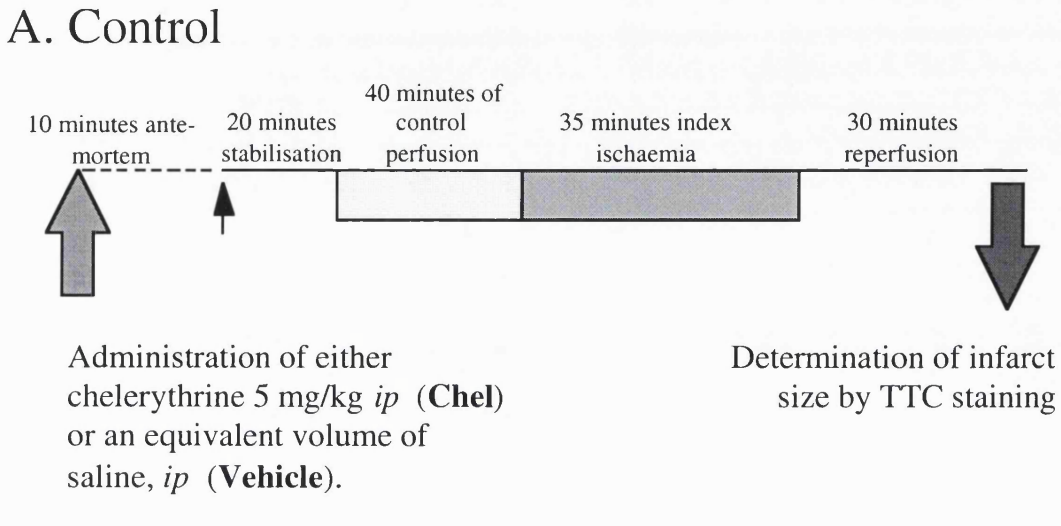

Table 3. Summary of body and heart weights plus baseline coronary and contractile function raw data.

No significant differences were noted between groups in body weight, heart weight, baseline contractile function, or baseline coronary flow.

Group	Body weight (grams)	Heart weight (grams)	Contractile function ($g.beat.min^{-1}$)	Coronary flow ($ml.min^{-1}$)
Control Vehicle (n = 6)	28.5 ± 1.0	0.15 ± 0.00	1354 ± 91	3.3 ± 0.2
Preconditioned vehicle (n = 6)	27.2 ± 0.7	0.14 ± 0.01	1328 ± 131	3.2 ± 2
Control chelerythrine (n = 6)	29.3 ± 1.6	0.16 ± 0.01	1502 ± 181	3.4 ± 0.4
Preconditioned chelerythrine (n = 6)	29.9 ± 0.6	0.15 ± 0.01	1183 ± 135	3.1 ± 0.3

Figure 4.13. Chelerythrine abrogates ischaemic preconditioning.
Hearts from chelerythrine treated animals failed to show any infarct limitation resulting from the preconditioning regime that resulted in significant attenuation of infarction in hearts of animals treated with a saline vehicle bolus. Furthermore, control hearts in chelerythrine treated group had an infarct size identical to that observed in the vehicle control group. Therefore PKC is essential for murine ischaemic preconditioning, and the harvesting technique does not result in preconditioning.

Abbreviations used in figure:

Vehicle: hearts from saline vehicle pre-treated animals,

Chel: hearts from chelerythrine pre-treated animals,

IPC: ischaemic preconditioning,

Control: time matched perfusion.

** p = 0.012 versus vehicle control, and p = 0.016 versus chelerythrine IPC group. 6 hearts were used per group.

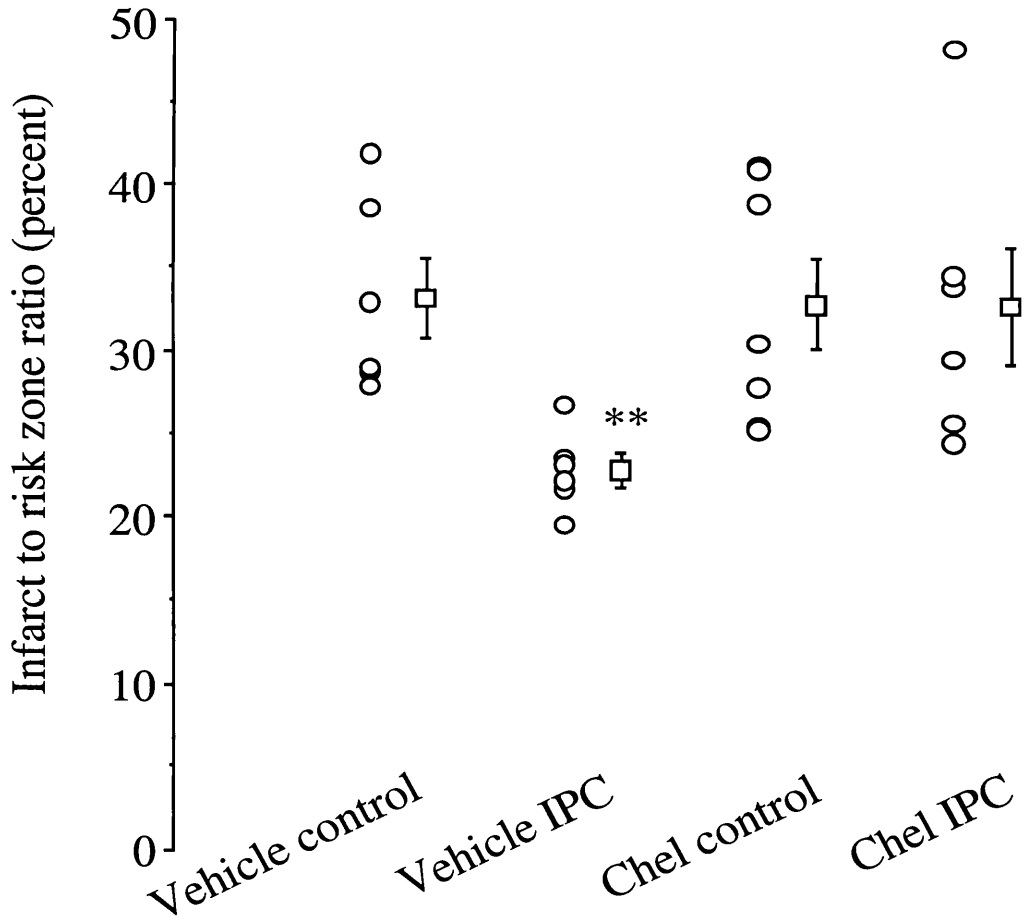

FIGURE 4.14. PRECONDITIONING AGAINST STUNNING REQUIRES PKC.

Post-ischaemic contractile dysfunction is modestly, but significantly, reduced by ischaemic preconditioning (**A**, ** p = 0.001). This resistance to stunning is completely abrogated by the prior administration of the PKC inhibitor, chelerythrine (**B**, p = 0.001 chelerythrine (Chel) versus vehicle pre-treated preconditioned hearts). n = 6 per group. Baseline fibures are included in table 3.

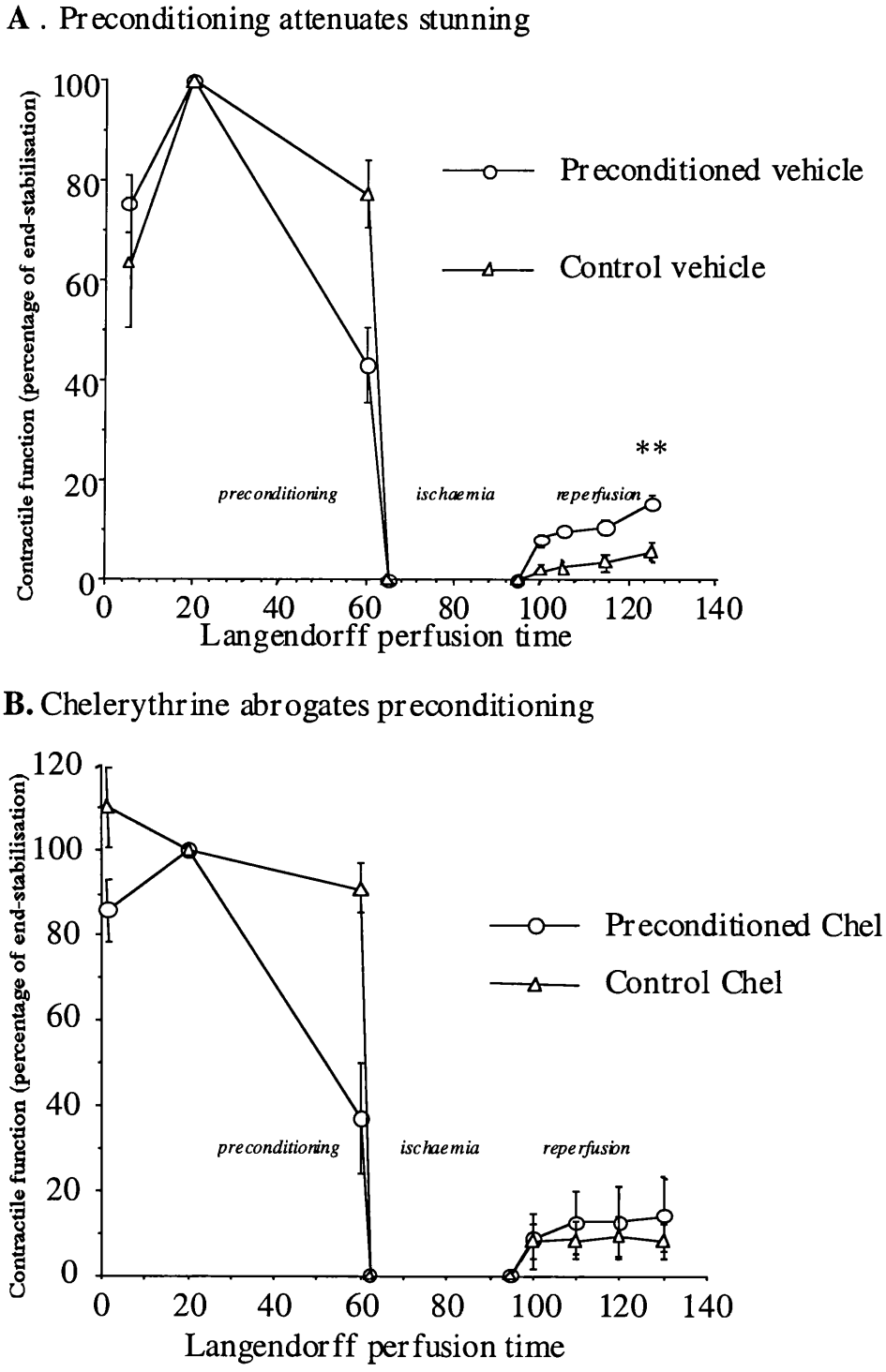

4.4 The influence of strain and gender upon ischaemic injury

4.4.1 The influence of genetics upon infarct susceptibility

The planned investigations of the role of NO in ischaemia/reperfusion injury required the use of a number of mouse strains sourced from a number of separate suppliers, including eNOS wild type and knockouts, iNOS wild types and knockouts, signal transducer and activator of transcription factor 1 (STAT-1, a gene transcription factor that up regulates a number of genes, including that of iNOS[316]) wild types and knockouts, and proprietary Swiss White mice. Whilst the eNOS and iNOS animals are bred at UCL, under licence from Jackson Laboratory Inc. (Bar Harbor, ME USA), STAT-1 and Swiss White animals are bought in from Washington University (shipped by Taconic Inc., and maintained in Rabies quarantine in UCL Biological services), and Harland Ltd respectively. Therefore, given the potential influences of genetic background and environmental factors upon infarct size, isolated hearts from these four groups of animals were compared with respect to susceptibility to infarction following the standardised ischaemia/reperfusion regime.

To test the hypothesis that each mouse strain would have equivalent infarct susceptibility following an ischaemic insult, 6 adult male mice from each group (the wild type strain were appropriate) were subjected to 35 minutes global ischaemia and 30 minutes reperfusion prior to infarct size determination (protocol, figure 4.15). All mice were aged between 2 to 3 months, weighing between 25 to 30 grams; the morphometric summary is shown in figure 4.16; heart size to body weight ratio in each strain examined were identical.

Following the ischaemia/reperfusion protocol, myocardial infarct sizes and coronary flow were examined, and the results are summarised in figures 4.17 and 4.18. Significantly each strain of mouse appear to posses different sensitivities to lethal ischaemic injury. NOS B6,129 wild type mouse strains had the largest infarcts (eNOS WT, 35 ± 2%, iNOS WT 33 ± 3%), whilst the Swiss white (20 ± 2%) and the STAT-1 wild type strain (129/SvEv) (15 ± 3%) mice had significantly smaller infarcts ($p < 0.001$, compared to eNOS and iNOS strains). Comparing coronary flow between the strains, no difference between either baseline coronary flow rate (eNOS 3.77 ± 0.42, iNOS 4.00 ± 0.52, STAT-1 3.10 ± 0.17, Swiss White 3.217 ± 0.28 ml/min) measured at the end of the reperfusion period, or following the ischaemic insult. Therefore, it would appear that microvascular function is not responsible for the variation in infarct size.

Similar findings to those presented here were found in a recent study in rat which a number of strains of rat were examined and infarct size and function examined over a 3

hour reperfusion period following a 27 minute global ischaemic insult.[317] Associated with genetic polymorphisms found between the in-bred strains examined, Brown Norway rats were found to have the greatest resistance to ischaemic injury, implying genetic variability to infarct resistance. Unlike the mouse strains presented here, the greater infarct size resistance in Brown Norway rats was also concomitant with better post-ischaemic vascular function. The mechanisms of the differences in infarction between groups were not investigated further in this study. However, these data do emphasise the importance of genetic differences that need to be considered when using different strains of animal in studies involving cardioprotection. For purposes of consistency and comparison, the studies presented here, unless otherwise stated, used B6,129 (eNOS wild type) strain mice.

FIGURE 4.15. PERFUSION PROTOCOL: ASSESSMENT OF GENETIC RESISTANCE TO INFARCTION.

Isolated mouse hearts from each strain investigated were subjected to an identical standardised ischaemia/reperfusion regime as previously described. In brief, hearts were perfused on the Langendorff rig and allowed to stabilise for 20 minutes. The hearts were then subjected to a 35 minute, normothermic, global ischaemic insult, prior to entering reperfusion for 30 minutes. At this time the experiment was terminated, and the hearts stained with TTC to determine infarct size.

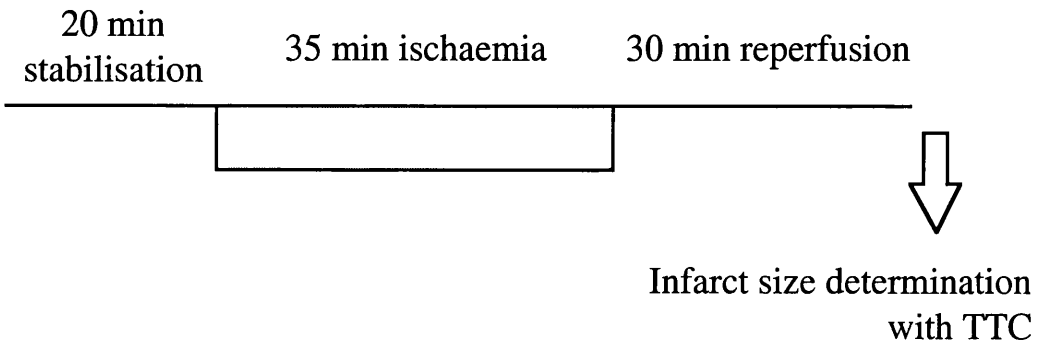

FIGURE 4.16. MORPHOMETRICS

To exclude the possibility of confounding variables due to species variation in (**A**) body weight or (**B**) myocardial weight, were compared and controlled across the four groups studied. No significant difference was observed for either variable (summarised below: Swiss white mice, NIH/SW; eNOS WT, eNOS wild type B9,129; iNOS WT, iNOS wild type B9, 129; and STAT-1 WT, STAT-1 wild type, 129 Sv Ev mice).

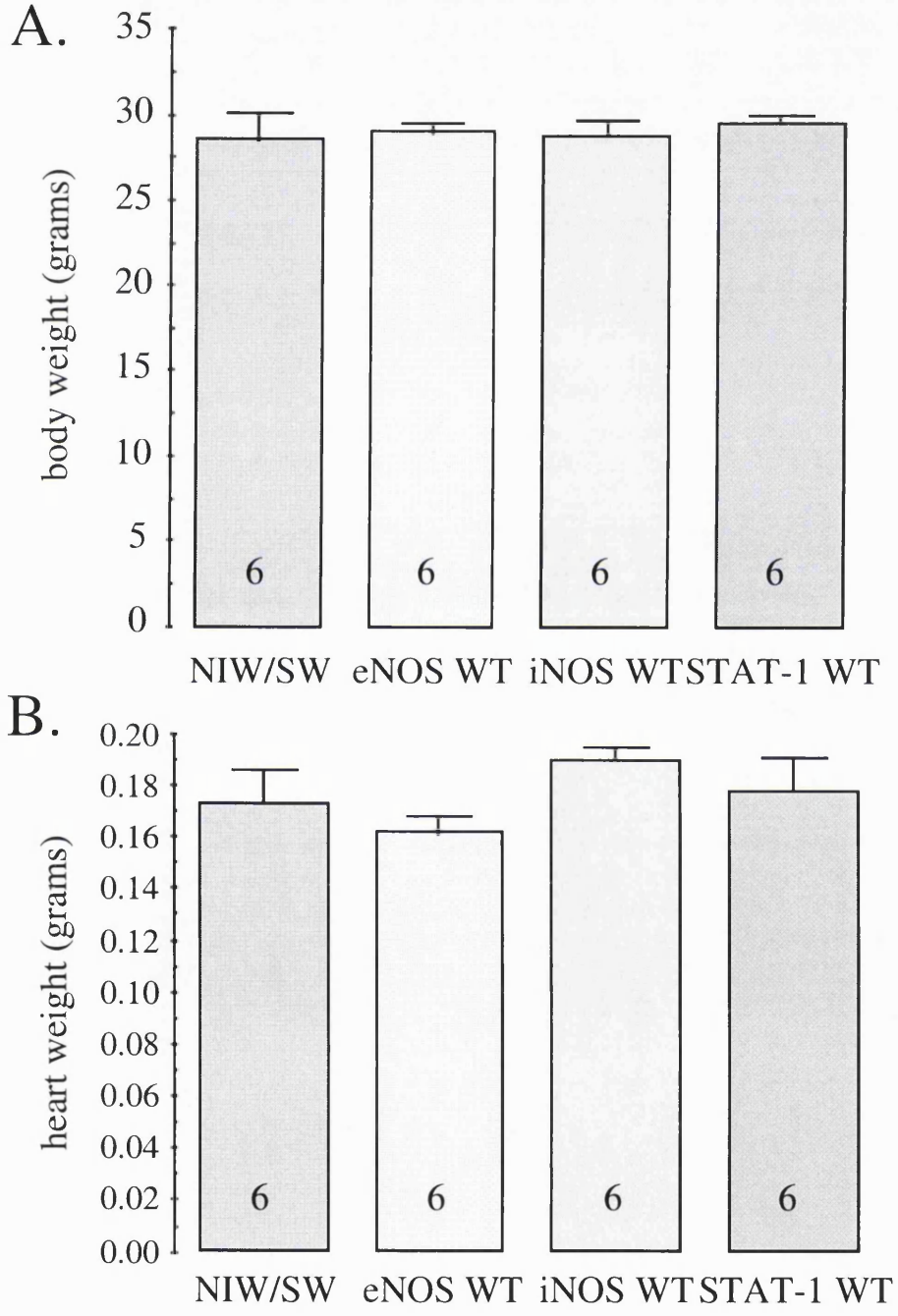

FIGURE 4.17. GENETIC SUSCEPTIBILITY TO INFARCT SIZE.

Commercially available Swiss white mice were compared to mouse strains used in the generation of transgenic mice. B6,129 hybrids used as controls for both the eNOS and iNOS knockout mice were used, as were C57/BL6 mice used as controls for the STAT-1 knockouts. Both the STAT-1 wild types and the Swiss white mice had infarcts that were significantly less than those observed in either of the NOS wild type strains. (** $p < 0.001$.)

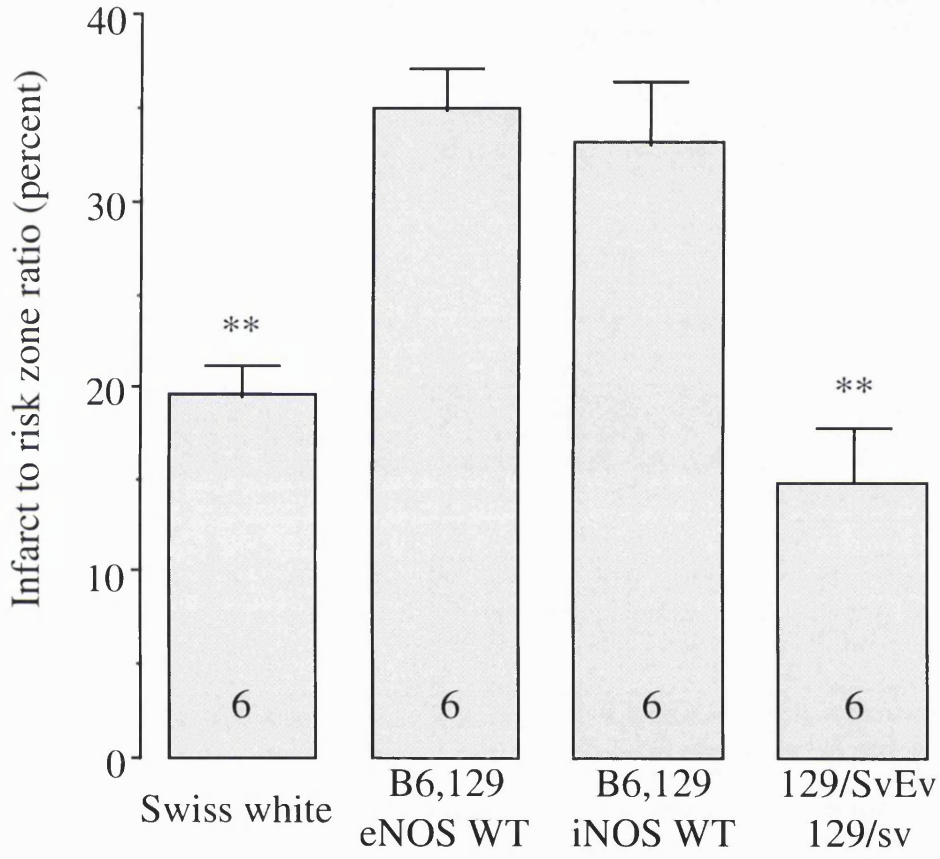

FIGURE 4.18. CORONARY FLOW RATE IN REPERFUSION.

To exclude the possibility that coronary vasculature may be responsible for the difference in infarct size (summarised figure 4.17), coronary flow rates were compared at reperfusion. The data displayed below are expressed as a percentage of base line coronary flow after 20 minutes stabilisation. No significant difference was observed between groups (summarised below: Swiss white mice, NIH/SW; eNOS WT, eNOS wild type B9,129; iNOS WT, iNOS wild type B9, 129; and STAT-1 WT, STAT-1 wild type, 129 Sv Ev mice). Base line coronary flow for each group respectively was 3.76 ± 0.42, 4.00 ± 0.52, 3.10 ± 0.17 and 3.22 ± 0.28 ml/min, p = NS. n = 6 per group. There was no significant difference in baseline coronary flow between groups.

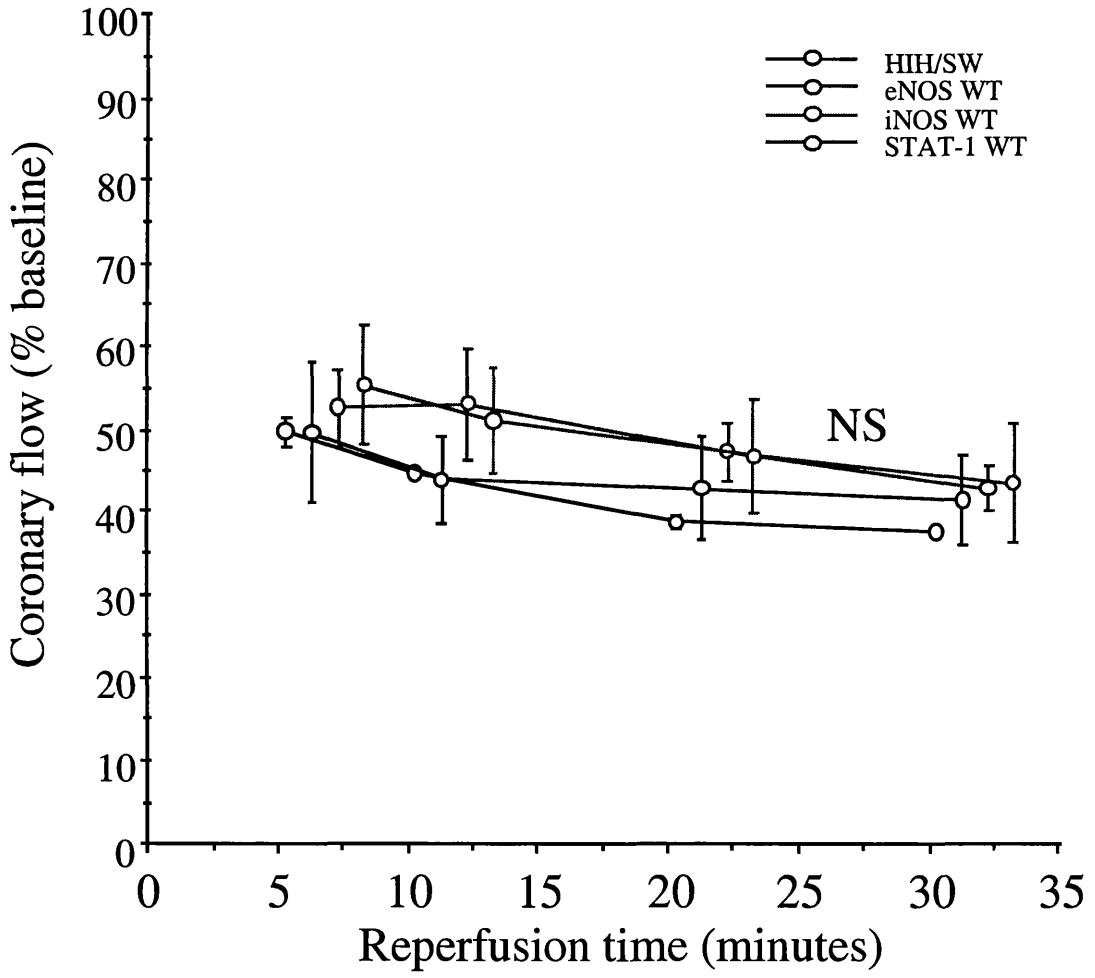

4.4.2 The influence of gender upon infarct size

Mouse strain appears to influence susceptibility to myocardial infarction in mouse (section 4.4.1). The influence of gender upon ischaemia/reperfusion injury in this species has not been previously documented, although data from rat and dog suggest that gender does not influence infarct size.[318, 319] However, oestrogen levels have been demonstrated to modify vascular responses to vasodilators, and resistance to hypoxic injury. Chronic administration of 17β oestradiol resulted in an increase of nitric oxide mediated vasodilatory response observed in the coronary vasculature of isolated perfused guinea pig hearts, although baseline coronary tone was unaltered by the treatment.[320] 17β oestradiol administration (in male dogs) is also associated with preserved endothelial function and reduced frequency of arrhythmias after 15 minute regional ischaemia.[321] Furthermore, oestrogen receptor-α knockout mice had reduced myocardial viability associated with reduced reperfusion coronary flow compared to their wild types following a 45 minute global ischaemic insult, associated with diminished NO metabolite accumulation.[322] Of potential importance to myocardial infarct size where eNOS has recently been shown to modify ischaemia/reperfusion injury,[243] 17β oestradiol upregulates vascular eNOS activity and NO generation,[323] a mechanism that may lead to greater myocardial tolerance to ischaemic injury.

Both male and female mice are used in the studies presented here. It is therefore important to determine whether there is a gender susceptibility to ischaemia/reperfusion injury in this species.

To determine whether gender influenced infarct size of isolated Langendorff perfused mouse hearts, 8 adult male and 8 adult female mice of equal body weight (25-30 grams, figure 4.20) were subjected to 35 minutes of global, normothermic ischaemia and 30 minutes reperfusion prior to determination of infarct size (protocol, figure 4.19).

The infarct size data are summarised in figure 4.21. Male hearts had an infarct to risk zone ratio of 31 ± 3% compared to female hearts which had infarct sizes of 31 ± 3% ($p = 0.998$). Therefore there appears to be no difference between the genders with respect to infarct resistance. To determine the difference between the two genders and vascular function, post ischaemic coronary flows were compared. Data from studies using chronic administration of 17β- oestradiol appear to suggest that base line and post ischaemic coronary flows would be greater in the females in the males. The coronary flow rate data are presented in figure 4.22. Base line coronary flows, measured after 20 minutes of stabilisation, were no different between groups, although flow in the females were marginally greater (4.00 ± 0.52 compared to 3.50 ± 0.25 ml/min in female and male groups respectively). Contrary to what was expected, hearts from female animals had lower coronary flow at reperfusion than the hearts from male mice

($p = 0.202$, not significant on actual values, but when expressed as a proportion of flow at the end of stabilisation, $p < 0.001$). The explanation of this difference in post-ischaemic vascular function remains unclear, but may represent a component of 17β-oestradiol withdrawal that may warrant further investigation.

As data from rat and dog suggest, the influence of gender upon myocardial infarct size appears to be minimal. Whilst post ischaemic flow appears to be worse in hearts from female animals, this appears to have no correlation to myocardial infarction resulting from global ischaemia. Therefore, infarct data from male and female mice may be compared in future ischaemia/reperfusion injury studies.

FIGURE 4.19. GENDER AND INFARCT RESISTANCE PROTOCOL.

All hearts were subjected to the standardised ischaemia/reperfusion regime characterised earlier. Thus male and female animals were randomly allocated to perfusion and ischaemia/reperfusion prior to infarct size assessment by TTC staining.

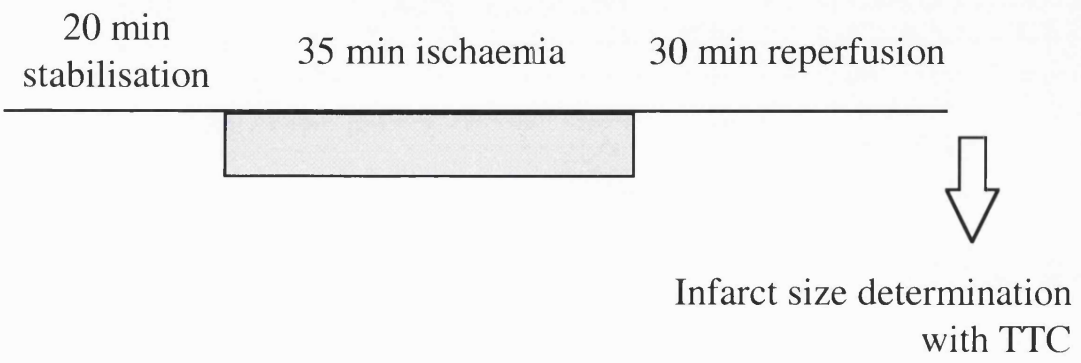

Infarct size determination
with TTC

FIGURE 4.20. COMPARISON OF MORPHOMETRICS BETWEEN THE GENDER GROUPS

No potential confounding influences of body or heart weight were detectable between the male and female groups in this study.

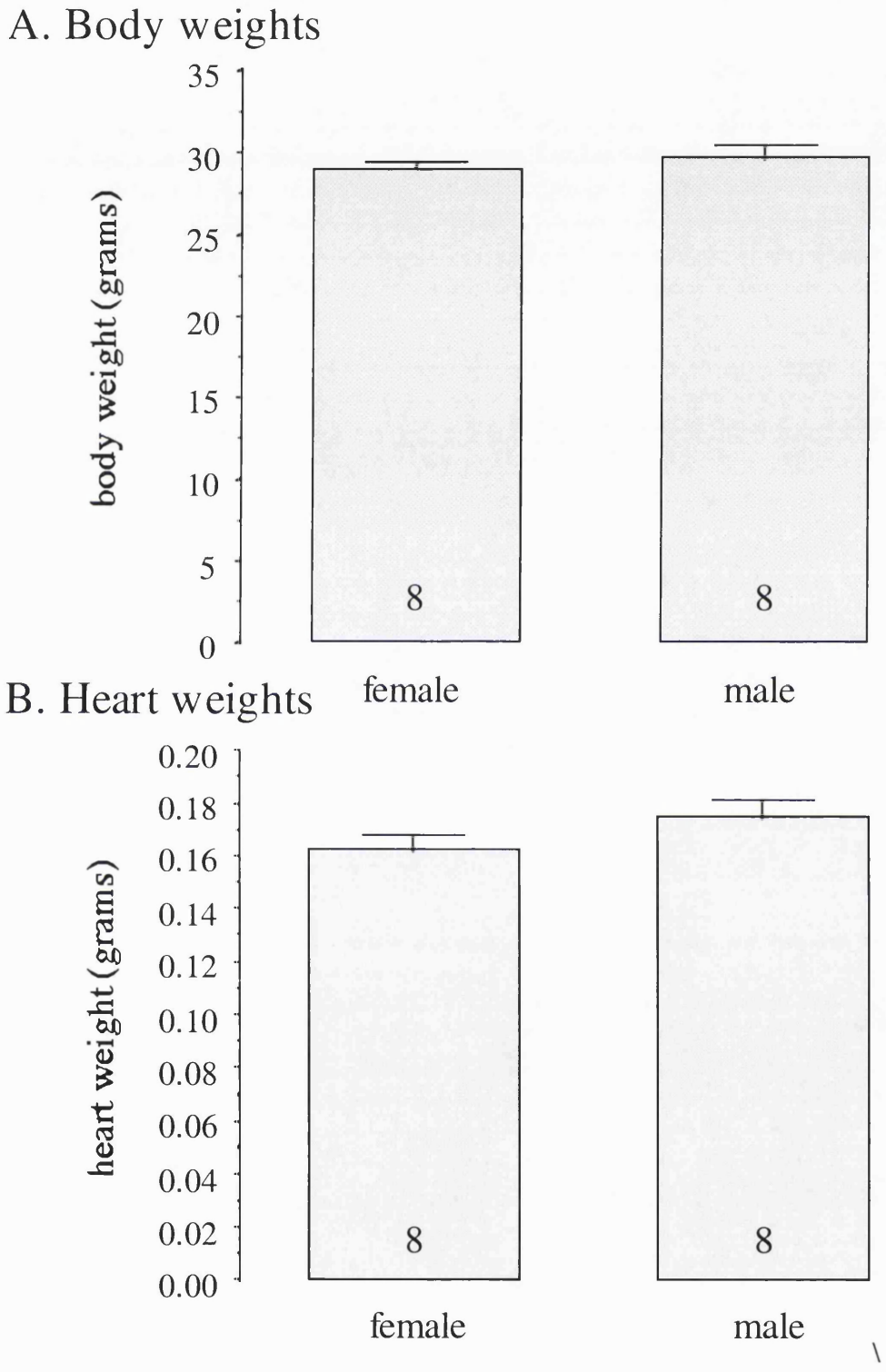

FIGURE 4.21. GENDER AND INFARCT RESISTANCE.

Both male and female B6.129 mice, subjected to an identical ischaemia/reperfusion regime, have the same susceptibility to necrosis as by determined by TTC staining. 8 experiments were performed per group.

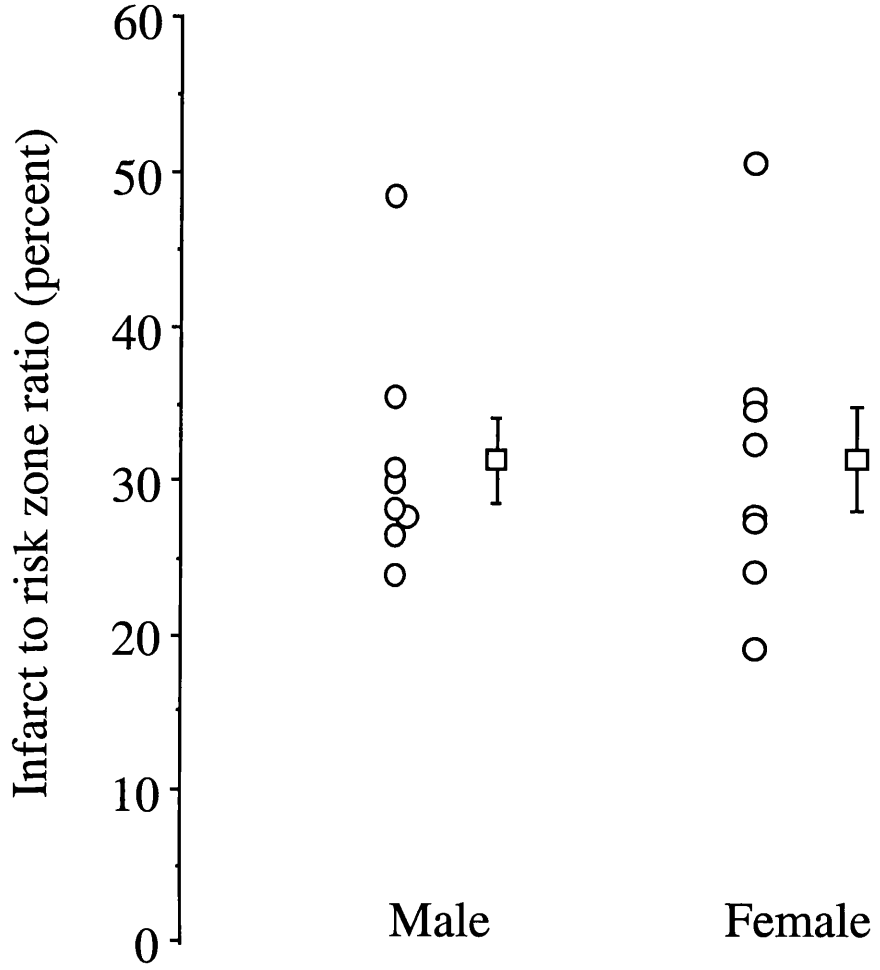

FIGURE 4.22. CORONARY FLOW RATE IN REPERFUSION

Post-ischaemic coronary flow measurement failed to demonstrate a significant difference between either the male or female groups. However, presenting the data as a percentage of baseline coronary flows, males have proportionately less ischaemia/reperfusion induced microvascular dysfunction. n = 8 per group.

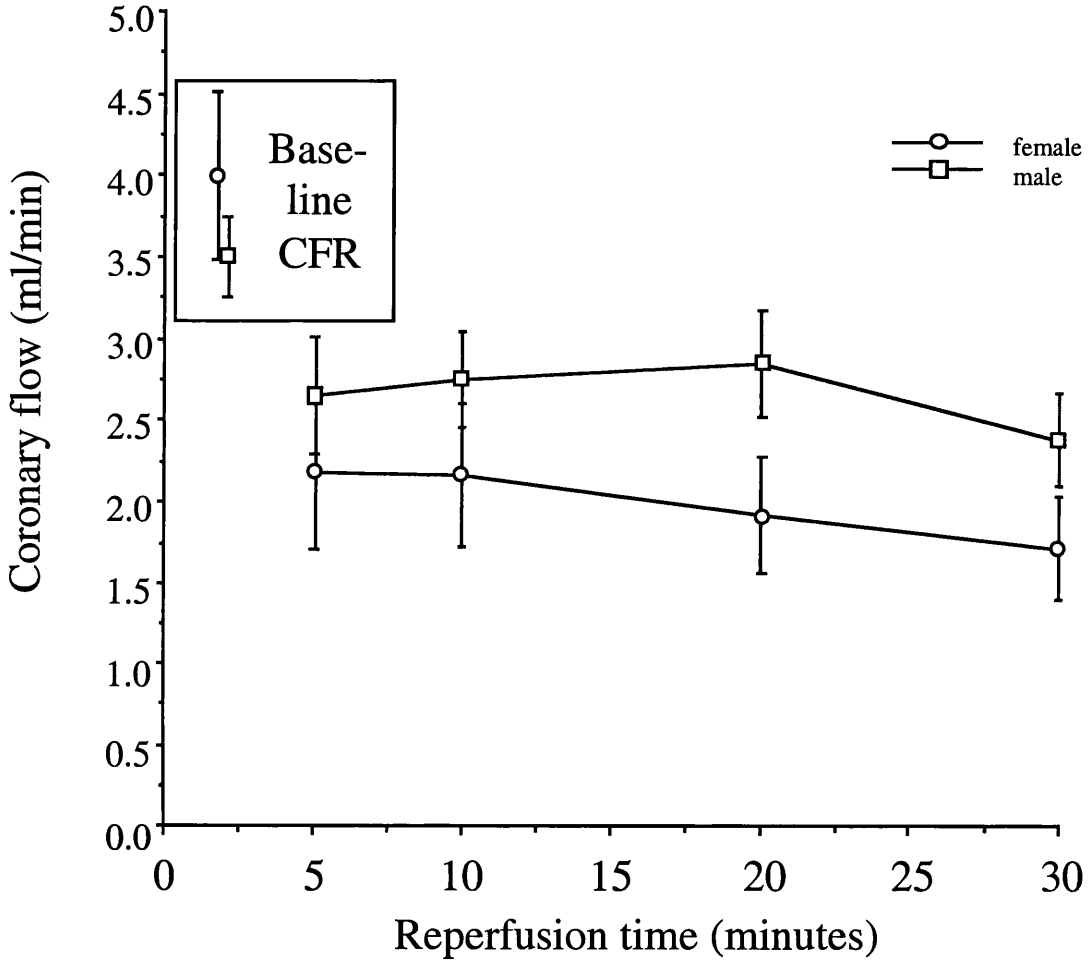

4.4.3. Role of gender upon early ischaemic preconditioning.

Having determined in section 4.4.2 that gender had no influence upon ischaemia/reperfusion induced necrosis, the ability to precondition male and female animals was compared. Subjected to an ischaemic preconditioning regime consisting of 2 cycles of 10 minute ischaemia and 10 minute reperfusion (protocol, figure 4.23), hearts from male and female animals were then subjected to the standardised ischaemia/reperfusion regime and the infarcts compared with those hearts that received control perfusion. The infarct data are summarised in figure 4.24. Hearts from both male and female animals had significantly attenuated infarction when compared to their respective controls (male group: control: 34 ± 2% versus IPC: 23 ± 1%, $p = 0.0008$; female group: control: 35 ± 2% versus IPC: 21 ± 3%, $p = 0.0002$). As found in section 4.4.2, control hearts from male and female animals had identical infarct sizes ($p = 0.828$). Moreover, the infarct sizes in the two preconditioning groups were also indistinguishable ($p = 0.633$), suggesting that the infarct size data in early ischaemic preconditioning are also directly comparable between genders. As seen in figure 4.25, preconditioning resulted not only in a significant attenuation of infarction, but of post-ischaemic contractile dysfunction as well, which was equivalent in both male and female heart groups. Therefore gender has no direct influence upon either infarct limitation or contractile recovery following index ischaemia.

Based upon these data, experiments were performed using male animals, however, where stated, female animals were also used. Given that infarct susceptibility and preconditioning responses in terms of infarct and contractile dysfunction attenuation were the same, data may be used interchangeably.

FIGURE 4.23. PRECONDITIONING PROTOCOL IN MALE AND FEMALE MOUSE HEARTS.

To determine whether gender has an influence upon preconditioning, hearts from male and female mice were harvested and randomly assigned to a control group (A), where stabilisation was followed by a prolonged control perfusion period to time match with the preconditioning regime, and the preconditioning (IPC) group (B), where hearts were subjected to 2 cycles of 10 minute ischaemia and 10 minutes reperfusion immediately prior to the index ischaemia.

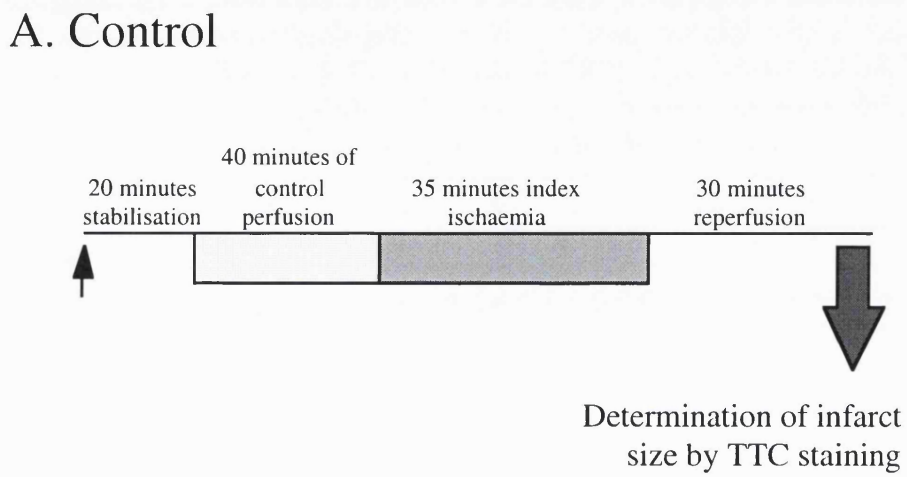

FIGURE 4.24. PRECONDITIONING ATTENUATES INFARCT SIZE IRRESPECTIVE OF GENDER.

Preconditioning results in significant attenuation of infarct size in both hearts from male and female mice. Preconditioning had similar potency in both groups.

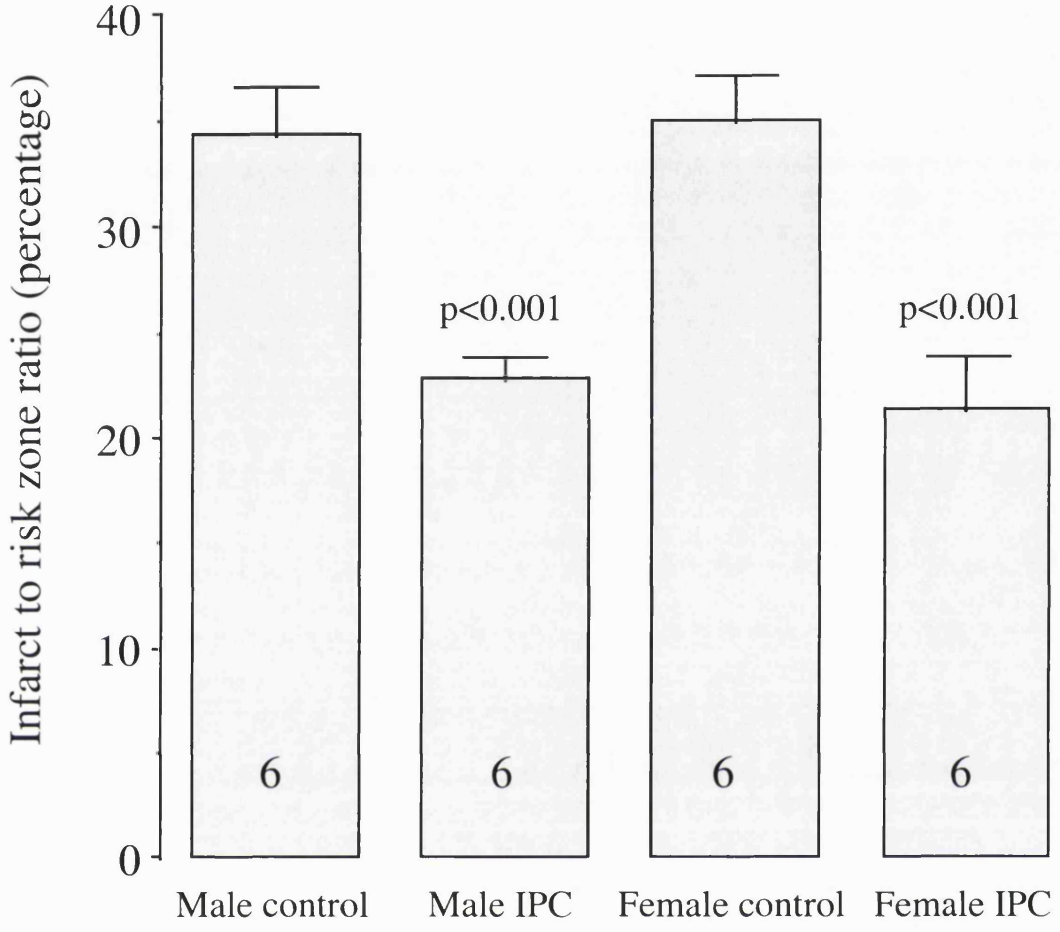

FIGURE 4.25. PRECONDITIONING ATTENUATES CONTRACTILE DYSFUNCTION.

In both male and female heart groups significant attenuation of contractile dysfunction was observed following preconditioning ($p = 0.002$ and $p < 0.001$ respectively). $n = 6$ per group.

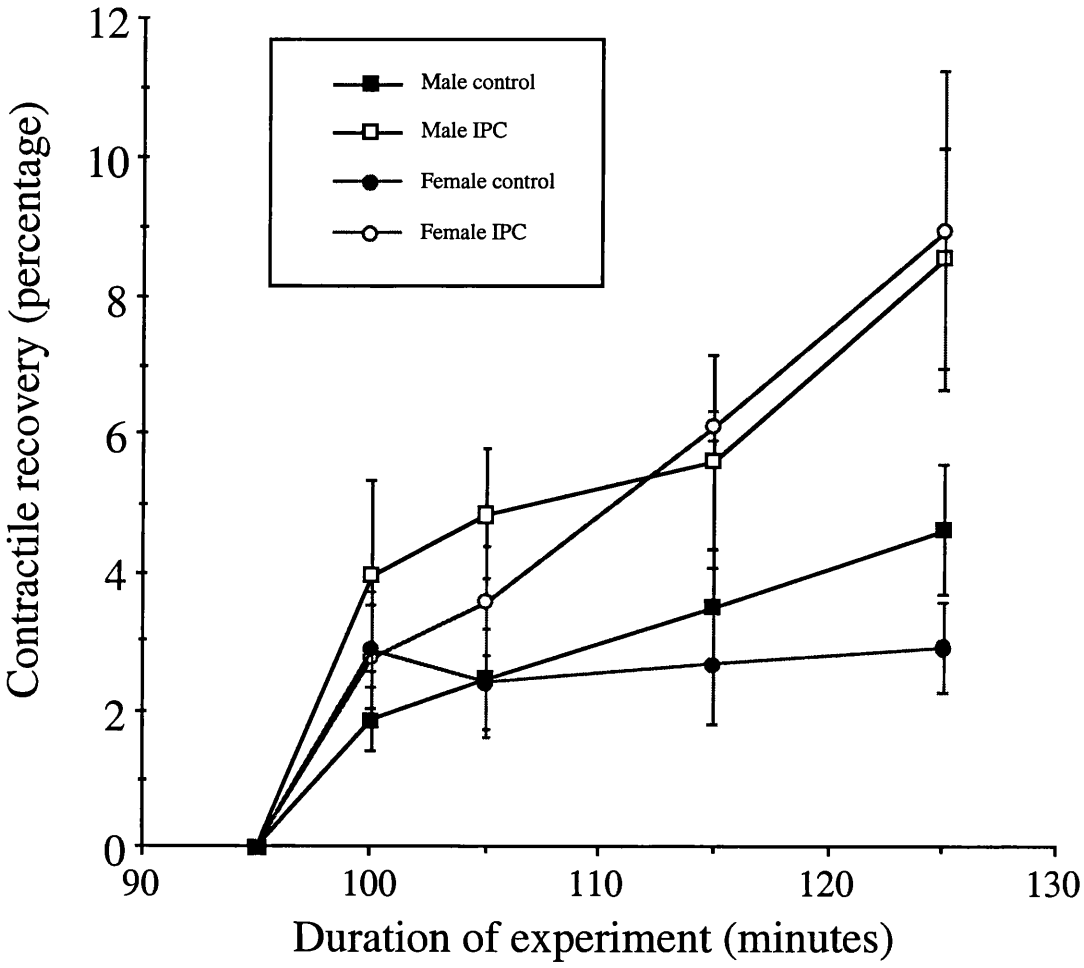

4.5. Morphometric characteristics.

The studies contained within this thesis, as outlined in chapter 2, use both eNOS and iNOS knockout animals. Little information regarding growth characteristics were available at the outset of these studies, particularly regarding the growth of internal organs such as the heart. Therefore the aim of this study was to descriptively map the wet weights of heart, liver and lung in both wild type and knockout animals with increasing age in both genders, to determine the age range of these animals suitable for study that avoided potential confounding myocardial hypertrophy and/or heart failure. This is particularly important with respect to the eNOS knockout animals where aortic valve abnormalities[292] and hypertension[291] have previously been reported. To this end, male and female mice with targeted knockouts of their eNOS or iNOS genes and their respective controls were sacrificed at the age of 3 and 8 months. As mice have a typical life span of 1.5 to 3 years,[297] 3 months represent early adulthood, whilst at 8 months the mice are entering middle age. Thus, at these time points, the heart, lung and liver were harvested and weighed to determine what effect, if any, the genetic mutations had upon organ weight. Congestive heart failure was expected to manifest as increased congestion and therefore weight of the liver and lungs in proportion to total body weight of the animal.

4.5.1. Body weight.

Weights of both male and female animals were compared, and the results are summarised in figure 4.26 (figure A and figure B for the iNOS and eNOS groups respectively). Targeted disruption of the iNOS gene had no effect upon the gross development of these mice compared to their wild type controls (figure 4.26.A), which is entirely consistent with the reported lack of effect of iNOS disruption upon phenotype. Male animals were however found to be significantly larger then their female litter mates in both wild type and knockout groups (at 3 months of age, male iNOS knockout mice weighed 33.98 $\pm$ 3.02 grams compared to the females who weighed 23.23 $\pm$ 0.29 grams, $p = 0.0004$).

Given the development of hypertension reported in eNOS knockout mice, these animals were expected to have different growth characteristics to their wild type controls. This was not observed (figure 4.26.B). Both groups of animals possessed the same body weights at both age points in both genders (for example in females, 3 months and 6 months of age $p = 0.332$ and $p = 0.463$ respectively). As found in the iNOS groups of animals, male animals were found to be significantly heavier than their female litter mates.

FIGURE 4.26. BODY WEIGHT OF iNOS/eNOS WILD TYPE & KNOCKOUT MICE.

Summary of body weight data. **A**, iNOS mice and **B**, eNOS mice. No significant difference is observed in the age range examined, although male mice are significantly heavier than female mice. n = 3 per group.

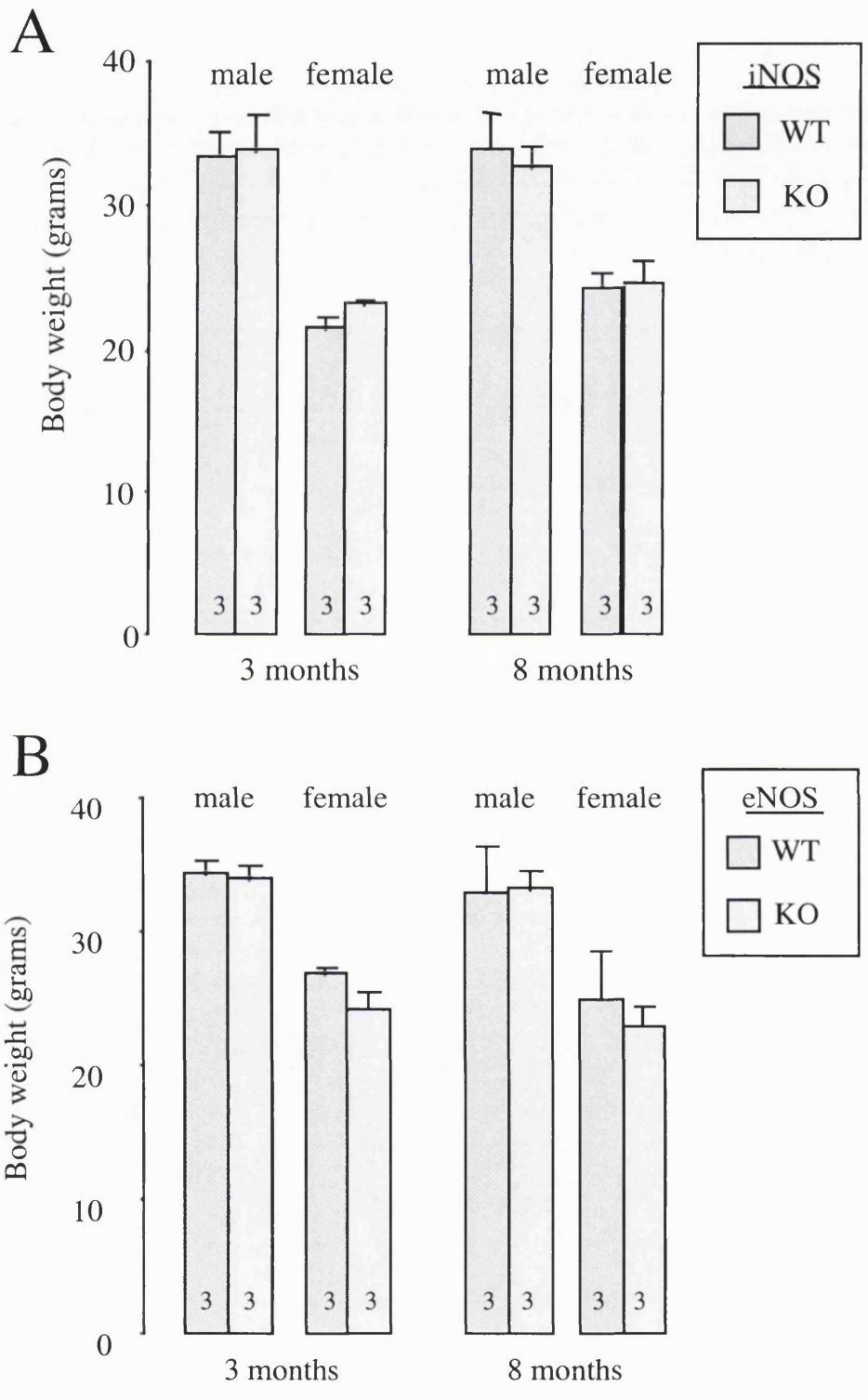

4.5.2. Mouse heart weights.

In iNOS wild type and knockout mice, no difference in heart weight was determined with increasing age. As with body weight, heart weights in males were significantly greater than in their female siblings. However, these animals heart:body weight ratios were no different: comparing male and female iNOS knockout mice, ratios of 0.62 ± 0.05% and 0.65 ± 0.05% in male and female animals respectively were observed ($p = 0.248$), and at 8 months, the ratios were 0.68 ± 0.02% and 0.63 ± 0.3% respectively ($p = 0.161$).

A difference in heart weights had been anticipated in eNOS knock out mice, as hypertension secondary to eNOS deficiency would be expected to trigger left ventricular hypertrophy. However, even at 8 months of age, there was no difference between eNOS wild types and knockouts (in female mice for example at 8 months, heart weights in knockouts and wild types were respectively 0.15 ± 0.01g and 0.16 ± 0.01g. As found in the iNOS group, males had larger hearts than the females, but the heart:body ratio were essentially identical: at 3 months, male mice had a heart:body weight ratio of 0.61 ± 0.1% compared to female mice with a heart:body weight ratio of 0.62 ± 0.01% ($p = 0.938$).

4.5.3. Lung and liver weights

Liver weight, like heart weight, followed a similar pattern of development in association to body weight. In both the iNOS and eNOS groups (figure 4.28 A and B respectively), males had larger livers than their female siblings. Disruption of either the iNOS or eNOS gene had no impact upon liver weight in either age group. In iNOS wild types and knockouts, the liver:body ratio was approximately 5%, whilst in the eNOS wild type and knockouts the ratio was approximately 4%. Liver weight demonstrated no relationship with increasing animal age: in female eNOS knockout mice for example, liver weights at 3 months and 8 months were 0.82 ± 0.03g and 0.99 ± 0.11g. Given the lack of association between total heart weight and age, the lack of increase of liver weight is not surprising.

Lung weight in these groups of mice had no measurable relationship with gender, age or gene status in either the iNOS (figure 4.29.A) or eNOS (figure 4.29.B) groups (ANOVA, $F = 0.592$, $p = 0.797$). Mean lung weight in all mice was 0.250g.

FIGURE 4.27. MOUSE HEART WEIGHT IN eNOS AND iNOS WT AND KOs.

Heart weights compared between iNOS wild types and knockouts (A) and eNOS wild types and knockouts (B). No significant difference were observed between wild types and knockouts at the time points studied. Male animals had significantly larger hearts than their female siblings however, concomitant with their greater body weight. n = 4 per group.

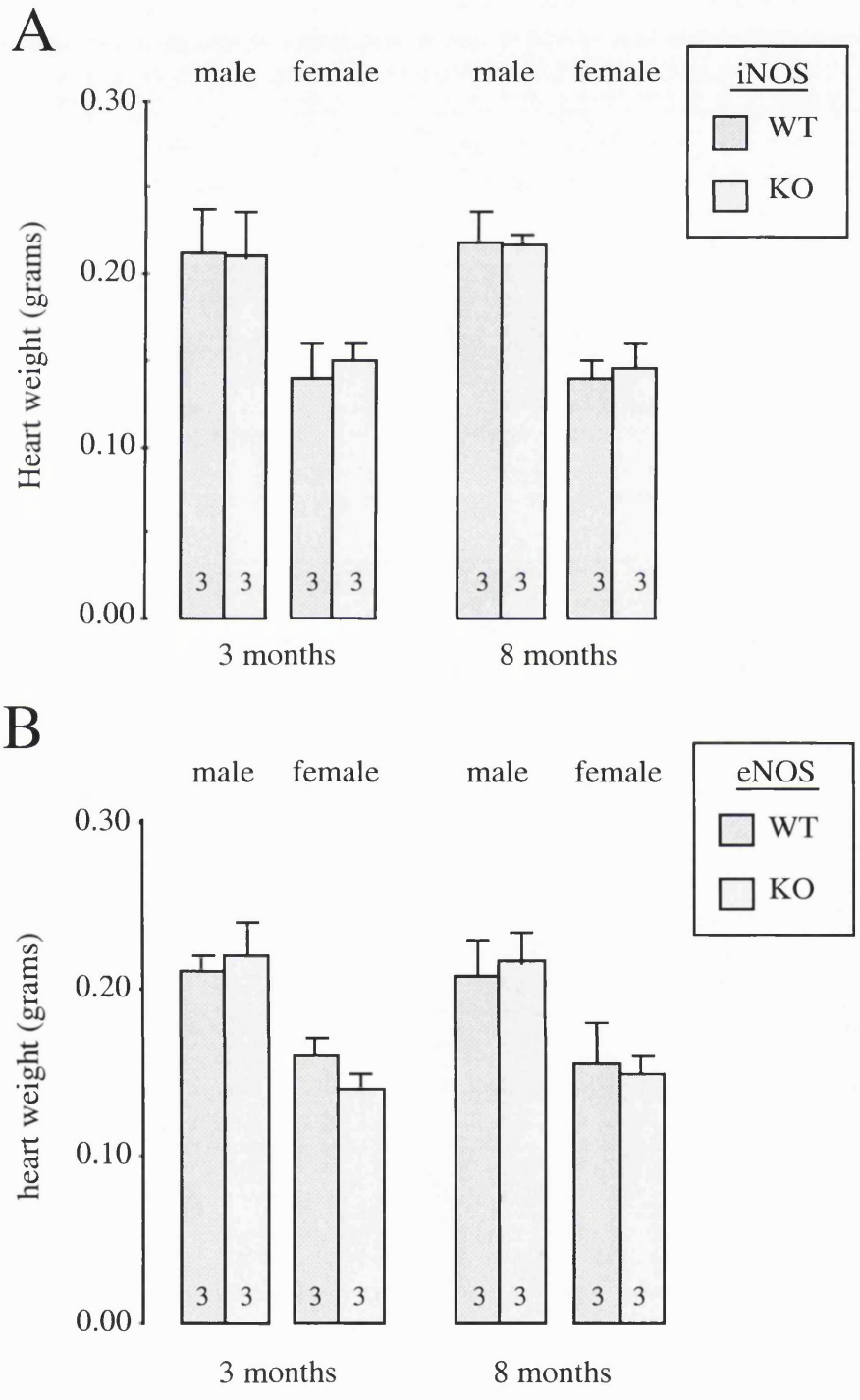

FIGURE 4.28. LIVER WEIGHT RELATIONSHIP TO eNOS AND iNOS STATUS.

No difference in gender matched wild type and knock out liver weights in either iNOS (**A**) or eNOS (**B**) groups. Male animals have significantly larger livers to females, in accordance to body weight. n = 4 per group.

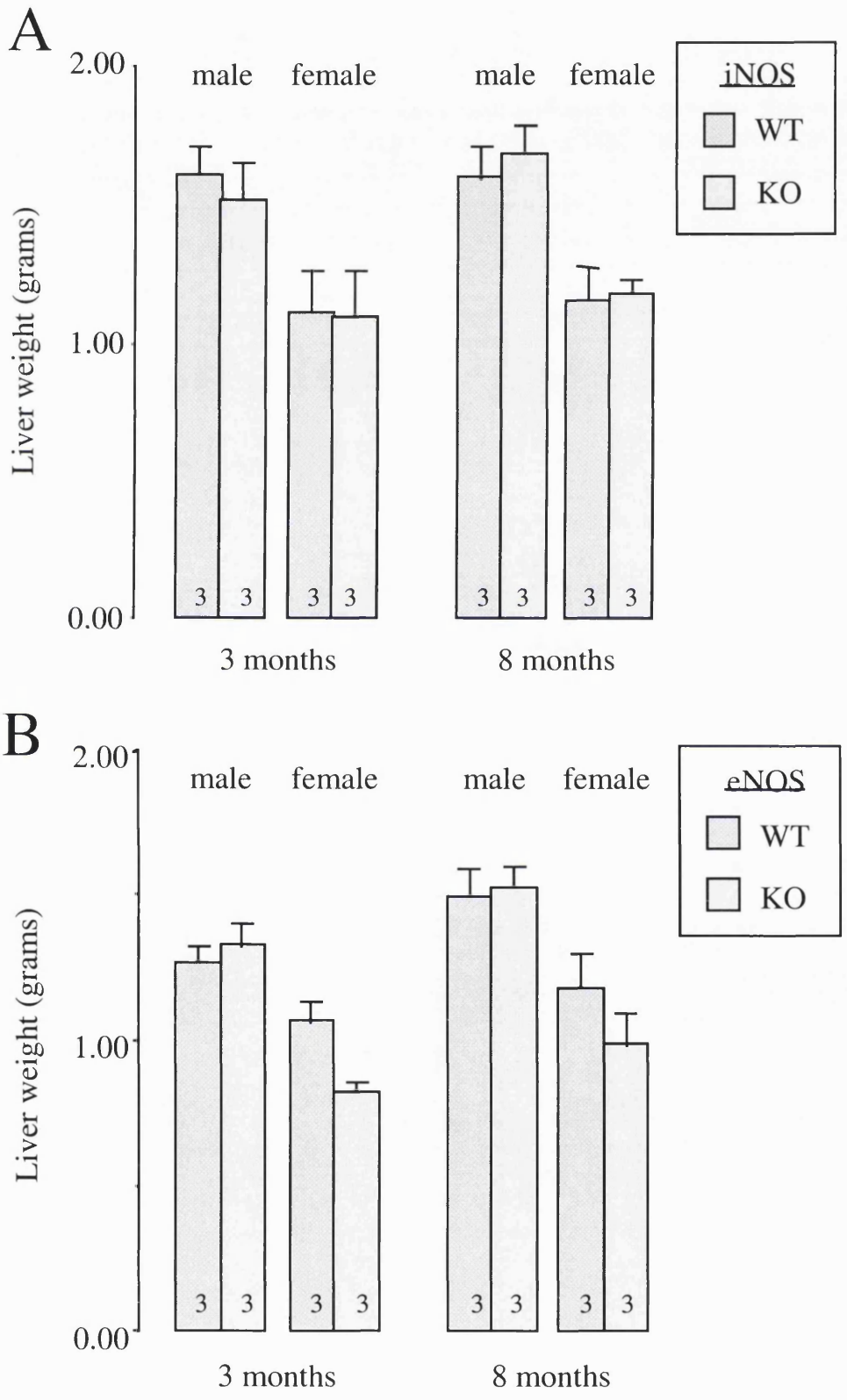

FIGURE 4.29. LUNG WEIGHT RELATIONSHIP TO eNOS AND iNOS STATUS.

No significant difference was detected between gender or genetic status in either iNOS (**A**) or eNOS (**B**) groups. n = 4 per group.

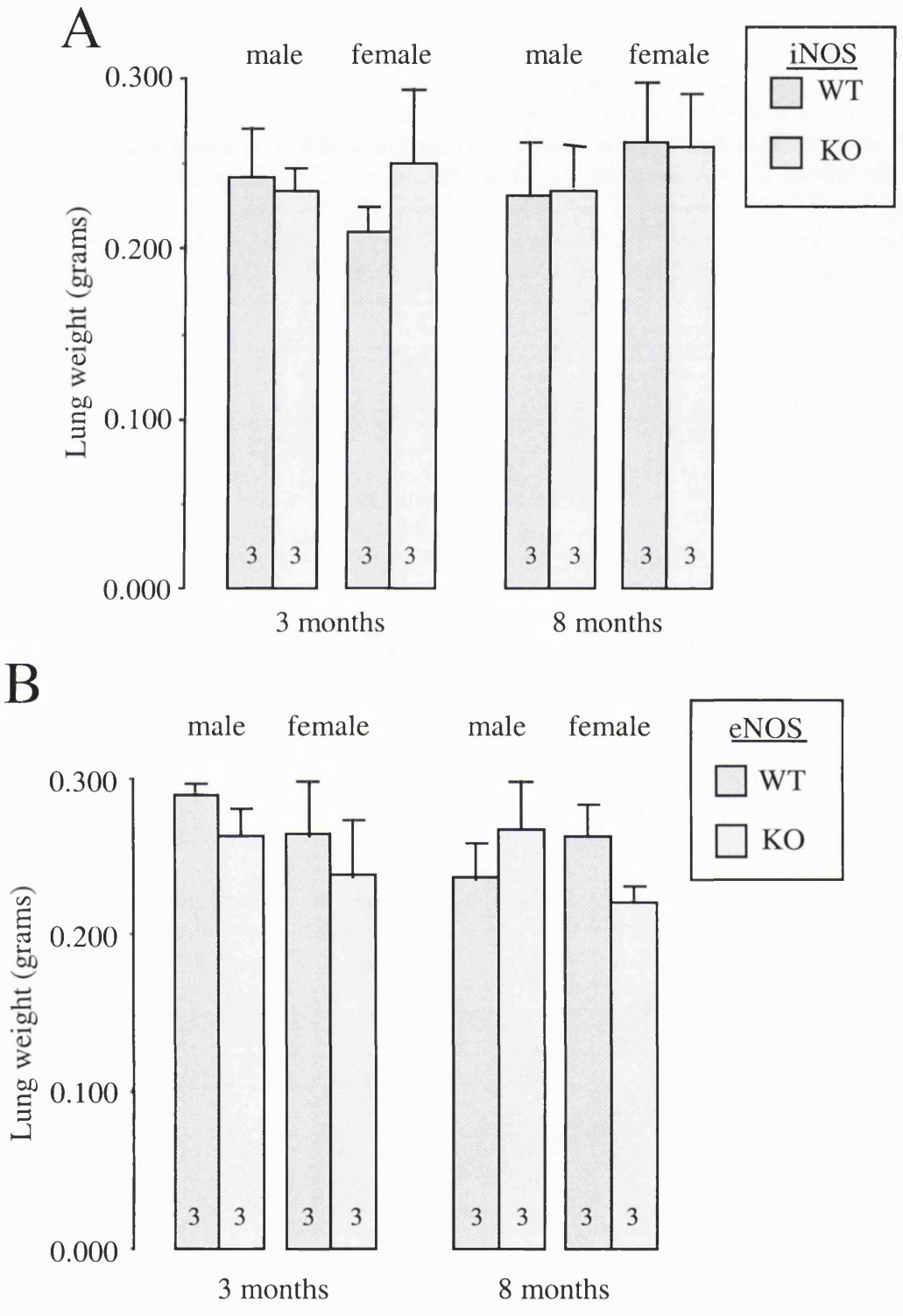

4.5.4. Conclusions.

This descriptive study provides morphometric information useful for the design of later studies, in that it confirms the lack of phenotypic differentiation between the NOS genotypes.

4.5.4.1. iNOS wild type versus iNOS knockouts.

Gender based development of the major internal organs is no different in either the iNOS wild type or iNOS knock out animals. There are no gross signs of cardiomyopathy or congestive cardiac failure, even in the middle aged mice. These data appear consistent with the original reports of the phenotype of this targeted gene disruption model (section 3.3). Given the lack of potential confounding morphological differences in iNOS knockouts and wild types in the age range of 3-8 months, all future studies using these animals were performed using 3-4 month old mice.

4.5.4.2. eNOS wild type versus eNOS knockouts.

Despite previous reports of aortic valve malformations[292] and spontaneous hypertension,[291] neither young adult (3 month old) or middle aged adult (8 month old) mice of either gender demonstrated any evidence of gross cardiac hypertrophy associated with hypertension, or increases in liver of lung weight associated with congestive heart failure. Therefore the animals used in the later studies described in this thesis are typically 3 to 4 months of age. On the basis of this gross descriptive morphological study, there is no reason to suspect confounding cardiac hypertrophy or heart failure in the results comparing eNOS knockouts with wild type animals.

Chapter 5: The role of nitric oxide in early preconditioning

5.1 Aims and protocol

As described in chapter 1, ischaemic preconditioning results in the release of a number of metabolites and neuro-humeral agents that trigger the preconditioning response, including adenosine, bradykinin, angiotensin, opioids and cytokines. These triggers of preconditioning summate to generate the signal for preconditioning. This 'threshold' hypothesis proposed by Downey and colleagues, is supported by investigations in both rabbit[45] and human myocardium[46] and is discussed in greater detail in section 1.2.2. Interestingly, many of these triggers of the preconditioning response also alter eNOS activity (section 1.7.4). Bradykinin receptor activation in particular can lead to the disassociation of eNOS from inhibitory binding sites both on the receptor itself and from sarcolemmal caveoli binding sites.

G-protein linked receptors are associated with both the activation of PI3 kinase (section 1.5.1.1) which is linked to the activity of protein kinase B (PKB or Akt) and the activation of cAMP linked protein kinases through the interaction of the Gsα subunit with adenylate cyclase (section 1.5.1.1). With the activation of either or both PKB/Akt[85, 86] and cAMP linked protein kinase, [79, 80] eNOS may be phosphorylated at serine 1177,[79, 80, 85, 86] increasing the activity of eNOS 40 fold.

Whilst there is evidence that eNOS activity is upregulated by the same signals that trigger preconditioning, the hypothesis that NO generated from eNOS may play an important role in the mediation of classical preconditioning is controversial. Perhaps surprisingly, all pharmacological studies to date have failed to implicate a role for nitric oxide (NO) in early preconditioning,[263-265] whilst the strongest evidence that NO is being released in this early phase following ischaemic preconditioning is derived from studies implicating a role for constitutive nitric oxide synthesis in triggering delayed preconditioning,[324, 325] and evidence for NO generation in the ischaemic zone by electron spin resonance techniques.[326] Moreover, substantive evidence exists for reactive oxygen species triggering the preconditioning response.[70, 327] It is surprising therefore that NO (through the generation of peroxynitrite species) appears to have no role to play in this paradigm. Therefore to determine whether eNOS plays a role in the induction and mediation of classical preconditioning, adult mice (22-28 grams, morphometric summary in table 4, mixed sex in group A, 3 male mice and the balance made up with females per group, and all females in group B) with either a targeted disruption of the eNOS gene (KO) or their wild types (WT) where subjected to ischaemic preconditioning (protocol, figure 5.1.A). Furthermore, to determine whether exogenous NO can emulate preconditioning protection, the NO donor, S-Nitroso N-

acetyl DL penicillamine (SNAP) was used to construct an infarct size limitation dose response curve (protocol, figure 5.1.D).

Table 4. Chapter 5: Morphometrics and baseline functional parameters.

No significant differences were noted between groups. Group **A**- animals used in the initial investigation to determine the role of endogenous nitric oxide in early preconditioning. Group **B**- animals used in the second phase of the study investigating the cardioprotective properties of exogenous nitric oxide.

Group	Body weight (g)	Heart weight (mg)	Baseline coronary flow (ml/min)	Baseline contractile function (g/beat/min)	Baseline resting tension (g)
A					
WT control (n = 6)	26.99 ± 1.21	170 ± 16	3.32 ± 0.13	1465 ± 187.3	1.04 ± 0.06
KO control (n = 7)	23.86 ± 0.99	163 ± 11	3.00 ± 0.20	1484 ± 168.9	1.14 ± 0.04
WT 4PC (n = 6)	26.97 ± 1.79	172 ± 9	3.28 ± 0.14	1697 ± 199.0	1.04 ± 0.05
KO 4PC (n = 6)	24.96 ± 0.38	158 ± 9	2.78 ± 0.16	1217 ± 142.5	1.06 ± 0.04
WT SNAP (n = 6)	27.79 ± 1.36	180 ± 9	3.33 ± 0.08	1553 ± 149.2	1.04 ± 0.05
KO SNAP (n = 6)	27.30 ± 0.81	182 ± 3	3.03 ± 0.23	1364 ± 240.4	1.04 ± 0.05
WT 3PC (n = 6)	23.56 ± 1.27	166 ± 13	2.48 ± 0.20	1420 ± 192.7	1.15 ± 0.13
KO 3PC (n = 6)	24.52 ± 0.69	171 ± 7	2.59 ± 0.10	1100 ± 88.6	1.09 ± 0.04
WT 2PC (n = 6)	26.28 ± 0.81	153 ± 6	2.98 ± 0.18	1175 ± 156.9	1.17 ± 0.08
KO 2PC (n = 6)	25.27 ± 0.92	157 ± 7	2.47 ± 0.17	1250 ± 176.1	1.10 ± 0.10
B					
Control (n = 11)	26.59 ± 1.13	158 ± 4	2.75 ± 0.25	1241 ± 138.8	1.32 ± 0.09
SNAP 0.2 μM (n = 5)	26.35 ± 0.10	158 ± 5	2.68 ± 0.23	1240 ± 188.0	1.25 ± 0.14
SNAP 1.0 μM (n = 6)	27.34 ± 0.83	154 ± 5	3.04 ± 0.21	1485 ± 112.3	1.03 ± 0.03
SNAP 2.0 μM (n = 6)	27.49 ± 0.59	165 ± 5	2.80 ± 0.43	1013 ± 71.8	1.22 ± 0.03
SNAP 6 μM (n = 6)	26.49 ± 0.68	155 ± 11	2.75 ± 0.35	1300 ± 92.2	1.19 ± 0.07
SNAP 20 μM (n = 6)	26.28 ± 0.67	157 ± 7	3.03 ± 0.21	1158 ± 103.6	1.27 ± 0.08

FIGURE 5.1. EXPERIMENTAL PROTOCOLS.

All hearts were subjected to 35 minutes global index ischaemia and 30 minutes reperfusion.

Group A. WT and eNOS KO mice were randomly assigned to control or ischaemic preconditioning groups consisting of 4 cycles of 5 minutes ischaemia and reperfusion.

Group B. As part of the initial study, WT and KO hearts were also randomly assigned to an ischaemia/reperfusion group in the presence of a NO donor, SNAP (2 μM). Perfusion was time matched with group A.

Group C. To determine whether eNOS contributed to the preconditioning threshold, the number of preconditioning cycles were reduced to 3 and 2 cycles (3PC and 2PC respectively). WT and KO hearts were randomised to control, 3PC and 2PC groups.

Group D. The exogenous NO donor, SNAP was added in incremental doses of 0, 0.2, 1, 2, 6, 20 μM to the perfusate. WT hearts were then subjected to the same ischaemia reperfusion protocol as groups A, B and C.

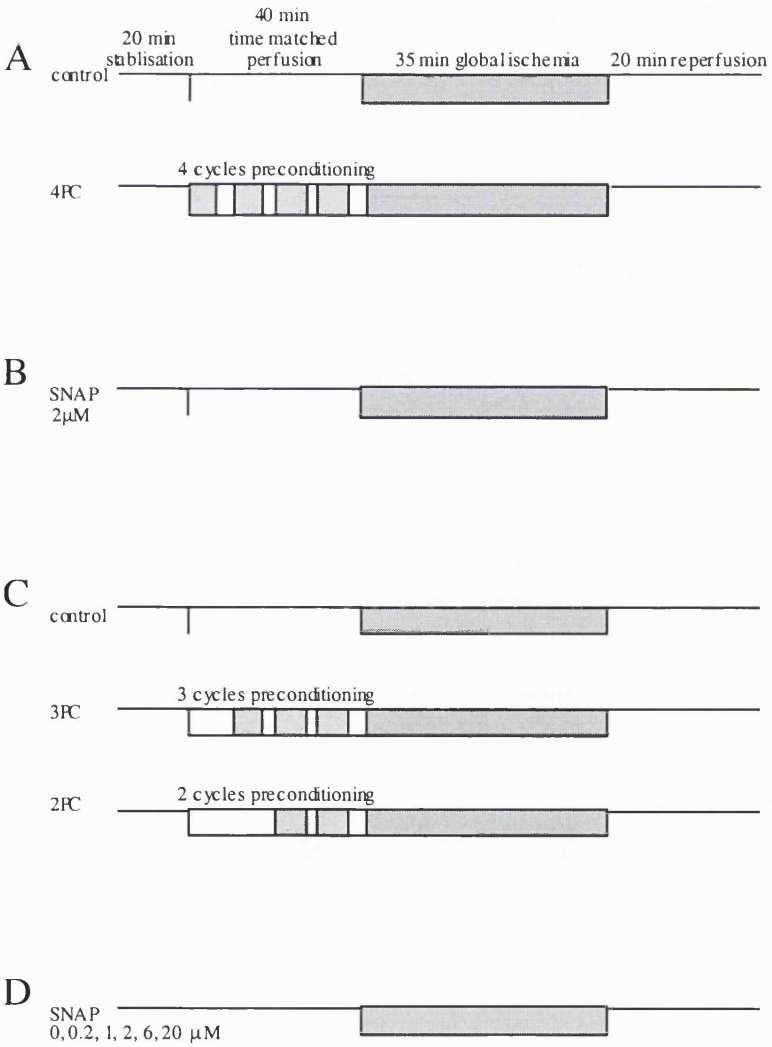

5.2 Results

No significant differences between groups were documented in terms of body or heart weight, end-stabilisation baseline contractile function (expressed as a force-rate product), baseline coronary flow or resting tension (table 4). Group A in table 4 describes baseline parameters for animals used in the initial investigation to determine the role of endogenous nitric oxide in early preconditioning. Group B in table 4 describes baseline parameters for animals used in the second phase of the study investigating the cardioprotective properties of exogenous nitric oxide.

5.2.1 Is eNOS activity required for early preconditioning?

To determine whether the presence and therefore activity of eNOS is essential to elicit early ischaemic preconditioning, hearts from eNOS WT and KO animals were subjected to a 4 cycle, 5 minute ischaemia and 5 minute reperfusion preconditioning regime (protocol, figure 5.1.A), based upon the preconditioning regimes described in chapter 4 and the published work of Sumeray et al.[310] The hearts were then subjected to index ischaemia and reperfusion, as described. The hypothesis that eNOS would be pivotal to early ischaemic preconditioning appeared to be discounted as significant infarct limitation was observed in both WT and KO hearts, with infarct reduction from 35 ± 2% to 21 ± 3% and 31 ± 2% to 23 ± 3% in the WT and KO groups respectively ($p = 0.001$ and $p = 0.037$, summarised in figure 5.2.A). The infarct sparing effect was concomitant with improved contractile recovery in both the preconditioned groups (figure 5.2.B; $p = 0.008$ and $p = 0.021$ in KO and WT preconditioned groups versus their respective controls). The result implies that eNOS and NO appear not to be essential in the evolution of cardioprotection observed from early ischaemic preconditioning, but does not exclude a potential cardioprotective role for NO itself.

5.2.2 Is exogenous NO cardioprotective?

To confirm that the mechanisms for NO mediated resistance to ischaemia reperfusion injury exist in both WT and KO hearts, naive hearts were subjected to index ischaemia and reperfusion in the presence of SNAP (2 μM) (protocol, figure 5.1.B), a dose previously demonstrated to elicit an early pharmacological preconditioning response.[327] In both SNAP treated groups, significant attenuation of infarction was observed, with WT infarct size reduced to 15 ± 1% ($p < 0.0001$ versus control) and KO infarct size to 17 ± 3% ($p = 0.0006$ versus control) (results summarised figure 5.3.A). As with the preconditioning regimen, the administration of exogenous SNAP resulted in a significant improvement in contractile function in SNAP treated WT and KO hearts,

mimicking the preconditioning effect (figure 5.3.B; $p < 0.001$ in both SNAP treated groups versus their respective controls). Therefore, whilst preconditioning may not be dependent upon NO, exogenous NO can imbue significant resistance to ischaemia/reperfusion injury in both WT and KO animals, thus implying that the mechanisms and targets of NO mediated protection are present in eNOS KO as well as in eNOS WT hearts.

5.2.3 Does eNOS contribute to the preconditioning threshold?

To determine whether eNOS contributes to the threshold to preconditioning, the preconditioning stimulus was progressively reduced from 4 cycles (4PC) to 2 cycles (2PC) of 5 minutes ischaemia and 5 minutes reperfusion (protocol figure 5.1.C). If eNOS contributes to the preconditioning threshold, it was hypothesised that by reducing the intensity of the preconditioning stimulus, eNOS knockouts would lose the protection before the eNOS wild type hearts.

Significant attenuation of infarct size was observed in the hearts from WT animals, both from 3 and from 2 cycles of preconditioning (figure 5.4.A; 3PC 26 ± 3% and 2PC 27 ± 2%, $p = 0.026$ and $p = 0.039$ respectively versus the control group). The infarcts in these two preconditioning groups were not significantly larger than that seen in the 4 cycle preconditioning group (21 ± 3%). The incremental ischaemic preconditioning resulted in a highly correlated reduction of infarct size ($p = 0.022$, $r^2 = 0.954$) in a dose-responsive fashion (figure 5.4.1.A). In contrast however, the infarct sparing effect in the hearts from KO animals was not observed with either the 2 or 3 cycle preconditioning regimes (figure 5.4.B; 3PC 33 ± 3%, 2PC 29 ± 3%; $p = 0.664$ and $p = 0.568$ versus control respectively). Moreover, these infarct sizes were significantly larger than that observed following 4 cycles of preconditioning in hearts from the same group of animals (23 ± 3%, $p = 0.0.015$ versus the 3 cycle preconditioned group). Nor was there any correlation between preconditioning ischaemia cycles and infarct reduction, with an evident threshold at 3 to 4 cycles of preconditioning ischaemia (figure 5.4.1.B).

These data therefore suggest that there is a role for eNOS in early ischaemic preconditioning by contributing to the preconditioning trigger stimulus and thus lowering the ischaemic threshold for preconditioning.

FIGURE 5.2.A. eNOS IS NOT PIVOTAL FOR CLASSICAL PRECONDITIONING.

4 cycles of preconditioning resulted in significant attenuation of infarction in both WT and KO mice (*, p = 0.037 and **, p = 0.001 versus respective controls). n = 6 per group.

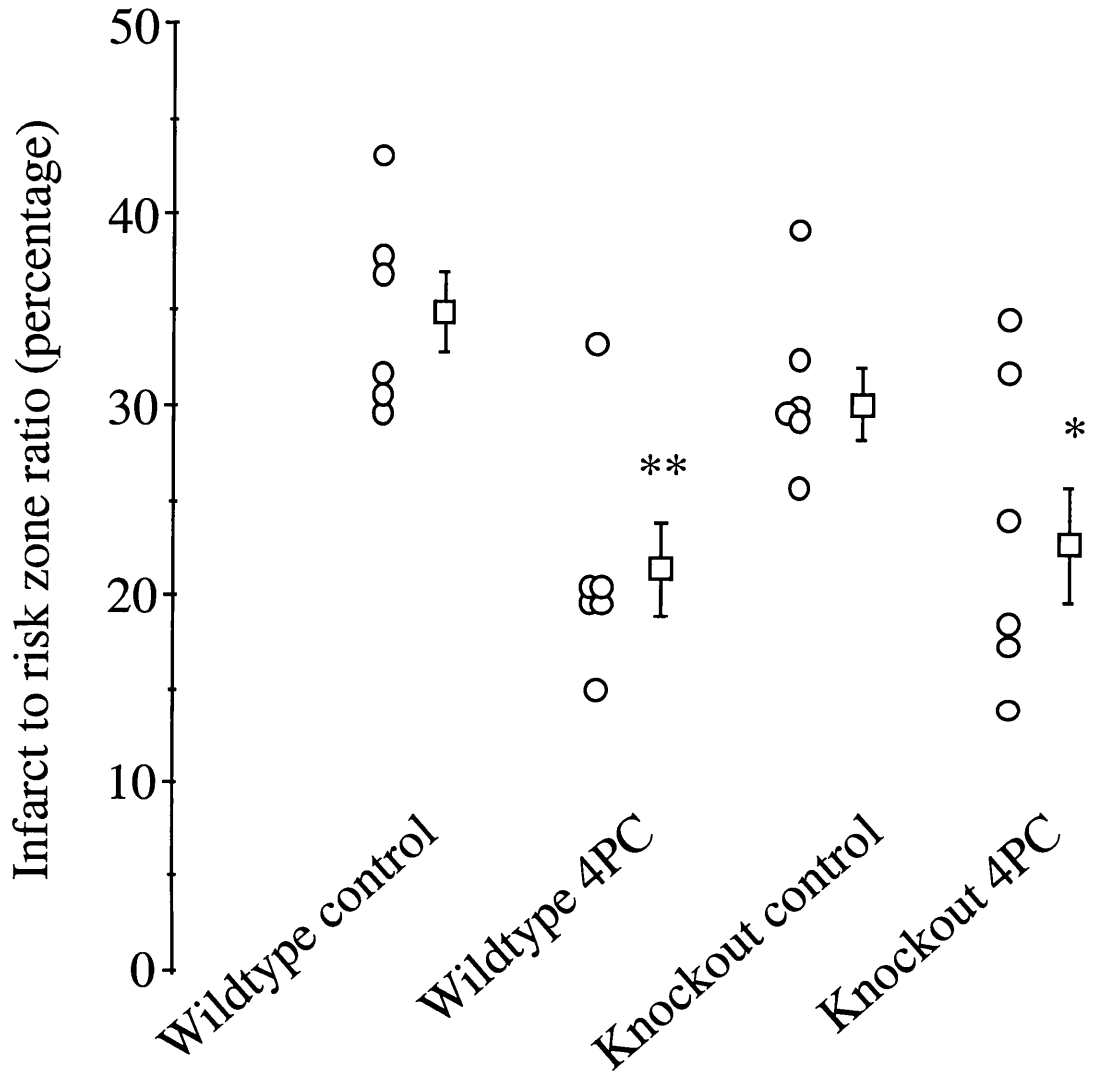

FIGURE 5.2.B. POST-ISCHAEMIC CONTRACTILE RECOVERY AFTER PRECONDITIONING.

Four cycles of ischaemic preconditioning (**4IPC**) resulted in significantly improved post-ischaemic contractile function in both wild type (**WT**) and eNOS knockout (**KO**) hearts. Compared to the respective controls, p = 0.021 and p = 0.008 for the WT and KO groups respectively. n = 6 per group.

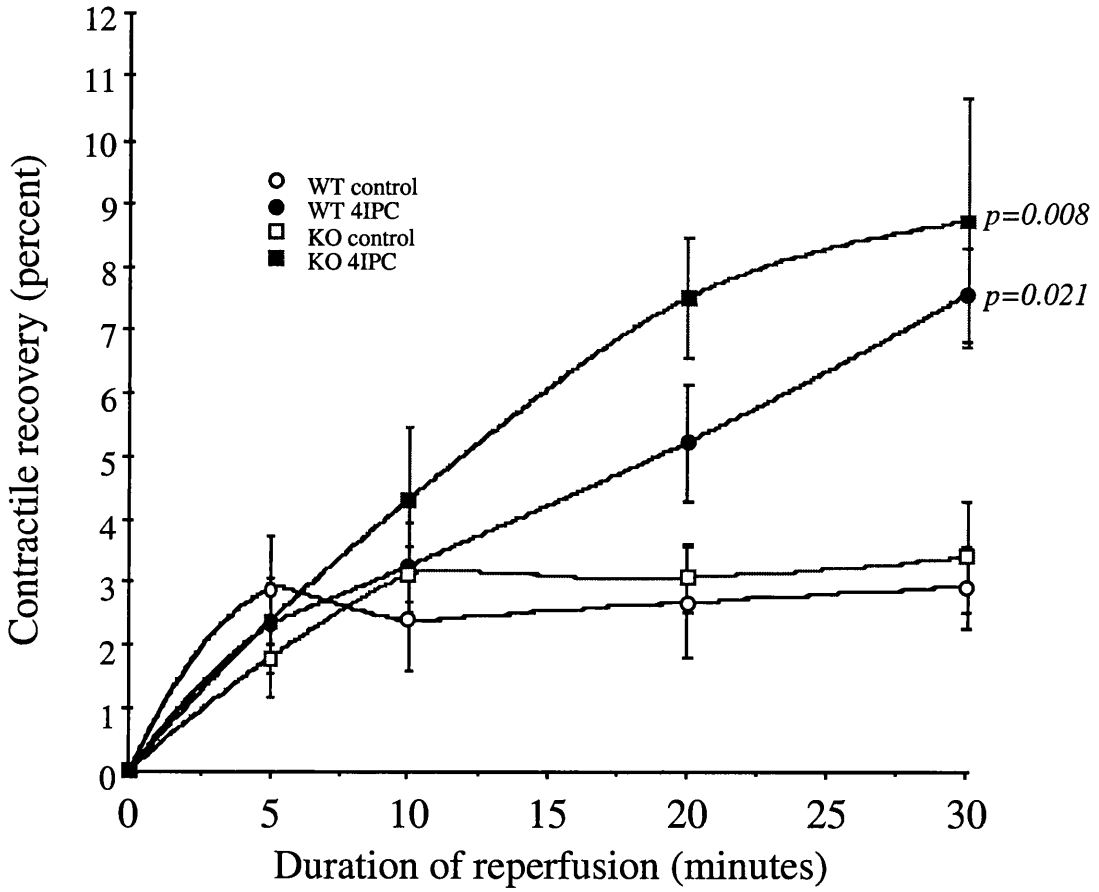

FIGURE 5.3.A. EXOGENOUS NO MIMICS CLASSICAL PRECONDITIONING.

SNAP 2 μM resulted in significant limitation of infarct size in both eNOS WT and eNOS KO groups suggesting that the targets of nitric oxide mediated protection are evident in all hearts subjected to ischaemia/reperfusion.

*, $p = 0.0006$ and **, $p < 0.0001$ versus respective controls.

n = 6 per group.

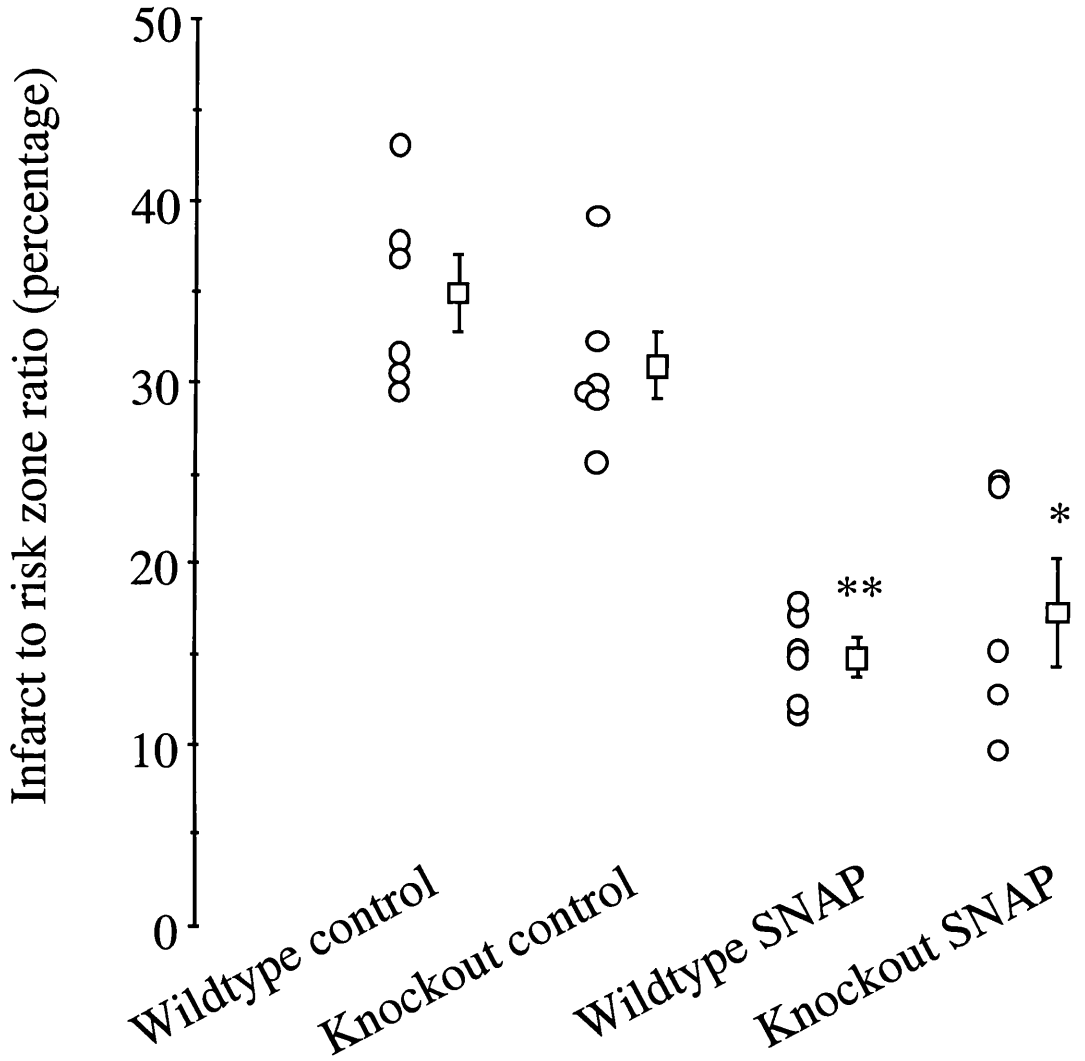

FIGURE 5.3.B. POST-ISCHAEMIC CONTRACTILE FUNCTION WITH SNAP

In addition to an infarct sparing effect, 2 μM SNAP also resulted in significant attenuation of contractile dysfunction (both groups, compared to controls, $p < 0.001$).

n = 6 per group.

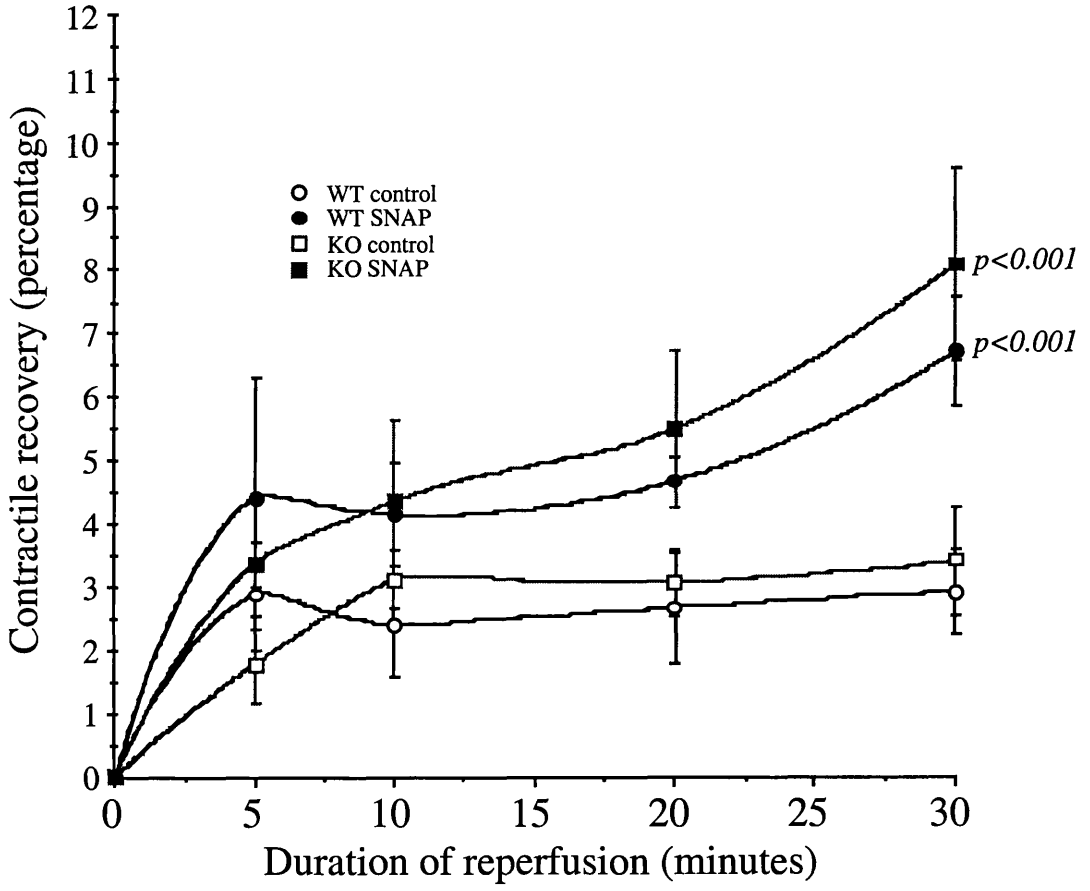

FIGURE 5.4. SUBTHRESHOLD PRECONDITIONING AND THE ROLE OF eNOS.

Reducing the number of cycles of preconditioning had no effect upon WT hearts (**A**), which continued to be significantly protected against infarction. However, the protection in KO mice (**B**) was lost. (* p = 0.039, ** p = 0.026 versus control).

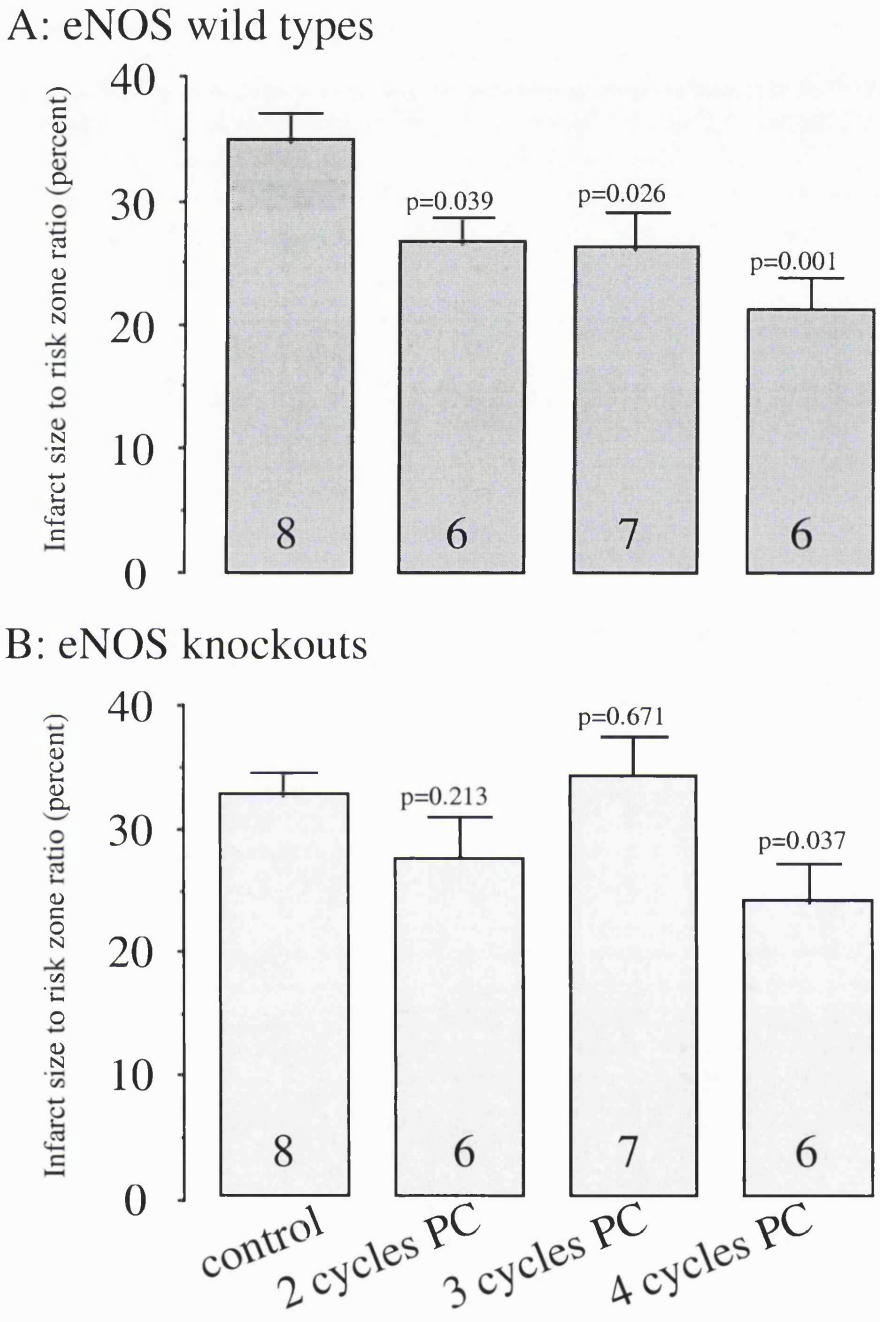

FIGURE 5.4.1. SUBTHRESHOLD PRECONDITIONING DOSE-RESPONSE CURVES.

A strong correlation between the number of preconditioning cycles and the infarct reduction observed is found in eNOS wild type, but not in eNOS knockout hearts. The threshold of preconditioning in knockout hearts appears to be 3 cycles of preconditioning.

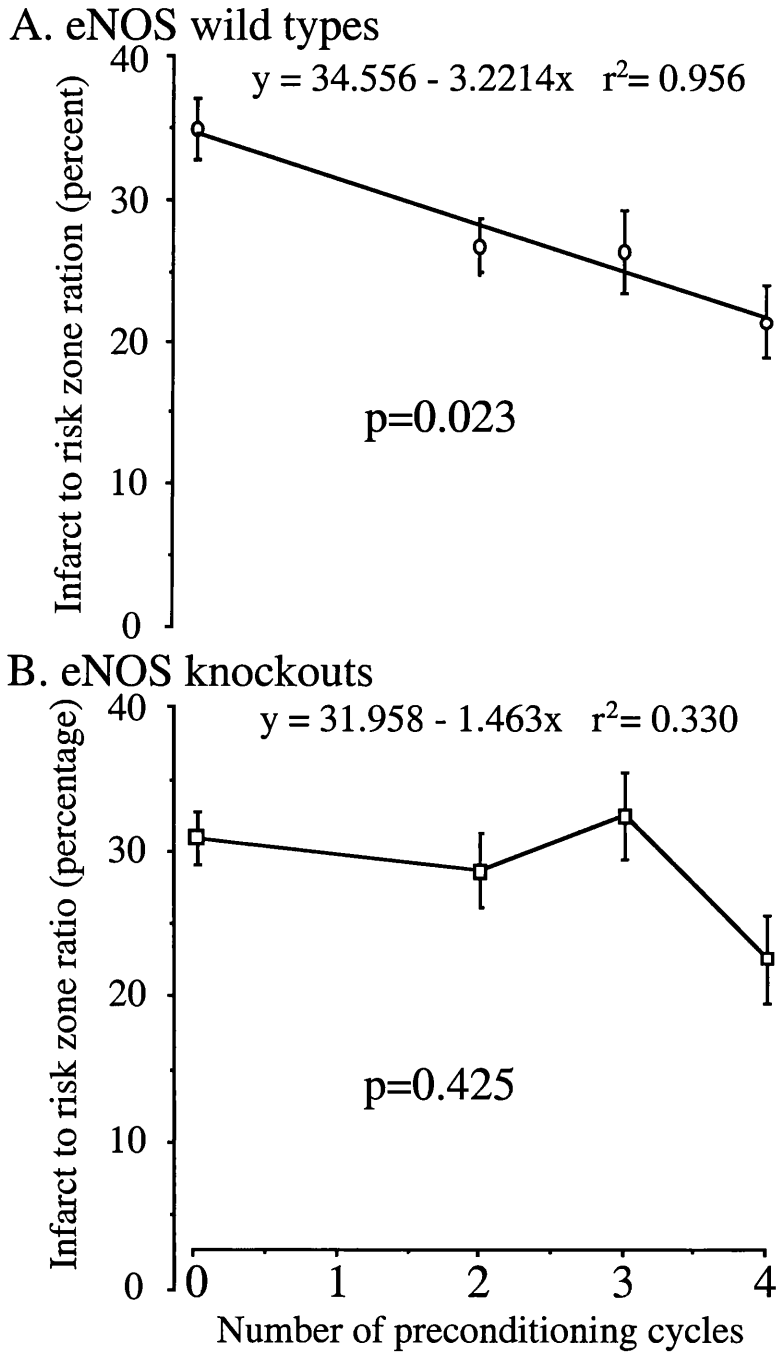

5.2.4 Exogenous NO and cardioprotection against infarction.

The role of NO in resistance to myocardial injury is controversial, and often likened to a double edged sword. The benefits of NO with respect to ischaemia/reperfusion in the heart has not been fully elaborated, but benefit is thought to be derived from lower concentrations, whilst the detrimental aspects of NO are seen at higher doses. Therefore, to determine the optimal cardioprotective concentration of NO in isolated perfused mouse heart, and to determine the concentration at which the detrimental aspects of NO are observed, hearts from naive eNOS wild type mice were perfused with increasing doses of the NO donor, SNAP, from 0.02 μM to 20 μM (protocol figure 1D) throughout the ischaemia/reperfusion protocol.

5.2.4.1. SNAP results in attenuation of infarct size.

Low dose SNAP (0.02 and 0.2 μM) failed to provide any significant resistance to injury from the ischaemia/reperfusion insult, although by 0.2 mM the mean infarct size was lower than that observed in control hearts (results summarised in figure 5.5; 32 ± 3% in control versus 28 ± 2% in the SNAP 0.2 μM group, $p = 0.392$). Intermediate doses of SNAP (1 and 2 μM) resulted in significant attenuation of infarct size compared to control, with the higher concentration of SNAP resulting in the greater protection (1 μM SNAP, 21 ± 1% and 2 μM SNAP, 17 ± 4%, $p = 0.029$ and $p = 0.002$ respectively versus control group). At higher concentrations (6 and 20 μM SNAP), the infarct sparing was lost, with infarct sizes approaching those in the low dose and control groups (6 μM SNAP, 28 ± 4%, 20 μM SNAP, 29 ± 3%, $p = 0.304$ and $p = 0.456$ respectively versus control hearts).

Examining the mean infarct sizes in the low and intermediate SNAP dose ranges revealed a linear logarithmic dose response curve between SNAP concentration and infarct size limitation up to the optimal cardioprotective concentration of 2 μM (figure 5.6, $r^2 = 0.941$).

SNAP concentrations equal to or greater than 6 μM were detrimental to cardioprotection and infarct sparing, confirming the potential hypothesis that the beneficial and detrimental effects of NO upon ischaemia/reperfusion injury may be concentration dependant.

5.2.4.2. SNAP results in attenuation of contractile dysfunction.

Concomitant with the infarct sparing effect of increasing doses of SNAP to the optimal concentration of 2 μM, there was also an improvement in contractile recovery, as summarised in figures 5.7 and 5.8. Figure 5.7 demonstrates the contractile recovery over time. As found in chapter 4, contractile recovery is poor and appears to be a model dependent phenomenon. However, within the modest functional recovery observed, this measured parameter was more sensitive to the cardioprotective effects of NO

concentration. Significant improvement in function was found at lower SNAP concentrations than thoose found to protect against myocardial necrosis, with 0.2 mM SNAP resulting in significantly better function than control hearts ($p = 0.007$). As with infarct reduction, the optimal dose of SNAP was found to be 2 μM (mean recovery figures summarised in figure 5.8; SNAP 2 mM mean contractile recovery 11.37 ± 1.54% versus control 3.25 ± 0.62%, $p < 0.001$). Whilst the curve is again bell-shaped, the contractile recovery associated with 20 μM SNAP was still significantly greater than that observed in control hearts (mean functional recovery 6.878 ± 1.01% in SNAP 100 μM versus control, 3.25 ± 0.62%, $p = 0.003$), even though protection from necrosis was lost at this concentration of SNAP. Again, comparing the mean recovery data with low to intermediate SNAP doses (0.02 to 2.00 μM SNAP), a linear logarithmic curve can be demonstrated between increasing SNAP concentration and contractile recovery (figure 5.9, $r^2 = 0.986$). Therefore, as with infarct measures, there is a concentration of SNAP beyond which the detrimental effects of SNAP start to overwhelm any beneficial advantageous effect. The mechanisms by which this occurs have not been studied here.

FIGURE 5.5. SNAP MEDIATED CARDIOPROTECTION: DOSE RESPONSE CURVE.

Infarct size following ischaemia/reperfusion in the presence of incremental concentrations of the nitric oxide donor, SNAP. Optimal protection is observed at a dose of 2 μM, but is lost by 6 μM. The result therefore implies that the protection mediated by nitric oxide may have a narrow therapeutic index.

*, p = 0.018, **, p = 0.001 versus control group perfused with normal buffer.

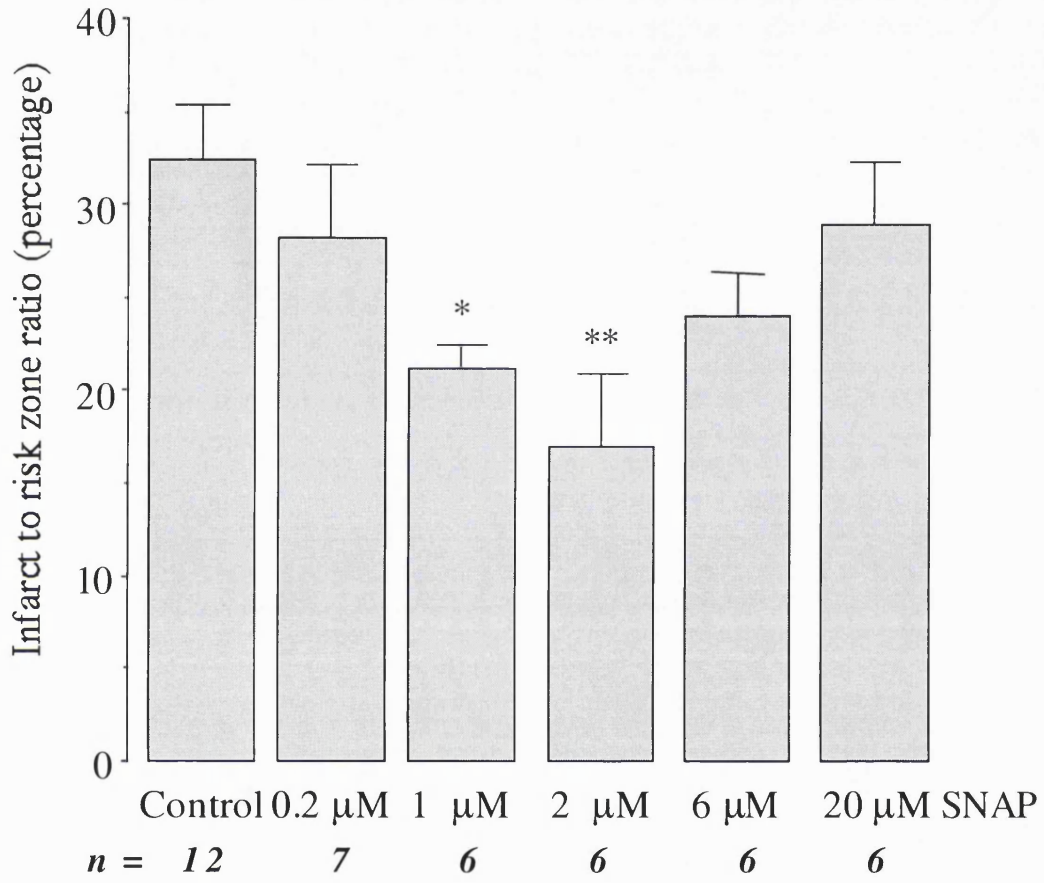

FIGURE 5.6. INFARCT REDUCTION IS PROPORTIONAL TO PERFUSATE CONCENTRATION OF SNAP.

Examining the infarct data revealed that SNAP attenuates necrosis with a logarithmic dose/response curve up to a concentration of 2 μM where optimal protection is observed. n = 6 per group.

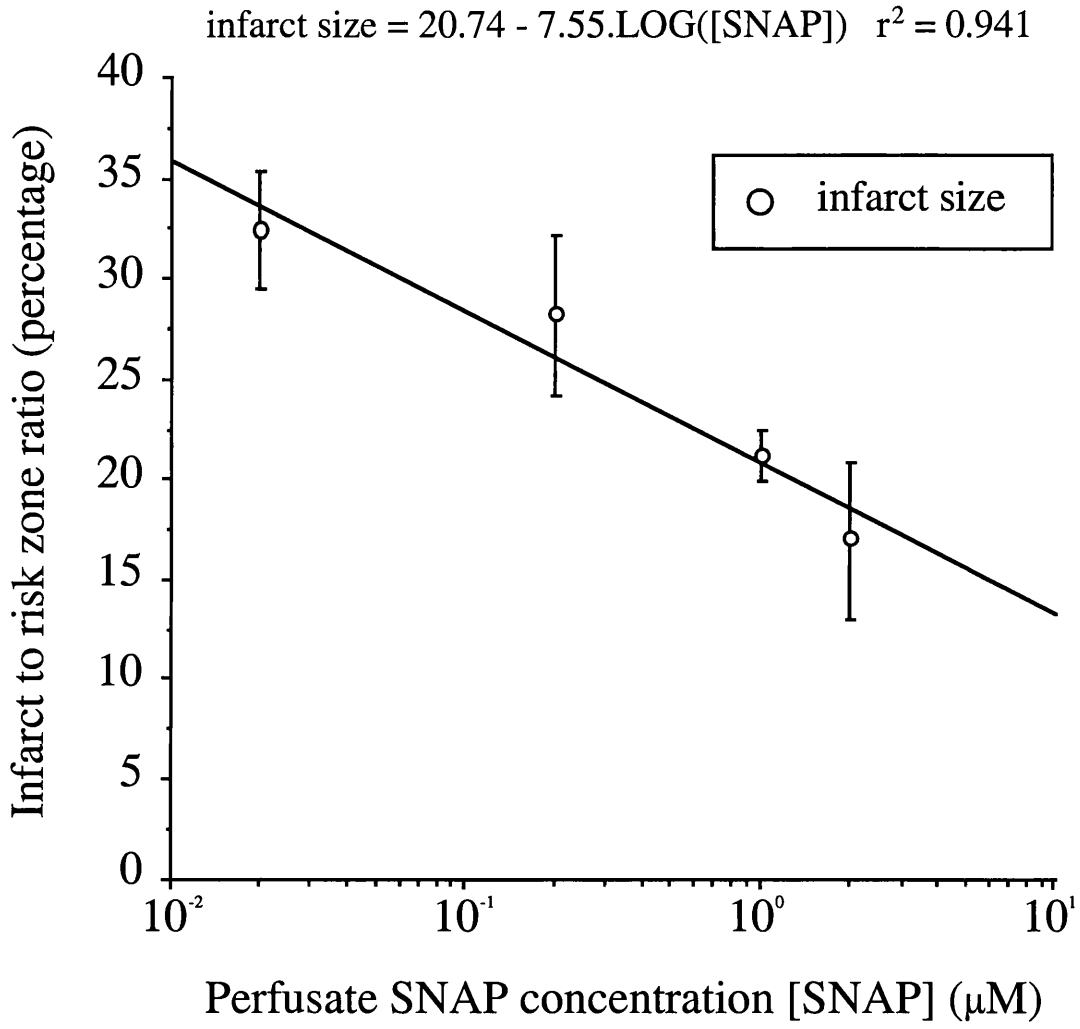

FIGURE 5.7. SNAP AND CONTRACTILE RECOVERY

Concentrations of up to 2 μM SNAP leads to an incremental improvement in post-ischaemic contractile function. At greater concentrations, SNAP confers less protection against ischaemia-induced contractile dysfunction. n = 6 per group.

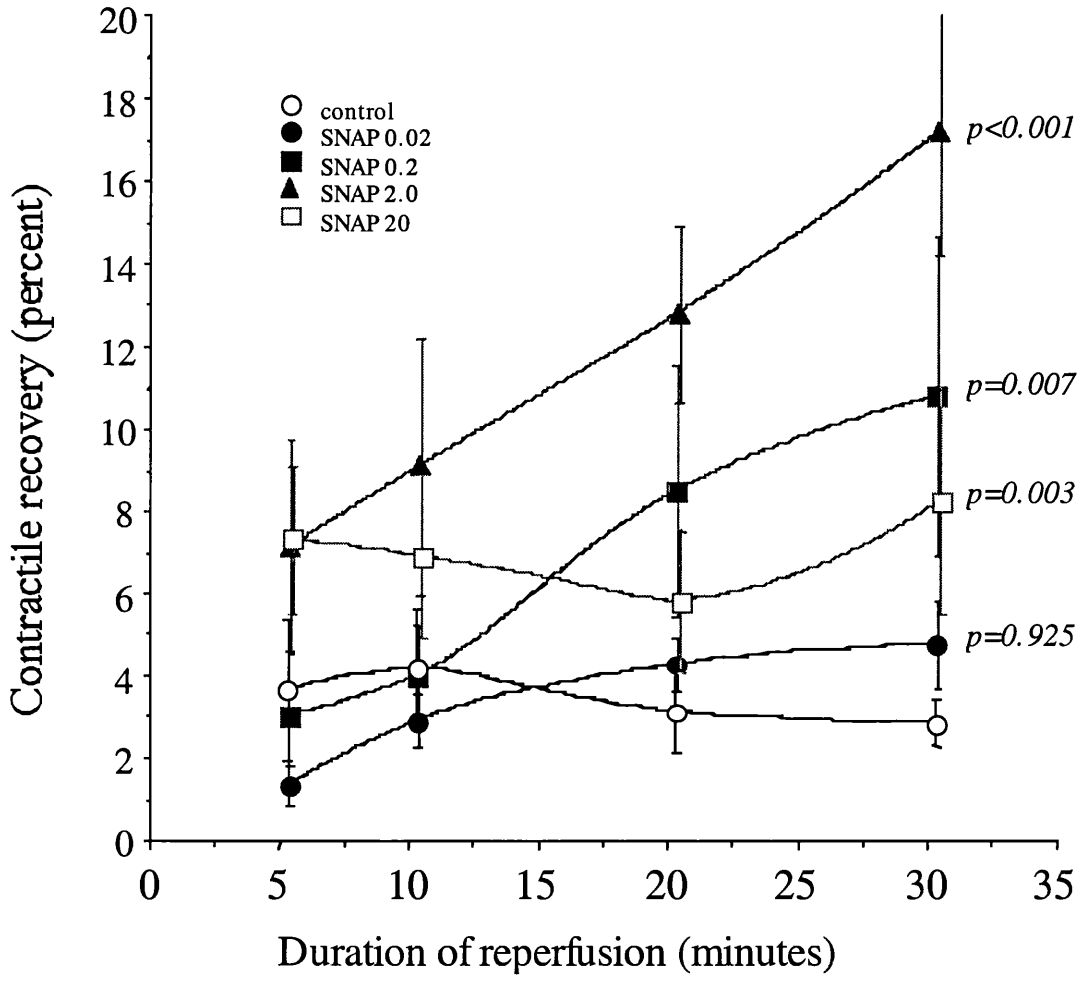

FIGURE 5.8. MEAN POST-ISCHAEMIC FUNCTION.

Presenting the same data as figure 5.7 in bar-graph form shows how increasing perfusate concentration of SNAP results in improved post-ischaemic function, up to an optimal concentration of 2 μM, where after post-ischaemic function deteriorates.

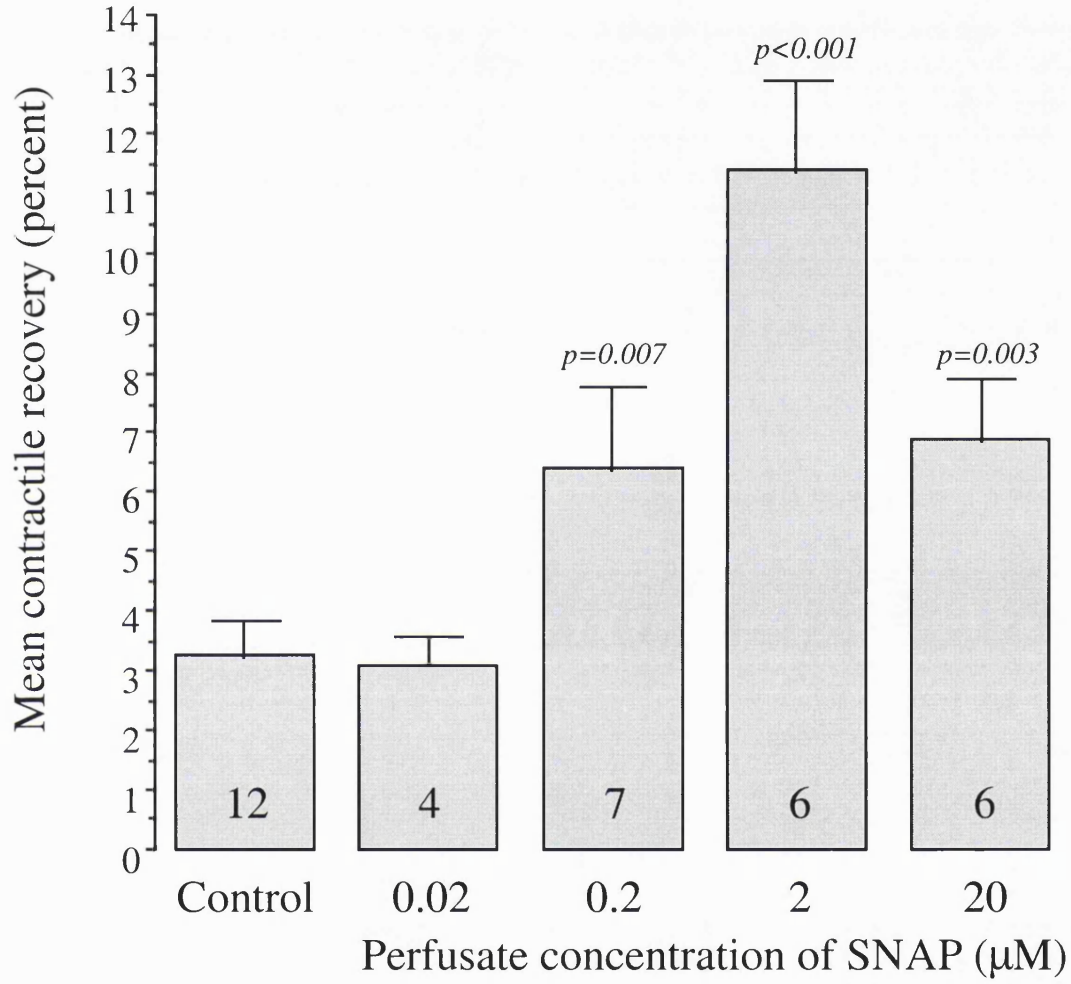

FIGURE 5.9. SNAP DOSE/RESPONSE AND CONTRACTILE RECOVERY.

Representing some of the data from figure 5.9, the improvement in contractile recovery is proportional to the log of the concentration of SNAP used, up to the optimal concentration of 2 μM. Beyond this concentration the protective relationship between SNAP dose and function is lost.

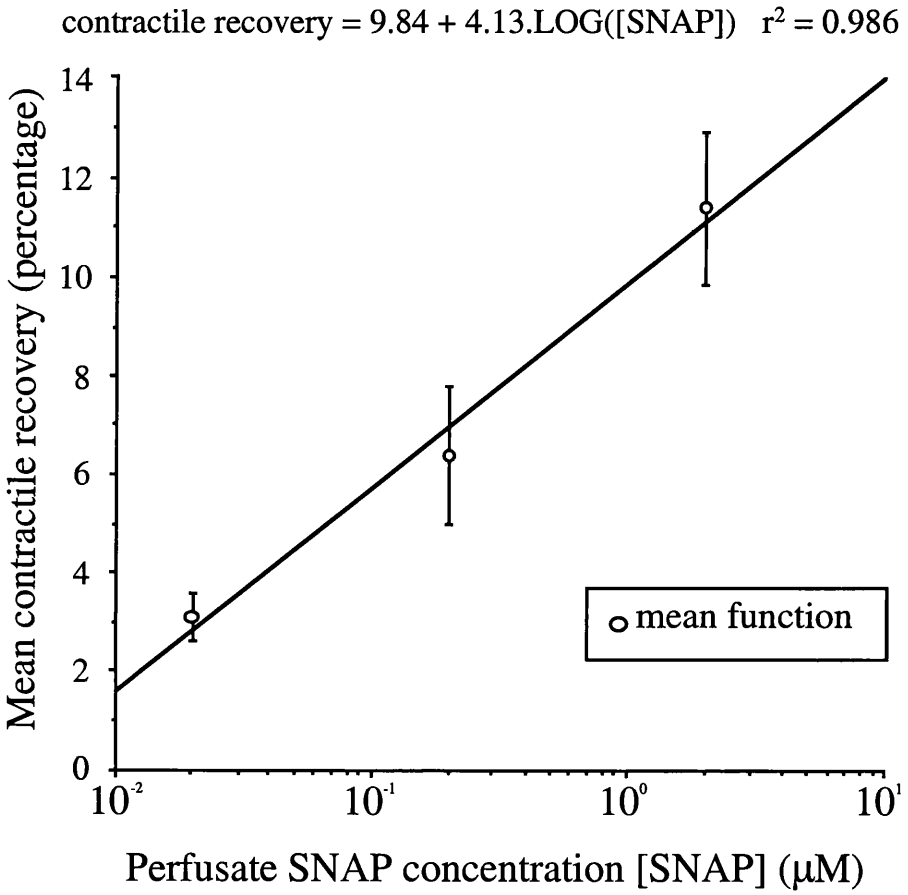

5.3 Discussion

5.3.1 The role of eNOS in early ischaemic preconditioning

A number of recently published pharmacological-based studies provide evidence that endogenous NO does not contribute towards ischaemic preconditioning,[327, 328] which is in accordance with earlier similarly designed studies.[263-265] The evidence presented here, with a robust preconditioning regime, appears to be consistent with these data; 4 cycles of preconditioning is equally efficacious at generating significant infarct size limitation in both eNOS WT and KO hearts. However, with less robust preconditioning stimuli of 3 or 2 cycles, protection is no longer observed in the KO animals and yet the WT hearts remain protected. These data suggest that enzymatic products of eNOS activity may contribute towards the multifactorial trigger signal required to induce early ischaemic preconditioning.

Exogenous NO has previously been shown to trigger preconditioning,[327] which is consistent with the data presented in figure 5.3. Exogenous NO derived from the spontaneous NO donor SNAP, even in the absence of eNOS, results in significant attenuation of infarct size, confirming that down stream targets of NO remain intact in the absence of eNOS, targets that may be pivotal in mediating the protection following less stringent preconditioning stimuli in WT hearts.

Thus, the contribution of NO and eNOS to trigger early preconditioning appear divergent from the published literature. These observations may have two explanations. The first may be the involve the magnitude of the preconditioning stimulus in these other studies.[263-265, 327, 328] At supra- threshold levels, ischaemic preconditioning may not obligatorily require *de novo* NO synthesis to trigger protection. A precedent exists for this hypothesis: the involvement of free radicals in early preconditioning where Baines et al demonstrated that one cycle but not 4 cycles of 5 minutes ischaemia 5 minutes reperfusion, preconditioning was reliant upon the generation of free radicals in the rabbit.[70] The second possibility concerns the catalytic properties of eNOS itself. NO is not the sole product of eNOS; under conditions of low intracellular BH_4 or L-arginine depletion, superoxide radicals may by be generated.[329, 330] Whilst L-arginine depletion is unlikely to occur during the relatively short duration of these experiments, neither BH_4 or free radicals were measured in this investigation, so the possibility of eNOS synthesised free radicals contributing to the preconditioning 'signal' cannot be excluded in the current study.

5.3.2. The double edged sword of NO in ischaemia/reperfusion injury

In section 5.2.2, exogenous NO (SNAP 2 μM) administered throughout the ischaemia/reperfusion protocol was demonstrated to result in significant infarct size reduction and improvement in post-ischaemic contractile function, consistent with findings of other investigators using both SNAP (1.5 μM)[331] and other NO donors such as FK409.[332] Other investigators have not found NO to be so benign. At higher doses (of greater than 10 μM), SNAP induces apoptosis (possibly via a cGMP mediated mechanism[232]) and becomes involved in peroxynitrite mediated injury.[333] Therefore to determine the concentrations of SNAP that were beneficial and detrimental in ischaemia/reperfusion injury, a concentration-response curve was constructed with regard to measurable infarction. Incremental concentrations of the NO donor resulted in significantly greater resistance to myocyte injury up to a concentration of 2 μM (a linear logarithmic relationship between infarct reduction and contractile function can be observed - figures 5.2.6 and 5.2.9). Beyond this concentration, the exogenous NO mediated protection to lethal ischaemic injury was lost, thus resulting in a clear benefit/detriment threshold.

The mechanisms of benefit and detriment are unclear, but it is interesting that the observed SNAP protection curve is similar to that observed by Brookes et al [280] between NO concentration and inhibition of mitochondrial swelling (a surrogate for mitochondrial permeability transition pore open probability). The inhibition of transition pore opening and the attenuation of release of cytochrome-c maybe one mechanism of protection, although NO may have many other potential targets, such as the mitochondrial K_{ATP} channel,[286] preserved p42/44 extracellular signal regulated protein kinase (ERK) phosphorylation[281] and nitrosylation and inhibition of members of the pro-apoptotic pathway, including caspase-3[282, 334] as discussed in section 1.7.7. The reasons for loss of protection between 2 and 6 μM SNAP are equally unclear, but may be related to free radical generation- possibly by the accumulation of peroxinitrite.[333]

5.3.3. Implications of a potential role of eNOS in early preconditioning.

In this chapter, eNOS has been shown to modify the preconditioning threshold, an observation that may have implications to preconditioning in gender. The role of gender and its effect upon preconditioning is explored in section 4.4.2 using a preconditioning regime (two cycles of 10 minutes ischaemia and 10 minutes reperfusion) that was equivalent to the four cycle 5 minute ischaemia/ 5 minute reperfusion protocol used in these studies (section 5.2.1). The influence of gender upon preconditioning was not found to be significant with respect to infarct resistance. However, using this robust preconditioning regime, no difference between infarct size resistance was noted in hearts from eNOS wild type and eNOS knockout mice whilst less robust

preconditioning regimes there *was* a difference comparing eNOS WT and KO hearts. This may be significant in interpreting the gender preconditioning data. In section 4.4.2, it was noted that 17 β-oestradiol regulates eNOS activity. This being the case, the threshold to preconditioning may be lower in female animals, but as noted above, the preconditioning regime used is suprathreshold. To more accurately determine a difference in the preconditioning threshold in male versus female mice, a much smaller preconditioning threshold needs to be explored- possibly using 1 cycle of 2.5 minutes or 5 minutes of transient ischaemia and re-oxygenation. That there may be a difference in the preconditioning threshold is a novel hypothesis has not been investigated before, and could of clinical interest/relevance in the investigation and management of male and female patients with acute coronary syndromes.

5.4 Conclusions

A number of novel observations regarding the role of nitric oxide in early ischaemic preconditioning can be made. Firstly, nitric oxide appears to play a nonessential role in early ischaemic preconditioning, contributing to the preconditioning stimulus, and thus reducing the duration of antecedent ischaemia required to induce protection against a subsequent lethal ischaemic insult. Secondly, in the eNOS knockout hearts, despite the absence of the synthase, the cellular targets for nitric oxide mediated protection remain intact, as ischaemic preconditioning can be clearly mimicked with the administration of an exogenous nitric oxide donor. Finally, the nitric oxide dose response curve and the injury observed as a result of ischaemia/reperfusion demonstrates a clear benefit/detriment threshold that appears to exist at a concentration of SNAP of 2 μM. With these data, it is possible to predict the benefit/detriment of nitric oxide in various pathologies based upon the concentration of nitric oxide. Thus, nitric oxide synthesis during an ischaemia/reperfusion insult may be cardioprotective when synthesized in modest quantities, whereas the considerable synthesis of NO, as associated with iNOS induction in endotoxic shock, may be detrimental to myocyte survival in the context of ischaemic injury.

Chapter 6. The role of nitric oxide in delayed pharmacologicai preconditioning.

6.1. Aims and protocols

As described in chapter 1 (section 1.6.3), delayed preconditioning is associated with new protein synthesis; inhibition of translation or transcription of protein abrogates the protection associated with this phase of preconditioning.[179] Nitric oxide has been associated with increased resistance to myocardial infarction. With the administration of exogenous nitric oxide using spontaneous donors, significant attenuation of infarction can be observed (chapter 5). The inducible isoform of nitric oxide synthase has been shown to be increased following a number of stressful stimuli; as such it is attractive to hypothesize that delayed preconditioning is associated with the induction of iNOS, and mediated by the resulting increased NO synthesis. This hypothesis has been strengthened by recent studies using pharmacological inhibitors of iNOS transcription[209] or activity,[209, 271] and using transgenic mouse models where the iNOS gene has undergone targeted disruption.[230, 272] Whilst evidence for the role of iNOS in delayed *ischaemic* preconditioning is strong, comparatively little is known about delayed *pharmacological* preconditioning, and in particular, following the administration of an adenosine A_1 receptor agonist. Ischaemic preconditioning results in the release of numerous neuro-humoral agents, and inflammatory cytokines.[335] These cytokines appear to preferentially signal via the p42/p44 ERK pathway to upregulate gene products such as inducible isoforms of nitric oxide synthase.[169, 170] Adenosine A_1 receptor activation appears to signal via PKC[143] and thus may preferentially upregulate p38 MAPK activity. Therefore, there may be clear differences between pharmacological and ischaemic delayed preconditioning that have yet to be fully elucidated.

Recent peripheral vascular based studies by Bhagat and colleagues, investigating the role of cytokines in shock,[275] have demonstrated that eNOS activity can be significantly up-regulated by increased BH_4 availability through the induction of the synthesising enzyme, GTP-cyclohydrolase-1. The increased NO synthesis from eNOS, in the absence of significant iNOS upregulation, was said to be an example of eNOS "masquerading" as iNOS. The potential importance of this observation in context of preconditioning has not, until now, been explored.

To investigate the comparative importance of the NOS isoforms in the mediation of delayed *pharmacological* preconditioning, a model of delayed pharmacological preconditioning needed to be developed. Whilst the adenosine A_1 receptor agonist, 2-chloro N^6 cyclopentyl adenosine (CCPA) is a known trigger of delayed preconditioning in rabbit[143, 203, 336] and rat,[96] CCPA triggered delayed preconditioning in mouse had not

been characterised. Therefore, a dose-response curve was performed, prior to determining the effect of prior administration of CCPA in both wild type (WT) mice and mice with targeted disruption of the iNOS gene (KO).

FIGURE 6.1. CCPA TRIGGERED DELAYED PRECONDITIONING PROTOCOLS.

Experimental protocols. **A**. Determination of CCPA dose: 25 or 100 μg/kg *iv* administered 24 hours prior to index ischaemia compared to control group. **B**. Saline vehicle treatment versus CCPA preconditioning in WT and KO hearts. **C**. As for protocol B, with the co-infusion of L-NAME (100 μM) throughout the perfusion protocol. **D**. Effect of SNAP 1 μM to iNOS KO hearts, present throughout the perfusion protocol. **E**. Hearts from pre-treated animals were excised and perfused for 20 minutes before snap freezing and storage for later Western blot analysis.

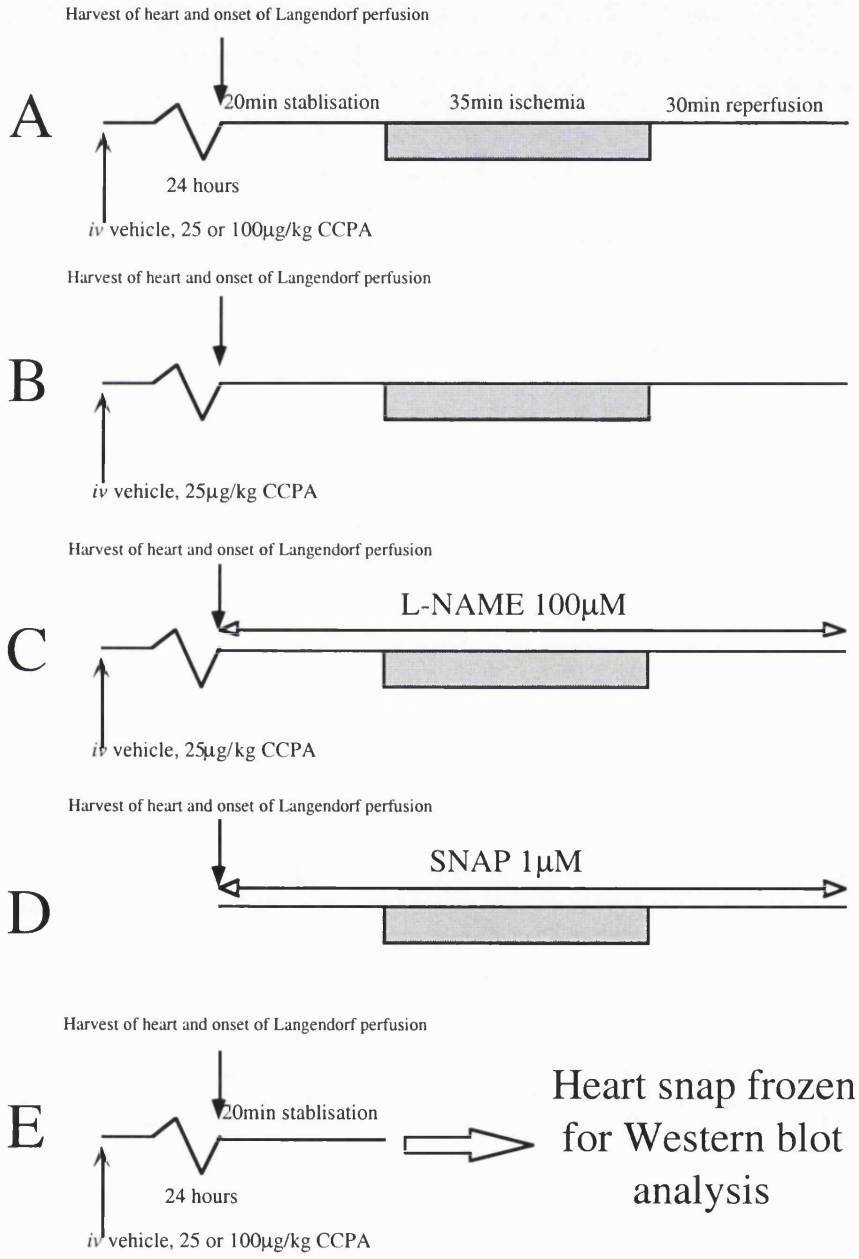

Table 5. Chapter 6: Morphometrics and baseline functional value.

*: baseline coronary flow was significantly reduced in hearts from animals that had received the higher CCPA dose of 100 μg/kg: p = 0.0028 versus control group and p = 0.0458 versus 25 μg/kg CCPA treated group. L-NAME resulted in significantly lower coronary flow rates in control WT and KO animals, and in CCPA treated KO. CCPA treated WT hearts had a lower mean flow rate, but was not significantly different from the non L-NAME treated group. †, P < 0.0001 vs equivalent non-L-NAME group, ‡, P < 0.002 vs equivalent non-L-NAME group, §, P < 0.004 vs equivalent non-L-NAME group.

Group	Mouse body weight (g)	Heart weight (mg)	Coronary flow rate ($ml.min^{-1}$)	Force-rate product ($g.b.min^{-1}$)	Resting tension (g)
A					
Control (n = 16)	26.23 ± 1.11	152 ± 1	3.66 ± 0.19	918 ± 62	1.00 ± 0.12
CCPA (25 μg/kg) (n = 9)	24.73 ± 0.85	149 ± 7	3.59 ± 0.22	1052 ± 91	1.22 ± 0.06
CCPA (100 μg/kg) (n = 9)	26.03 ± 0.48	150 ± 4	2.70 ± 0.11*	1035 ± 138	1.02 ± 0.05
B					
WT vehicle (n = 10)	22.81 ± 0.68	128 ± 2	3.61 ± 0.39	1100 ± 79	1.23 ± 0.10
WT CCPA (n = 9)	22.66 ± 0.47	129 ± 3	3.34 ± 0.53	1077 ± 61	1.60 ± 0.19
KO vehicle (n = 10)	22.02 ± 0.66	139 ± 4	3.51 ± 0.21	1125 ± 104	1.45 ± 0.16
KO CCPA (n = 10)	22.32 ± 0.42	138 ± 5	3.59 ± 0.25	894 ± 97	1.50 ± 0.11
C					
WT vehicle + L-NAME (n = 8)	21.06 ± 0.20	130 ± 5	1.59 ± 0.24†	800 ± 73	1.32 ± 0.14
WT CCPA + L-NAME (n = 8)	20.96 ± 0.46	130 ± 7	2.46 ± 0.37	778 ± 192	1.39 ± 0.08
KO vehicle + L-NAME (n = 8)	21.59 ± 0.40	133 ± 5	1.99 ± 0.10‡	891 ± 151	1.50 ± 0.19
KO CCPA + L-NAME (n = 9)	22.14 ± 0.52	139 ± 8	2.23 ± 0.25§	1143 ± 135	1.04 ± 0.04
D					
Control (n = 6)	26.30 ± 0.59	154 ± 5	3.11 ± 0.34	1002 ± 165	1.00 ± 0.02
SNAP (n = 6)	28.34 ± 1.20	162 ± 6	3.18 ± 0.18	1100 ± 168	1.00 ± 0.03

Table 6. Summary of rtPCR genotyping.

As described in section 3.9.1, liver of animals whose hearts were used in Langendorff perfusion were extracted and frozen for rtPCR analysis. These tissue samples were then later randomly selected and mRNA extracted to determine gene expression of iNOS. As shown below, livers from animals with the targeted disruption of iNOS had no detectable iNOS mRNA after 40 cycles of PCR amplification. In contrary, iNOS wild types had readily detectable iNOS expression. Interestingly, the livers from animals that had been pharmacologically preconditioned with CCPA appeared to have greater mRNA contents than those that had received the saline vehicle.

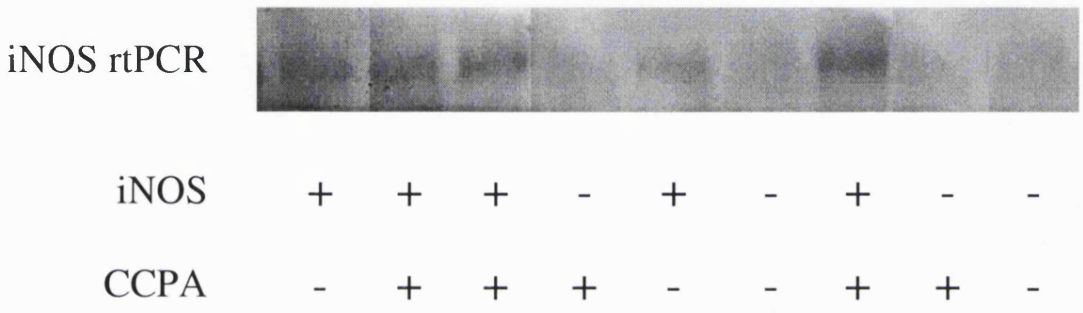

6.2. Results

No significant difference between groups were documented in terms of body or heart weights, end-stabilisation contractile function or resting tension load placed on the hearts to achieve maximal developed force (table 5). Significant differences in baseline coronary flows were observed. In group A, high dose administration of CCPA (100 μg/kg) resulted in lower coronary flow rates 24 hours later, compared to control and low dose CCPA (25 μg/kg). Similarly attenuated coronary flows were also documented in Group C, associated with the administration of the non-specific NOS inhibitor, L-NAME (100 μM), presumably associated with the consequence of attenuated vasodilator response. The rtPCR data shown in table 6 confirm the genotype of the animals used in the study, correlating with the protein estimations shown in figure 6.7.A.

6.2.1. Determination of optimal CCPA dosage regime

Whilst adenosine A_1 receptor activation has been demonstrated to elicit delayed cardioprotection against infarction in other mammalian species such as rabbit, until recently it was unknown whether A_1 receptor agonists such as 2-chloro N^6 cyclopentyl adenosine (CCPA) are able to trigger delayed preconditioning in mice. Therefore, WT hearts were subjected to the ischaemia reperfusion regime outlined in figure 6.1.A. The mice were injected *iv* with either the saline vehicle or the drug (CCPA 25 μg/kg or 100 μg/kg) 24 hours prior to the hearts being harvested and Langendorff perfused. The mice were observed during and following drug administration, their physical activity noted and recorded. Animals administered with 100 μg/kg CCPA displayed physical evidence of shock (pilo errection, haunched posture and minimal provoked behaviour) lasting over 1.5 hours. At the lower 25 μg/kg dose, treated animals demonstrated none of these features, although exploratory behaviour was subdued until returning to normal within 40 minutes.

Both doses of CCPA given 24 hours prior to lethal ischaemia resulted in equivalent significant infarct size reduction (figure 6.2). However, the hearts of animals treated with 100 μg/kg CCPA had significantly lower baseline coronary flow rates compared to vehicle and 25 μg/kg CCPA treated animals: coronary flow was 3.66 ± 0.19 ml/min and 3.59 ± 0.22 ml/min in controls and 25 μg/kg versus 2.7 ± 0.11 ml/min in the 100 μg/kg treated group ($p = 0.0028$ and $p = 0.0456$ versus control and 25 μg/kg groups respectively). Therefore, to avoid systemic haemodynamic shock (and therefore unwanted cytokine induction) and coronary haemodynamic sequelae, the lower 25 μg/kg dose of CCPA was employed for this study.

6.2.2. The role of iNOS in mediating delayed preconditioning

The aim of the study was to test the hypothesis that delayed pharmacological preconditioning was mediated by the induction of iNOS. Therefore, delayed pharmacological preconditioning was not expected to be observed in the hearts from iNOS KO animals. Using the low dose CCPA (25 μg/kg) regime characterised in 6.2.1, animals were pre-treated with either the saline vehicle (control) or CCPA, *iv*, 24 hours prior to harvesting the hearts and Langendorff perfusion (protocol, figure 6.1.B). Following the injurious ischaemia/reperfusion insult, both WT and KO hearts from animals treated with saline vehicle had equivalent infarct sizes- 37 ± 3% and 37 ± 2% respectively (figure 6.3.A). Prior CCPA administration significantly reduced infarct size in WT hearts to 22 ± 2% and also, unexpectedly, in KO hearts to 27 ± 2%, possibly implying that either (1) nitric oxide is not required for delayed pharmacological preconditioning, or (2) nitric oxide is required for protection, not necessarily derived from iNOS.

Whilst protection against infarction was observed, there was no significant diminution of contractile dysfunction in either WT or KO, CCPA treatment groups (figure 6.3.B). Whilst delayed ischaemic preconditioning reduces post ischaemic dysfunction (stunning), the protection observed following transient adenosine A_1 receptor activation has not been associated with improved myocardial function after ischaemia/reperfusion injury[337]- and this appears consistent with the data presented here.

6.2.3. NOS activity assessment

To determine whether the protection observed in KO hearts occurred independently of mechanisms involving the synthesis of NO, the rate of NO_X release into the coronary effluent was measured (results summarised in figure 6.4.A). The NO_X release rates are representative of synthesis throughout the perfusion protocol of each heart. NO_X release during stabilisation was negligible in both WT and KO control hearts (2.86 ± 2.86 and 0.00 ± 0.00 nmole/min/gram wet weight heart). Preconditioning with CCPA resulted in significant increases of NO_X release, 20.67 ± 7.40 and 16.37 ± 5.46 nmole/min/gram in WT and KO hearts respectively ($p = 0.010$ and $p = 0.017$ versus respective controls).

Therefore, delayed pharmacological preconditioning results in a sustained increase in basal nitric oxide generation that may be important in mediating the infarct sparing protection observed in this model. Moreover, because transient adenosine A_1 receptor activation results in a significant increase of nitric oxide synthesis in the absence of iNOS, the generation of nitric oxide could be by one of the other enzymatic sources of nitric oxide.

6.2.4. NO- cardioprotective mediator or epiphenomenon?

Whilst CCPA pre-treatment to iNOS WT and KO mice resulted in significant upregulation of NO synthesis, the NO generated need not necessarily be mediating the cardioprotection observed. Therefore, to determine whether NO is a cardioprotective mediator or epiphenomenon of delayed pharmacological preconditioning, two approaches were taken: first to determine whether attenuation of NO generation abrogated delayed preconditioning and second, to investigate whether exogenously administered NO could mimic preconditioning infarct limitation.

To attenuate all NOS activity during ischaemia and reperfusion, a non-specific NOS inhibitor, L-NAME (100 μM) was added to the Krebs Henseleit buffer (protocol, figure 6.1.C). Consistent with the hypothesis that NOS activity is essential for the infarct sparing effect of delayed preconditioning, protection against infarction was abrogated in the CCPA pre-treated groups (see table 4 and figure 6.5), concomitant with complete abrogation of NO_x release into the coronary effluent.

In the second phase, using naive KO hearts, the spontaneous NO donor, S-nitroso N-acetyl penicillamine (SNAP, 1 μM) was added to the perfusion buffer (protocol, figure 6.1.D). This dose was estimated, based upon the concentration of NO_x released from hearts of CCPA treated WT mice (20.67 ± 7.40 nM/min). SNAP donates NO with 1:1 stoichiometry at a high rate of degradation; 100 μM SNAP releases 1.4 μM NO/minute at 37 °C, linear over a wide temperature range[338], which equates to 1.4 μM SNAP to reproduce the coronary release measured. Compared to control hearts perfused with the unmodified Krebs Henseleit buffer, SNAP perfused hearts had significantly reduced infarction from 37 ± 3% to 21 ± 1% (figure 6.6, $p < 0.001$) - an equivalent reduction to that observed in preconditioned WT and KO hearts.

6.2.5. CCPA triggered preconditioning: eNOS and iNOS regulation.

Delayed pharmacological preconditioning triggered by transient adenosine A_1 receptor activation with the selective agonist, CCPA, appears to be mediated by the generation of NO in both iNOS wild types and iNOS knockouts. The generation of significantly greater NO in the iNOS KO group implies the upregulation of a constitutively expressed NOS isoform. Investigators have previously demonstrated that the eNOS isoform is widely expressed in the myocardium,[254] and the suggestion that eNOS activity can be significantly upregulated in the absence of iNOS activity,[275] the expression of the eNOS and iNOS isoforms were determined 24 hours following transient adenosine A_1 receptor activation. Therefore hearts from animals that had been pre-treated were isolated and Langendorff perfused for 20 minutes (to correspond with the coronary perfusate NO_x collection time at the end of the stabilisation period), and then snap frozen in liquid nitrogen (protocol, figure 6.1.E.). The results of the Western blot

analysis are summarised in figure 6.7. As previously reported preconditioning increases the expression of iNOS from modest expression in naive hearts to 2.31 times greater in hearts of CCPA pre-treated iNOS WT animals (figure 6.7.A, p = 0.002). Consistent with the knockout status, no iNOS protein was expressed in either vehicle control or CCPA treated iNOS KO groups (figure 6.7.A). Whereas in previous studies, eNOS was demonstrated not to be regulated following transient *ischaemia* 24 hours earlier,[230] the pre-administration of 25 μg/kg CCPA resulted in significant upregulation of eNOS protein in both iNOS WT and iNOS KO groups (summarised in figure 6.7.B, 210 ± 35% and 241 ± 21% of iNOS WT control iNOS expression respectively, with p values of 0.013 and 0.018 versus their respective controls in the wild type and knock out groups respectively). Comparing iNOS WT and iNOS KO control animals, baseline eNOS content was not found to be significantly greater in the control iNOS KO hearts (138 ± 19%) than compared to iNOS WT groups (100 ± 18%, p = 0.297). Therefore, delayed pharmacological preconditioning with the adenosine A_1 agonist, CCPA, at a dose of 25 μg/kg, is mediated via the upregulation of eNOS and iNOS; in the absence of iNOS the eNOS may become pivotal to the protection observed.

6.2.6. The role of eNOS in delayed pharmacological preconditioning.

The novel implication that eNOS is involved in delayed pharmacological preconditioning was explored further by testing the hypothesis that eNOS was essential for delayed pharmacological preconditioning. The protocol was essentially as shown in figure 6.1.B, whereby 25 μg/kg CCPA was used to trigger preconditioning in both eNOS WT and eNOS KO animals, whilst control animals received an equivalent volume of saline. The results are summarised in figure 6.9. CCPA preconditioning resulted in significant attenuation of infarct size in comparison with hearts from eNOS WT animals (34 ± 2% versus 24 ± 3% in control and preconditioned hearts respectively, p = 0.005). This protection was no longer evident in the eNOS KO hearts, where CCPA preconditioning results in a non-significant (p = 0.146) reduction in measured infarction (32 ± 1% versus 26 ± 3% in control and CCPA groups respectively). The data would therefore appear to support a role for eNOS, although more work needs to be performed to increase numbers in this study to ensure that the present result is correct, and to determine whether the role of eNOS is important for the triggering or mediation of delayed pharmacological preconditioning.

FIGURE 6.2. CCPA MYOCARDIAL RESISTANCE DOSE RESPONSE.

Both doses of CCPA, 25 μg/kg and 100 μg/kg resulted in similar infarct size limitation, but the lower dose had fewer haemodynamic sequelae (summarised table 5).

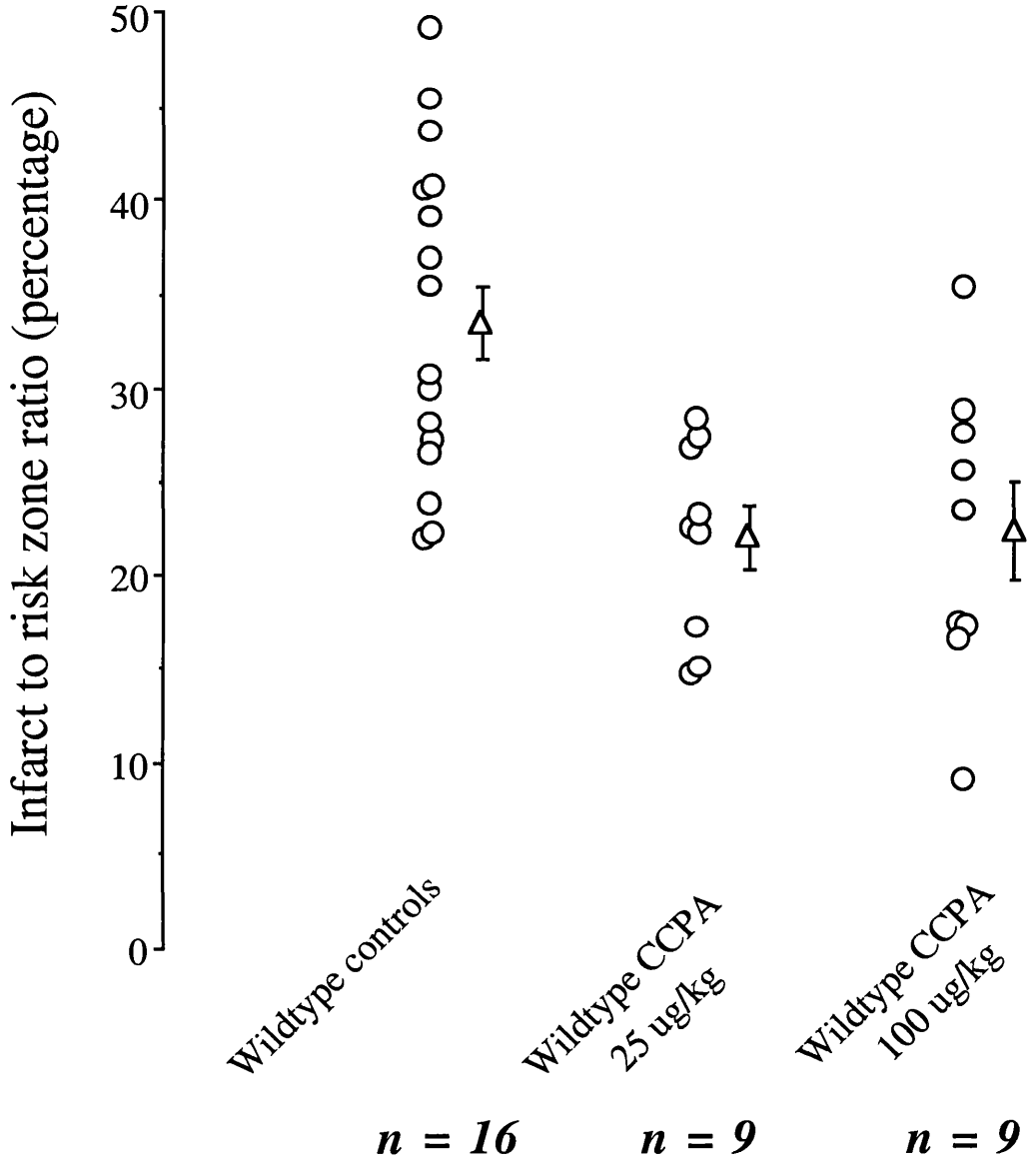

FIGURE 6.3.A. CCPA TRIGGERED SECOND WINDOW OF PROTECTION IN WT AND KO MICE.

The effect of CCPA delayed pharmacological preconditioning upon iNOS WT and KO hearts. Infarct size in control iNOS WT and KO hearts are the same. preconditioning with CCPA leads to attenuation of infarction in WT hearts and, unexpectedly, in KO hearts. **, $p < 0.0001$ versus WT vehicle and *, $p = 0.001$ versus KO vehicle hearts.

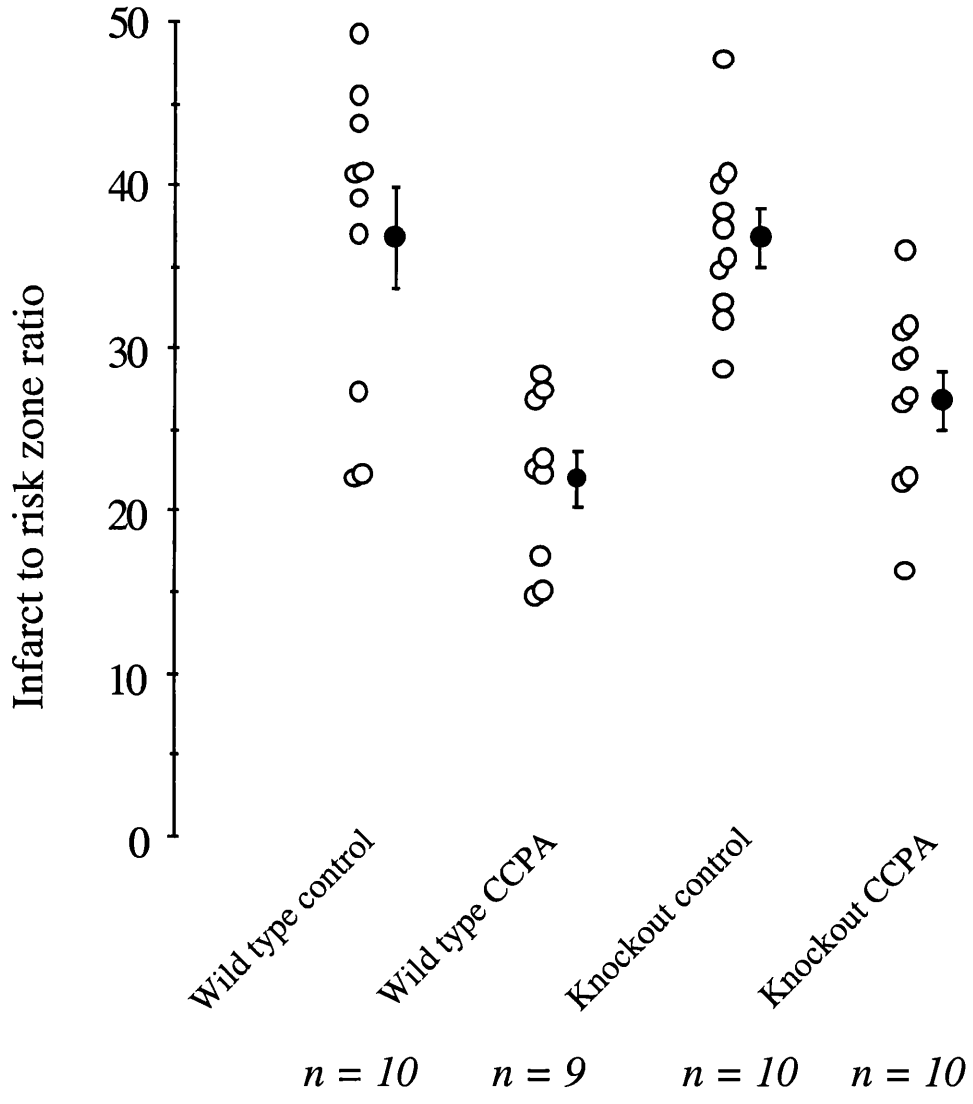

FIGURE 6.3.B. CCPA PRECONDITIONING AND HAEMODYNAMIC OUTCOMES.

Delayed pharmacological preconditioning with CCPA fails to attenuate stunning in this model.
(n = 9 to 10 per group)

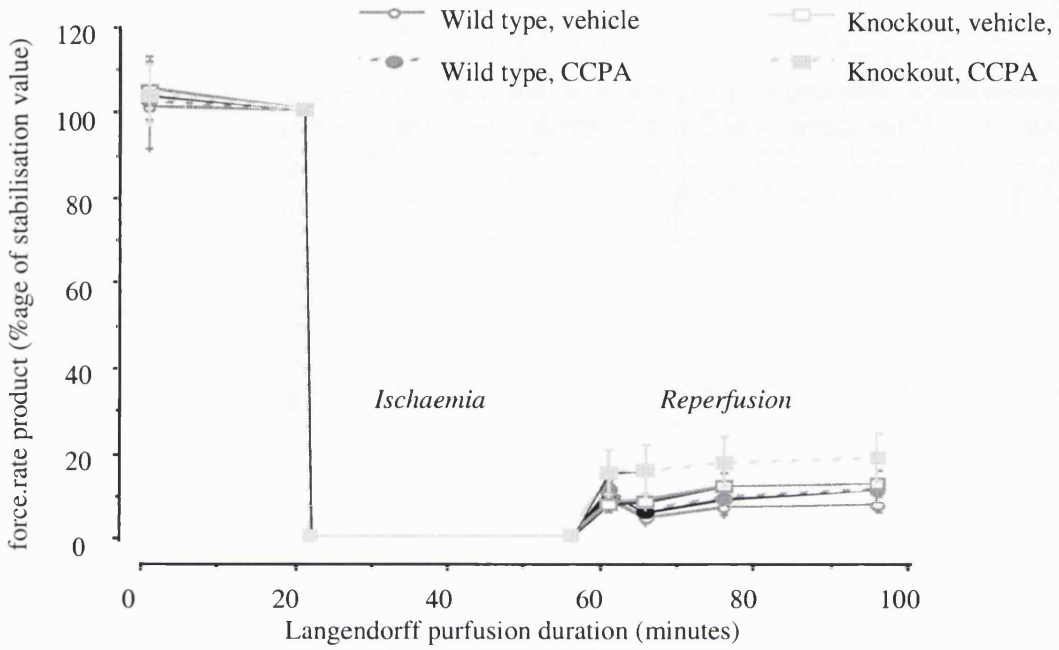

FIGURE 6.4.1. THE RATE OF RELEASE OF NO FROM CONTROL AND PRECONDITIONED HEARTS.

The rate of NO release into the coronary effluent, corrected for coronary flow rate and myocardial weight. Basal NO_X release in control hearts is minimal, but is significantly augmented by administration of CCPA 24 hours' earlier. **, p = 0.010 versus control. *, p = 0.017 versus control.

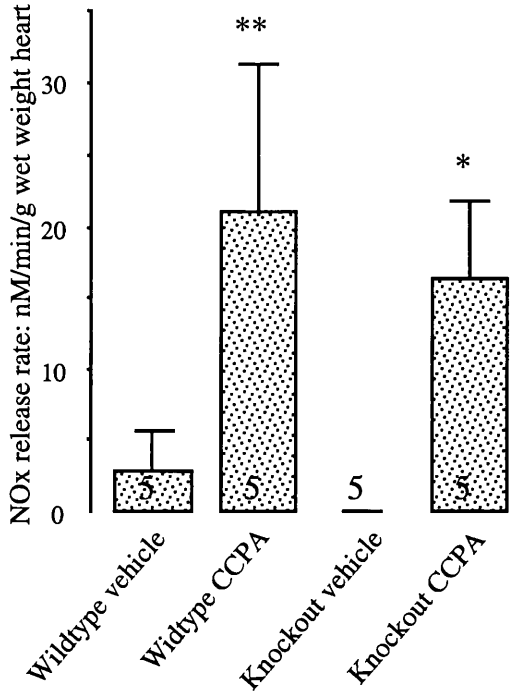

FIGURE 6.4.2. NO_X RELEASE WITH THE ADMINISTRATION OF L-NAME

Co-infusion of the non-specific NOS inhibitor, L-NAME (100 μM) totally abrogates NO_X release from the heart in all four groups.

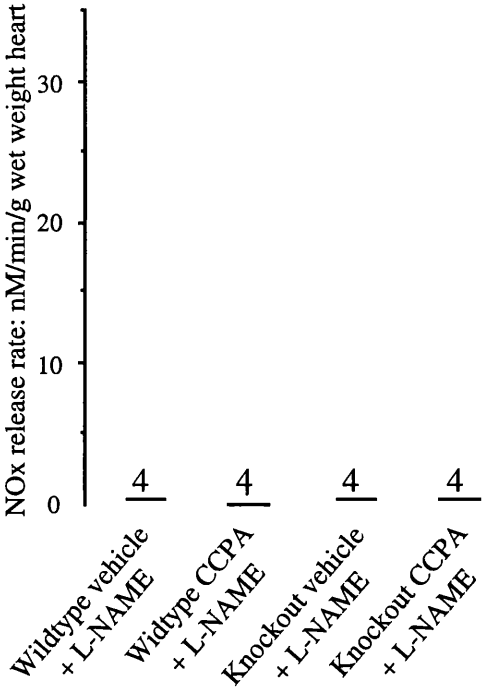

FIGURE 6.5. L-NAME ABROGATES DELAYED *PHARMACOLOGICAL* PRECONDITIONING.

The effect of L-NAME (100 μM) administered during the ischaemia/reperfusion insult upon the protective effect of delayed *pharmacological* preconditioning with CCPA. In both WT and knockouts pre-treated with CCPA, infarct limitation is abrogated in the presence of the non-specific NOS inhibitor, L-NAME. (n = 8 to 9 per group)

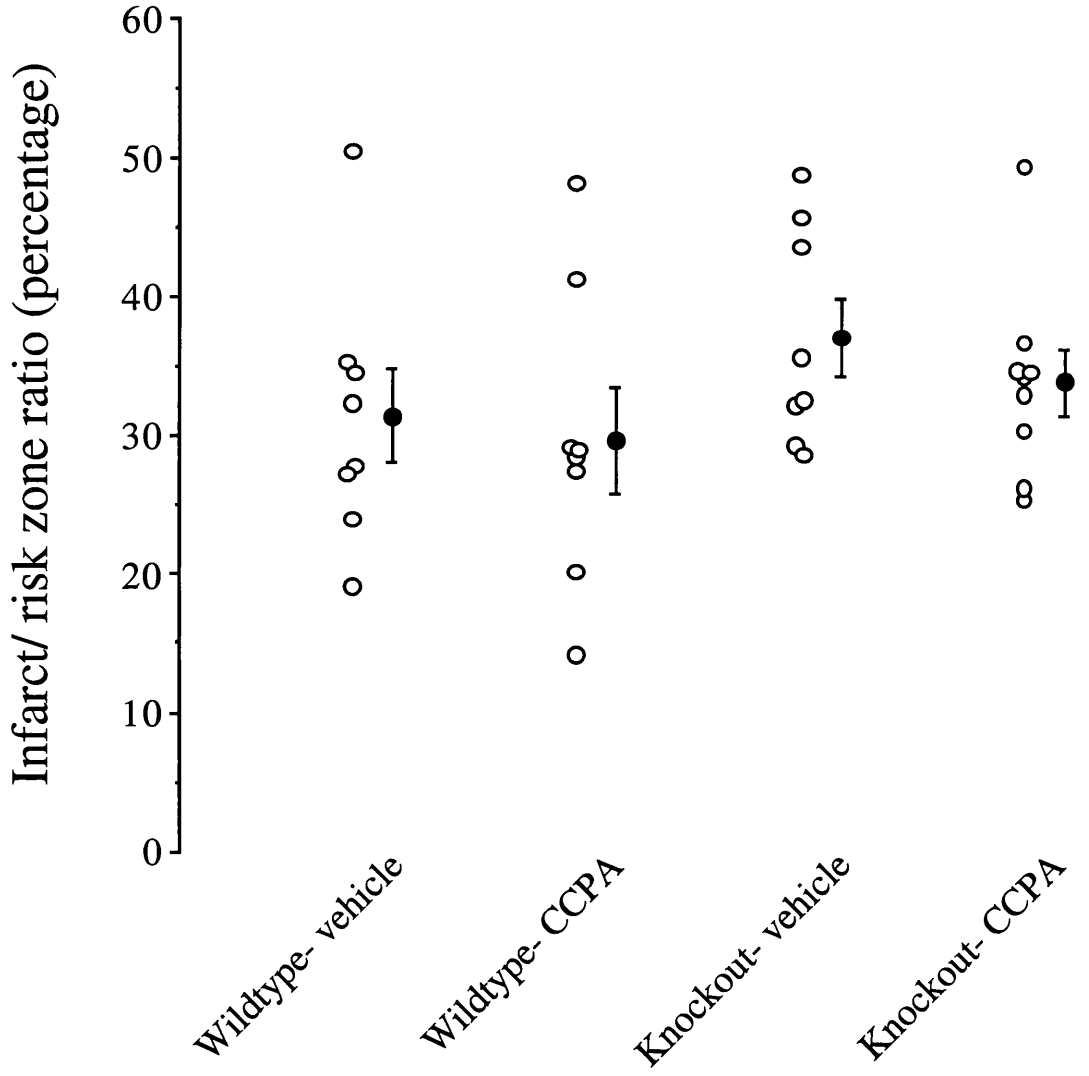

FIGURE 6.6. SNAP MIMICS PRECONDITIONING.

The effect of the administration of exogenous NO upon infarct size. 1.0 μM SNAP administered throughout the perfusion protocol leads to significant infarct size limitation equivalent to that observed with delayed preconditioning with CCPA. **, $p < 0.001$. $n = 6$ per group.

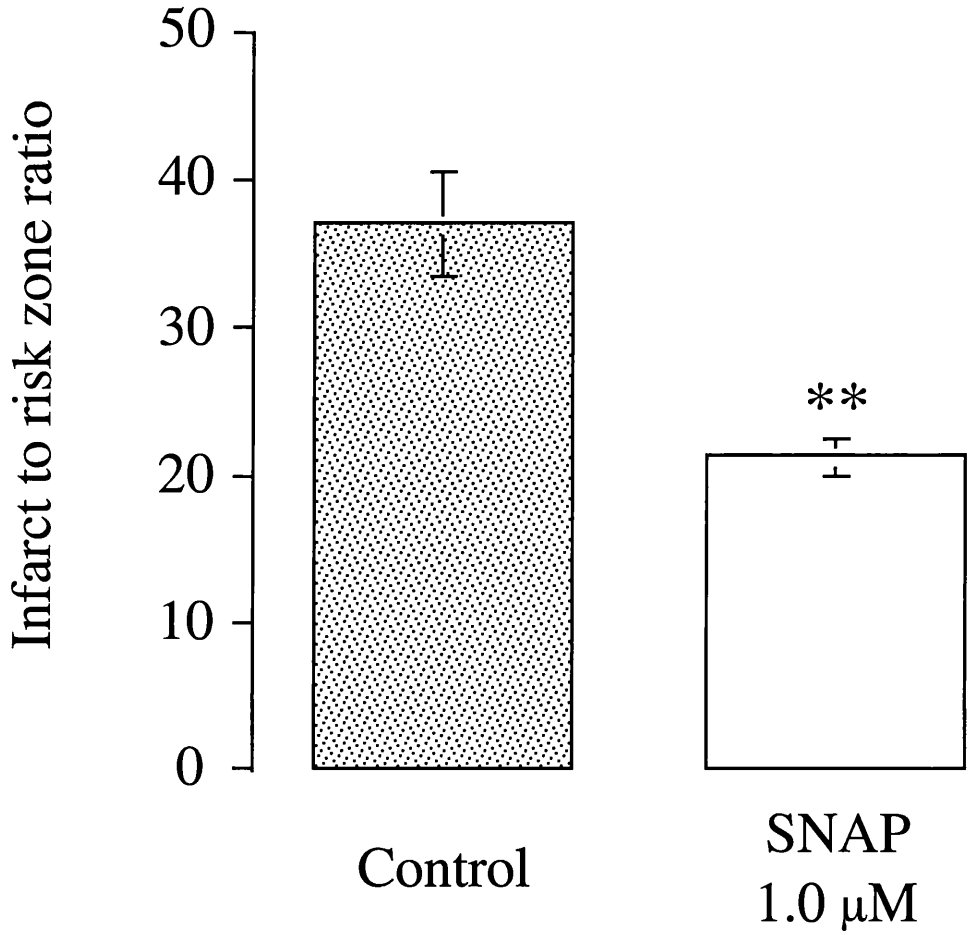

FIGURE 6.7 PROTEIN INDUCTION 24 HOURS AFTER CCPA ADMINISTRATION

A: iNOS is found expressed at low levels in isolated naive hearts, consistent with previous reports. Administration of CCPA as a pharmacological preconditioning stimulus results in a significant increase of iNOS protein in iNOS WT hearts. In iNOS KO hearts, no basal or induced expression of iNOS was observed.

B: eNOS was found to be basally expressed in both iNOS WT and iNOS KO hearts at similar levels. 'Preconditioning' with CCPA resulted in increased expression of eNOS in both WT and KO hearts.

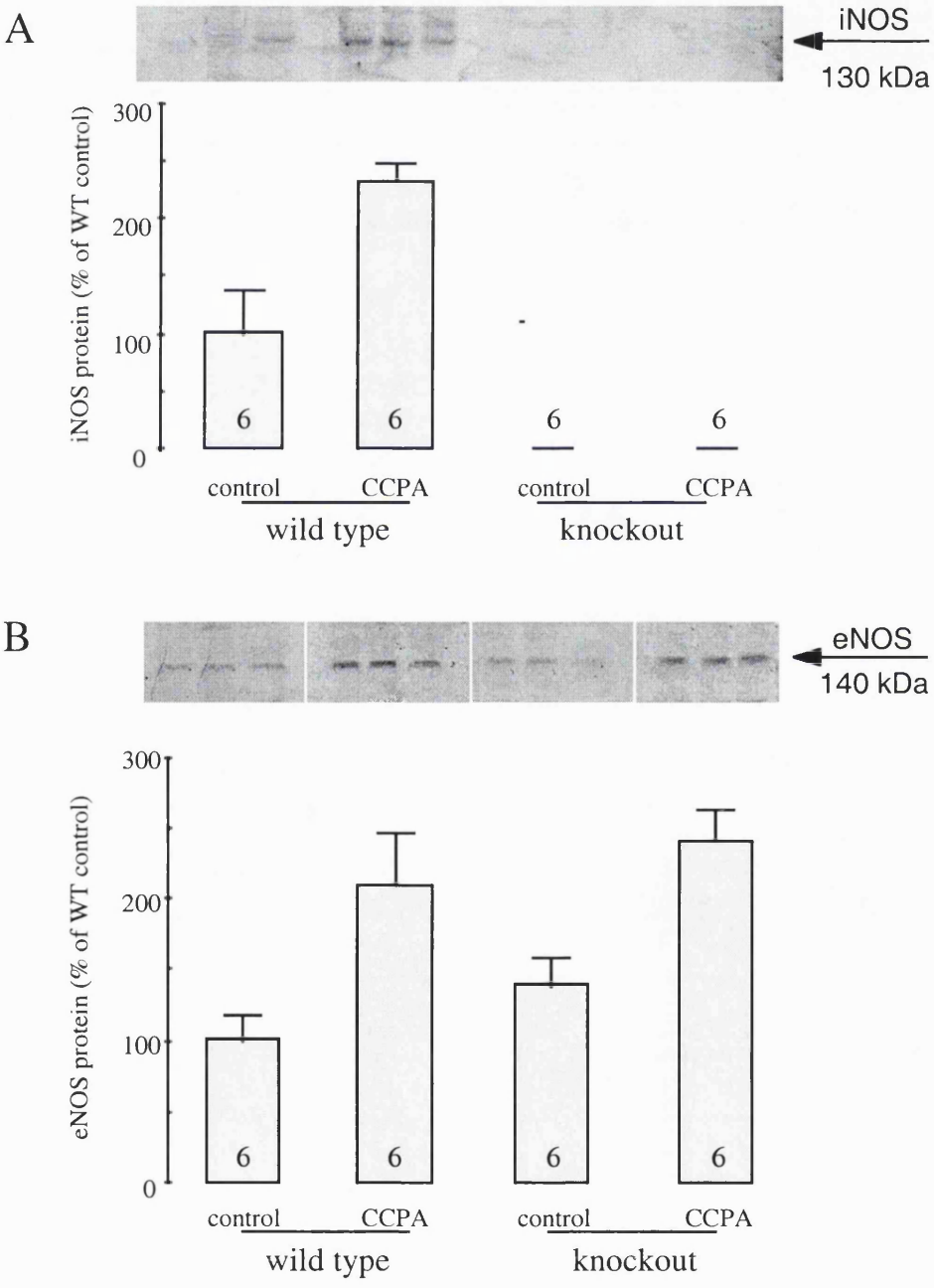

FIGURE 6.8. HSP90 EXPRESSION FOLLOWING CCPA IN iNOS WT AND KO.

Tissue samples were prepared as outlined in figure 6.1.E. CCPA administration to either iNOS WT or iNOS KO mice failed to result in significant upregulation of HSP90 α/β expression. Immuno-precipitation studies will need to be performed to demonstrate HSP90/eNOS interaction. n = 6 per group.

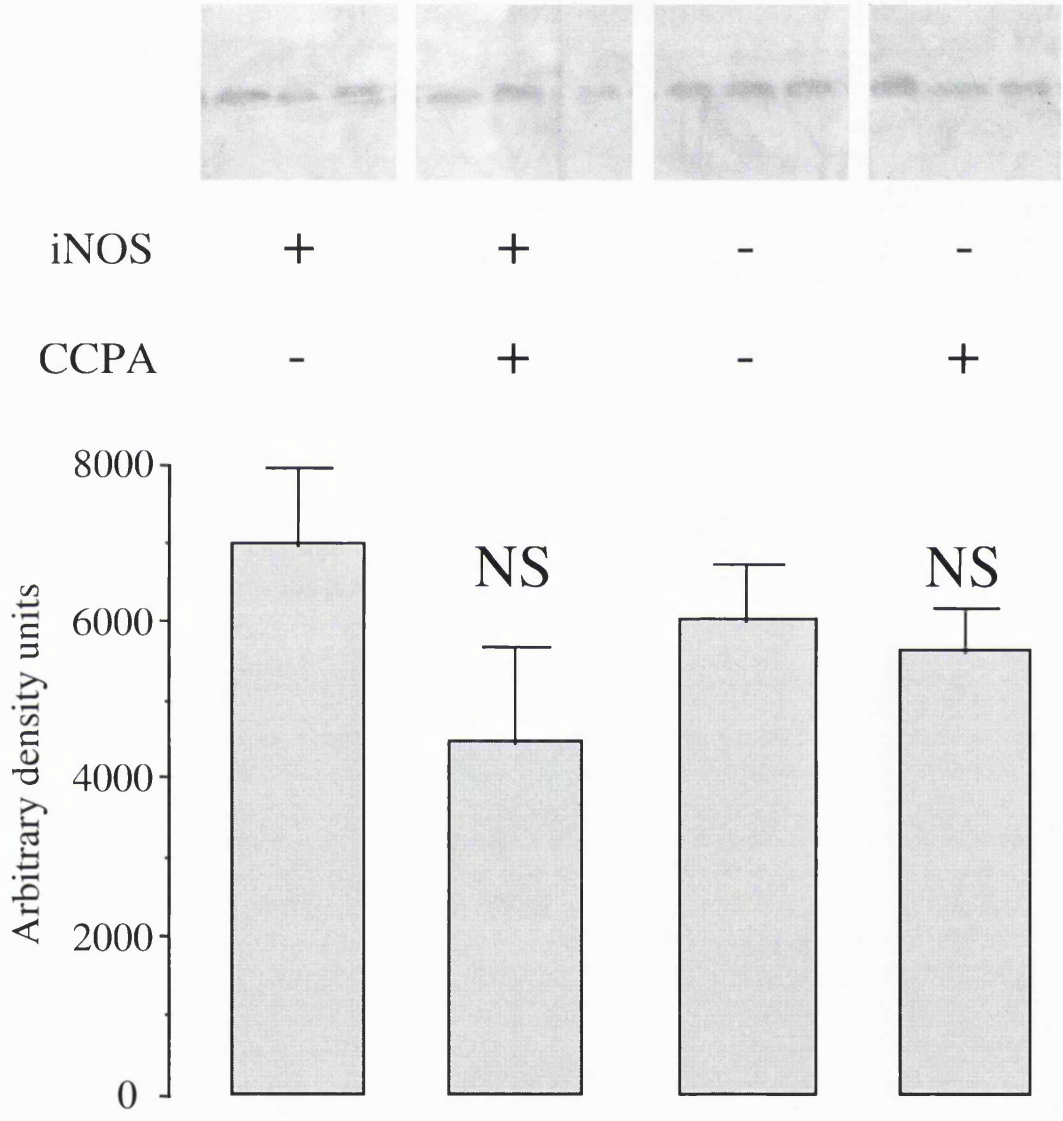

FIGURE 6.9. IS eNOS PIVOTAL TO DELAYED PHARMACOLOGICAL PRECONDITIONING?

To investigate the role of eNOS in delayed CCPA triggered preconditioning, eNOS WT and KO animals were injected *iv* with 25 μg/kg CCPA 24 hours before a 35 minute global ischaemic insult followed by 30 minutes reperfusion. As expected, CCPA pre-treatment resulted in significant attenuation of infarct size in the WT group. In the eNOS KO group, preconditioning resulted in a non-significant reduction of infarction. There is no significant difference between the CCPA treatment WT and KO groups.

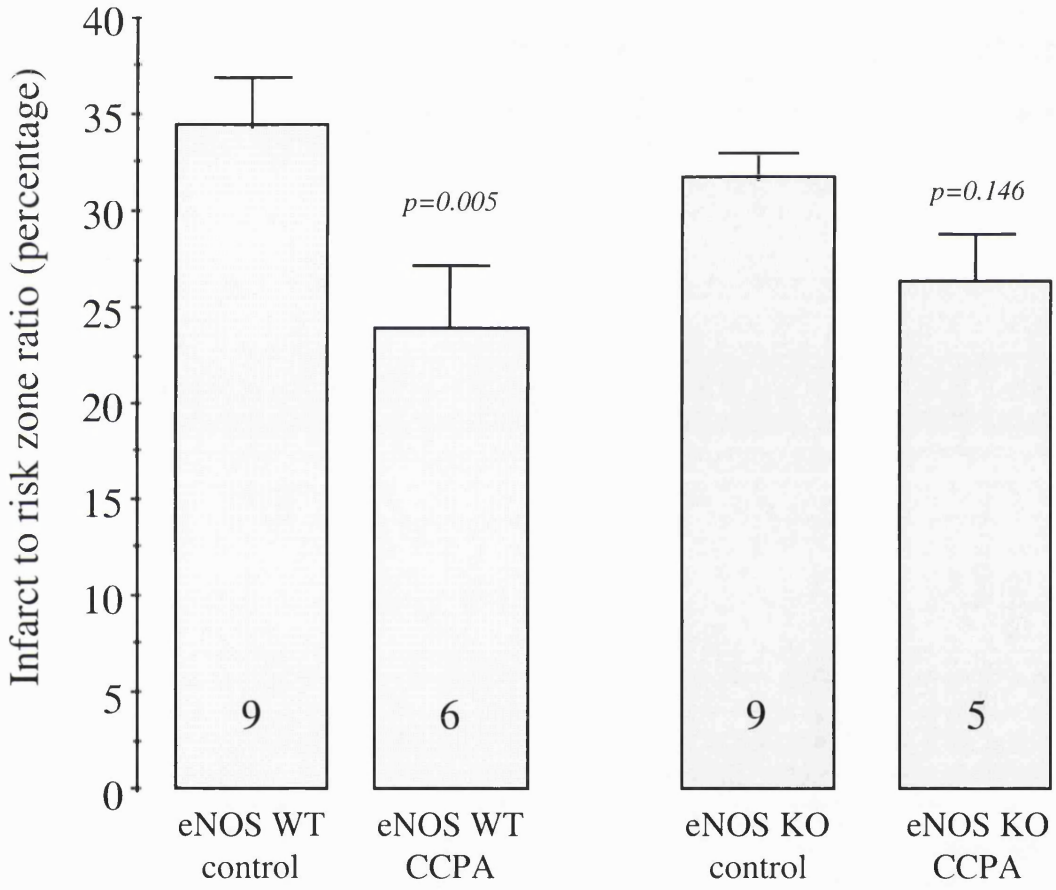

6.3. Discussion

6.3.1 The role of eNOS versus that of iNOS

Consistent with the published literature on delayed ischaemic and pharmacological preconditioning, CCPA preconditioning appears dependent upon the generation of NO. However, where previous investigations have shown the inducible isoform of NOS as being the obligatory source of NO in this phase of protection, the results presented here suggest that delayed pharmacological preconditioning is associated with constitutive nitric oxide synthase upregulation.

The NO hypothesis for delayed ischaemic preconditioning, as proposed by Bolli and colleagues[73], is attractive. In it, they propose that ischaemic preconditioning results in increased nitric oxide synthesis from constitutive nitric oxide synthases, which in turn leads to the activation of protein kinase C (PKCε). PKC results in the upregulation of the gene transcription factor, NF-κB, which upregulates the expression of iNOS. In support of this hypothesis, nitric oxide synthesis has been demonstrated following ischaemic preconditioning,[72] resulting in PKCε translocation,[273] NF-κB activation and iNOS induction.[163] Importantly, iNOS induction has been demonstrated to mediate delayed ischaemic preconditioning. In a number of recent studies, employing either selective pharmacological inhibitors[209, 271] or targeted deletion of iNOS,[230, 272] iNOS has been implicated as the potential source of nitric oxide in this form of preconditioning.

Based upon the available evidence, delayed *pharmacological* preconditioning was also predicted to be mediated via an iNOS dependent mechanism. Adenosine A_1 receptor activation has been shown to trigger delayed preconditioning in a number of animal species including rabbit[60] and rat.[96] The data presented in this chapter are the first to demonstrate that CCPA administration 24 hours prior to a lethal ischaemic insult results in a significant and marked reduction of infarction in WT mice. Moreover, this protection is associated with increased NO release from the heart 24 hours after the CCPA-preconditioning stimulus. This is entirely consistent with the previously proposed 'NO' hypothesis. Interestingly however, iNOS knock out mice (with no demonstrable iNOS mRNA or protein; figure 6.7) display a similar degree of infarct limitation with CCPA. One potential explanation for the continued evidence of protection resulting from delayed preconditioning in the absence of iNOS is that the protection is mediated via a nitric oxide independent signalling pathway. However, the NOS activity assay data appears to allude to another possibility (figure 6.4). In hearts of saline treated WT and KO mice there was negligible NO_X release into the coronary effluent. However, hearts of WT and KO CCPA treated animals released similar significantly greater quantities of NO_X into the coronary effluent. Therefore a second

hypothesis was proposed: NO is the mediator of delayed pharmacological preconditioning, *irrespective of enzymatic source*. This is further supported by data showing that CCPA triggered protection is attenuated by the non-specific NOS inhibitor, L-NAME, and emulated by the NO donor, SNAP (figures 6.5 and 6.6).

If NO is a mediator of delayed A_1 receptor triggered *pharmacological* preconditioning in iNOS KO hearts, it would suggest that one of the constitutive NOS isoforms is up-regulated. The most likely potential candidate is eNOS. Whilst eNOS may have the lowest intrinsic levels of catalytic activity relative to nNOS and iNOS,[236] it nonetheless has significant capacity to be up-regulated. Several mechanisms exist to augment eNOS activity, which include receptor mediated translocation from the sarcolemmal caveoli,[339] eNOS serine 1177 phosphorylation by Akt[85] and AMP-activated protein kinase,[80] and HSP90 association with eNOS.[225] HSP90α/β expression was determined by Western blotting in this study (figure 6.8); however, no significant upregulation of expression was observed, although binding with eNOS was not assessed: this would require the use of co-precipitation techniques that were not available at the time of submission of this thesis.

The potential for eNOS activity to be significantly increased following a stressful stimuli has been demonstrated by Bhagat et al., in a human vascular model of cytokine triggered septic shock.[275] They demonstrated that eNOS was capable of generating significant quantities of NO through the induction of GTP cyclohydrolase-1 expression and activity and thus increasing the bio-availability of the co-factor, tetrahydrobiopterin (BH_4). Therefore they suggest that it is feasible for eNOS to masquerade as iNOS under certain circumstances. It is therefore attractive to postulate that the data presented here are an example of eNOS "*masquerading*" as iNOS in delayed *pharmacological* preconditioning.

6.3.2 Pharmacological preconditioning and contractile dysfunction

Preconditioning with CCPA results in significant attenuation of infarction in the present model, with infarct size reduction of approximately 30% (figure 6.3.A). Delayed pharmacological preconditioning triggered by transient adenosine A_1 receptor activation does not, however, result in improved contractile function following the ischaemic insult. It is well established that ischaemically triggered delayed preconditioning does result in significant attenuation of contractile dysfunction,[340] so the failure of this form of cardioprotection in this model is unclear. However, the lack of contractile recovery from CCPA preconditioning is a repeatable and well-documented phenomenon in the literature, and found in all the animal species studied to date using this A_1 receptor agonist as a trigger of delayed protection, including rabbit,[203, 337] rat[96] and more recently, mouse.[341] Perhaps significantly, whilst delayed ischaemic preconditioning

against infarction can be abrogated by adenosine receptor antagonists, the resistance to stunning remains evident.[337, 340] The implication of these data are that ischaemic and pharmacological preconditioning are mediated by separate pathways. Such evidence of signalling pathway divergence may go some way to explain the difference between the data presented here, and the contradictory evidence presented by others in similar models of ischaemia/reperfusion. The dichotomy remains unexplored, and warrants further investigation; the explanation may lie in differential MAP kinase regulation (p38 MAPK versus p42/p44 ERK).

6.3.3 Conflicting evidence: is iNOS pivotal to delayed preconditioning?

These data presented in this chapter appears to contradict three recent investigations of delayed preconditioning in mice with targeted disruption of the iNOS gene. In an *in vivo* model of delayed *ischaemic* preconditioning, Bolli and colleagues demonstrated that delayed protection was abrogated in the iNOS KO mouse.[230] A similar observation was made by Kukreja and colleagues with a model of delayed *pharmacological* preconditioning, triggered with monophosphoryl lipid A (MLA).[272] The ischaemia and reperfusion was performed *ex-vivo* 24 hours after drug administration to the whole animal. There are two potential explanations for the observed difference between these two investigations and the data presented in this thesis. One would be the sex of the mice used in the studies. In this study female mice were used, although, from our observations, there is no difference between the sexes (either WT or KO) with respect to their infarct limiting cardioprotective response following preconditioning (sections 4.4.2 and 4.4.3). The other explanation involves the manner in which the protection has been triggered. Both transient ischaemia and MLA, used respectively in the two studies mentioned, could have multifarious effects upon the whole animal. Both are associated with significant cytokine induction,[335, 342] and thus neither stimulus will be acting via a specific signalling pathway. Cytokines are classically associated with iNOS induction.[228, 343] In the case of CCPA administration, signalling is selectively limited to A_1 receptor and associated pathways. The third contradiction is with the recently published work by Kukreja and colleagues.[341] In a model similar to the one presented here, they show no evidence of delayed CCPA preconditioning in iNOS KO mice. However, the dose of CCPA used was 100 μg/kg, a dose that in our hands was associated with physical evidence of shock at the time of administration, and diminished coronary flow 24 hours later (table 5.A). Given the haemodynamic consequence of high dose CCPA administration to the mice, it is possible that signalling cascades other than those mediated via the adenosine A_1 receptor could have masked or silenced the putative protective eNOS pathway in iNOS KO animals proposed here. Therefore, there may be subtlties in signalling cascade and transcription factor activation that may

explain the difference in results between this and the studies mentioned above; these differences warrant further investigation. One potential avenue of investigation is the differential activation of the MAP kinases; cytokines appear to preferentially signal via p42/p44 ERK, evidence to date implies that CCPA preconditioning is mediated via p38 MAPK.

6.3.4 Is eNOS pivotal to delayed pharmacological preconditioning?

The data presented in this chapter appear to imply a new and novel hypothesis, namely that eNOS has an important role to play in the induction and/or mediation of delayed pharmacological preconditioning triggered by transient adenosine A_1 receptor activation. The results, summarised in figure 6.9, demonstrate that CCPA administration in eNOS WT resulted, as expected, in significant attenuation of infarct size. However, this protection was not reciprocated in the eNOS KO animals; whilst CCPA administration resulted in a lowering of the mean infarct size compared to control hearts, the trend was not significant ($p = 0.146$). These data appear to support the hypothesis that eNOS is an important mediator of delayed pharmacological preconditioning, although further work needs to be performed to increase numbers to be confident of this observation.

If eNOS activity is essential for delayed pharmacological preconditioning, then this poses a further question: is eNOS essential to *trigger* delayed preconditioning, or does eNOS *mediate* delayed protection? If the former case is true, it would support Roberto Bolli's 'nitric oxide hypothesis.' This hypothesis proposes that nitric oxide synthesis, presumably from eNOS, is required for the induction of protection. The protection observed following CCPA preconditioning would therefore be expected to be abrogated by inhibiting eNOS activity at the time of the preconditioning stimulus. If this hypothesis were found to be correct, then it may be possible that eNOS triggers delayed protection in a similar way to that observed with early preconditioning (chapter 5), by lowering the preconditioning threshold. However, if inhibition of eNOS activity during the trigger phase fails to attenuate delayed protection, then eNOS is a *mediator* of delayed protection, synthesising the nitric oxide required for protection in this form of protection.

6.4 Conclusions

The data presented in this chapter provide, for the first time, evidence that there are clear differences in the mediation of delayed preconditioning depending on the triggering stimulus used. Whilst transient ischaemia or MLA administration appear to induce delayed protection in an iNOS dependent fashion, CCPA triggered delayed protection is also associated with the upregulation of eNOS. That eNOS may actually play a pivotal role in the triggering and/or mediation of this form of pharmacological preconditioning,

although unclear at this time, is underlined in preliminary studies with eNOS knock out mice. Further information is also required regarding the potential contrasts between the signalling pathways inferred by differences in eNOS regulation and myocardial functional preservation. The proposed hypothesis for such a difference is through differences in MAP kinase activation.

Chapter 7. Nitric oxide in ischaemia/reperfusion injury

7.1 Introduction, aims and protocol

Preconditioning has been proven to be a highly effective modality in reducing cell death resulting from injurious myocardial ischaemia/reperfusion injury, and examples of this have been described in this thesis (chapters 3-6). Clinical application of these techniques have proven problematic however, by virtue of the mismatch of characteristically unpredictable acute coronary syndromes, and, by definition, the premeditated nature of preconditioning modalities. Therefore to limit the sequelae of acute myocardial infarction, the ideal therapeutic agent would limit infarct size when administered at the time of thrombolysis, and therefore upon reperfusion of the ischaemic myocardium. Moreover, as reperfusion brings with it the paradoxical phenomenon of 'reperfusion injury,'[344, 345] a process that has been most closely associated with the onset of apoptosis. Therefore agents with anti-apoptotic or cell survival properties may be associated with a reduction of myocardial injury when administered upon reperfusion.

7.1.1. Ischaemia/reperfusion injury salvage agents

With respect to anti-apoptotic agents that may be of benefit administered upon reperfusion, peptide growth factors have recently been demonstrated to function as "survival factors", both during normal embryonic development,[49] and during pathological processes such as reperfusion injury.[23, 50, 346] These survival factors have been shown to signal through a reperfusion injury salvage kinase (RISK) pathway involving the activation of phosphatidyl inositide 3'-OH kinase (PI3 kinase), the serine/threonine kinase Akt/PKB[23] and through the phosphorylation and activation of p42/p44 ERK.[50, 346] Activation of these kinase cascades are adequate to attenuate cellular apoptosis in a number of cell types, including primary ventricular myocytes.[50] The administration insulin or insulin related growth factor-1 (IGF-1) either before[51] or upon reperfusion,[23] has demonstrated that growth factors are effective in reducing cell death resulting from lethal ischaemia reperfusion injury. The ischaemia/reperfusion injury salvage pathway elicited by insulin appears dependent upon the activation of the PI3 kinase pathway, as the myocardial preservation observed following insulin administration was sensitive to blockade by the selective PI3 kinase inhibitor, wortmannin.[23]

7.1.2. Nitric oxide and cell survival

The target protein of PI3 kinase is PKB/Akt (henceforth referred to as Akt). Akt has numerous targets,[52] many of which are thought to inhibit cell death cascades (as summarised in section 1.1). Of direct interest to the theme of this thesis, Akt has also been associated with the regulation of nitric oxide synthesis through the phosphorylation of the endothelial isoform of nitric oxide synthase,[85, 86, 229, 261, 262] increasing its activity some 40 fold. This link has not been explored with relation to reperfusion salvage, yet there is evidence that low concentration nitric oxide may function as a potent anti-apoptotic signalling moiety, inhibiting the release of cytochrome-c from mitochondria,[280] and directly reducing the activity of down stream elements of the apoptotic cascade, specifically caspase-3.[282] This is a controversial role for nitric oxide, which has also been associated, at much higher concentrations, with cell death.[232] Further circumstantial evidence of the potentially protective role of nitric oxide at reperfusion comes from observations from the measurement of nitric oxide release from isolated mouse hearts subjected to ischaemia/reperfusion injury (figure 7.1). These data are derived from the nitric oxide release measurements described in chapter 6, and therefore includes data from iNOS wild type and iNOS knock out mice that either received a vehicle (saline) or the adenosine A_1 receptor agonist, CCPA, 24 hours before isolation of the heart and being subjected to an ischaemia/reperfusion protocol. In control hearts, negligible release of nitric oxide is measured, yet upon reperfusion, nitric oxide generation is significantly augmented in these hearts, a state that persists for the duration of the perfusion protocol. In the preconditioned hearts where myocardial protection is observed, this reperfusion associated increase in nitric oxide generation is significantly augmented over controls, and again there is greater than baseline release of nitric oxide persisting for the duration of reperfusion. It is therefore attractive to speculate that the myocardial protection observed as a result of this form of preconditioning is mediated through increased reperfusion triggered nitric oxide synthesis.

7.1.3. Bradykinin as a cell survival signal.

Bradykinin has been shown to activate PI3 kinase and activation of the p70 S6 kinase,[347] a signalling pathway associated with cellular salvage from reperfusion injury. Bradykinin has also been demonstrated to have a direct effect upon eNOS activity, leading to the release of the enzyme from inhibitory binding sites in the sarcolemmal caveoli[260] and the bradykinin B2 receptors themselves.[259] Thus, with the activation of Akt through PI3 kinase, eNOS may be phosphorylated and its enzymatic activity increased.[261]

Therefore it was hypothesised that bradykinin, though B2 receptors and PI3 kinase activation, would mediate myocardial resistance to lethal reperfusion injury via a mechanism reliant upon the activity of the endothelial isoform of nitric oxide synthase.

7.1.4. The bradykinin/ nitric oxide hypothesis of reperfusion injury salvage.

To test the proposed hypothesis, wild type or mice with a targeted disruption of the eNOS gene were subjected to the standardised ischaemia/reperfusion regime as summarised in figure 7.2. At reperfusion, Krebs Henseleit buffer containing bradykinin (group A), SNAP (group B), wortmannin or wortmannin plus bradykinin (group C) were infused into the hearts. Functional parameters were monitored, and at the end of reperfusion, infarct sizes were determined by TTC staining.

FIGURE 7.1. NO RELEASE BY HEARTS DURING ISCHAEMIA/REPERFUSION

Nitric oxide release profiles from control and CCPA preconditioned hearts were analysed 24 hours after administration. In all hearts, reperfusion NO release was quadrupled compared to basal release values- and further significantly augmented by prior administration of CCPA. This pattern of release was maintained until the end of reperfusion 30 minutes later. * $p < 0.05$, CCPA treated group compared to respective control, vehicle treated group.

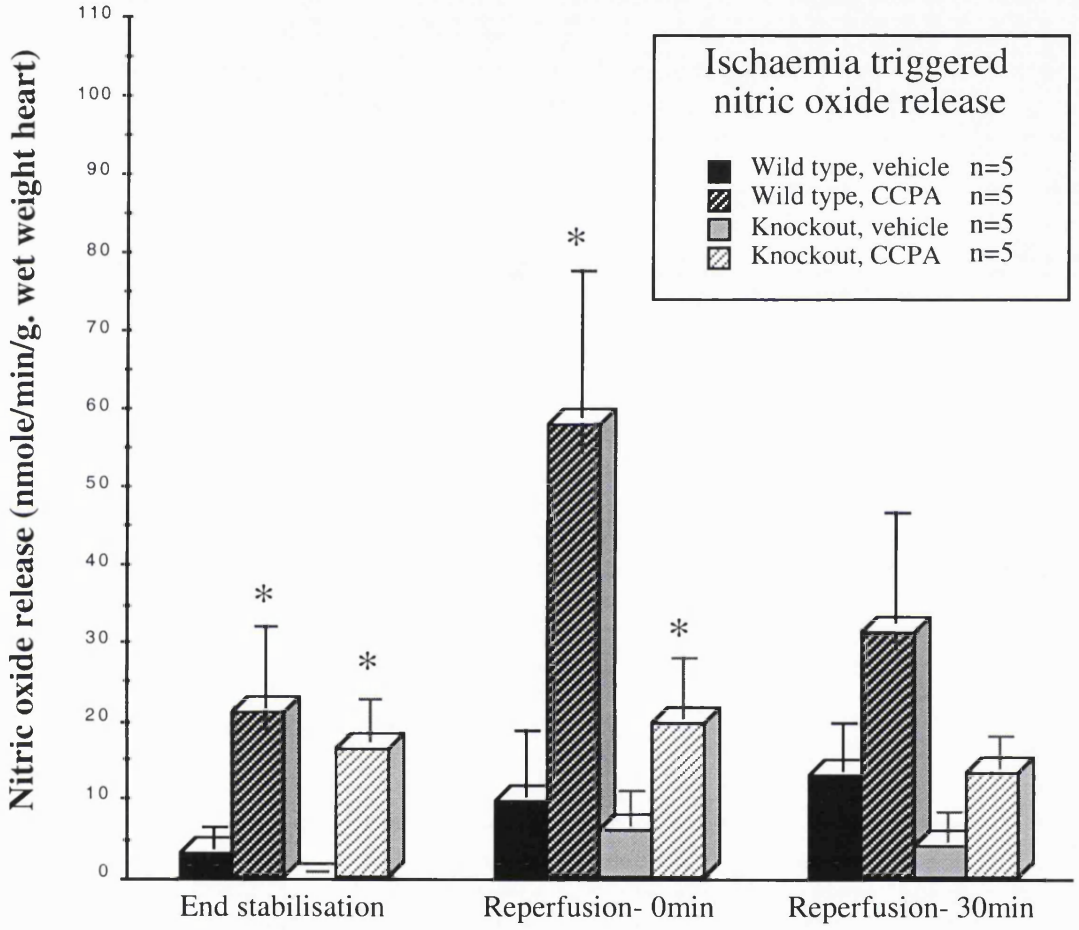

FIGURE 7.2. EXPERIMENTAL PROTOCOL.

All hearts were subjected to the standardised ischaemia/reperfusion regime. At the onset of global ischaemia, the bubble trap was drained of Krebs Henseleit buffer and sealed. At the onset of reperfusion, the chamber was rapidly re-filled with buffer containing drug (bradykinin 100 μM/ SNAP 1 μM/ wortmannin 100 μM) such that the drug would reach the ischaemic myocardium instantaneously. The protocol can be divided into three groups:

A: WT and eNOS KO hearts subjected to ischaemia/reperfusion comparing the effect of bradykinin at reperfusion to normal buffer perfused hearts.

B: eNOS KO hearts received either normal buffer or the NO donor, SNAP, to determine whether the mechanisms of ischaemia/reperfusion injury salvage are present in the KO, and whether NO plays a significant role.

C: To determine whether any infarct sparing effect observed was mediated via the hypothesised PI3 kinase mediated pathway, the specific PI3 kinase inhibitor, wortmannin was either co-perfused with bradykinin, or administered on its own to determine whether wortmannin had an independent effect upon infarction.

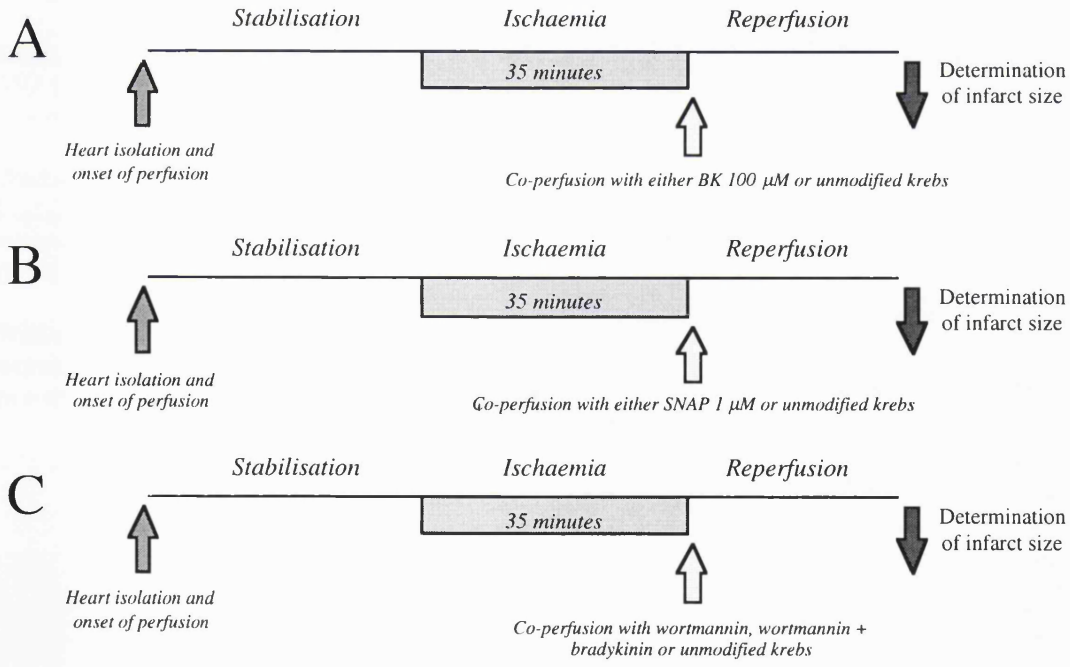

Table 7. Chapter 7: Morphometrics and baseline haemodynamics.

Groups were compared with respect to body and heart weight, baseline coronary flow, resting tension and contractile function. No difference in any of the parameters was observed between groups.

Group	Body weight (grams)	Heart weight (grams)	Baseline coronary flow rate ($ml.min^{-1}$)	Resting tension (grams)	Force rate product ($gram.beat.min^{-1}$)
Wild type control (n = 9)	24.87 ± 0.69	0.16 ± 0.007	3.62 ± 0.17	0.97 ± 0.04	1397.66 ± 100.02
Wild type bradykinin (n = 9)	26.07 ± 0.77	0.17 ± 0.004	3.50 ± 0.20	1.03 ± 0.04	1262.50 ± 114.29
Knockout control (n = 6)	23.98 ± 0.47	0.17 ± 0.008	3.73 ± 0.67	1.04 ± 0.05	1227.08 ± 145.40
Knockout bradykinin (n = 6)	24.29 ± 0.55	0.17 ± 0.006	3.13 ± 0.48	1.08 ± 0.05	1200.78 ± 138.46
Knockout SNAP (n = 6)	25.28 ± 0.56	0.17 ± 0.007	3.25 ± 0.26	1.13 ± 0.09	1201.25 ± 79.00
Wild type bradykinin + wortmannin (n = 6)	23.50 ± 0.64	0.16 ± 0.003	3.13 ± 0.18	1.00 ± 0.03	1310.42 ± 44.90
Wild type wortmannin (n = 6)	25.80 ± 1.31	0.17 ± 0.004	3.62 ± 0.20	0.98 ± 0.03	1325.00 ± 82.14

7.2 Results

No significant difference between groups were documented in terms of body or heart weight, baseline coronary flow rate, resting tension or contractile function (expressed as a force-rate product), as summarised in table 7.

7.2.1. Reperfusion salvage: infarct size.

7.2.1.1. Does bradykinin mediate reperfusion injury salvage?

Both eNOS WT and eNOS KO hearts were subjected to an ischaemia/reperfusion regime, to which hearts were randomly allocated into treatment or control groups (protocol, figure 7.2). The results are summarised in figure 7.3. In WT hearts, the data provide the first evidence that bradykinin mediates ischaemia/reperfusion injury salvage (IRIS). At a concentration of 100 μM, bradykinin mediates a 32% reduction of infarct size from 32 ± 2% to 22 ± 2% ($p = 0.002$), an equivalent reduction to that seen elicited by both early and delayed preconditioning in this model of isolated mouse heart ischaemia/reperfusion injury (chapters 4, 5 and 6). In the hearts of eNOS KO mice, the protective effect of bradykinin was completely absent, with infarct sizes in the control and bradykinin groups being 31 ± 2% and 32 ± 2% respectively ($p = 0.779$). Therefore, bradykinin triggered IRIS appears to require the presence of eNOS to mediate protection.

7.2.1.2. Can an exogenous NO donor mimic reperfusion salvage in eNOS KO hearts?

To determine whether, in the absence of eNOS, ischaemia/reperfusion injury salvage can be elicited by the exogenous administration of nitric oxide, and thus effectively bypassing the nitric oxide synthase, SNAP (1 μM) was administered to KO hearts at reperfusion (protocol, figure 7.2.B; results summarised in figure 7.4). Consistent with the hypothesis that NO is required for infarct sparing effect of bradykinin at reperfusion, the NO donor resulted in significant attenuation of infarction, from 31 ± 2% in controls to 17 ± 4% in the SNAP treated group ($p = 0.001$). Therefore, NO appears to mediate the infarct size limitation associated with bradykinin administration at reperfusion, and moreover, NO donors themselves appear to have significant ischaemia/reperfusion injury salvage properties.

7.2.1.3. Is bradykinin reperfusion salvage mediated by PI3 kinase?

The signalling pathway associated with bradykinin administration and consequential myocardial salvage remains undetermined. One potential signalling pathway may involve the activation of the PI3 kinase/RISK cascade. Therefore, using the PI3 kinase selective inhibitor, wortmannin, hearts subjected to ischaemia/reperfusion were reperfused in the presence of wortmannin (100 μM) alone, to exclude the potential of

non-specific infarct effects of the drug, or in the presence of bradykinin at the same concentration used previously to elicit cardioprotection. The results are summarised in figure 7.5. Wortmannin alone had no influence upon infarct size measured at the end of reperfusion, the infarct size being equivalent to that observed in the control hearts: 32 ± 2% compared to 30 ± 1% in control and wortmannin treated hearts respectively. The administration of wortmannin in addition to bradykinin abrogated the observed protection resulting from bradykinin perfusion at reperfusion: infarct size in the bradykinin treatment group being 22 ± 2%, increasing to 31 ± 2% when co-administered with wortmannin, an infarct size equivalent to that seen in the control hearts ($p = 0.723$).

FIGURE 7.3. BRADYKININ AT REPERFUSION ATTENUATES INFARCTION.

Administration of bradykinin at reperfusion resulted in significant attenuation in infarct size in eNOS WT hearts. The infarct sparing cardioprotective effect of bradykinin was completely absent in the hearts from eNOS KO mice.

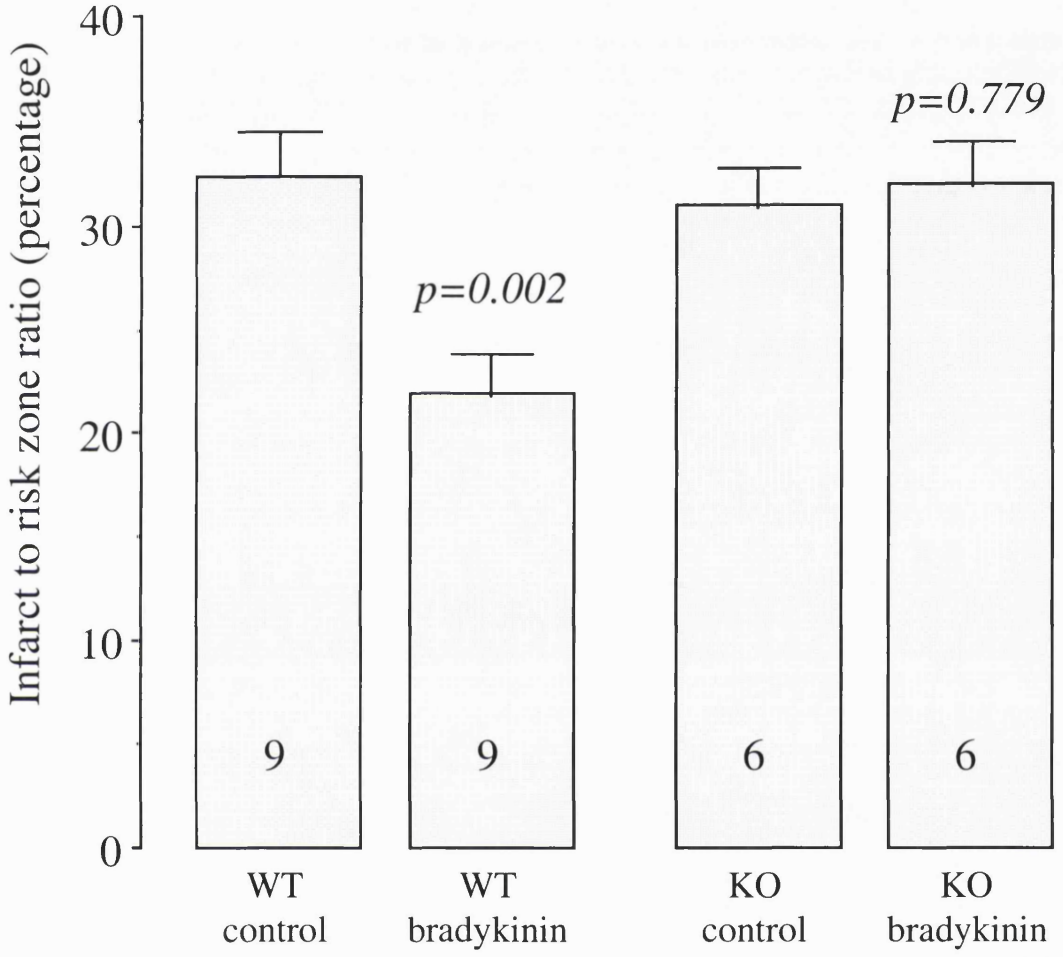

FIGURE 7.4. ADMINISTRATION OF SNAP AT REPERFUSION ATTENUATES INFARCTION.

The administration of the exogenous NO donor, SNAP, at the onset of reperfusion results in significant attenuation of infarction in the hearts eNOS KO mice, mimicking the protection of bradykinin administration in the hearts of eNOS WT mice.

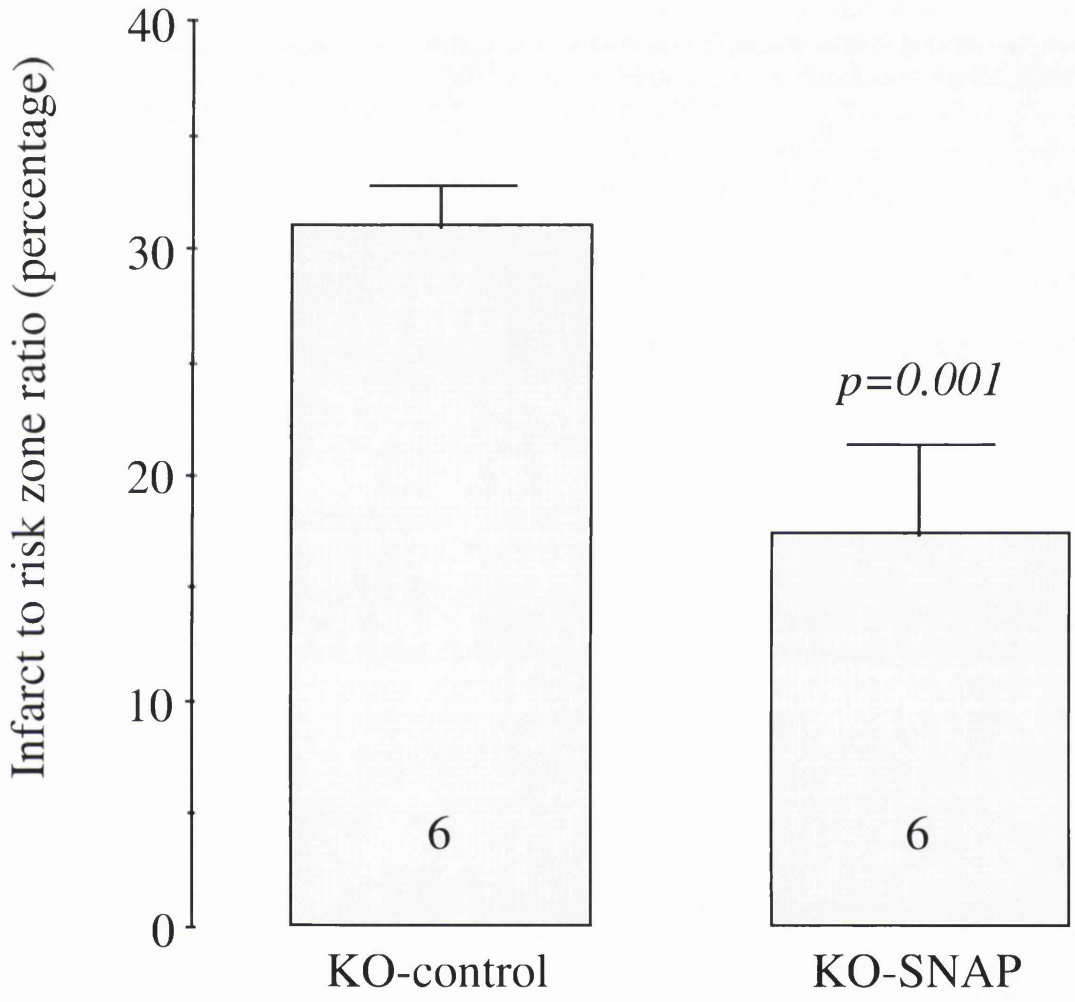

FIGURE 7.5. INFARCT SPARING EFFECT OF BRADYKININ IS ABROGATED BY WORTMANNIN.

The PI3 kinase specific inhibitor, wortmannin, had no effect upon infarction when administered alone at the onset of reperfusion. Co-administration with bradykinin, resulted in the abrogation of the protection conferred by bradykinin upon the reperfused heart against necrotic damage.

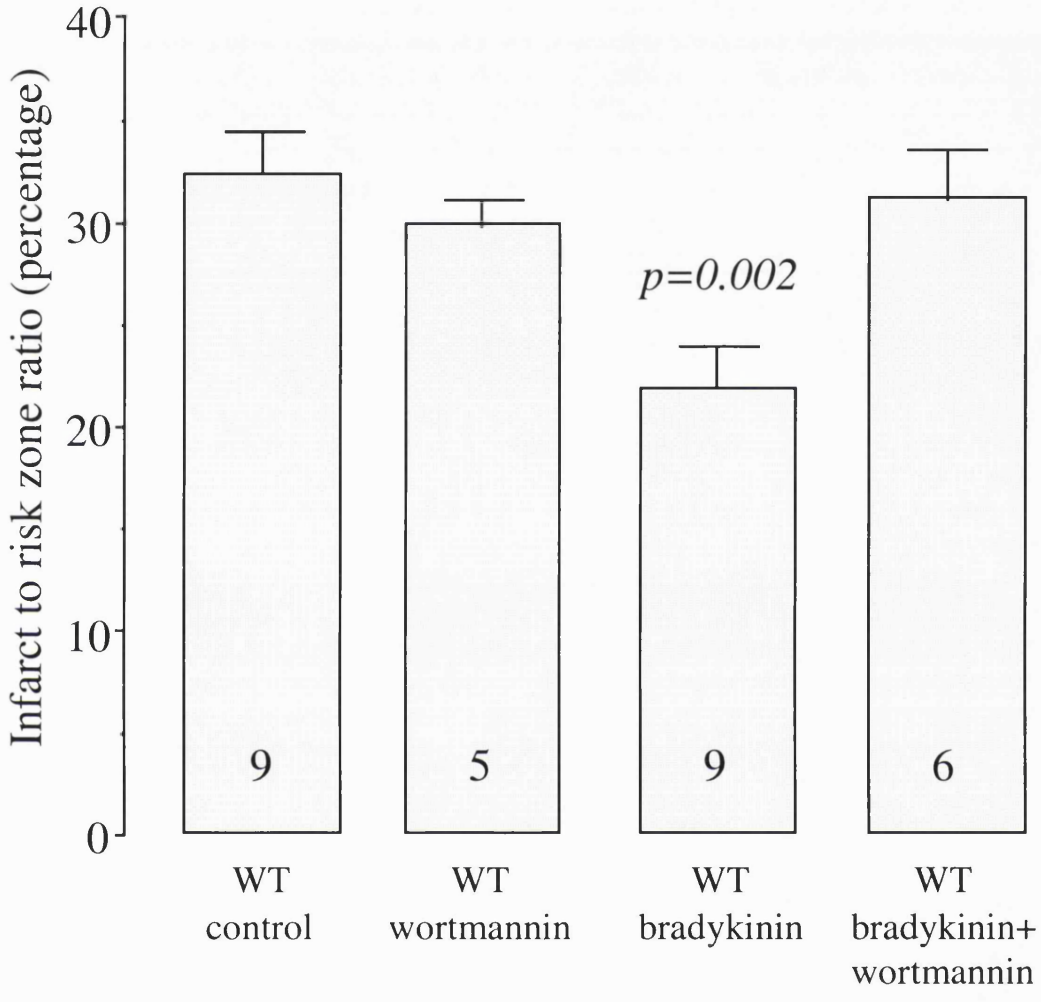

7.2.2. Reperfusion salvage: coronary flow rate.

The data from the coronary flow measures are summarised in figures 7.6-7.8. As bradykinin appears to mediate an infarct sparing effect though PI3 kinase and the upregulation of eNOS activity, an expected corollary was the improvement of post-ischaemic coronary flow. As summarised in figure 7.6, bradykinin had no impact on the coronary flow in eNOS KO hearts, which in turn was significantly lower than that observed in the eNOS WT hearts ($p < 0.001$). Unexpectedly however, bradykinin failed to impact upon eNOS WT control coronary flows, with flow rates equivalent to those seen in WT control hearts ($p = 0.363$). The administration of exogenous nitric oxide with SNAP significantly increased the coronary flow rate in the knockout hearts compared to the wild type hearts over the duration of the reperfusion period (figure 7.7, $p < 0.001$), to a rate equivalent to that observed in both WT control and WT bradykinin groups (versus WT control, KO SNAP, $p = 0.280$). The possibility of a reperfusion coronary flow ceiling was not explored here, but the data may suggest that damage to the vasculature occurs during the ischaemic period that is not amenable to reperfusion injury salvage agents.

The administration of wortmannin, either on its own or in conjunction with bradykinin, had a small, but significant, detrimental effect upon coronary flow during the reperfusion period (summarised in figure 7.8, versus WT eNOS control hearts, $p < 0.001$ and $p = 0.019$ respectively for wortmannin plus bradykinin and wortmannin alone groups). The possibility that this is mediated through attenuation of basal eNOS activity was not explored.

FIGURE 7.6. BRADYKININ DID NOT IMPROVE REPERFUSION VASCULAR FUNCTION.

Hearts from eNOS KO animals had significantly worse reperfusion coronary flow rates compared to hearts from eNOS WT animals ($p < 0.001$). The administration of bradykinin had no protective effect against coronary dysfunction measured as a function of flow. (n = 6 to 9 per group.)

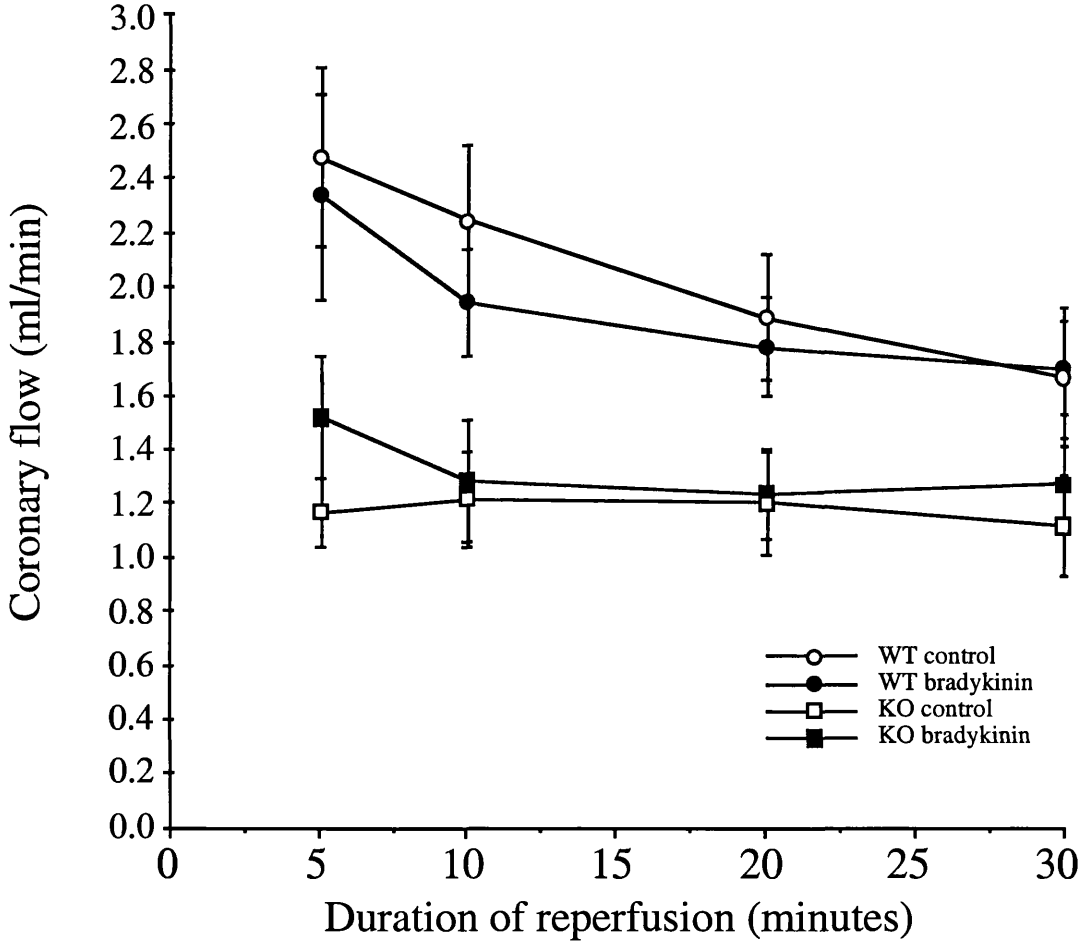

FIGURE 7.7. ADMINISTRATION OF SNAP IMPROVES eNOS HEART CORONARY FLOW.

The administration of SNAP at the onset of reperfusion to hearts of eNOS KO animals resulted in significant improved coronary flow rates ($p = 0.012$), which were equivalent to those seen in the hearts of eNOS WT animals (SNAP versus eNOS WT control, $p = 0.978$). ($n = 6$ to 9 per group.)

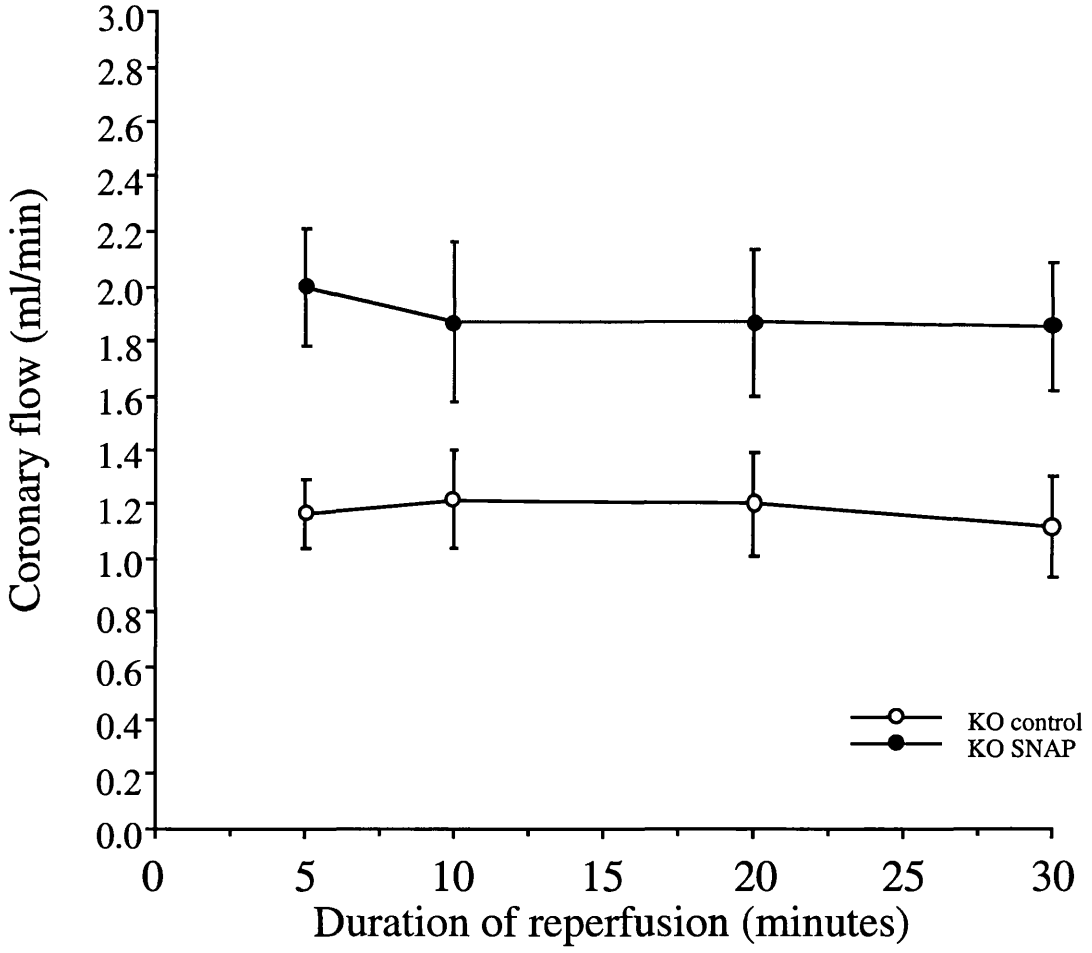

FIGURE 7.8. WORTMANNIN RESULTS IN A MODEST REDUCTION OF CORONARY FLOW.

The administration of wortmannin at reperfusion resulted in a modest but significant reduction of reperfusion coronary flows compared to the respective non-wortmannin treated group (control versus wortmannin, p = 0.019; bradykinin versus bradykinin + wortmannin, p = 0.004). Coronary flows in wortmannin treated hearts remained, however, significant greater than that found in hearts of eNOS KO mice (p = 0.038). (n = 6 to 9 per group.)

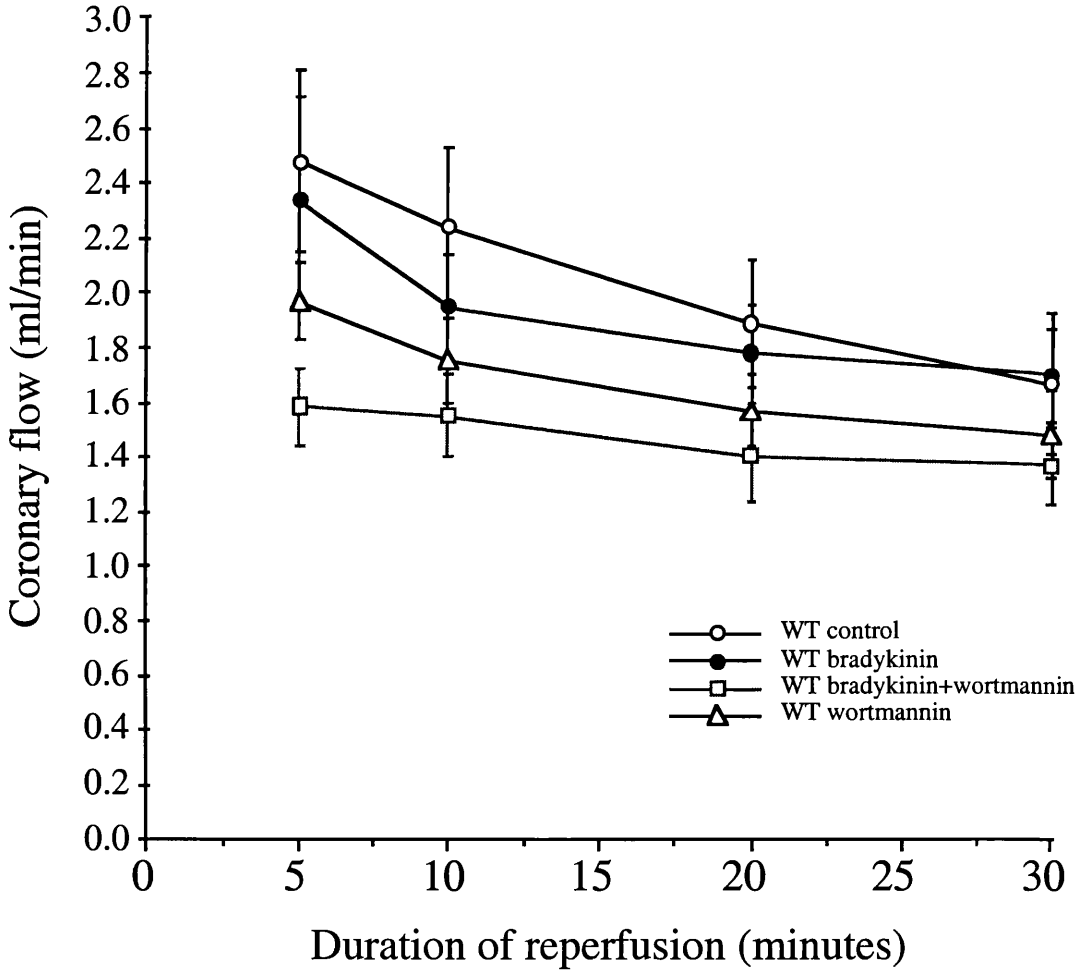

7.2.3. Reperfusion salvage: contractile function.

Contractile function was monitored throughout the study as previously described. The functional data in figures 7.9-7.12 are presented as a percentage of the individual heart's baseline function prior to ischaemia, and thus confounding factors such as variable myocardial weight are accounted for. As in previous studies using this model of ischaemia/reperfusion injury, there was significant stunning recorded in the hearts. As seen in figure 7.9, contractile recovery in the hearts from control wild type and knockout mice was equivalent ($p = 0.460$).

7.2.3.1 Does bradykinin mediate protection against contractile dysfunction?

As summarised in figure 7.10, bradykinin mediates a modest but significant improvement in post-ischaemic contractile function ($p = 0.050$), concomitant with the infarct sparing effect observed in the hearts of eNOS WT mice.
In eNOS KO mice (figure 7.11), despite no evidence of infarct size limitation resulting from bradykinin administration at reperfusion, there was a significant reduction of contractile dysfunction resulting from bradykinin infusion at reperfusion (versus control, $p < 0.001$). This result may allude to disparate pathways between preservation in contractile function and infarct limitation hitherto unknown. The administration of SNAP to these KO hearts also results in a significant improvement in contractile function (versus control, $p < 0.001$), equivalent to that observed in the bradykinin treated group ($p = 0.483$).

7.2.3.2 Is the reduction of contractile dysfunction mediated by PI3 kinase?

As seen in section 7.2.1, infarct size limitation appears to be mediated by the activity of PI3 kinase; inhibition of PI3 kinase activity abrogated the infarct sparing effect. Unexpectedly therefore, the administration of wortmannin appeared to have no impact upon the contractile recovery triggered by the administration of bradykinin (figure 7.12). Compared to the WT control hearts, hearts perfused at reperfusion with both bradykinin and wortmannin had a modest but significant improvement of contractile recovery ($p = 0.046$), comparable to that observed with bradykinin alone. The administration of wortmannin in isolation at reperfusion resulted in a non-significant improvement in contractile function compared to control hearts ($p = 0.062$).

FIGURE 7.9. CONTRACTILE RECOVERY IN CONTROL WT AND KO HEARTS.

Contractile recovery was poor in both WT and KO hearts; no significant difference was determined between groups (p = 0.460). (n = 6 to 9 per group.)

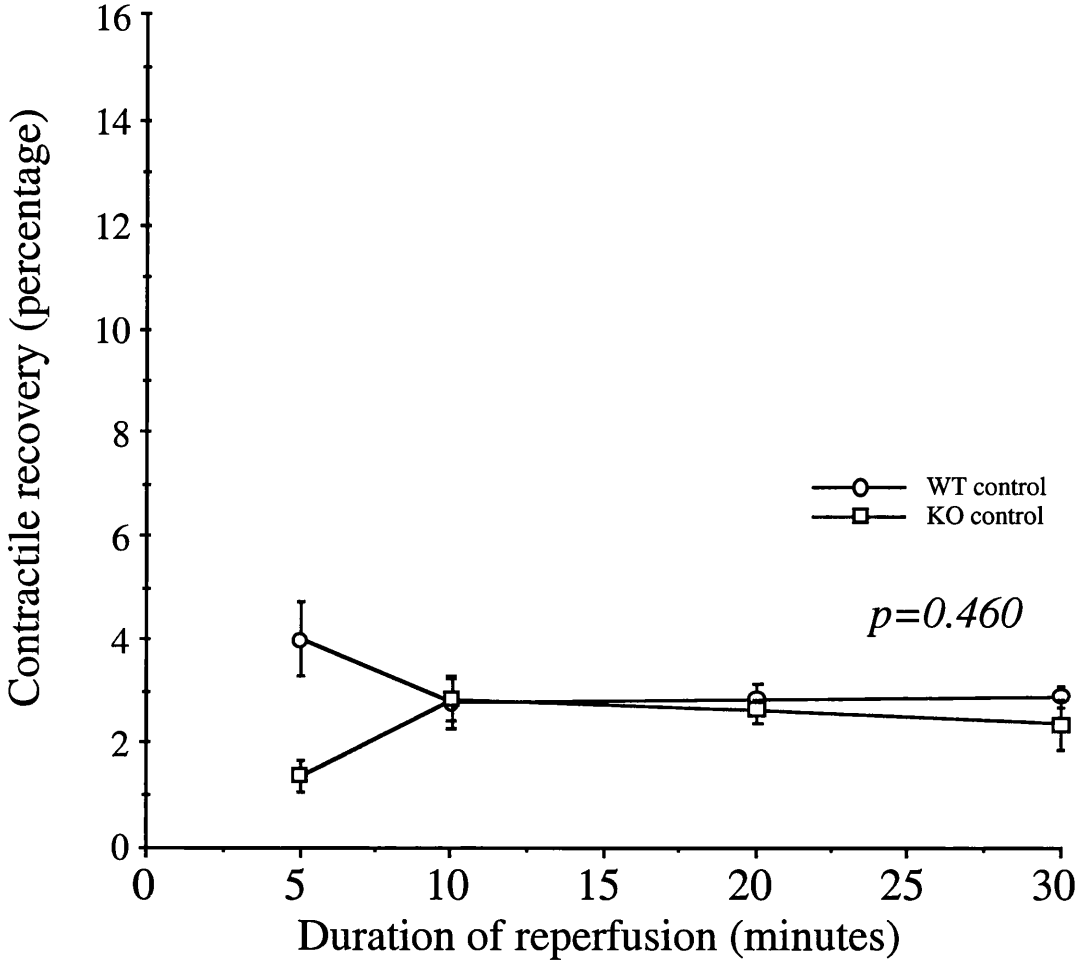

FIGURE 7.10. BRADYKININ IMPROVED CONTRACTILE DYSFUNCTION IN WT HEARTS.

The administration of bradykinin at reperfusion resulted in a modest, but significant improvement in the measured contractile function ($p = 0.050$). ($n = 6$ to 9 per group.)

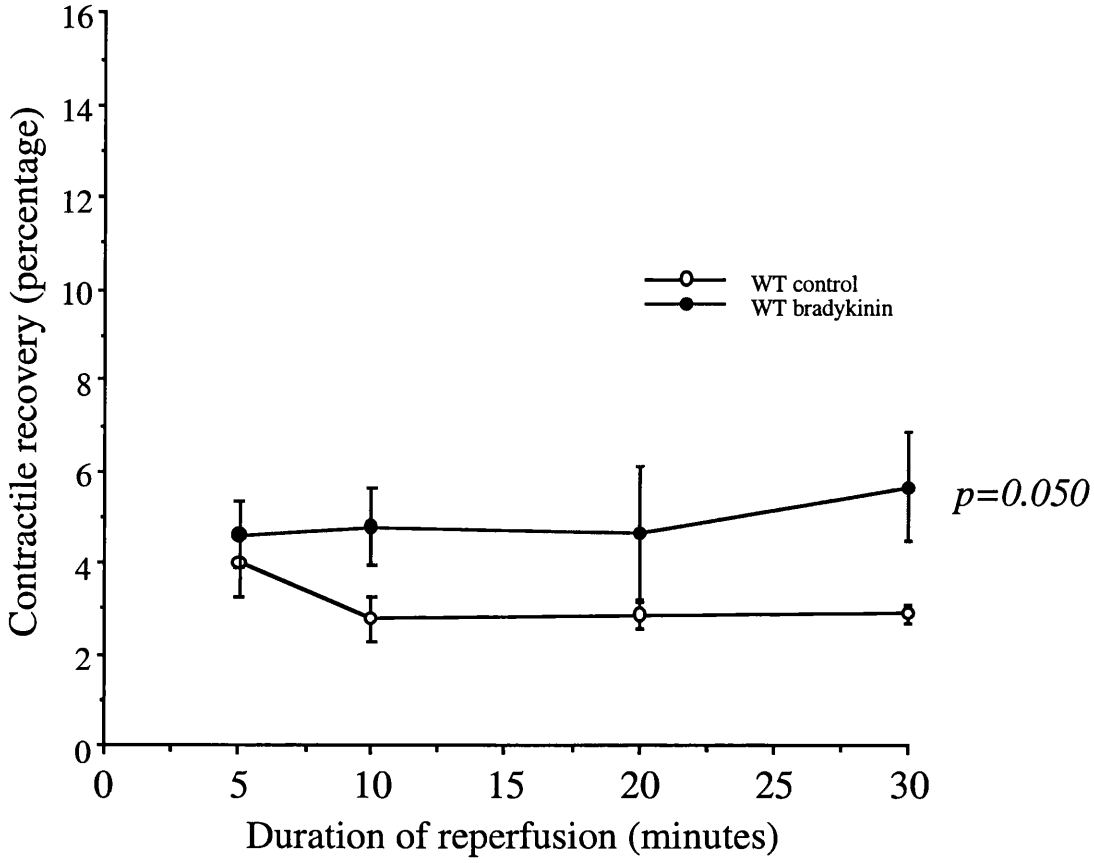

FIGURE 7.11. BRADYKININ AND SNAP REDUCED CONTRACTILE DYSFUNCTION IN KO HEARTS.

Unexpectedly, bradykinin resulted in a significant improvement of contractile recovery in eNOS KO hearts, independently of a reduction of infarction ($p < 0.001$). A similar reduction of contractile dysfunction was observed in SNAP treated KO hearts compared to KO control hearts ($p < 0.001$), but was also concomitant with an infarct sparing effect (figure 7.4). ($n = 6$ to 9 per group.)

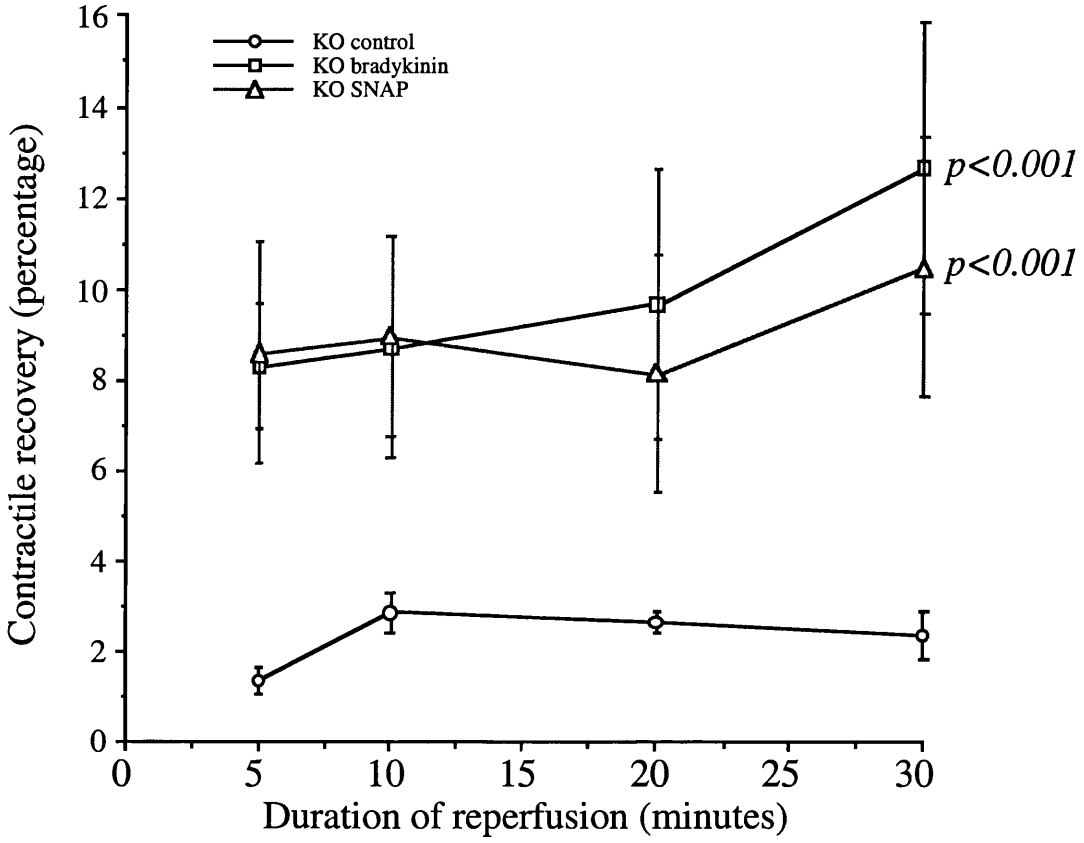

FIGURE 7.12. WORTMANNIN DOES NOT ATTENUATE BRADYKININ-CONTRACTILE RECOVERY.

Wortmannin administration resulted in a modest improvement in post-ischaemic function compared to control hearts, but the trend was not significant ($p = 0.062$). Wortmannin administration to bradykinin treated hearts failed to attenuate the contractile recovery associated with bradykinin administration (versus control, $p = 0.046$; versus the bradykinin group, $p = 0.483$). ($n = 6$ to 9 per group.)

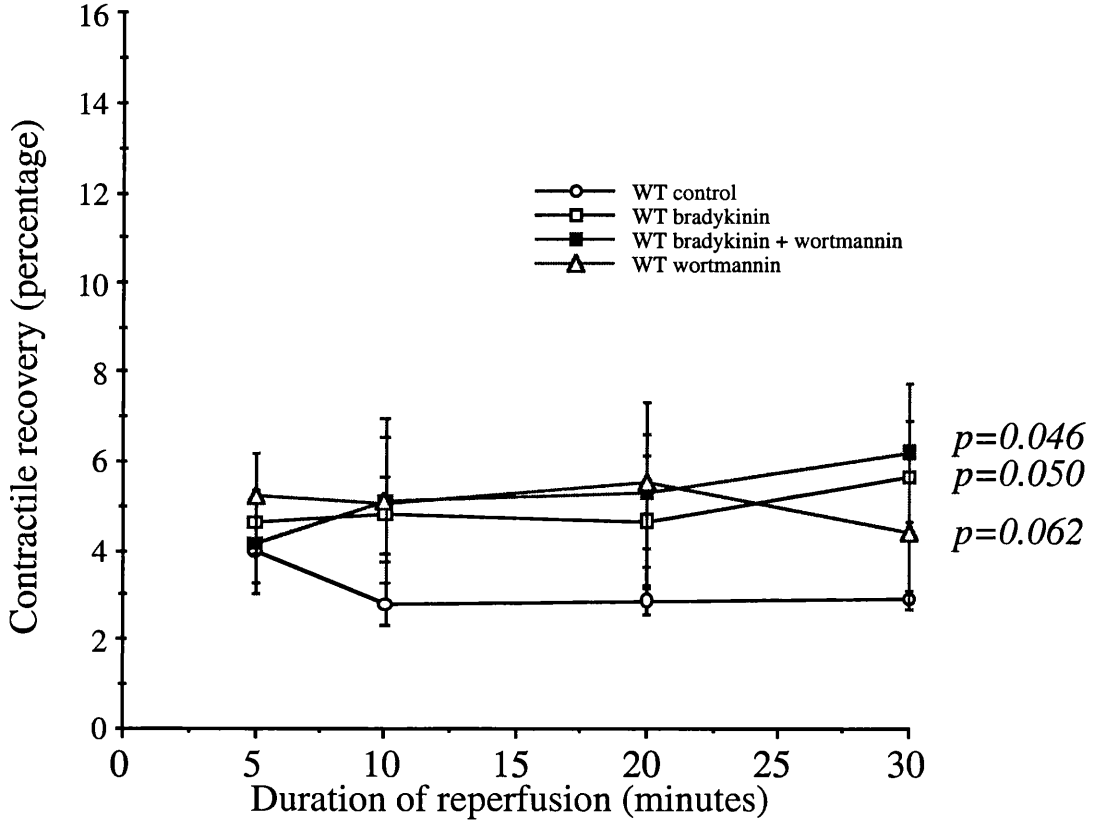

7.3. Discussion.

The data presented in this chapter represent a number novel findings, and these are discussed below.

7.3.1. Reperfusion salvage with bradykinin.

In this study, there is a clear demonstration that bradykinin, when administered at reperfusion, results in a significant and robust attenuation of infarct size in the hearts from eNOS wild type mice. Conversely, no protection was observed in eNOS knockout mouse hearts subjected to an identical ischaemia/reperfusion protocol. Therefore bradykinin directly mediates infarct limitation via a mechanism that appears reliant upon the activity of eNOS. These data may therefore provide evidence and a mechanism by which drugs that attenuate the breakdown of bradykinin in the extracellular milieu may have significant benefit in reducing reperfusion injury. Indeed the administration of an angiotensin converting enzyme inhibitor (ACE inhibitor) 5 minutes prior to reperfusion has been found to be significantly protective against infarction[348] and contractile dysfunction[349] in eNOS WT mouse hearts, protection that, as found here with bradykinin, was absent in the hearts of eNOS KO animals.[348] In a separate recent study, angiotensin II type 1 receptor antagonists and angiotensin converting enzymes have been shown to be cardioprotective against contractile dysfunction via a mechanism sensitive to blockade by HOE 140, a bradykinin B2 receptor agonist.[350] Therefore the bradykinin signalling system may be a powerful tool for the attenuation of ischaemia/reperfusion injury both experimentally and clinically.

7.3.2. Nitric oxide donors mimic bradykinin reperfusion salvage.

Given the controversy surrounding the potential detrimental[351, 352] versus advantageous effects of nitric oxide[230, 272] upon cellular systems, a potentially advantageous effect of nitric oxide donors at reperfusion may not appear to be an ideal ischaemia/reperfusion injury salvage agent. However, based on evidence of the augmentation of nitric oxide generation in the myocardium in the reperfusion period (figure 7.1), nitric oxide at reperfusion was hypothesised to be beneficial. Initial observations in eNOS wild type versus eNOS knockout mouse hearts appear to support a role for nitric oxide in attenuating reperfusion injury. The data presented here, with the administration of SNAP at reperfusion is the first demonstration of exogenous nitric oxide having a direct anti-infarct effect upon the myocardium when administered at the moment of reperfusion. Interestingly, similar findings have been documented following the administration of another nitric oxide donor, FK409, whereby FK409 has been shown

to reduces myocardial CK release, and improve coronary vascular flows and contractile function.[332]

Given the widespread use of nitrates in the context of cardiovascular disease, and following acute myocardial infarction, it is perhaps surprising that no cardiovascular morbidity or mortality advantages have been found with intravenous nitrates. Two large scale studies conducted in the early nineties, GISI-3[353] and ISIS-4,[354] failed to demonstrate any advantage following successful thrombolysis. The reasons for this are not clear, but the most likely explanation being the time of administration relative to the restoration of blood flow to the area at risk in the ischaemic myocardium following successful thrombolysis. The NO donor administered in this study was present from the onset of reperfusion; nitrate therapy in the GISI-3 and ISIS-4 trials could be started up to 24 hours after hospitalisation, potentially missing the therapeutic window for reperfusion salvage with nitrates. Interestingly, small scale clinical trials performed prior to the advent of widespread clinical application of thrombolysis in the management of acute myocardial infarction were more favourable with respect to nitrate therapy. In these studies, nitrates were commenced upon admission to hospital; reperfusion was dependent upon spontaneous revascularisation, and therefore nitrates were present in the coronary circulation at the time of myocardial reperfusion.[355-359] Whilst other explanations exist for the disparity in results and mechanisms of protection observed, it may be appropriate to re-assess the role of nitrates in the context of reperfusion in acute myocardial infarction.

Furthermore, by effectively bypassing the endogenous eNOS-nitric oxide synthesis system, the administration of exogenous NO donors at reperfusion may have potential advantages over mechanisms that involve the upregulation of eNOS activity. In patient based studies, patients at risk of, or who have recently suffered from acute coronary infarction appear significantly more likely to have eNOS polymorphisms (G-- > T polymorphism in exon 7 of the gene which encodes a Glu-- > Asp amino acid substitution at residue 298 of eNOS).[360] Such a polymorphism may adversely effect the nitric oxide generation resulting from activation of bradykinin mediated pathways, and therefore potentially limit the clinical effectiveness of such therapies.

7.3.3. The involvement of wortmannin in reperfusion salvage.

The data presented in this report clearly demonstrates that the infarct sparing effect of bradykinin administration is reliant upon the activity of the pro-survival PI3 kinase pathway; the benefit of infarct limitation with bradykinin administered at reperfusion is completely abrogated with the administration of the PI3 kinase inhibitor, wortmannin. Immediately downstream of PI3 kinase is PKB/Akt. Akt has numerous targets in the cellular death cascade, that include the Bcl-2 family member, Bad. Bcl-2 related

proteins comprise a family that are closely involved in the initiation and regulation of the apoptotic programme.[52] Pro-apoptotic family members, Bax and Bid, promote the release from mitochondria of both cytochrome-c[53] and, in neurones and myocytes, the precursor protease, pro-caspase-9.[54] Cytochrome-c binds with the adapter protein, Apaf-1 to activate caspase-9 and bind to form the apoptosome.[55] Anti-apoptotic family members, Bcl-2 and Bcl-X_L, inhibit the release of cytochrome-c and the activation of caspase-9 by Apaf-1 respectively.[56] Bad plays an important regulatory role. Constitutively active, it dimerises and inactivates both Bcl-2 and Bcl-X_L.[52] However, Akt dual phosphorylates Bad, inactivating the protein, and enabling Bad to bind to a chaperone protein 14-3-3.[57] Therefore, with Bad inactivated, Bcl-2 and Bcl-XL are enabled to exert their anti-apoptotic function. There are further targets of Akt including caspase-9[58] and the Forkhead family of proapoptotic gene transcription factors[52] and of direct relevance to the present study, eNOS.[85, 86, 229, 261, 262]

The evidence presented in the study so far appears to support the original bradykinin/nitric oxide hypothesis of reperfusion salvage' (section 7.1.4); protection against infarction is abrogated by both wortmannin and by the absence of eNOS, therefore bradykinin, through the activation of PI3 kinase, presumably leads to the phosphorylation and activation of eNOS via the catalytic activity of Akt.

7.3.4. Bradykinin mediated preservation of contractile function.

The contractile recovery data appear to allude to an interesting dichotomy between the signalling pathways preventing cell death and those attenuating myocardial stunning resulting from an ischaemia/reperfusion insult. However, the results need to be interpreted with some caution; the experimental model used in this investigation is not optimised for the monitoring of contractile function. There are a number of reasons for this: (*i*) global ischaemia and reperfusion in the mouse heart is associated with significant stunning (sections 4.2 and 4.3), making extrapolation to other experimental models difficult; (*ii*) the duration of reperfusion is short- monitoring of myocardial stunning should ideally be performed over a number of days; and (*iii*) the method of monitoring contractile function via isometric contraction with a linear force transducer may not be a good measure of left ventricular free wall function. With these limitations in mind, the current study proffers two interesting findings:

1. bradykinin mediates contractile recovery, even in the absence of eNOS (an observation not reflected in the recent paper of Yang et al with ACE inhibitors, using mean arterial pressure as the only measure of function, failed to demonstrate any benefit in function in either eNOS WT and KO mice[348]);
2. bradykinin mediated contractile recovery occurred independently of the PI3 kinase RISK pathway.

In order to validate these data, the experiment requires repetition in a functionally appropriate model before any definitive conclusions can be made, but as a preliminary result and observation, it appears to suggest that infarct limitation and resistance to myocardial stunning are mediated via separate signalling pathways.

7.4 Cardioprotection and clinical therapies

The current data provides a testable hypothesis for the mechanism of action of ischaemia/reperfusion injury salvage agents, namely that reperfusion salvage can be elicited via activation of the PI3 kinase/ Akt pathway and the upregulation of eNOS. Based upon this novel hypothesis, drugs that have already of proven benefit and are currently used in the management of cardiovascular disease may be re-examined in the context of ischaemia/reperfusion injury. Of particular interest are drugs, based on the observation of the benefits of bradykinin at reperfusion, that increase the bioavailability of this peptide by attenuating its metabolic breakdown, namely ACE and NEP inhibitors.[361, 362] More recently, HMG CoA reductase inhibitors, currently used in the clinical management of hypercholesterolaemia in patients at risk of coronary vascular disease, have been demonstrated to increase eNOS activity through upregulation of PI3 kinase.[363, 364] Therefore, HMG CoA reductase inhibitors may of significant benefit in the management of acute myocardial infarction to reduce myocardial necrosis and improve post-ischaemic contractile function. Further basic and clinical research is required into this phenomena.

Chapter 8. Nitric oxide and mitochondria.

8.1. Introduction.

In chapters 5, 6 and 7, nitric oxide has been shown to have significant cardioprotective properties, lowering the preconditioning threshold in early ischaemic preconditioning, mediating the protective effect of delayed pharmacological preconditioning as well as demonstrating an association with bradykinin mediated reperfusion salvage. However, the mechanisms by which these infarct sparing effects are observed remain undetermined. One potential target however could be the mitochondria. Myocardial mitochondria are sensitive to ischaemia and reperfusion mediated injury. Ischaemia is associated with mitochondrial swelling, progressive amorphism, disruption and loss of cristae, and reduction of matrix volume.[2-6] In turn, reperfusion is associated either with resolution of the ultrastructural changes associated with reversible myocyte injury,[5] or with considerable mitochondrial accumulation of calcium[14-17] associated with irreversible injury. Calcium entry into mitochondria appears to be closely linked with the opening of the non-specific mitochondrial transition pore (or permeability transition pore, PTP),[365] an event associated with the release of cytochrome-c (and possibly pro-caspase-9[54]) from the inter-membrane space into the cytosol[279] with subsequent activation of cell death cascades through binding to Apaf-1 and activation of caspase-9.[366]

Nitric oxide has been demonstrated to have a direct influence upon mitochondrial function. As an inhibitor of the electron transport chain (reversibly binding to the heme a3 component of cytochrome-c oxidase/ complex IV[367-370]) it reduces oxygen consumption by the mitochondria. This attenuation of oxygen consumption has been demonstrated in whole tissue under normoxic conditions,[371, 372] and may provide a potential beneficial protective mechanism during sustained ischaemia, particularly in terms of increasing the O_2 diffusion distance from arterioles and modifying mitochondrial respiration in response to altering oxygen tension.[373] This increase in diffusion distance is mediated by modulation of mitochondrial respiration: where the O_2 tension is highest near the arteriole, so is the nitric oxide concentration. Thus, O_2 up take in the immediate vicinity of the vessel wall is reduced- increasing O_2 tension distal from the vessel in computer models examined.[373] Exogenous nitric oxide has also been shown to influence the PTP open probability by attenuating reperfusion triggered calcium loading of the mitochondria,[374] and thus maintaining the PTP in a closed state.[280] Additionally, recent work has suggested that mitochondrial calcium overload may be abrogated by the opening of the mitochondrial K_{ATP} channel,[285, 375] a putative end effector of the preconditioning phenomenon, whose opening is associated with

cardioprotection.[182] Nitric oxide has been linked to an increase of mitochondrial K_{ATP} channel open probability.[286] It is therefore attractive to hypothesise that the cardioprotective effects of nitric oxide are potentially mediated through the alteration of mitochondrial function and the attenuation of calcium overload during reperfusion, possibly via a direct effect upon the mitochondrial K_{ATP} channel.

Curiously, whilst there is evidence for nitric oxide acting upon and interacting with the mitochondria, surprisingly little evidence exists to support the nitric oxide/ mitochondrial hypothesis of myocardial infarct size limitation, although some data do exist linking the clinical therapeutic exogenous nitric oxide donor, glyceryl trinitrate and the mitochondrial K_{ATP} channel with improved post-ischaemic functional recovery and attenuated lactate dehydrogenase (LDH) release.[287]

Therefore, the aim of this study was to determine whether nitric oxide interacts with mitochondria, and whether the cardioprotective effects of nitric oxide are mediated via the mitochondrial K_{ATP} channel.

Phase 1.

Electron immuno cytochemistry was performed to determine the subcellular location and distribution of the NOS isoforms following a preconditioning stimulus.

Phase 2.

To determine whether nitric oxide has a direct effect upon mitochondria, exogenous nitric oxide was administered to isolated rat mitochondria loaded with the membrane potential sensitive probe, tetramethyl rhodamine methyl ester (TMRM), and the effect of K_{ATP} channel blockade determined.

Phase 3.

Hearts were perfused with buffer containing the nitric oxide donor, SNAP (2 μM) to elicit an infarct sparing effect. To elucidate whether this protection was mediated via the mitochondrial K_{ATP} channel, the selective mitochondrial K_{ATP} channel blocker, 5 hydroxydecanoate (5-HD) was co-administered with the nitric oxide donor.

8.2. Phase 1: Electron immunocytochemistry.

To determine the patterns of cellular induction and distribution of nitric oxide synthase following a preconditioning stimulus, hearts were examined 24 hours following a pharmacological trigger. Delayed phase pharmacological preconditioning was studied because nitric oxide synthesis was found to be an essential component for mediating the protection observed, and furthermore, both eNOS and iNOS proteins were demonstrated to be upregulated (figure 6.7). Therefore, consistent with the protocol used in chapter 6, mice were treated with a selective adenosine A_1 receptor agonist, CCPA (protocol, figure 8.1; 25 mg/kg, *iv*), 24 hours prior to harvesting the hearts and perfusion with paraformaldehyde based fixative (method described in section 3.11).

8.2.1. Pattern of iNOS induction.

In control hearts, minimal iNOS expression was observed in the myocardium of mice pre-treated with the saline vehicle. As shown in figure 8.2.A, no iNOS expression is evident in the myocytes, although surprisingly, basal expression of iNOS was evident in the endothelium of the microvasculature (arrowed). Other investigators have also demonstrated low-level basal expression of iNOS in the myocardium of naive mice,[230, 254] although the cellular location of the this synthase in these circumstances had not previously described. Whether it is conceivable that iNOS has a role to play in the normal physiology of endothelium remains to be determined, but it is conceivable that iNOS may contribute to the regulation of O_2 consumption by mitochondria, thus increasing diffusion distances under circumstances of low O_2 tension,[373] but with non-specific pharmacological techniques this may be difficult to elucidate.

Preconditioning resulting from transient activation of A_1 receptor activation results in a marked upregulation of iNOS protein expression. In contrast to control hearts, iNOS can now be found in myocytes, with electron dense aggregates found localised to mitochondrial outer membrane and to the intercalated discs (figure 8.2.B). The subcellular localisation of iNOS to mitochondria may be an artefactual finding arising as a consequence of the peroxidase immuno cytochemistry technique employed; iNOS does not possess the N-terminus protein region that enables eNOS and nNOS to be compartmentalised within the cell.[239-241] Thus, iNOS is freely soluble, and would therefore be found unbound in the cytosol. Nonetheless, the product of iNOS activity, nitric oxide, could have a close functional relationship to the mitochondria of the myocyte as the diffusion distance from the cytoplasm to the mitochondria is small. Interestingly, iNOS induction is also observed in the endothelium of the microvasculature (figure 8.2.C), perhaps serving to preserve microvascular function in the delayed phase of preconditioning.

FIGURE 8.1. TREATMENT AND HEART ISOLATION PROTOCOL.

Conscious adult mice were treated to a pharmacological preconditioning regime comprising the adenosine A_1 receptor agonist, CCPA. 24 hours later, the animals were anaesthetised and the hearts harvested. The aorta cannulated with a 21 gauge needle through which fixative was infused as a slow (5 minute) bolus in preparation for electron immuno cytochemistry.

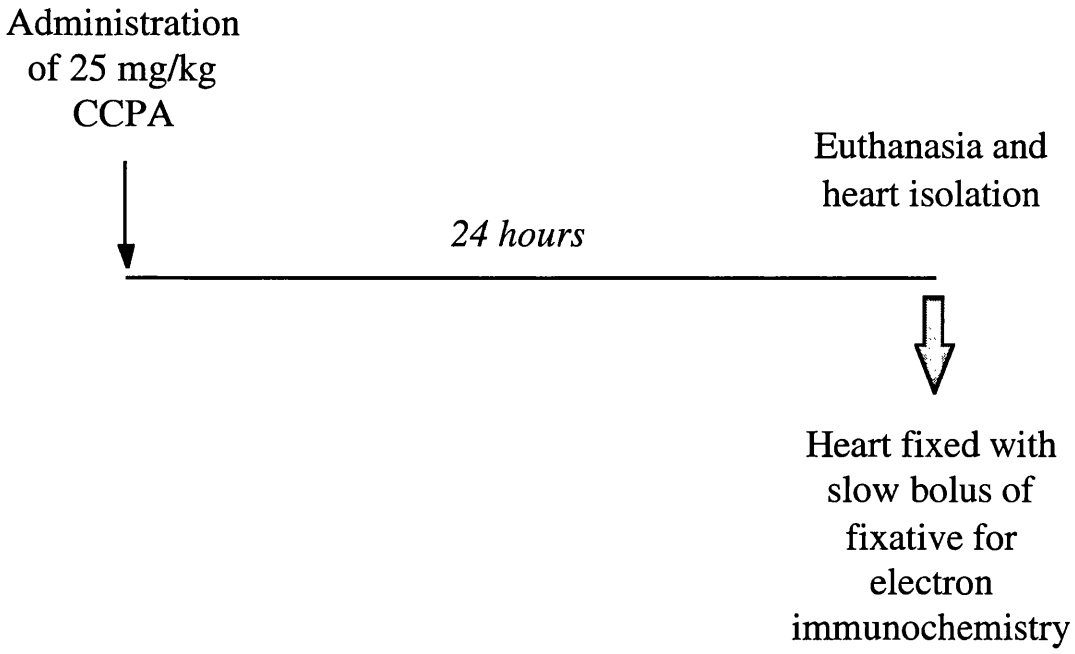

FIGURE 8.2.A. ELECTRON MICROGRAPH: INOS STAINING IN CONTROL HEARTS.

Mice were administered with a saline vehicle bolus 24 hours prior to euthanasia and harvesting of the heart. These control hearts were fixed and prepared and stained for iNOS as described in section 3.11. 12,000x magnification electron micrograph is shown below.

Abbreviations used in figure:

Myo: myocyte;

M: mitochondria;

Epi: epithelial cell;

BM: basement membrane.

In this control heart, very little basal iNOS staining was observed, with minimal basal expression in the vascular endothelium (arrowed), and none in the myocytes.

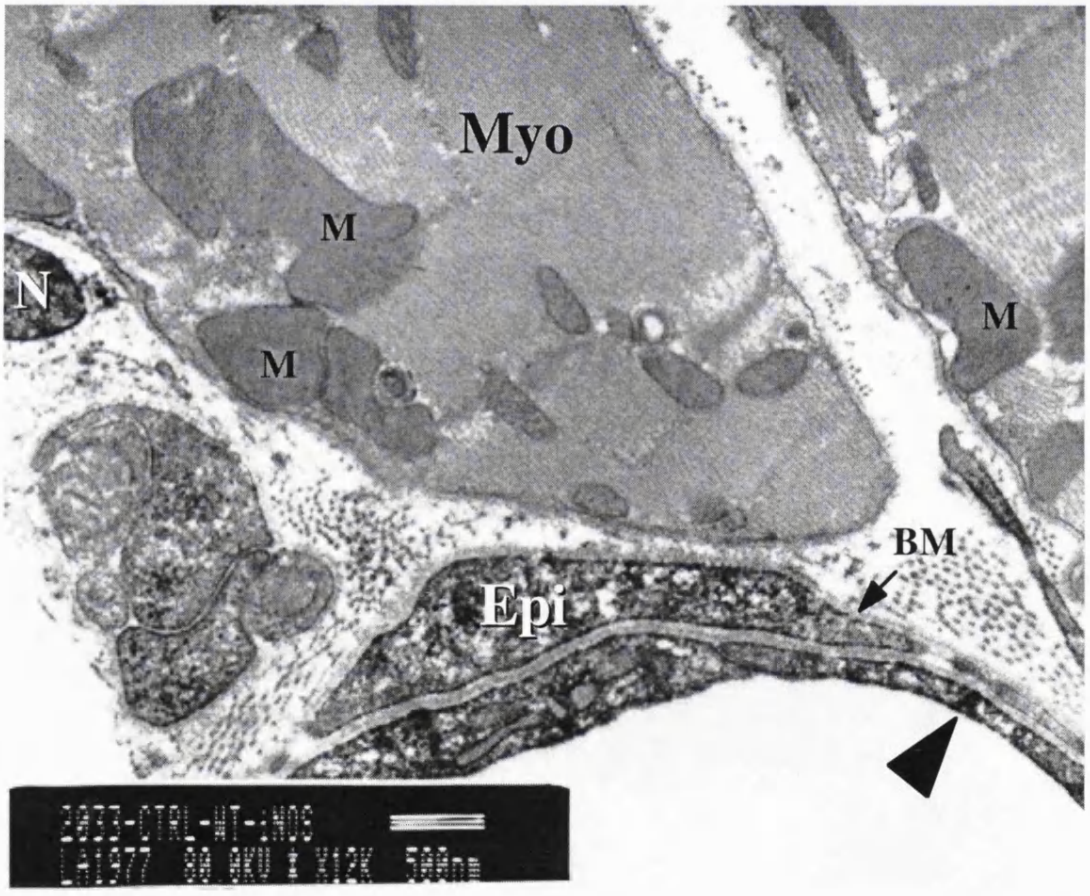

FIGURE 8.2.B. ELECTRON MICROGRAPH: INOS STAINING AFTER CCPA.

Prior to harvesting the hearts, preparing and staining for iNOS, the mice were 'preconditioned' with a bolus of 25 μg/kg CCPA 24 hours earlier. Electron micrograph (below) is at 10,000x magnification.

Abbreviations used in figure:

M: mitochondria.

ICD: intercalated disc.

Myo: myocyte.

Following pharmacological preconditioning, significantly greater expression of iNOS was observed in the myocardium. Unlike control hearts, iNOS is now found expressed in the myocytes. iNOS appears to aggregate towards the mitochondria and the ICD (arrowed). Given the lack of N-terminal coding of the iNOS protein to enable sub-cellular localisation, this is likely to be artefactual, secondary to the peroxidase staining method used, but may alternatively indicate a functional relationship between iNOS activity and the mitochondria.

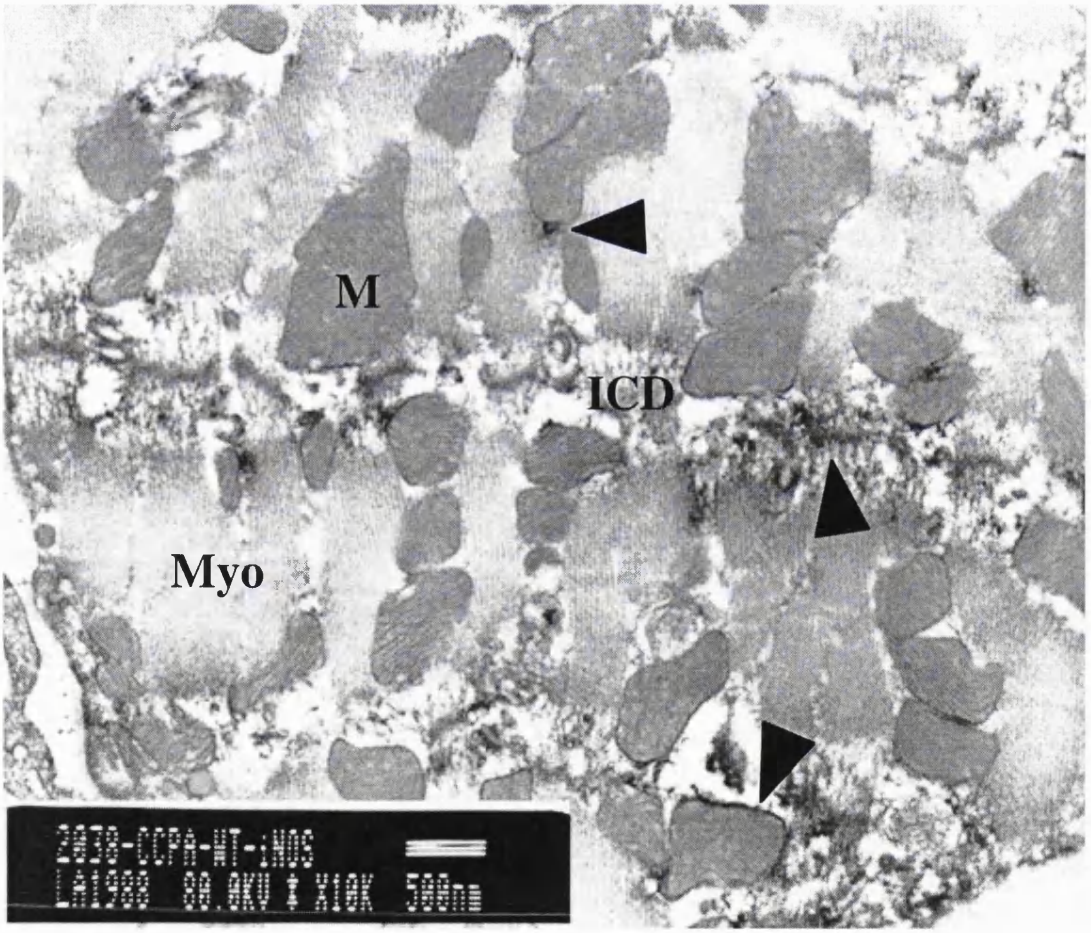

FIGURE 8.2.C. ELECTRON MICROGRAPH: INOS STAINING AFTER CCPA.

Lower magnification view of iNOS staining in a slice from a CCPA-preconditioned heart (6000x).

Abbreviations used in figure:

M: mitochondria.

N: nucleus.

Ca: coronary arteriole.

As found in control hearts, iNOS is also expressed in the endothelium (arrowed) of the microvasculature. The functional role that iNOS is performing is undetermined, but it may conceivably be altering the O_2 diffusion distance through nitric oxide's ability to reversibly inhibit cytochrome-c oxidase/ complex IV activity.

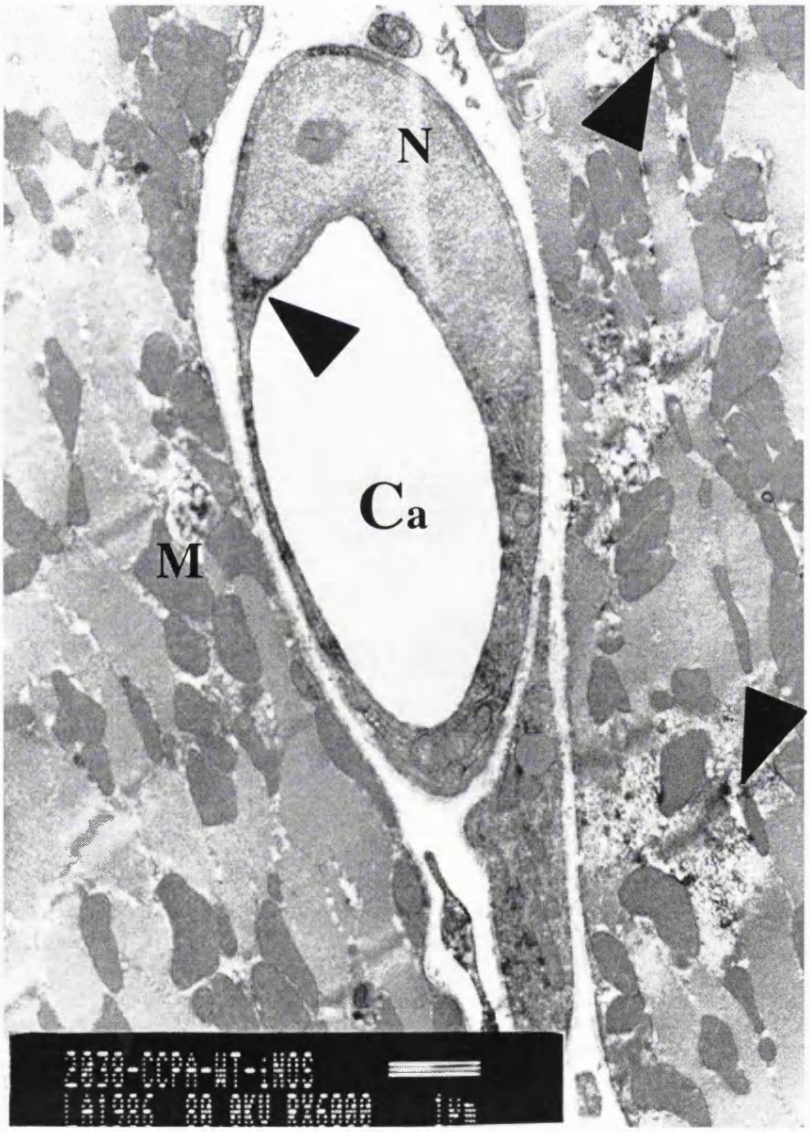

8.2.2 Pattern of eNOS induction.

The basal expression of eNOS in control hearts in the slices imaged (figure 8.3.A) was considerably lower than anticipated based upon the Western blot analysis (figure 6.7) and reports in the literature.[230, 254] The reasons for this apparent failure of the antibody stain are unclear, and for better interpretation of the sub-cellular localisation of eNOS these electron micrographs need to be repeated, but were not available at the time of the submission of this thesis. One potential problem relates to the distribution of eNOS in the myocardium; it is heterogeneous,[254] with more eNOS staining in the epicardial myocardium then the endocardium; the low eNOS staining in these electron micrographs may be as a result of a sampling error. Unfortunately, low eNOS signal makes interpretation of the eNOS electron immuno cytochemistry difficult. In the control hearts, where electron dense eNOS binding has occurred, it is predominantly in the endothelium of the microvasculature. Practically no staining is observed in the myocytes; the electron densities near the peripheries of the image (figure 8.3.A) are probably not related to myocyte expression of eNOS.

Preconditioning with CCPA 24 hours previously resulting in a modest increase in eNOS binding (figure 8.3.B). A number of electron densities are found in association with the endothelium, and with the mitochondria of myocytes. However, given the problem associated with the staining in these hearts, no definitive conclusions are therefore drawn.

8.2.3. Discussion.

Pre-treatment with CCPA elicited a significant increase of iNOS expression in the endothelium and the myocyte. The apparent association of iNOS to mitochondria is likely to be artefactual, although iNOS expression in the cytosol represents a short diffusion distance for nitric oxide from the inducible synthase to the mitochondrion. There is a suggestion that a similar process occurs with eNOS, although the immuno cytochemistry results were disappointingly inconclusive. The evidence does however suggest a plausible link between nitric oxide synthases, nitric oxide and mitochondria that requires further investigation.

FIGURE 8.3.A. ELECTRON MICROGRAPH: ENOS STAINING IN CONTROL HEARTS.

Mice were administered with a saline vehicle bolus 24 hours prior to euthanasia and harvesting of the heart. These control hearts were fixed and prepared and stained for eNOS as described in section 3.11. 4,000x magnification electron micrograph is shown below.

Abbreviations used in figure:

M: mitochondria;

Ca: coronary arteriole.

In this control heart, very little basal eNOS staining was observed, with minimal basal expression in the vascular endothelium and myocytes.

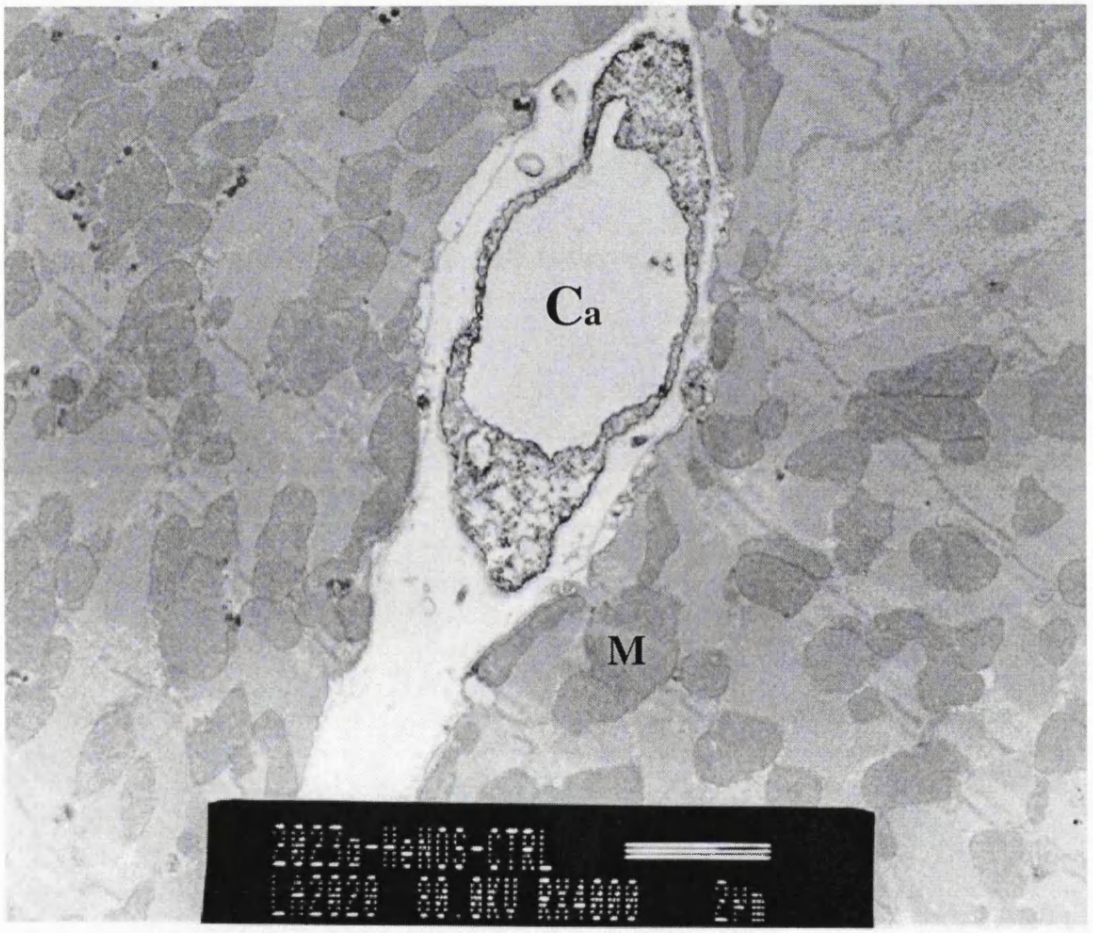

FIGURE 8.3.B. ELECTRON MICROGRAPH: ENOS STAINING AFTER CCPA.

Prior to harvesting the hearts, preparing and staining for eNOS, the mice were 'preconditioned' with a bolus of 25 μg/kg CCPA 24 hours earlier. Electron micrograph (below) is at 4,000x magnification.

Abbreviations used in figure:

M: mitochondria.

Epi: epithelial cell of the vascular endothelium.

Following pharmacological preconditioning, greater expression of eNOS was observed in the myocardium (arrowed). Some eNOS aggregates are observed adjacent to myocyte mitochondria.

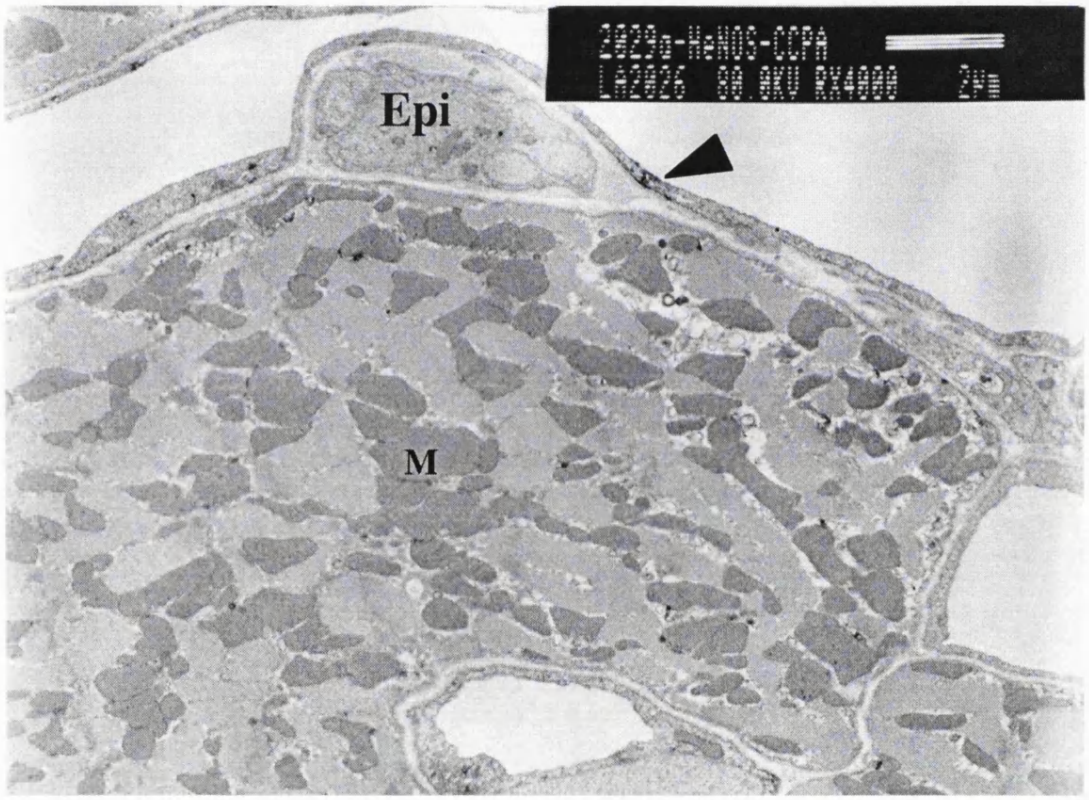

8.3. Phase 2. NO and mitochondrial membrane potential ($\Delta\psi_m$).

As demonstrated in section 8.2, the subcellular localisation of nitric oxide synthase (particularly iNOS) following preconditioning appears to couple the enzyme to within an extremely short diffusion distance of mitochondria. This potentially implicates a functional relationship between nitric oxide and mitochondria following preconditioning stimuli. To determine whether nitric oxide has a direct effect upon mitochondria and specifically the mitochondrial K_{ATP} channel independently of cellular signalling cascades, the effect of exogenous nitric oxide administration upon isolated mitochondria was determined. K_{ATP} channel opening has previously been associated with mitochondrial membrane depolarisation, as determined by the measurement of $\Delta\psi_m$[376] or flavoprotein auto-fluorescence.[286] Therefore, determination of mitochondrial membrane potential ($\Delta\psi_m$) change associated with the administration of exogenous nitric oxide and the effect of selective K_{ATP} channel blockers upon nitric oxide's relationship with $\Delta\psi_m$ would therefore implicate nitric oxide as a K_{ATP} channel modulator. Thus this result would provide new insight into the action of nitric oxide as a cardioprotective agent and its interaction with the putative end-effector of preconditioning.

To study the effect of nitric oxide upon mitochondria, mitochondria were isolated as described in section 3.10. Following confirmation of normal respiration and the effect of respiratory chain uncoupling (section 3.10.2.2), the mitochondria were then incubated with incremental concentrations of nitric oxide to form a dose/response curve with respect to $\Delta\psi_m$, and the effect of the administration of the selective mitochondrial K_{ATP} channel blocker, 5 hydroxydecanoate (5-HD) determined (protocol, figure 8.4).

FIGURE 8.4. SNAP AND ISOLATED MITOCHONDRIA.

Mitochondria were isolated as detailed in section 3.10, and normal respiration confirmed by the influences of electron chain uncoupling as described in section 3.10.2.2. Aliquots where then briefly incubated with SNAP at concentrations ranging from 0.01 to 10 μM. Membrane potential was then assessed by flow cytometry over 15,000 events. Each concentration was repeated in triplicate to ensure reproducible results.

Once an optimal concentration of SNAP was determined, as defined by maximal membrane depolarisation, the mitochondria were incubated with this concentration of SNAP in conjunction with the K_{ATP} channel blocker, 5-HD (100 μM). A further group of mitochondria were incubated with 5-HD alone, and the membrane potential compared with control mitochondria that were incubated with the membrane potential dye alone.

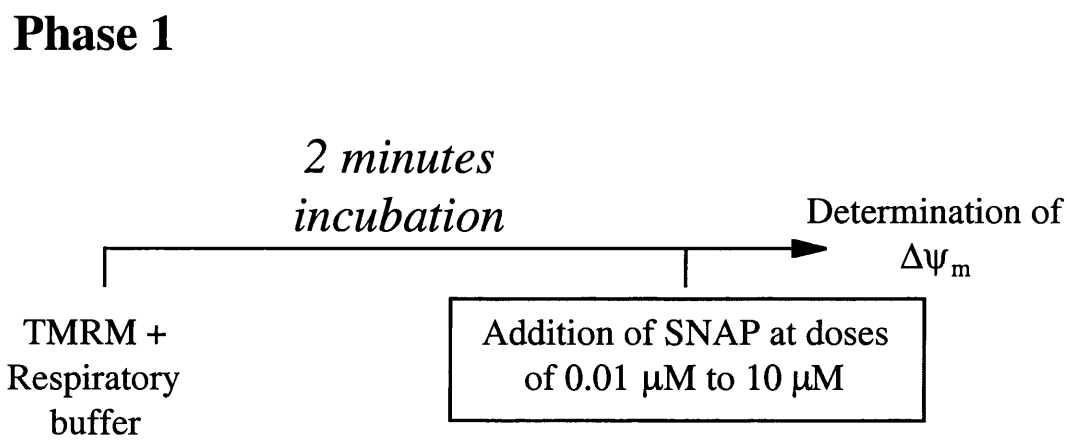

FIGURE 8.5. SNAP AND MITOCHONDRIAL $\Delta\Psi_M$ DOSE RESPONSE.

The effect of increasing concentrations of SNAP upon mitochondrial membrane potential was determined. SNAP concentrations of up to 1 μM resulted in significant depolarisation of mitochondria, whilst at higher doses SNAP resulted in mitochondrial hyperpolarisation (*$p < 0.05$).

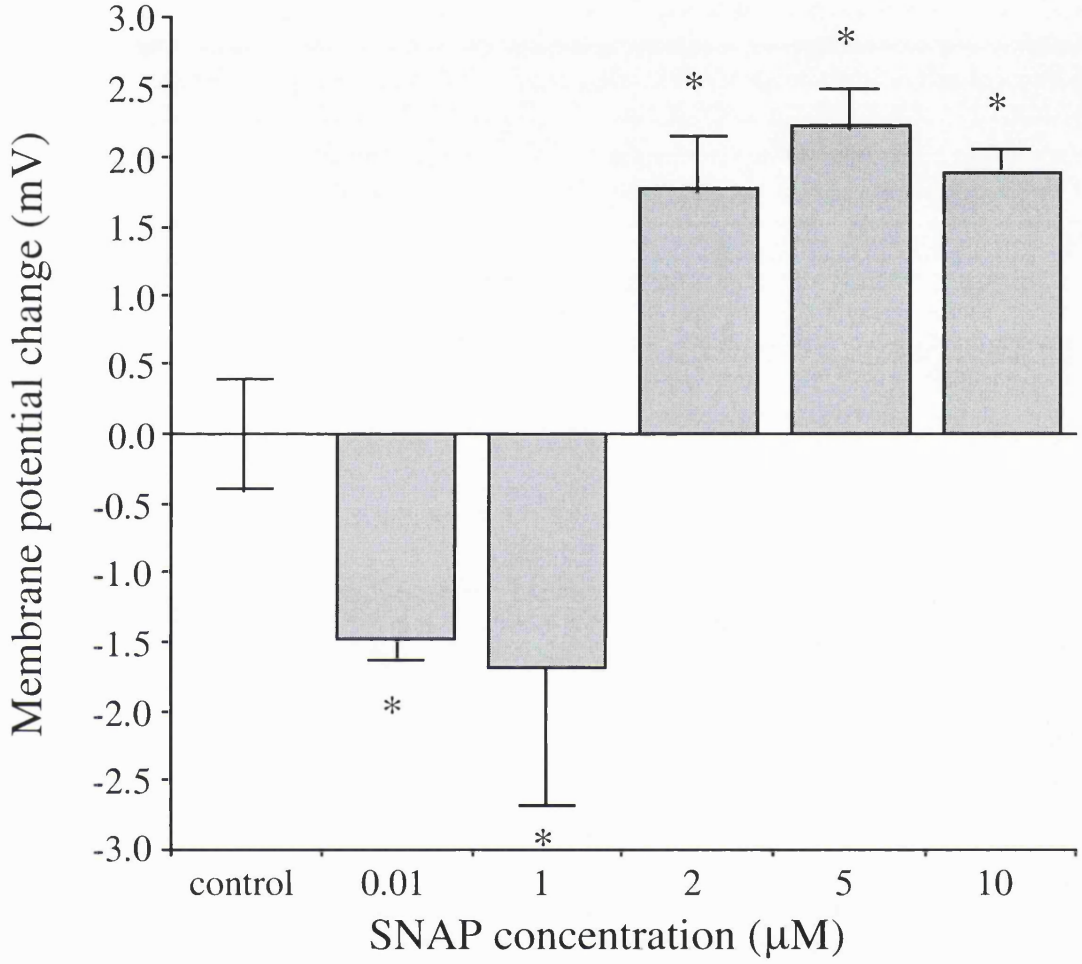

FIGURE 8.6. 5-HD ABROGATES SNAP INDUCED DEPOLARISATION.

To determine whether the depolarisation of mitochondria with low dose SNAP was dependent upon the opening of the K_{ATP} channel, mitochondria were co-incubated with 1 μM SNAP and 5-HD. 5-HD abrogated the membrane potential change associated with SNAP administration, whilst 5-HD on its own had no effect upon $\Delta\psi m$.

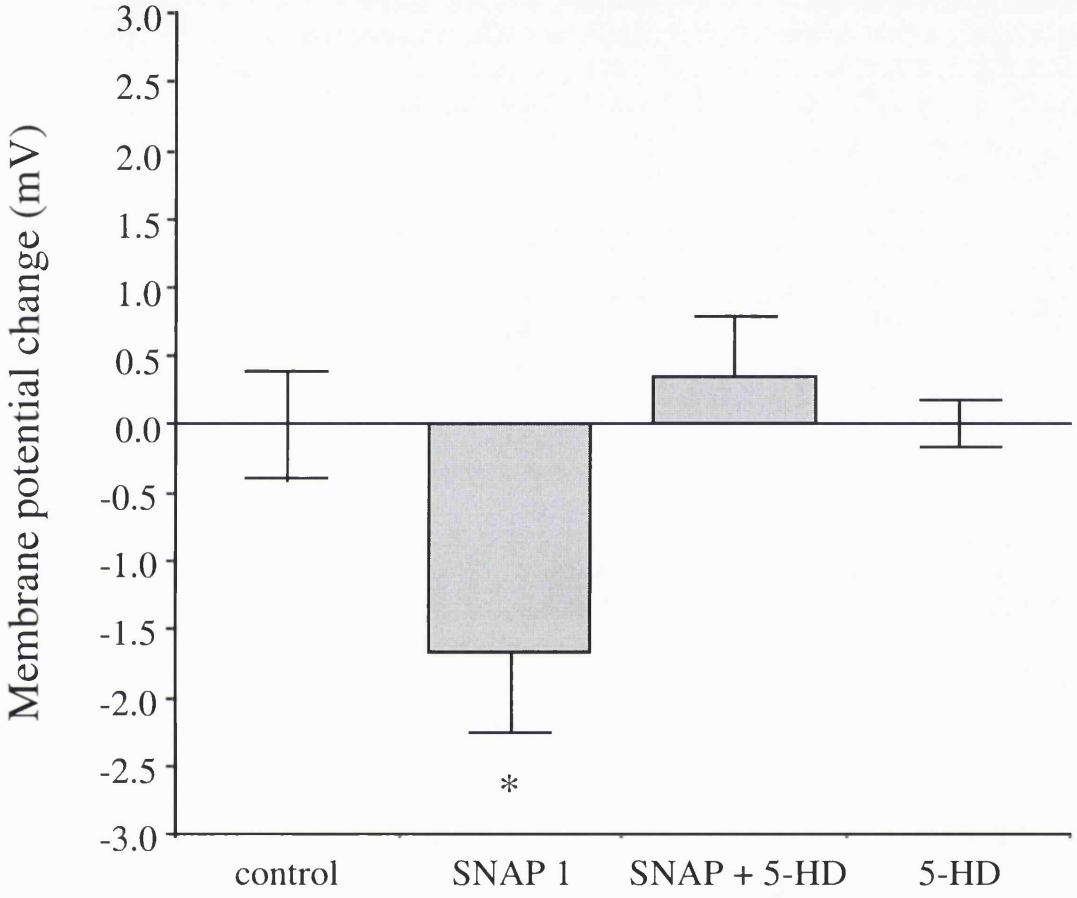

FIGURE 8.7. TMRM FLUORESCENCE RAW DATA.

This figure shows representative results from the flow cytometer, demonstrating the event/fluorescence data from the isolated rat mitochondria experiments. In **A**, CCCP resulted in rapid and near complete depolarisation of the mitochondria, as shown by the left-shift of the fluorescence curve. 1 μM SNAP (**B**), also resulted in mitochondrial depolarisation, although the left-shift is modest. Higher concentrations, the mitochondria tended to hyperpolarise, as seen with 10 μM SNAP in **C**. In **D**, the effect of 5-HD administration is shown- the depolarisation associated with SNAP 1 μM administration is abrogated.

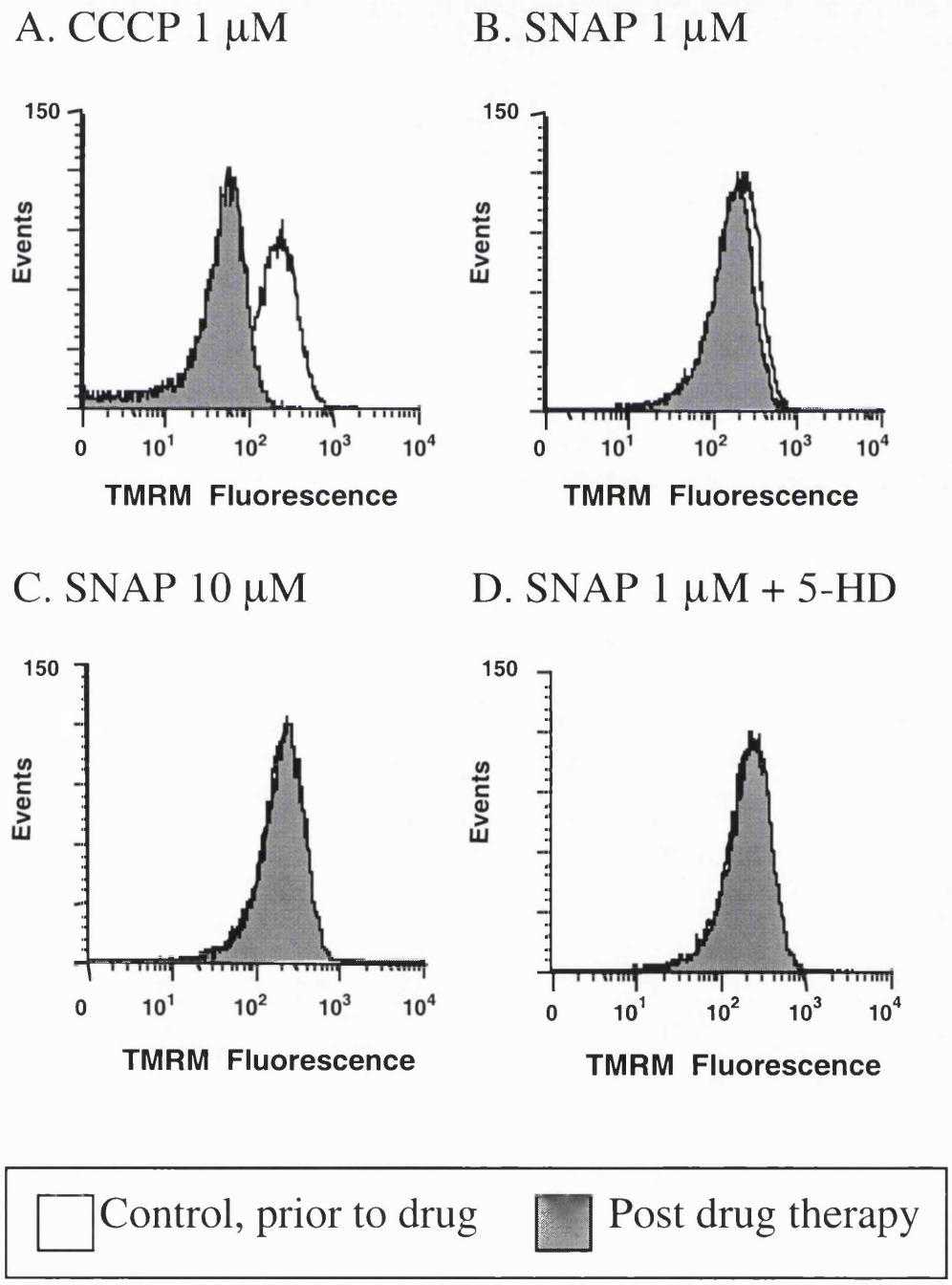

8.3.1. Results.

Incremental concentrations of SNAP resulted in a bi-modal membrane potential response, with a reversal concentration of 1 μM SNAP (figure 8.5). With concentrations of less than or equal to 1 μM, there was a modest, but significant drop of membrane potential compared to control mitochondria (1.51 ± 0.02 mV to 1.71 ± 0.02 mV associated with 0.01 and 1 μM SNAP respectively, versus controls, $p = 0.024$ and $p = 0.023$). At concentrations greater than 1 μM, the mitochondria were found to significantly hyperpolarise (1.76 ± 0.02 mV, 2.21 ± 0.01 mV and 1.88 ± 0.01 mV at SNAP concentrations 2, 5 and 10 μM respectively, with p values of 0.020, 0.007 and 0.015).

The depolarisation associated with lower concentrations of SNAP was found to be sensitive to the administration of the mitochondrial K_{ATP} channel blocker 5-HD, with complete attenuation of membrane potential change associated with 1 μM SNAP in the presence of 5-HD, whilst 5-HD on its own had no effect upon the membrane potential (figure 8.6, 149.85 ± 0.395, 150.19 ± 0.43 and 149.85 ± 0.15 mV in control, SNAP plus 5-HD and 5-HD alone groups, and is also shown figuratively in figure 8.7). Thus, the membrane potential change associated with low dose SNAP therefore appears to be mediated via the mitochondrial K_{ATP} channel.

8.3.2. Discussion.

Exogenous nitric oxide applied to isolated mitochondria has a direct effect upon mitochondrial membrane potential, an effect that is bi-model and concentration dependent. This result appears to suggest a *direct* effect of nitric oxide upon the mitochondria, as the isolation/washing process removes second messenger systems associated with the sarcolemma and the cytosol. The depolarisation effect observed with the lower concentrations of nitric oxide appears sensitive to blockade by 5-HD, suggesting that the nitric oxide mediated effect upon the mitochondria is mediated by opening of the K_{ATP} channel, and appears consistent with the literature demonstrating that K_{ATP} channel opening is associated with a lowering of the membrane potential.[376] Thus it is attractive to postulate that cardioprotective low dose nitric oxide is mediated via the mitochondrial K_{ATP} channel.

Higher dose nitric oxide (released from SNAP at concentrations greater than 1 μM) is associated with membrane hyperpolarisation. Whilst not investigated here, previous reports have suggested that hyperpolarisation of mitochondria is associated with the induction of apoptosis by triggering the release of cytochrome-c,[377] suggesting a potential mechanism whereby high dose SNAP resulted in lost cardioprotection in Langendorff hearts (section 5.2.4) compared to low dose SNAP. The dose/response

curves for cardioprotection in whole hearts and for membrane potential are not identical. In whole hearts (figure 5.5), the optimal concentration of SNAP to imbue cardioprotection is 2 μM, a dose that, in isolated mitochondria triggers membrane hyperpolarisation. Mitochondrial hyperpolarisation maybe associated with toxic respiratory chain inhibition and later membrane potential collapse. The disparity between the whole organ and the mitochondrial isolate is likely to be secondary to diffusion distance of nitric oxide from the microvasculature to the myocyte mitochondrion. As nitric oxide has a notably short half life (typically less than 2 seconds, but dependent upon conditions), the nitric oxide concentration surrounding *in situ* mitochondria in the *in-vivo* heart will be less than the nitric oxide concentration found in the vessel itself. Where in isolated mitochondria 1 μM SNAP induces small membrane depolarisation and 2 μM hyperpolarisation, in the isolated heart the optimal cardioprotective concentration is 2 μM, one might speculate that the concentration at the mitochondria in isolated heart is 50% of that in the vasculature.

The modest changes of membrane potential are surprising. In context, the addition of GTP (50 μM), used a K_{ATP} channel opener under the same respiratory buffer conditions resulted in a 14 ± 0.9% reduction of population fluorescence intensity.[378] In comparison, the change of fluorescence associated with 1 μM SNAP administration was 4 ± 0.5%, which represents approximately a third of the fluorescence change. The modest change in membrane potential associated with SNAP administration may have two explanations: (*i*) nitric oxide is a pure K_{ATP} channel opener, with a modest efficacy compared to GTP. (*ii*) Nitric oxide has other effects upon mitochondria other than a direct effect upon the mitochondrial K_{ATP} channel. Indeed, as discussed at the beginning of this chapter, nitric oxide reversibly inhibits the respiratory chain at complex IV,[370] as well as inhibiting complex I through the generation of peroxynitrite free radicals in rat heart.[379] How such a modest mitochondrial membrane change as those associated with SNAP administration may imbue protection upon the myocyte, was not investigated in this series of experiments. In the present study, $\Delta\Psi_m$ is used primarily as a marker of an "effect" upon mitochondria, and therefore no causal association with infarct size is drawn or demonstrated. Assuming that $\Delta\Psi_m$ reflects mitochondrial function, then an explanation of the disproportionate effect of $\Delta\Psi_m$ change upon cellular survival would be that a small change of membrane potential has a large effect upon the mechanisms of mitochondria. If this were the case, then mitochondrial membrane potential would require rigorous control to avoid instability of mitochondrial systems. In this study, under control conditions, resting mitochondrial membrane potential was 149.9 ± 0.4 mV perhaps indicating the necessary tight control. The alternative (and possibly more likely) explanation is that membrane potential is an indirect and somewhat insensitive marker of other processes in the mitochondria. Thus, whilst nitric oxide administration may have significant effects upon the mitochondria, this is manifest as very modest

changes of membrane potential. At the present time, it is unclear as to which potential explanation is correct, and warrants further investigation.

The results here and from section 8.2 appear to suggest that nitric oxide may have a functional relationship with the mitochondria. The following series of experiments were designed to determine whether opening of the mitochondrial K_{ATP} channel mediates the cardioprotective effect of exogenous nitric oxide.

8.4. Phase 3: nitric oxide and the mitochondrial K_{ATP} channel.

From the evidence in the literature implicating a role for nitric oxide regulating the function of mitochondria, possibly though a direct action upon the mitochondrial K_{ATP} channel (sections 8.1 and 8.3), and evidence from electron immuno cytochemistry implicating a possible association between nitric oxide synthases and the mitochondria on a sub-cellular level (section 8.2), the aim of this study was to determine whether exogenous nitric oxide mediated its infarct-sparing cardioprotective effect via the modulation of mitochondrial K_{ATP} channels.

Based upon the dose/response infarct resistance data prepared in chapter 5 (infarct size resistance associated with increasing concentrations of nitric oxide donor summarised in figures 5.5 and 5.6), the nitric oxide donor, S-nitroso N-acetyl DL penicillamine, SNAP, at the optimal infarct and functional sparing dose, 2 μM, was used. To determine whether the infarct sparing effect of nitric oxide is associated with the mitochondrial K_{ATP} channel, the mitochondrial selective mitochondrial K_{ATP} channel blocker, 5 hydroxydecanoate, 5-HD,[380, 381] was used at a concentration of 100 μM to determine whether the cardioprotective effects of exogenous nitric oxide would be blocked and therefore mediated via the modulation of the open probability of the K_{ATP} channel.

Therefore, hearts were randomly allocated into one of four groups: control with normal Krebs Henseleit buffer (figure 8.8.A), buffer plus SNAP 2 μM (figure 8.8.B), buffer, SNAP 2 μM plus 5-HD 100 μM (figure 8.8.C), and buffer plus 5-HD 100 μM (figure 8.8.D). The final group received 5-HD alone to determine whether the K_{ATP} channel blocker had an effect upon infarct size resistance in naive hearts.

FIGURE 8.8. PROTOCOL FOR ISCHAEMIA/REPERFUSION.

To determine whether nitric oxide donors mediated their protection via a mechanism that is reliant upon the mitochondrial K_{ATP} channel, hearts were perfused in one of 4 groups.:

A: control; hearts perfused with normal Krebs Henseleit buffer.

B: SNAP; 2 μM SNAP was added to the perfusate and was present throughout the perfusion protocol.

C: SNAP + 5-HD: 2 μM SNAP + 100 μM 5-HD were added to the perfusate, and present throughout the perfusion

D: 5-HD: 100 μM 5-HD added to the perfusate and present throughout the perfusion protocol.

Primary end point in the study was infarct size. Secondary functional measures were also monitored.

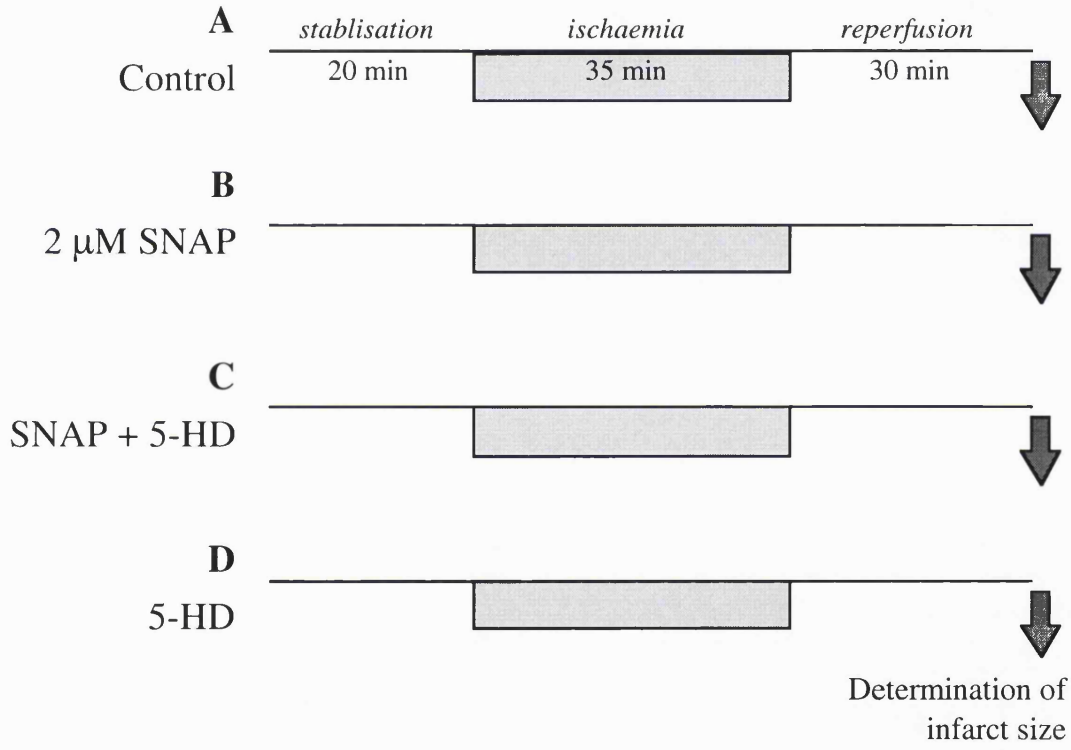

Table 8. Chapter 8: Morphometrics and baseline figures.

No significant differences in body or heart weights were observed between the groups. No significant difference in baseline resting tension was determined. Group B, the SNAP treated group, had significantly greater resting coronary flow than that observed in the other groups (* $p < 0.001$ versus control and 5-HD treatment groups); this increased coronary flow was not observed in the 5-HD co-treatment group, suggesting that the K_{ATP} channel blocker attenuated the vasodilatory effects of SNAP.

Group	Body weight (grams)	Heart weight (grams)	Coronary flow rate ($ml.min^{-1}$)	Resting tension (grams)
A: Control *(n = 7)*	24.75 ± 0.31	0.163 ± 0.004	2.41 ± 0.14	1.21 ± 0.15
B: SNAP *(n = 6)*	25.13 ± 0.57	0.160 ± 0.004	3.77 ± 0.15*	1.04 ± 0.04
C: SNAP +5-HD *(n = 6)*	25.15 ± 0.52	0.170 ± 0.006	2.52 ± 0.16	1.08 ± 0.04
D: 5-HD *(n = 5)*	25.55 ± 0.80	0.164 ± 0.011	2.66 ± 0.14	1.07 ± 0.05

8.4.1. Results.

The morphometrics of the animals used in the study are summarised in table 8. No differences in either body or heart weight were observed in the four groups studied. Baseline functional parameters were also equivalent, although the baseline coronary flow was higher in the SNAP treated hearts, an increase that was abrogated by the co-infusion of the K_{ATP} channel blocker, 5-HD. 5-HD had no independent effect upon baseline coronary flow rates.

8.4.1.1. Nitric oxide limits infarction via mitochondrial K_{ATP} channels.

As found in previous studies (section 5.2.4), the administration of 2 μM SNAP resulted in significant attenuation of infarct size compared to that observed in control hearts (figure 8.9; control: 32± 3% SNAP: 17 ± 4%, p = 0.004). In hearts where SNAP was administered in the presence of the mitochondrial K_{ATP} channel blocker, 5-HD, the protection against myocardial infarction was abrogated, with the infarct size increasing to 38 ± 3% (p = 0.214 versus control). 5-HD on its own did not influence infarct size (36 ± 3%). These results suggest that infarct limitation is mediated by a mechanism sensitive to blockade with 5-HD, and thus point to a potential role of mitochondrial K_{ATP} as an effector mechanism of nitric oxide mediated cardioprotection,

8.4.1.2. Nitric oxide improves post-ischaemic function.

SNAP administration throughout the perfusion protocol resulted in a modest, but significant improvement in post-ischaemic function (figure 8.10; mean post-ischaemic recovery in controls and SNAP treated groups were, respectively, 2.64 ± 0.34% and 4.47 ± 0.37%, p < 0.001). The administration of the mitochondrial K_{ATP} channel blocker, 5-HD, abrogated this functional improvement (mean functional recovery, 3.33 ± 0.38%, p = 0.147 versus control and p = 0.021 versus SNAP treated group). 5-HD administered on its own had no influence upon contractile recovery (mean function, 2.29 ± 0.22%, p = 0.918 versus control). Thus, nitric oxide mediates post-ischaemic contractile functional recovery that, as with infarct sparing, is also sensitive to the administration of 5-HD.

FIGURE 8.9. SNAP CARDIOPROTECTION IS BLOCKED WITH 5-HD.

Administration of 2 μM SNAP was significantly cardioprotective resulting in attenuation of infarct size. This protection was completely abrogated in the presence of the mitochondrial K_{ATP} channel blocker, 5-hydroxydecanoate. 5-hydroxydecanoate had no detrimental effect upon infarct size when administered to hearts in isolation.

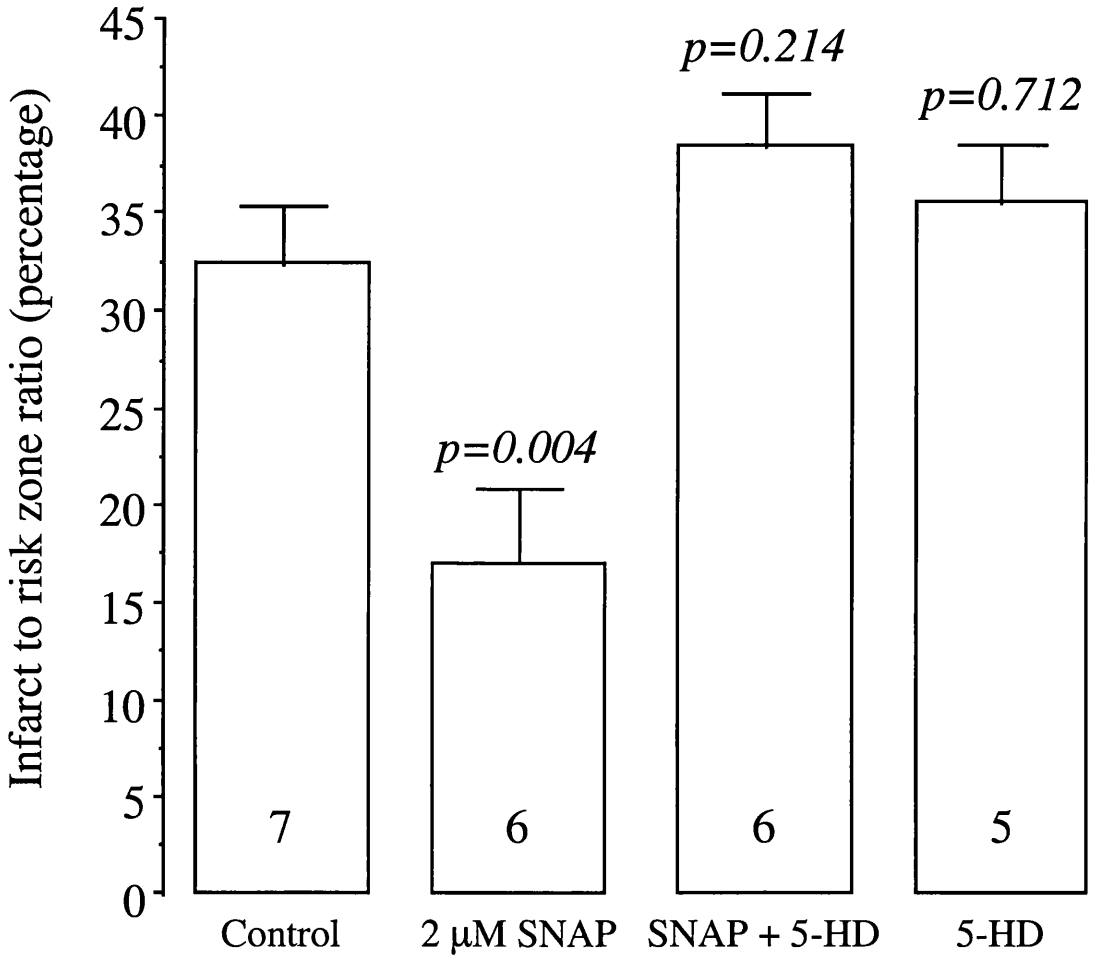

FIGURE 8.10. POST-ISCHAEMIC CONTRACTILE RECOVERY.

2 μM SNAP resulted in a significant increase in post-ischaemic contractile recovery compared to the control group ($p < 0.001$). The addition of the mitochondrial K_{ATP} channel blocker, 5-HD (100 μM) abolished this improvement in function. (n = 5 to 7 per group.)

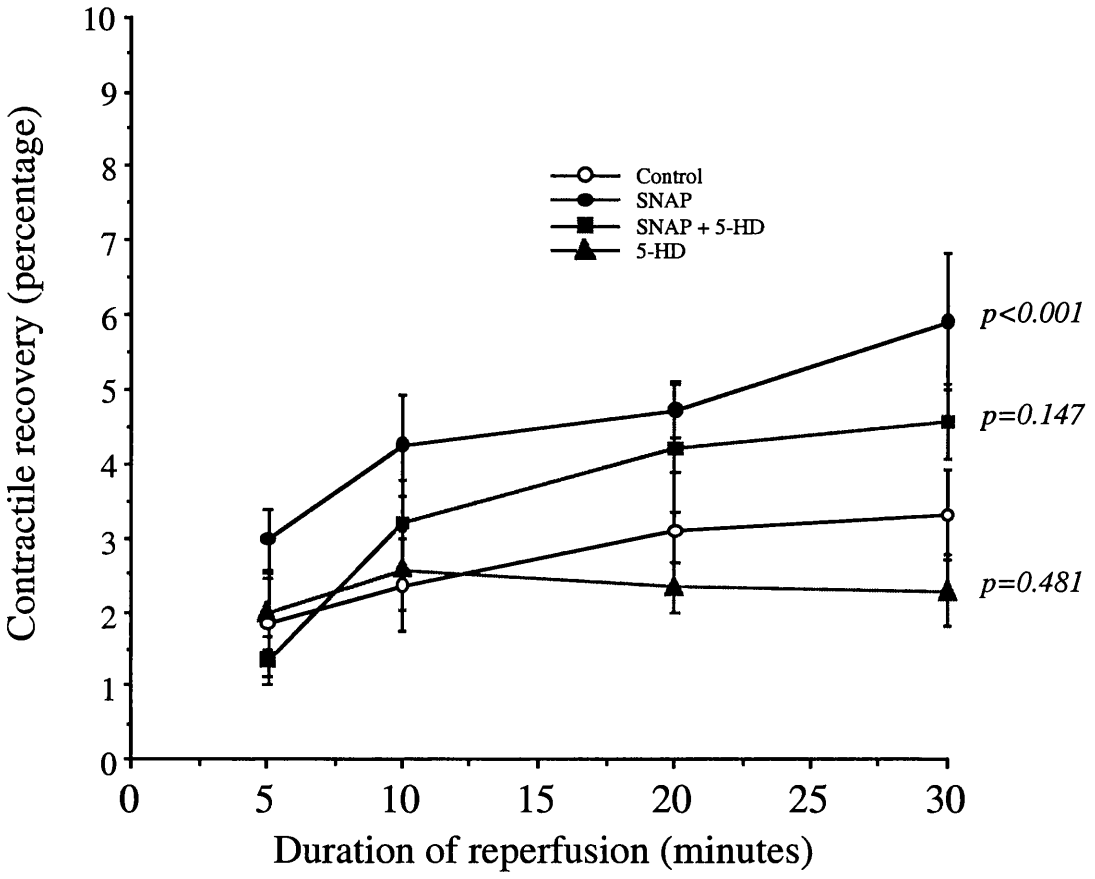

8.4.2. Discussion.

As found in section 5.2.4, exogenously administered nitric oxide results in significant attenuation of myocardial infarction and contractile dysfunction. The mechanisms by which nitric oxide may mediate protection have not been previously elaborated upon, and the data presented here indicate for the first time a link between nitric oxide infarct limitation and the mitochondrial K_{ATP} channel. The results demonstrate that the cardioprotective effects (both in terms of contractile function preservation and infarct limitation) of nitric oxide administration are abrogated by the co-administration of the mitochondrial selective K_{ATP} channel blocker, 5-HD.

The data contained within this chapter therefore provide evidence of a link between myocardial preconditioning, nitric oxide generation, mitochondrial K_{ATP} channel opening by nitric oxide, and cardioprotection. Delayed preconditioning, as demonstrated in chapter 6 is closely associated with the synthesis of nitric oxide. The subcellular localisation of induced iNOS as a consequence of transient adenosine A_1 receptor activation clearly shows that nitric oxide generated by nitric oxide synthase has a very short diffusion distance to the mitochondria, providing biological plausibility to the hypothesis that nitric oxide may mediate protection by modulating the respiratory functions of this organelle. This hypothesis is strengthened further from the results obtained from isolated mitochondria (section 8.3) where nitric oxide causes a dose dependent bi-modal membrane potential change. K_{ATP} channels have been associated with cardioprotection (as described in sections 1.6.2.2 and 1.6.3.2) and with mitochondrial membrane depolarisation.[376] Interestingly, the depolarisation caused by the administration of 1 μM SNAP is blocked by 5-HD implicating that the reduced $\Delta\psi_m$ is mediated by K_{ATP} channel opening. In the absence of second messenger systems in this isolated mitochondria preparation, it appears that nitric oxide is capable of acting directly, modifying mitochondrial function. Examining the role of nitric oxide and its potential interaction with the K_{ATP} channel in the isolated, Langendorff perfused mouse heart model of ischaemia/reperfusion, the data summarised here in section 8.4.1 demonstrate that the protective, anti-necrotic effects of nitric oxide upon the heart are abrogated by the K_{ATP} channel blocker, 5-HD. Thus this provides further evidence for the link between nitric oxide and mitochondria. The mechanisms by which K_{ATP} channel opening imbues protection requires further investigation; mitochondria is just one of many potential targets of nitric oxide that may imbue the heart with resistance against infarction (discussed in section 1.7.7.2).

Potential schema of preconditioning and nitric oxide mediated protection:

Preconditioning → increased cytosolic nitric oxide synthase → diffusion of nitric oxide to mitochondria → opening of K_{ATP} channels → Cardioprotection

Chapter 9. Summary, conclusions and future directions.

The primary aim of the studies contained within this thesis was to determine the role of nitric oxide as a signalling moiety in mediating myocardial protection. In this thesis, the investigation centred on the forms of receptor activated endogenous myocardial protection so far discovered, namely, early preconditioning, delayed preconditioning as well as protection against reperfusion injury.

9.1. Summary of findings:

9.1.1. eNOS lowers the threshold of preconditioning

Hitherto, studies using pharmacological inhibitors of eNOS activity have failed to demonstrate any contribution of nitric oxide to early ischaemic preconditioning. Given evidence of the ability of agents released into the cellular milieu by transient ischaemia to translocate and phosphorylate eNOS, these results are surprising. The data presented in this thesis demonstrate a clear shift of the ischaemic preconditioning dose-response curve to the left in the presence of eNOS; preconditioning eNOS knockout hearts requires more repeated cycles of ischaemia to trigger a similar level of infarct resistance. The studies contained within this report are, we believe, the first to demonstrate a beneficial link between eNOS and early ischaemic preconditioning.

9.1.2. Exogenous nitric oxide mediates cardioprotection

The transient administration of nitric oxide has previously been demonstrated to trigger a preconditioning-like response, but the cardioprotective properties of nitric oxide donors, present throughout the duration of ischaemia and reperfusion, were undetermined. In this thesis, it was demonstrated that exogenous nitric oxide mediates significant cardioprotection in a dose-responsive fashion (infarct to risk zone ratio = 20.74 - 7.55*Log([SNAP]), significantly correlated, with a coefficient of $r^2 = 0.941$). Equally, resistance to post-ischaemic contractile dysfunction was also mediated in a similar dose-responsive manner. A further novel finding of this study was the demonstration that there appears to be a clear dose threshold beyond which the beneficial infarct limiting effects are lost. Whilst the '*supra-protective*' concentrations of nitric oxide donor examined in this report resulted in infarct sizes what were no greater than that found in control hearts, this is the clearest demonstration thus far of the benefit/ detriment character of nitric oxide with relation to cell survival.

9.1.3. Nitric oxide synthesised by eNOS mediates delayed *pharmacological* protection

Previous reports investigating the role of nitric oxide in delayed ischaemic or monophosholipid-A triggered preconditioning have emphasised the pivotal role of iNOS in the paradigm of protection. Contrary to these reports, low dose CCPA (25 mg/kg), was found to mediate cardioprotection via a mechanism that also involves the novel upregulation of eNOS. As in previous investigations, CCPA triggered cardioprotection was found to be dependent upon the synthesis of nitric oxide as non-specific nitric oxide inhibitors were seen to attenuate the protection observed. Moreover, the infarct size reduction could be demonstrated to be mimicked by the administration of a nitric oxide donor.

9.1.4. eNOS activation by PI3 kinase/Akt mediates reperfusion salvage

The ability to salvage myocardium from the consequences of lethal ischaemic injury is a goal that has eluded cardiologists for many years. The exact mechanisms by which it may be possible to protect the myocardium at reperfusion are unknown, but the hypothesis that the PI3 kinase/Akt pathway plays a pivotal role in this form of protection is new and has been the basis of a number of studies in our laboratories. Furthermore, as Akt has been demonstrated to phosphorylate and activate eNOS, it was hypothesised that reperfusion protection may be dependent upon nitric oxide synthesis. In this thesis, one of the known activators of PI3 kinase, namely bradykinin, was examined when administered at reperfusion. The protection observed was found to be reliant upon the presence of eNOS, and thus nitric oxide was found be critical to the induction of infarct resistance. That protection against infarction could also be observed following the administration of a nitric oxide donor at reperfusion strengthens the link between nitric oxide and reperfusion salvage.

9.1.5. Mitochondria is a target of nitric oxide

As a potential signalling moiety, nitric oxide has cellular targets that effect the resistance to cell death. Some investigators have demonstrated that nitric oxide may impact directly upon anti-apoptotic cascades, whilst others have implied a potential interaction with mitochondria, and specifically the putative end-effector of preconditioning, namely the mitochondrial K_{ATP} channel. Electron immunocytochemistry established the biological plausibility of a link between nitric oxide synthase sub-cellular localisation, nitric oxide synthesis and mitochondria. In isolated mitochondria, nitric oxide could be demonstrated to alter membrane potential at nitric oxide concentrations that were previously demonstrated to be cardioprotective. The membrane depolarisation appeared

consistent with mitochondrial K_{ATP} channel opening, and could be attenuated by the administration of mitochondrial K_{ATP} channel blocker, 5-HD. In the absence of second messenger systems, this would suggest that nitric oxide has a direct effect upon mitochondrial function. Returning to whole hearts subjected to ischaemia/reperfusion, the cardioprotection resultant from exogenously administered nitric oxide was totally abrogated with the administration of 5-HD, again supporting the link between preconditioning, nitric oxide synthesis and mitochondrial K_{ATP} channels.

9.1.6. Conclusions:

Nitric oxide synthases have been demonstrated to be involved in all forms of cardioprotection. The role of eNOS in particular was found to be far more involved in myocardial resistance than hitherto thought, contributing to the preconditioning threshold, mediating with iNOS delayed *pharmacological* preconditioning, and proving essential for reperfusion salvage. The product of nitric oxide synthase activity, nitric oxide, was demonstrated to mediate resistance to injury, with the protection observed closely correlated to its concentration. Therefore it would appear that nitric oxide is an important signalling moiety in both preconditioning protection and reperfusion salvage. That there is a concentration of nitric oxide beyond which cardioprotection is lost is a significant observation for the clinical use of nitric oxide donors, where nitric oxide concentrations are not determined.

With the demonstration of nitric oxide having a direct impact upon mitochondrial function, and that mitochondrial K_{ATP} channel blockers attenuate nitric oxide elicited protection, also suggest this to be an important mediator of cellular protection. Therefore, the following schema are proposed:

1. Nitric oxide hypothesis of preconditioning:

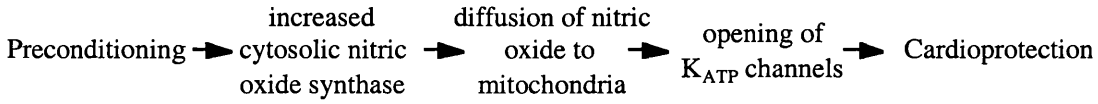

2. Nitric oxide hypothesis of reperfusion salvage:

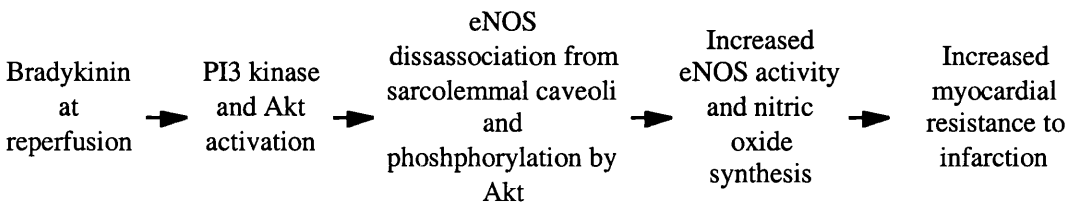

9.2. Clinical implications.

As a number of therapeutic agents used in the management of patients with cardiovascular disease may influence directly or indirectly tissue concentrations of nitric oxide, the data contained in this thesis may have profound implications with regard to future potential clinical management of acute coronary syndromes.

9.2.1. Nitrate therapy.

Use of nitrates in the management of acute coronary syndromes is primarily one of anginal symptom control. The implication that nitrates may be directly cardioprotective is important, as is the observation that the concentration of nitrate donor that elicits maximal cardioprotection is only a third of the dose that is associated with loss of protection implying a narrow therapeutic index. As clinical nitrate therapy is not monitored, the opportunity of inducing myocardial preservation in these patients may not be realised.

Nitrates in current clinical usage could be used to reduce the preconditioning threshold prior to surgical coronary interventions, mediate cardioprotection during acute myocardial ischaemia, and even be used as a reperfusion injury salvage agent in its own right. However, controlled clinical studies need to be undertaken if this observation is to be proven. Furthermore, given the evidence that nitric oxide therapy may have a narrow therapeutic index, it may be prudent to use drugs that upregulate endogenous synthesis of nitric oxide, such as bradykinin, to avoid potentially deleterious effects of nitrate therapy. One example of one such class of agent currently clinically available would be the angiotensin converting enzyme inhibitors.

9.2.2. Cardiovascular drugs that upregulate eNOS activity.

Agents that upregulate eNOS activity may be classified into two categories: drugs that activate PI3 kinase indirectly and drugs that activate PI3 kinase directly. Agents that fall into the first group include those agents that increase bradykinin in the extracellular milieu, such as angiotensin converting enzymes and neutral endopeptidase inhibitors. These agents would be expected to be found (and in some instances have already been shown) to lower the preconditioning threshold, mediate increased resistance to cell death if present during ischaemia, and result in attenuated infarction when administered at reperfusion. Similarly, drugs that can activate PI3 kinase directly, such as HMG CoA reductase inhibitors may be anticipated to posses similar qualities. As yet this has not been explored, but may go some way to explain the benefits of these lipid lowering drugs beyond their ability to lower cholesterol. Again, further basic and clinical

research needs to be undertaken to demonstrate and prove or disprove these hypothesis in the context of ischaemia/reperfusion injury.

9 .4. Further investigations.

9.4.1. Early preconditioning

- The relative contribution of nitric oxide and free radicals synthesised by eNOS in the paradigm of early ischaemic preconditioning.
- Can low dose exogenous nitric oxide lower the early preconditioning threshold?
- Is the preconditioning threshold in female mouse hearts different from that in male mouse hearts?

9.4.2. Delayed preconditioning

- Determination of whether differential regulation of p38 MAPK and p42/p44 ERK occurs following A_1 receptor activation compared to cytokine/endotoxic induction of delayed protection.
- As nitric oxide synthesis mediates delayed preconditioning, with evidence that nitric oxide concentrations are at their greatest at reperfusion (figure 7.1), might delayed protection be mediated via a mechanism of reperfusion injury salvage as found in chapter 7?
- Further characterisation of eNOS in delayed pharmacological preconditioning. Is eNOS required during the trigger phase of protection, or during the mediator phase during the ischaemia/reperfusion insult?

9.4.3. Mechanisms of exogenous nitric oxide protection and injury.

- Is the deleterious effects of high dose exogenous nitric oxide mediated through the induction of apoptosis? Is the mitochondrial hyperpolarisation observed with nitric oxide administration associated with PTP opening and cytochrome-c release?
- Would the clinically used nitric oxide donor, glyceryl trinitrate, in whole animal model of ischaemia/reperfusion injury mimic the cardioprotection observed with SNAP.
- What influence of blood products upon the nitric oxide/cardioprotection dose-response curve.
- What effect has vascular nitrate tolerance have upon nitric oxide mediated cardioprotection?

9.4.4. Reperfusion injury salvage.

- Determination of the mechanisms by which nitric oxide mediates infarct reduction.
- Do cardiovascular drugs that activate PI3 kinase also result reperfusion injury salvage? Therefore, do HMG CoA reductase inhibitors have this effect?

Publications and Communications.

Bell, RM, Rees, D, Yellon, DM (1998). *The protection resulting from delayed pharmacological preconditioning appears independently of iNOS: a study in iNOS knockout mice.* September 1999, Autumn meeting of the British Society of Cardiovascular Research.

Bell, RM, Rees, D, Yellon DM (1999). *The protection observed during delayed preconditioning appears independent of iNOS: a study in iNOS knockout mice.* November 1999, Atlanta meeting of the American Heart Association.

Bell, RM, Yellon, DM (2000). *Early preconditioning of the mouse heart: the role of nitric oxide and endothelial nitric oxide synthase. Investigations in transgenic mice.* February 2000, Glasgow meeting of the British Cardiac Society.

Bell RM, Yellon DM (1998). *Molecular mechanisms of preconditioning: therapeutic implications.* Rev Port Cardiol. 1998 Oct;17 Suppl 2:II49-61. (Review)

Bell, RM, Smith C, Yellon, DM (2001). *Constitutive nitric oxide synthases may masquerade as inducible nitric oxide synthase in delayed pharmacological preconditioning*. Manuscript submitted to Circulation Research.

Bell, RM, Yellon DM (2001). *Nitric oxide's nonessential role in early preconditioning. An investigation with eNOS knockout mice.* Manuscript submitted to Basic Research in Cardiology.

Bell RM, Yellon, DM (2001). *Bradykinin triggers eNOS mediated reperfusion salvage via the PI3 kinase pathway*. Manuscript submitted to Circulation.

Bibliography

1. Murray C, Lopez A. Mortality by cause for eight regions of the world: Global Burden of Disease Study. Lancet 1997; 349:1269-76.

2. Decker RS, Wildenthal K. Lysosomal alterations in hypoxic and reoxygenated hearts. I. Ultrastructural and cytochemical changes. Am J Pathol 1980; 98:425-44.

3. Banka VS, Bodenheimer MM, Ramanathan KB, Hermann GA, Helfant RH. Progressive transmural electrographic, myocardial potassium ion/sodium ion ratio and ultrastructural changes as a function of time after acute coronary occlusion. Am J Cardiol 1978; 42:429-43.

4. Hegstad AC, Ytrehus K, Lindal S, Jorgensen L. Ultrastructural alterations during the critical phase of reperfusion: a stereological study in buffer-perfused isolated rat hearts. Cardiovasc Pathol 1999; 8:279-89.

5. Jennings RB, Schaper J, Hill ML, Steenbergen C, Reimer KA. Effect of reperfusion late in the phase of reversible ischemic injury. Changes in cell volume, electrolytes, metabolites, and ultrastructure. Circ Res 1985; 56:262-78.

6. Lichtig C, Brooks H. Myocardial ultrastructure and function during progressive early ischemia in the intact heart. J Thorac Cardiovasc Surg 1975; 70:309-15.

7. Murry CE, Jennings RB, Reimer KA. Preconditioning with ischemia: a delay of lethal cell injury in ischemic myocardium. Circulation 1986; 74:1124-36.

8. Murry CE, Richard VJ, Reimer KA, Jennings RB. Ischemic preconditioning slows energy metabolism and delays ultrastructural damage during a sustained ischemic episode. Circ Res 1990; 66:913-31.

9. Steenbergen C, Murphy E, Levy L, London RE. Elevation in cytosolic free calcium concentration early in myocardial ischemia in perfused rat heart. Circ Res 1987; 60:700-7.

10. Allen DG, Orchard CH. Myocardial contractile function during ischemia and hypoxia. Circ Res 1987; 60:153-68.

11. Simoons ML, Boersma E, Maas AC, Deckers JW. Management of myocardial infarction: the proper priorities. Eur Heart J 1997; 18:896-9.

12. Jennings RB, Ganote CE. Mitochondrial structure and function in acute myocardial ischemic injury. Circ Res 1976; 38:I80-91.

13. Humphrey SM, Vanderwee MA. Factors affecting the development of contraction band necrosis during reperfusion of the isolated isovolumic rat heart. J Mol Cell Cardiol 1986; 18:319-29.

14. Shen AC, Jennings RB. Kinetics of calcium accumulation in acute myocardial ischemic injury. Am J Pathol 1972; 67:441-52.

15. Shen AC, Jennings RB. Myocardial calcium and magnesium in acute ischemic injury. Am J Pathol 1972; 67:417-40.

16. Jennings RB, Shen AC. Calcium in experimental myocardial ischemia. Recent Adv Stud Cardiac Struct Metab 1972; 1:639-55.

17. Allen SP, Darley-Usmar VM, McCormack JG, Stone D. Changes in mitochondrial matrix free calcium in perfused rat hearts subjected to hypoxia-reoxygenation. J Mol Cell Cardiol 1993; 25:949-58.

18. Whalen DA, Hamilton DG, Ganote CE, Jennings RB. Effect of a transient period of ischemia on myocardial cells. I. Effects on cell volume regulation. Am J Pathol 1974; 74:381-97.

19. Holly TA, Drincic A, Byun Y, et al. Caspase inhibition reduces myocyte cell death induced by myocardial ischemia and reperfusion in vivo. J Mol Cell Cardiol 1999; 31:1709-15.

20. Freude B, Masters TN, Robicsek F, et al. Apoptosis is initiated by myocardial ischemia and executed during reperfusion. J Mol Cell Cardiol 2000; 32:197-208.

21. Mocanu MM, Baxter GF, Yellon DM. Caspase inhibition and limitation of myocardial infarct size: protection against lethal reperfusion injury. Br J Pharmacol 2000; 130:197-200.

22. Shimizu S, Eguchi Y, Kamiike W, et al. Retardation of chemical hypoxia-induced necrotic cell death by Bcl-2 and ICE inhibitors: possible involvement of common mediators in apoptotic and necrotic signal transductions. Oncogene 1996; 12:2045-50.

23. Jonassen AK, Brar BK, Mjos OD, Sack MN, Latchman DS, Yellon DM. Insulin administered at reoxygenation exerts a cardioprotective effect in myocytes by a possible anti-apoptotic mechanism. J Mol Cell Cardiol 2000; 32:757-64.

24. Jonassen AK, Sack NS, Mjøs OD, Yellon DM. Mycardial protection by insulin at reperfusion requires early administration and is dependent on the PI3-kinase, Akt/PKB and p70S6 kinase signaling pathway. Circulation 2000:In Press.

25. Zhao ZQ, Budde JM, Morris C, et al. Adenosine Attenuates Reperfusion-induced Apoptotic Cell Death by Modulating Expression of Bcl-2 and Bax Proteins. J Mol Cell Cardiol 2001; 33:57-68.

26. Gottlieb RA, Engler RL. Apoptosis in myocardial ischemia-reperfusion. Ann N Y Acad Sci 1999; 874:412-26.

27. Jeremias I, Kupatt C, Martin-Villalba A, et al. Involvement of CD95/Apo1/Fas in cell death after myocardial ischemia. Circulation 2000; 102:915-20.

28. Varfolomeev EE, Schuchmann M, Luria V, et al. Targeted disruption of the mouse Caspase 8 gene ablates cell death induction by the TNF receptors, Fas/Apo1, and DR3 and is lethal prenatally. Immunity 1998; 9:267-76.

29. Bialik S, Cryns VL, Drincic A, et al. The mitochondrial apoptotic pathway is activated by serum and glucose deprivation in cardiac myocytes. Circ Res 1999; 85:403-14.

30. Rosse T, Olivier R, Monney L, et al. Bcl-2 prolongs cell survival after Bax-induced release of cytochrome c. Nature 1998; 391:496-9.

31. Cryns V, Yuan J. Proteases to die for. Genes Dev 1998; 12:1551-70.

32. Reimer KA, Murry CE, Yamasawa I, Hill ML, Jennings RB. Four brief periods of ischaemia cause no cumulative ATP loss or necrosis. Am J Physiol. 1986; 251:H1306-H1315.

33. Baxter G, Goma F, Yellon D. Characterisation of the infarct-limiting effect of delayed preconditioning: time course and dose-dependency studies in rabbit myocardium. Basic Res Cardiol 1997; 92:159-67.

34. Sekili S, Jeroudi MO, Tang XL, Zughaib M, Sun JZ, Bolli R. Effect of adenosine on myocardial 'stunning' in the dog. Circ Res 1995; 76:82-94.

35. Sun JZ, Tang XL, Park SW, Qiu Y, Turrens JF, Bolli R. Evidence for an essential role of reactive oxygen species in the genesis of late preconditioning against myocardial stunning in conscious pigs. J Clin Invest 1996; 97:562-76.

36. Richard V, Kaeffer N, Tron C, Thuillez C. Ischemic preconditioning protects against coronary endothelial dysfunction induced by ischemia and reperfusion. Circulation 1994; 89:1254-61 issn: 0009-7322.

37. Loktionova SA, Ilyinskaya OP, Kabakov AE. Early and delayed tolerance to simulated ischemia in heat-preconditioned endothelial cells: a role for HSP27. Am J Physiol 1998; 275:H2147-58.

38. Vegh A, Komori S, Szekeres L, Parratt J. Antiarrhythmic effects of preconditioning in anaesthetised dogs and rats. Cardiovasc Res 1992; 26:487-95.

39. Parratt JR, Vegh A. Delayed protection against ventricular arrhythmias by cardiac pacing. Heart 1997; 78:423-5.

40. Thornton JD, Thornton CS, Downey JM. Effect of adenosine receptor blockade: preventing protective preconditioning depends on time of initiation. Am J Physiol 1993; 265:H504-8.

41. Jin ZQ, Chen X. Bradykinin mediates myocardial ischaemic preconditioning against free radical injury in guinea-pig isolated heart. Clin Exp Pharmacol Physiol 1998; 25:932-5.

42. Schultz JE, Hsu AK, Gross GJ. Morphine mimics the cardioprotective effect of ischemic preconditioning via a glibenclamide-sensitive mechanism in the rat heart. Circ Res 1996; 78:1100-4.

43. Diaz RJ, Wilson GJ. Selective blockade of AT1 angiotensin II receptors abolishes ischemic preconditioning in isolated rabbit hearts. J Mol Cell Cardiol 1997; 29:129-39.

44. Miki T, Miura T, Ura N, et al. Captopril potentiates the myocardial infarct size-limiting effect of ischemic preconditioning through bradykinin B_2 receptor activation. J Am Coll Cardiol 1996; 28:1616-22.

45. Goto M, Liu Y, Yang X, M, Ardell J, L, Cohen M, V, Downey J, M. Role of bradykinin in protection of ischemic preconditioning in rabbit hearts. Circ Res. 1995; 77:611-21.

46. Morris SD, Yellon DM. Angiotensin-converting enzyme inhibitors potentiate preconditioning through bradykinin B_2 receptor activation in human heart. J Am Coll Cardiol 1997; 29:1599-1606.

47. Parratt JR, Vegh A, Zeitlin IJ, et al. Bradykinin and endothelial-cardiac myocyte interactions in ischemic preconditioning. Am J Cardiol 1997; 80:124A-131A.

48. Pan HL, Chen SR, Scicli GM, Carretero OA. Cardiac interstitial bradykinin release during ischemia is enhanced by ischemic preconditioning. Am J Physiol Heart Circ Physiol 2000; 279:H116-21.

49. Fisher SA, Langille BL, Srivastava D. Apoptosis during cardiovascular development. Circ Res 2000; 87:856-64.

50. Brar BK, Jonassen AK, Stephanou A, et al. Urocortin protects against ischemic and reperfusion injury via a MAPK-dependent pathway. J Biol Chem 2000; 275:8508-14.

51. Fujio Y, Walsh K. Akt mediates cytoprotection of endothelial cells by vascular endothelial growth factor in an anchorage-dependent manner. J Biol Chem 1999; 274:16349-54.

52. Datta SR, Brunet A, Greenberg ME. Cellular survival: a play in three Akts. Genes Dev 1999; 13:2905-27.

53. Desagher S, Osen-Sand A, Nichols A, et al. Bid-induced conformational change of Bax is responsible for mitochondrial cytochrome c release during apoptosis. J Cell Biol 1999; 144:891-901.

54. Krajewski S, Krajewska M, Ellerby LM, et al. Release of caspase-9 from mitochondria during neuronal apoptosis and cerebral ischemia. Proc Natl Acad Sci U S A 1999; 96:5752-7.

55. Tsujimoto Y. Role of Bcl-2 family proteins in apoptosis: apoptosomes or mitochondria? Genes Cells 1998; 3:697-707.

56. Dragovich T, Rudin CM, Thompson CB. Signal transduction pathways that regulate cell survival and cell death. Oncogene 1998; 17:3207-13.

57. Datta SR, Katsov A, Hu L, et al. 14-3-3 proteins and survival kinases cooperate to inactivate BAD by BH3 domain phosphorylation. Mol Cell 2000; 6:41-51.

58. Cardone MH, Roy N, Stennicke HR, et al. Regulation of cell death protease caspase-9 by phosphorylation. Science 1998; 282:1318-21.

59. Liu GS, Thornton J, Van Winkle DM, Stanley AW, Olsson RA, Downey JM. Protection against infarction afforded by preconditioning is mediated by A1 adenosine receptors in rabbit heart. Circulation 1991; 84:350-6.

60. Baxter GF, Marber MS, Patel VC, Yellon DM. Adenosine receptor involvement in a delayed phase of myocardial protection 24 hours after ischemic preconditioning. Circulation 1994; 90:2993-3000.

61. Fryer R, Hsu A, Eells J, Nagase H, Gross G. Opioid-induced second window of cardioprotection: potential role of mitochondrial KATP
channels. Circ Res 1999; 84:846-51.

62. Bell R, Yellon D. Molecular mechanisms of preconditioning: therapeutic implications. Rev Port Cardiol 1998; 17 Suppl 2:1149-61.

63. Liu GS, Jacobson KA, Downey JM. An irreversible A1-selective adenosine agonist preconditions rabbit heart. Can J Cardiol 1996; 12:517-21.

64. Liu GS, Richards SC, Olsson RA, Mullane K, Walsh RS, Downey JM. Evidence that the adenosine A3 receptor may mediate the protection afforded by preconditioning in the isolated rabbit heart. Cardiovasc Res 1994; 28:1057-61.

65. Qian YZ, Levasseur JE, Yoshida K, Kukreja RC. KATP channels in rat heart: blockade of ischemic and acetylcholine-mediated preconditioning by glibenclamide. Am J Physiol. 1996; 271:H23-8.

66. Cohen MV, Walsh RS, Goto M, Downey JM. Hypoxia preconditions rabbit myocardium via adenosine and catecholamine release. J Mol Cell Cardiol 1995; 27:1527-34.

67. Liu Y, Tsuchida A, Cohen MV, Downey JM. Pretreatment with angiotensin II activates protein kinase C and limits myocardial infarction in isolated rabbit hearts. J Mol Cell Cardiol 1995; 27:883-92.

68. Starkopf J, Bugge E, Ytrehus K. Preischemic bradykinin and ischaemic preconditioning in functional recovery of the globally ischaemic rat heart. Cardiovasc Res 1997; 33:63-70.

69. Schultz JJ, Hsu A, K, Gross GJ. Ischemic preconditioning and morphine-induced cardioprotection involve the delta (delta)-opioid receptor in the intact rat heart. J Mol Cell Cardiol 1997; 29:2187-95.

70. Baines CP, Goto M, Downey JM. Oxygen radicals released during ischemic preconditioning contribute to cardioprotection in the rabbit myocardium. J Mol Cell Cardiol 1997; 29:207-16.

71. Zhou X, Zhai X, Ashraf M. Direct evidence that initial oxidative stress triggered by preconditioning contributes to second window of protection by endogenous antioxidant enzyme in myocytes. Circulation 1996; 93:1177-84.

72. Bolli R, Bhatti ZA, Tang XL, et al. Evidence that late preconditioning against myocardial stunning in conscious rabbits is triggered by the generation of nitric oxide. Circ Res 1997; 81:42-52.

73. Bolli R, Dawn B, Tang X, et al. The nitric oxide hypothesis of late preconditioning. Basic Res Cardiol 1998; 93:325-38.

74. Nishizawa J, Nakai A, Matsuda K, Komeda M, Ban T, Nagata K. Reactive Oxygen Species Play an Important Role in the Activation of Heat Shock Factor 1 in Ischemic-Reperfused Heart. Circulation 1999; 99:934-941.

75. Csukai M, Mochly-rosen D. Pharmacologic modulation of protein kinase c isozymes: the role of racks and subcellular localisation. Pharmacol Res 1999; 39:253-9.

76. Nagao M, Yamauchi J, Kaziro Y, Itoh H. Involvement of protein kinase C and Src family tyrosine kinase in Galphaq/11-induced activation of c-Jun N-terminal kinase and p38 mitogen-activated protein kinase. J Biol Chem 1998; 273:22892-8.

77. Thornton JD, Liu GS, Downey JM. Pretreatment with pertussis toxin blocks the protective effects of preconditioning: evidence for a G-protein mechanism. J Mol Cell Cardiol 1993; 25:311-20.

78. Ge C, Anand-Srivastava MB. Involvement of phosphatidylinositol 3-kinase and mitogen-activated protein kinase pathways in AII-mediated enhanced expression of Gi proteins in vascular smooth muscle cells. Biochem Biophys Res Commun 1998; 251:570-5.

79. Butt E, Bernhardt M, Smolenski A, et al. Endothelial nitric-oxide synthase (type III) is activated and becomes calcium independent upon phosphorylation by cyclic nucleotide-dependent protein kinases. J Biol Chem 2000; 275:5179-87.

80. Chen ZP, Mitchelhill KI, Michell BJ, et al. AMP-activated protein kinase phosphorylation of endothelial NO synthase. FEBS Lett 1999; 443:285-9.

81. Kehrl J. Heterotrimeric G protein signaling: roles in immune function and fine-tuning by RGS proteins. Immunity 1998; 8:1-10.

82. Downey JM, Cohen MV. Signal transduction in ischemic preconditioning. Z Kardiol 1995; 4:77-86.

83. Ytrehus K, Liu Y, Downey JM. Preconditioning protects ischemic rabbit heart by protein kinase C activation. Am J Physiol 1994; 266:H1145-52.

84. Speechly Dick ME, Mocanu MM, Yellon DM. Protein kinase C. Its role in ischemic preconditioning in the rat. Circ Res 1994; 75:586-90.

85. Dimmeler S, Fleming I, Fisslthaler B, Hermann C, Busse R, Zeiher AM. Activation of nitric oxide synthase in endothelial cells by Akt-dependent phosphorylation. Nature 1999; 399:601-5.

86. Luo Z, Fujio Y, Kureishi Y, et al. Acute modulation of endothelial Akt/PKB activity alters nitric oxide-dependent vasomotor activity in vivo. J Clin Invest 2000; 106:493-9.

87. Headrick JP. Ischemic preconditioning: bioenergetic and metabolic changes and the role of endogenous adenosine. J Mol Cell Cardiol 1996; 28:1227-40.

88. Ganote CE, Armstrong S, Downey JM. Adenosine and A1 selective agonists offer minimal protection against ischaemic injury to isolated rat cardiomyocytes. Cardiovasc Res 1993; 27:1670-6.

89. Cave AC, Collis CS, Downey JM, Hearse DJ. Improved functional recovery by ischaemic preconditioning is not mediated by adenosine in the globally ischaemic isolated rat heart. Cardiovasc Res 1993; 27:663-8.

90. Miura T, Ishimoto R, Sakamoto J, et al. Suppression of reperfusion arrhythmia by ischemic preconditioning in the rat: is it mediated by the adenosine receptor, prostaglandin, or bradykinin receptor? Basic Res Cardiol 1995; 90:240-6.

91. Bugge E, Ytrehus K. Ischaemic preconditioning is protein kinase C dependent but not through stimulation of alpha adrenergic or adenosine receptors in the isolated rat heart. Cardiovasc Res 1995; 29:401-6.

92. Asimakis GK, Inners McBride K, Conti VR. Attenuation of postischaemic dysfunction by ischaemic preconditioning is not mediated by adenosine in the isolated rat heart. Cardiovasc Res 1993; 27:1522-30.

93. Li Y, Kloner RA. The cardioprotective effects of ischemic 'preconditioning' are not mediated by adenosine receptors in rat hearts. Circulation 1993; 87:1642-8.

94. Boutros A, Wang J. Ischemic preconditioning, adenosine and bethanechol protect spontaneously hypertensive isolated rat hearts. J-Pharmacol-Exp-Ther 1995; 275:1148-56 *LHM: This title is currently taken by UCL: Medical Sciences ISSN: 0022-3565.

95. de Jonge R, de Jong JW. Ischemic preconditioning and glucose metabolism during low-flow ischemia: role of the adenosine A1 receptor. Cardiovasc Res 1999; 43:909-18.

96. Dana A, Jonassen AK, Yamashita N, Yellon DM. Adenosine A(1) receptor activation induces delayed preconditioning in rats mediated by manganese superoxide dismutase. Circulation 2000; 101:2841-8.

97. Walker DM, Walker JM, Pugsley WB, Pattison CW, Yellon DM. Preconditioning in isolated superfused human muscle. J Moll Cell Cardiol 1995; 27:1349-57.

98. Htun P, Ito W, Hoefer I, Schaper J, Schaper W. Intramyocardial infusion of FGF-1 mimics ischemic preconditioning in pig myocardium. J Mol Cell Cardiol 1998; 30:867-77.

99. Vogt A, Htun P, Kluge A, Zimmermann R, Schaper W. Insulin-like growth factor-II delays myocardial infarction in experimental coronary artery occlusion. Cardiovasc Res 1997; 33:469-77.

100. Bogoyevitch M, Glennon P, Andersson M, et al. Endothelin-1 and fibroblast growth factors stimulate the mitogen-activated protein kinase signaling cascade in cardiac myocytes. The potential role of the cascade in the integration of two signaling pathways leading to myocyte hypertrophy. J Biol Chem 1994; 269:1110-9.

101. Kitakaze M, Node K, Minamino T, et al. Role of activation of protein kinase C in the infarct size-limiting effect of ischemic preconditioning through activation of ecto-5'-nucleotidase. Circulation 1996; 93:781-791.

102. Liu Y, Cohen MV, Downey JM. Chelerythrine, a highly selective protein kinase C inhibitor, blocks the anti-infarct effect of ischemic preconditioning in rabbit hearts. Cardiovasc Drugs Ther 1994; 8:881-2.

103. Vahlhaus C, Schulz R, Post H, Onallah R, Heusch G. No prevention of ischemic preconditioning by the protein kinase C inhibitor staurosporine in swine. Circ Res 1996; 79:407-414.

104. Vahlhaus C, Schulz R, Post H, Rose J, Heusch G. Prevention of ischemic preconditioning only by combined inhibition of protein kinase C and protein tyrosine kinase in pigs. J Mol Cell Cardiol 1998; 30:197-209.

105. Ping P, Zhang J, Qiu Y, Tang XL, Manchikalapudi S, Bolli R. Repetitive episodes of myocardial ischemia and reperfusion induce translocation of protein kinase C epsilon isoform in conscious rabbits which is associated with late preconditioning against myocardial stunning. Circulation 1996; 94(suppl):I-660 (abstract).

106. Ping P, Zhang J, Qiu Y, et al. Ischemic preconditioning induces selective translocation of protein kinase C isoforms epsilon and eta in the heart of conscious rabbits without subcellular redistribution of total protein kinase C activity. CircRes 1997; 81:404-414.

107. Goldberg M, Zhang HL, Steinberg SF. Hypoxia alters the subcellular distribution of protein kinase C isoforms in neonatal rat ventricular myocytes. J Clin Invest 1997; 99:55-61.

108. Armstrong S, Ganote CE. Preconditioning of isolated rabbit cardiomyocytes: effects of glycolytic blockade, phorbol esters, and ischaemia. Cardiovasc Res 1994; 28:1700-6.

109. Gray MO, Karliner JS, Mochly-Rosen D. A selective epsilon-protein kinase C antagonist inhibits protection of cardiac myocytes from hypoxia-induced cell death. J Biol Chem 1997; 272:30945-30951.

110. Baines C, Cohen M, Downey J. Protein tyrosine kinase inhibitor, genistein, blocks preconditioning in isolated rabbit hearts. Circulation 1996; 94 (suppl):I-661 (abstract).

111. Dana A, Baxter GF, Yellon DM. Both protein kinase C and protein tyrosine kinase mediate adenosine induced delayed cardioprotection in rabbits. Circulation 1997; 96:I-312 (abstract).

112. Baines C, Wang L, Cohen M, Downey J. Protein tyrosine kinase is downstream of protein kinase C for ischemic preconditioning's anti-infarct effect in the rabbit heart. J Mol Cell Cardiol 1998; 30:383-392.

113. Sugden P, Clerk A. "Stress-responsive" mitogen-activated protein kinases (c-Jun N-terminal kinases and p38 mitogen-activated protein kinases) in the myocardium. Circ Res 1998; 83:345-52.

114. Clerk A, Fuller SJ, Michael A, Sugden PH. Stimulation of "stress-regulated" mitogen-activated protein kinases (stress-activated protein kinases/c-Jun N-terminal kinases and p38-mitogen-activated protein kinases) in perfused rat hearts by oxidative and other stresses. J Biol Chem 1998; 273:7228-34.

115. Sugden P, Clerk A. Regulation of the ERK subgroup of MAP kinase cascades through G protein-coupled receptors. Cell Signal 1997; 9:337-51.

116. Zhou J, Li DX. Effects of tetrahydroberberine on isoproterenol-stimulated mitochondrial 45Ca uptake in rabbit myocardia. J Tongji Med Univ 1993; 13:199-201.

117. Lee JD, Ulevitch RJ, Han J. Primary structure of BMK1: a new mammalian map kinase. Biochem Biophys Res Commun 1995; 213:715-24.

118. Abe MK, Kartha S, Karpova AY, et al. Hydrogen peroxide activates extracellular signal-regulated kinase via protein kinase C, Raf-1, and MEK1. Am J Respir Cell Mol Biol 1998; 18:562-569.

119. Ping P, Zhang J, Cao X, et al. PKC-dependent activation of p44/p42 MAPKs during myocardial ischemia- reperfusion in conscious rabbits. Am J Physiol 1999; 276:H1468-81.

120. Seko Y, Tobe K, Ueki K, Kadowaki T, Yazaki Y. Hypoxia and hypoxia/reoxygenation activate Raf-1, mitogen-activated protein kinase kinase, mitogen-activated protein kinases, and S6 kinase in cultured rat cardiac myocytes. Circ Res 1996; 78:82-90.

121. Knight RJ, Buxton DB. Stimulation of c-Jun kinase and mitogen-activated protein kinase by ischemia and reperfusion in the perfused rat heart. Biochem Biophys Res Commun 1996; 218:83-8.

122. Bogoyevitch MA, Gillespie-Brown J, Ketterman AJ, et al. Stimulation of the stress-activated mitogen-activated protein kinase subfamilies in perfused heart. p38/RK mitogen-activated protein kinases and c-Jun N-terminal kinases are activated by ischaemia/reperfusion. Circ Res 1996; 79:162-73.

123. Yamauchi J, Nagao M, Kaziro Y, Itoh H. Activation of p38 mitogen-activated protein kinase by signaling through G protein-coupled receptors. Involvement of Gbetagamma and Galphaq/11 subunits. J Biol Chem 1997; 272:27771-7.

124. Maulik N, Watanabe M, Zu YL, et al. Ischemic preconditioning triggers the activation of MAP kinases and MAPKAP kinase 2 in rat hearts. FEBS-Lett 1996; 396:233-7.

125. Weinbrenner C, Liu G, Cohen MV, Downey JM. Phosphorylation of tyrosine 182 of p38 mitogen-activated protein kinase correlates with the protection of preconditioning in the rabbit heart. J Mol Cell Cardiol 1997; 29:2383-91.

126. Saurin AT, Martin JL, Heads RJ, et al. The role of differential activation of p38-mitogen-activated protein kinase in preconditioned ventricular myocytes. Faseb J 2000; 14:2237-46.

127. Ma XL, Kumar S, Gao F, et al. Inhibition of p38 mitogen-activated protein kinase decreases cardiomyocyte apoptosis and improves cardiac function after myocardial ischemia and reperfusion. Circulation 1999; 99:1685-91.

128. Mackay K, Mochly-Rosen D. An inhibitor of p38 mitogen-activated protein kinase protects neonatal cardiac myocytes from ischemia. J Biol Chem 1999; 274:6272-9.

129. Nagarkatti DS, Sha'afi RI. Role of p38 MAP kinase in myocardial stress. J Mol Cell Cardiol 1998; 30:1651-64.

130. Sato M, Cordis GA, Maulik N, Das DK. SAPKs regulation of ischemic preconditioning. Am J Physiol Heart Circ Physiol 2000; 279:H901-7.

131. Yue TL, Wang C, Gu JL, et al. Inhibition of extracellular signal-regulated kinase enhances Ischemia/Reoxygenation-induced apoptosis in cultured cardiac myocytes and exaggerates reperfusion injury in isolated perfused heart. Circ Res 2000; 86:692-9.

132. Omura T, Yoshiyama M, Shimada T, et al. Activation of mitogen-activated protein kinases in in vivo ischemia/reperfused myocardium in rats. J Mol Cell Cardiol 1999; 31:1269-79.

133. Turner N, Xia F, Azhar G, Zhang X, Liu L, Wei J. Oxidative stress induces DNA fragmentation and caspase activation via the c-Jun NH2-terminal kinase pathway in H9c2 cardiac muscle cells. J Mol Cell Cardiol 1998; 30:1789-801.

134. Punn A, Mockridge JW, Farooqui S, Marber MS, Heads RJ. Sustained activation of p42/p44 mitogen-activated protein kinase during recovery from simulated ischaemia mediates adaptive cytoprotection in cardiomyocytes. Biochem J 2000; 350 Pt 3:891-9.

135. Sakamoto K, Urushidani T, Nagao T. Translocation of HSP27 to sarcomere induced by ischemic preconditioning in isolated rat hearts. Biochem Biophys Res Commun 2000; 269:137-42.

136. Nakano A, Baines CP, Kim SO, et al. Ischemic preconditioning activates MAPKAPK2 in the isolated rabbit heart: evidence for involvement of p38 MAPK. Circ Res 2000; 86:144-51.

137. Maulik N, Yoshida T, Zu YL, Sato M, Banerjee A, Das DK. Ischemic preconditioning triggers tyrosine kinase signaling: a potential role for MAPKAP kinase 2. Am J Physiol 1998; 275:H1857-64.

138. Barancik M, Htun P, Strohm C, Kilian S, Schaper W. Inhibition of the cardiac p38-MAPK pathway by SB203580 delays ischemic cell death. J Cardiovasc Pharmacol 2000; 35:474-83.

139. Mocanu MM, Baxter GF, Yue Y, Critz SD, Yellon DM. The p38 MAPK inhibitor, SB203580, abrogates ischaemic preconditioning in rat heart but timing of administration is critical. Basic Res Cardiol 2000; 95:472-8.

140. Strohm C, Barancik T, Bruhl ML, Kilian SA, Schaper W. Inhibition of the ER-kinase cascade by PD98059 and UO126 counteracts ischemic preconditioning in pig myocardium. J Cardiovasc Pharmacol 2000; 36:218-29.

141. Kim SO, Baines CP, Critz SD, et al. Ischemia induced activation of heat shock protein 27 kinases and casein kinase 2 in the preconditioned rabbit heart. Biochem Cell Biol 1999; 77:559-67.

142. Behrends M, Schulz R, Post H, et al. Inconsistent relation of MAPK activation to infarct size reduction by ischemic preconditioning in pigs. Am J Physiol Heart Circ Physiol 2000; 279:H1111-9.

143. Dana A, Skarli M, Papakrivopoulou J, Yellon DM. Adenosine A(1) receptor induced delayed preconditioning in rabbits: induction of p38 mitogen-activated protein kinase activation and Hsp27 phosphorylation via a tyrosine kinase- and protein kinase C-dependent mechanism. Circ Res 2000; 86:989-97.

144. Eaton P, Awad WI, Miller JI, Hearse DJ, Shattock MJ. Ischemic preconditioning: a potential role for constitutive low molecular weight stress protein translocation and phosphorylation? J Mol Cell Cardiol 2000; 32:961-71.

145. Carroll R, Yellon DM. Delayed cardioprotection in a human cardiomyocyte-derived cell line: the role of adenosine, p38MAP kinase and mitochondrial KATP. Basic Res Cardiol 2000; 95:243-9.

146. Mockridge JW, Punn A, Latchman DS, Marber MS, Heads RJ. PKC-dependent delayed metabolic preconditioning is independent of transient MAPK activation. Am J Physiol Heart Circ Physiol 2000; 279:H492-501.

147. Li RC, Ping P, Zhang J, et al. PKCepsilon modulates NF-kappaB and AP-1 via mitogen-activated protein kinases in adult rabbit cardiomyocytes. Am J Physiol Heart Circ Physiol 2000; 279:H1679-89.

148. Erhardt P, Schremser EJ, Cooper GM. B-Raf inhibits programmed cell death downstream of cytochrome c release from mitochondria by activating the MEK/Erk pathway. Mol Cell Biol 1999; 19:5308-15.

149. Frodin M, Gammeltoft S. Role and regulation of 90 kDa ribosomal S6 kinase (RSK) in signal transduction. Mol Cell Endocrinol 1999; 151:65-77.

150. Bonni A, Brunet A, West AE, Datta SR, Takasu MA, Greenberg ME. Cell survival promoted by the Ras-MAPK signaling pathway by transcription-dependent and -independent mechanisms. Science 1999; 286:1358-62.

151. Takahashi E, Abe J, Gallis B, et al. p90(RSK) is a serum-stimulated Na+/H+ exchanger isoform-1 kinase. Regulatory phosphorylation of serine 703 of Na+/H+ exchanger isoform-1. J Biol Chem 1999; 274:20206-14.

152. Scheid MP, Schubert KM, Duronio V. Regulation of bad phosphorylation and association with Bcl-x(L) by the MAPK/Erk kinase. J Biol Chem 1999; 274:31108-13.

153. Bertolotto C, Maulon L, Filippa N, Baier G, Auberger P. Protein kinase C theta and epsilon promote T-cell survival by a rsk-dependent phosphorylation and inactivation of BAD. J Biol Chem 2000; 275:37246-50.

154. Kato Y, Tapping RI, Huang S, Watson MH, Ulevitch RJ, Lee JD. Bmk1/Erk5 is required for cell proliferation induced by epidermal growth factor. Nature 1998; 395:713-6.

155. Kato Y, Kravchenko VV, Tapping RI, Han J, Ulevitch RJ, Lee JD. BMK1/ERK5 regulates serum-induced early gene expression through transcription factor MEF2C. Embo J 1997; 16:7054-66.

156. Assefa Z, Vantieghem A, Garmyn M, et al. p38 mitogen-activated protein kinase regulates a novel, caspase-independent pathway for the mitochondrial cytochrome c release in ultraviolet B radiation-induced apoptosis. J Biol Chem 2000; 275:21416-21.

157. Hsu SC, Gavrilin MA, Tsai MH, Han J, Lai MZ. p38 mitogen-activated protein kinase is involved in Fas ligand expression. J Biol Chem 1999; 274:25769-76.

158. Wang Y, Huang S, Sah VP, et al. Cardiac muscle cell hypertrophy and apoptosis induced by distinct members of the p38 mitogen-activated protein kinase family. J Biol Chem 1998; 273:2161-8.

159. Nemoto S, Xiang J, Huang S, Lin A. Induction of apoptosis by SB202190 through inhibition of p38beta mitogen-activated protein kinase. J Biol Chem 1998; 273:16415-20.

160. Fuchs SY, Adler V, Pincus MR, Ronai Z. MEKK1/JNK signaling stabilizes and activates p53. Proc Natl Acad Sci U S A 1998; 95:10541-6.

161. Webster KA, Discher DJ, Kaiser S, Hernandez O, Sato B, Bishopric NH. Hypoxia-activated apoptosis of cardiac myocytes requires reoxygenation or a pH shift and is independent of p53. J Clin Invest 1999; 104:239-52.

162. Li C, Browder W, Kao R. Early activation of transcription factor NF-kappaB during ischemia in perfused rat heart. Am J Physiol 1999; 276:H543-52.

163. Xuan Y, Tang X, Banerjee S, et al. Nuclear factor-kappaB plays an essential role in the late phase of ischemic preconditioning in conscious rabbits. Circ Res 1999; 84:1095-109.

164. Ritchie ME. Nuclear factor-kappaB is selectively and markedly activated in humans with unstable angina pectoris. Circulation 1998; 98:1707-13.

165. Hattori Y, Nakanishi N, Kasai K. Role of nuclear factor kappa B in cytokine-induced nitric oxide and tetrahydrobiopterin synthesis in rat neonatal cardiac myocytes. J Mol Cell Cardiol 1997; 29:1585-92.

166. Nie Z, Mei Y, Ford M, et al. Oxidative stress increases A1 adenosine receptor expression by activating nuclear factor kappa B. Mol Pharmacol 1998; 53:663-9.

167. Zechner D, Craig R, Hanford DS, McDonough PM, Sabbadini RA, Glembotski CC. MKK6 activates myocardial cell NF-kappaB and inhibits apoptosis in a p38 mitogen-activated protein kinase-dependent manner. J Biol Chem 1998; 273:8232-9.

168. Craig R, Larkin A, Mingo AM, et al. p38 MAPK and NF-kappa B collaborate to induce interleukin-6 gene expression and release. Evidence for a cytoprotective autocrine signaling pathway in a cardiac myocyte model system. J Biol Chem 2000; 275:23814-24.

169. Kan H, Xie Z, Finkel MS. TNF-alpha enhances cardiac myocyte NO production through MAP kinase-mediated NF-kappaB activation. Am J Physiol 1999; 277:H1641-6.

170. Kan H, Xie Z, Finkel MS. Norepinephrine-stimulated MAP kinase activity enhances cytokine-induced NO production by rat cardiac myocytes. Am J Physiol 1999; 276:H47-52.

171. Adderley SR, Fitzgerald DJ. Oxidative damage of cardiomyocytes is limited by extracellular regulated kinases 1/2-mediated induction of cyclooxygenase-2. J Biol Chem 1999; 274:5038-46.

172. Han J, Molkentin JD. Regulation of MEF2 by p38 MAPK and its implication in cardiomyocyte biology. Trends Cardiovasc Med 2000; 10:19-22.

173. Korb H, Hoeft A, Hunneman DH, et al. Changes in myocardial substrate utilisation and protection of ischemic stressed myocardium by oxfenicine [(S)-4-hydroxyphenylglycine]. Naunyn-Schmiedebergs-Arch-Pharmacol 1984; 327:70-4 issn: 0028-1298.

174. Thorburn J, Carlson M, Mansour SJ, Chien KR, Ahn NG, Thorburn A. Inhibition of a signaling pathway in cardiac muscle cells by active mitogen-activated protein kinase kinase. Mol Biol Cell 1995; 6:1479-90.

175. Shimizu T, Kinugawa K, Yao A, et al. Platelet-derived growth factor induces cellular growth in cultured chick ventricular myocytes. Cardiovasc Res 1999; 41:641-53.

176. Paradis P, MacLellan WR, Belaguli NS, Schwartz RJ, Schneider MD. Serum response factor mediates AP-1-dependent induction of the skeletal alpha-actin promoter in ventricular myocytes. J Biol Chem 1996; 271:10827-33.

177. Kovacic-Milivojevic B, Wong VS, Gardner DG. Selective regulation of the atrial natriuretic peptide gene by individual components of the activator protein-1 complex. Endocrinology 1996; 137:1108-17.

178. Thornton J, Striplin S, Liu GS, et al. Inhibition of protein synthesis does not block myocardial protection afforded by preconditioning. Am J Physiol 1990; 259:H1822-5.

179. Rizvi A, Tang XL, Qiu Y, et al. Increased protein synthesis is necessary for the development of late preconditioning against myocardial stunning. Am J Physiol 1999; 277:H874-84.

180. Light P, Sabir A, Allen B, Walsh M, French R. Protein kinase C-induced changes in the stoichiometry of ATP binding activate cardiac ATP-sensitive K+ channels. Circ Res 1996; 79:399-406.

181. Speechly Dick ME, Grover GJ, Yellon DM. Does ischemic preconditioning in the human involve protein kinase C and the ATP-dependent K+ channel? Studies of contractile function after simulated ischemia in an atrial in vitro model. Circ Res 1995; 77:1030-5.

182. Mizumura T, Nithipatikom K, Gross GJ. Bimakalim, an ATP-sensitive potassium channel opener, mimics the effects of ischemic preconditioning to reduce infarct size, adenosine release, and neutrophil function in dogs. Circulation 1995; 92:1236-45.

183. Ferdinandy P, Szilvassy Z, Koltai M, Dux L. Ventricular overdrive pacing-induced preconditioning and no-flow ischemia-induced preconditioning in isolated working rat hearts. J Cardiovasc Pharmacol 1995; 25:97-104.

184. Armstrong SC, Liu GS, Downey JM, Ganote CE. Potassium channels and preconditioning of isolated rabbit cardiomyocytes: effects of glyburide and pinacidil. J Mol Cell Cardiol 1995; 27:1765-74.

185. Walsh RS, Tsuchida A, Daly JJ, Thornton JD, Cohen MV, Downey JM. Ketamine-xylazine anaesthesia permits a KATP channel antagonist to attenuate preconditioning in rabbit myocardium. Cardiovasc Res 1994; 28:1337-41.

186. Auchampach JA, Grover GJ, Gross GJ. Blockade of ischaemic preconditioning in dogs by the novel ATP dependent potassium channel antagonist sodium 5-hydroxydecanoate. Cardiovasc Res 1992; 26:1054-62.

187. Koning MM, Gho BC, van Klaarwater E, Opstal RL, Duncker DJ, Verdouw PD. Rapid ventricular pacing produces myocardial protection by nonischemic activation of KATP channels. Circulation 1996; 93:178-86.

188. Schulz R, Rose J, Heusch G. Involvement of activation of ATP-dependent potassium channels in ischemic preconditioning in swine. Am J Physiol 1994; 267:H1341-52.

189. Yao Z, Gross G. Effects of KATP channel opener bimakalim on coronary blood flow, monophasic action potential duration, and infarct size in dogs. Circulation 1994; 89:1769-1775.

190. Grover GJ. Pharmacology of ATP-sensitive potassium channel (KATP) openers in models of myocardial ischemia and reperfusion. Can J Physiol Pharmacol 1997; 75:309-15.

191. Liu Y, Sato T, O'Rourke B, Marban E. Mitochondrial ATP-dependent potassium channels: novel effectors of cardioprotection? Circulation 1998; 97:2463-2469.

192. Birincioglu M, Yang XM, Critz SD, Cohen MV, Downey JM. S-T segment voltage during sequential coronary occlusions is an unreliable marker of preconditioning. Am J Physiol 1999; 277:H2435-41.

193. Baines C, Liu G, Birincioglu M, Critz S, Cohen M, Downey J. Ischemic preconditioning depends on interaction between mitochondrial KATP channels and actin cytoskeleton. Am J Physiol 1999; 276:H1361-8.

194. Golenhofen N, Htun P, Ness W, Koob R, Schaper W, Drenckhahn D. Binding of the stress protein alpha B-crystallin to cardiac myofibrils correlates with the degree of myocardial damage during ischemia/reperfusion in vivo. J Mol Cell Cardiol 1999; 31:569-80.

195. Golenhofen N, Ness W, Koob R, Htun P, Schaper W, Drenckhahn D. Ischemia-induced phosphorylation and translocation of stress protein alpha B-crystallin to Z lines of myocardium. Am J Physiol 1998; 274:H1457-64.

196. Eaton P, Awad WI, Miller JI, Hearse DJ, Shattock MJ. Ischemic preconditioning: a potential role for constitutive low molecular weight stress protein translocation and phosphorylation? J Mol Cell Cardiol 2000; 32:961-71.

197. Landry J, Huot J. Modulation of actin dynamics during stress and physiological stimulation by a signaling pathway involving p38 MAP kinase and heat-shock protein 27. Biochem Cell Biol 1995; 73:703-7.

198. Knauf U, Jakob U, Engel K, Buchner J, Gaestel M. Stress- and mitogen-induced phosphorylation of the small heat shock protein Hsp25 by MAPKAP kinase 2 is not essential for chaperone properties and cellular thermoresistance. Embo J 1994; 13:54-60.

199. Sakamoto K, Urushidani T, Nagao T. Translocation of HSP27 to cytoskeleton by repetitive hypoxia-reoxygenation in the rat myoblast cell line, H9c2. Biochem Biophys Res Commun 1998; 251:576-9.

200. Huot J, Houle F, Spitz DR, Landry J. HSP27 phosphorylation-mediated resistance against actin fragmentation and cell death induced by oxidative stress. Cancer Res 1996; 56:273-9.

201. Guay J, Lambert H, Gingras-Breton G, Lavoie JN, Huot J. Regulation of actin filament dynamics by p38 map kinase-mediated phosphorylation of heat shock protein 27. J Cell Sci 1997; 110:357-68.

202. Armstrong SC, Delacey M, Ganote CE. Phosphorylation state of hsp27 and p38 MAPK during preconditioning and protein phosphatase inhibitor protection of rabbit cardiomyocytes. J Mol Cell Cardiol 1999; 31:555-67.

203. Bernardo NL, Okubo S, Maaieh MM, Wood MA, Kukreja RC. Delayed preconditioning with adenosine is mediated by opening of ATP-sensitive K(+) channels in rabbit heart. Am J Physiol 1999; 277:H128-35.

204. Mei D, Elliot G, Gross G. KATP channels mediate late preconditioning against infarction produced by monophosphoryl lipid A. Am J Physiol 1996; 271:H2723-9.

205. Baxter GF, Yellon DM. KATP channel blockade abolishes delayed anti-ischaemic actions of transient adenosine A1 receptor activation. J Mol Cell Cardiol 1998; 30:A10 (abstract).

206. Pell TJ, Yellon DM, Goodwin RW, Baxter GF. Myocardial ischemic tolerance following heat stress is abolished by ATP-sensitive potassium channel blockade. Cardiovasc Drugs Ther 1997; 11:679-86.

207. Hoag JB, Qian YZ, Nayeem MA, D'Angelo M, Kukreja RC. ATP-sensitive potassium channel mediates delayed ischemic protection by heat stress in rabbit heart. Am J Physiol 1997; 273:H2458-64.

208. Shinbo A, Iijima T. Potentiation by nitric oxide of the ATP-sensitive K+ current induced by K+ channel openers in guinea-pig ventricular cells. Br J Pharmacol 1997; 120:1568-74.

209. Imagawa J, Yellon DM, Baxter GF. Pharmacological evidence that inducible nitric oxide synthase is a mediator of delayed preconditioning. Br J Pharmacol 1999; 126:701-8.

210. Yamashita N, Hoshida s, Taniguchi N, Kuzuya T, Hori M. Whole-Body Hyperthermia Provides Biphasic Cardioprotection Against Ischemia/Reperfusion Injury in the Rat. Circulation 1998; 98:1414-21.

211. Yamashita N, Nishida M, Hoshida S, et al. Induction of manganese superoxide dismutase in rat cardiac myocytes increases tolerance to hypoxia 24 hours after preconditioning. J Clin Invest 1994; 94:2193-9.

212. Benjamin I, McMillan D. Stress (heat shock) proteins: molecular chaperones in cardiovascular biology and disease. Circ Res 1998; 83:117-32.

213. Uehara T, Kaneko M, Tanaka S, Okuma Y, Nomura Y. Possible involvement of p38 MAP kinase in HSP70 expression induced by hypoxia in rat primary astrocytes. Brain Res 1999; 823:226-30.

214. Ahn JH, Ko YG, Park WY, Kang YS, Chung HY, Seo JS. Suppression of ceramide-mediated apoptosis by HSP70. Mol Cells 1999; 9:200-6.

215. Gabai VL, Meriin AB, Yaglom JA, Volloch VZ, Sherman MY. Role of Hsp70 in regulation of stress-kinase JNK: implications in apoptosis and aging. FEBS Lett 1998; 438:1-4.

216. Sheikh-Hamad D, Di Mari J, Suki WN, Safirstein R, Watts BA, 3rd, Rouse D. p38 kinase activity is essential for osmotic induction of mRNAs for HSP70 and transporter for organic solute betaine in Madin-Darby canine kidney cells. J Biol Chem 1998; 273:1832-7.

217. Suzuki K, Sawa Y, Kagisaki K, et al. Reduction in myocardial apoptosis associated with overexpression of heat shock protein 70. Basic Res Cardiol 2000; 95:397-403.

218. Brar BK, Stephanou A, Wagstaff MJ, et al. Heat shock proteins delivered with a virus vector can protect cardiac cells against apoptosis as well as against thermal or hypoxic stress. J Mol Cell Cardiol 1999; 31:135-46.

219. Marber MS, Latchman DS, Walker JM, Yellon DM. Cardiac stress protein elevation 24 hours after brief ischemia or heat stress is associated with resistance to myocardial infarction. Circulation 1993; 88:1264-72.

220. Heads RJ, Latchman DS, Yellon DM. Stable high level expression of a transfected human HSP70 gene protects a heart-derived muscle cell line against thermal stress. J Mol Cell Cardiol 1994; 26:695-9.

221. Marber MS, Mestril R, Chi SH, Sayen MR, Yellon DM, Dillmann WH. Overexpression of the rat inducible 70-kD heat stress protein in a transgenic mouse increases the resistance of the heart to ischemic injury. J Clin Invest 1995; 95:1446-56.

222. Cornelussen R, Garnier A, van der Vusse G, Reneman R, Snoeckx L. Biphasic effect of heat stress pretreatment on ischemic tolerance of isolated rat hearts. J Mol Cell Cardiol 1998; 30:365-72.

223. Stancato LF, Silverstein AM, Owens-Grillo JK, Chow YH, Jove R, Pratt WB. The hsp90-binding antibiotic geldanamycin decreases Raf levels and epidermal growth factor signaling without disrupting formation of signaling complexes or reducing the specific enzymatic activity of Raf kinase. J Biol Chem 1997; 272:4013-20.

224. Grammatikakis N, Lin JH, Grammatikakis A, Tsichlis PN, Cochran BH. p50(cdc37) acting in concert with Hsp90 is required for Raf-1 function. Mol Cell Biol 1999; 19:1661-72.

225. Garcia-Cardena G, Fan R, Shah V, et al. Dynamic activation of endothelial nitric oxide synthase by Hsp90. Nature 1998; 392:821-4.

226. Pandey P, Saleh A, Nakazawa A, et al. Negative regulation of cytochrome c-mediated oligomerization of apaf-1 and activation of procaspase-9 by heat shock protein 90. Embo J 2000; 19:4310-22.

227. Nayeem MA, Hess ML, Qian YZ, Loesser KE, Kukreja RC. Delayed preconditioning of cultured adult rat cardiac myocytes: role of 70- and 90-kDa heat stress proteins. Am J Physiol 1997; 273:H861-8.

228. Moncada S, Palmer RM, Higgs EA. Nitric oxide: physiology, pathophysiology, and pharmacology. Pharmacol Rev 1991; 43:109-42.

229. Gallis B, Corthals GL, Goodlett DR, et al. Identification of flow-dependent endothelial nitric-oxide synthase phosphorylation sites by mass spectrometry and regulation of phosphorylation and nitric oxide production by the phosphatidylinositol 3-kinase inhibitor LY294002. J Biol Chem 1999; 274:30101-8.

230. Guo Y, Jones WK, Xuan YT, et al. The late phase of ischemic preconditioning is abrogated by targeted disruption of the inducible NO synthase gene. Proc Natl Acad Sci U S A 1999; 96:11507-12.

231. Patel VC, Yellon DM, Singh KJ, Neild GH, Woolfson RG. Inhibition of nitric oxide limits infarct size in the in situ rabbit heart. Biochem-Biophys-Res-Commun 1993; 194:234-8 issn: 0006-291x.

232. Taimor G, Hofstaetter B, Piper HM. Apoptosis induction by nitric oxide in adult cardiomyocytes via cGMP-signaling and its impairment after simulated ischemia. Cardiovasc Res 2000; 45:588-94.

233. Andrew PJ, Mayer B. Enzymatic function of nitric oxide synthases. Cardiovasc Res 1999; 43:521-31.

234. Abu-Soud HM, Stuehr DJ. Nitric oxide synthases reveal a role for calmodulin in controlling electron transfer. Proc Natl Acad Sci U S A 1993; 90:10769-72.

235. Abu-Soud HM, Yoho LL, Stuehr DJ. Calmodulin controls neuronal nitric-oxide synthase by a dual mechanism. Activation of intra- and interdomain electron transfer. J Biol Chem 1994; 269:32047-50.

236. Abu-Soud HM, Ichimori K, Presta A, Stuehr DJ. Electron transfer, oxygen binding, and nitric oxide feedback inhibition in endothelial nitric-oxide synthase. J Biol Chem 2000; 275:17349-57.

237. Gorren AC, Schrammel A, Schmidt K, Mayer B. Thiols and neuronal nitric oxide synthase: complex formation, competitive inhibition, and enzyme stabilization. Biochemistry 1997; 36:4360-6.

238. Gorren AC, List BM, Schrammel A, et al. Tetrahydrobiopterin-free neuronal nitric oxide synthase: evidence for two identical highly anticooperative pteridine binding sites. Biochemistry 1996; 35:16735-45.

239. Brenman JE, Chao DS, Gee SH, et al. Interaction of nitric oxide synthase with the postsynaptic density protein PSD-95 and alpha1-syntrophin mediated by PDZ domains. Cell 1996; 84:757-67.

240. Garcia-Cardena G, Oh P, Liu J, Schnitzer JE, Sessa WC. Targeting of nitric oxide synthase to endothelial cell caveolae via palmitoylation: implications for nitric oxide signaling. Proc Natl Acad Sci U S A 1996; 93:6448-53.

241. Ghosh S, Gachhui R, Crooks C, Wu C, Lisanti MP, Stuehr DJ. Interaction between caveolin-1 and the reductase domain of endothelial nitric-oxide synthase. Consequences for catalysis. J Biol Chem 1998; 273:22267-71.

242. Laine R, de Montellano PR. Neuronal nitric oxide synthase isoforms alpha and mu are closely related calpain-sensitive proteins. Mol Pharmacol 1998; 54:305-12.

243. Sumeray MS, Rees DD, Yellon DM. Infarct size and nitric oxide synthase in murine myocardium. J Mol Cell Cardiol 2000; 32:35-42.

244. Inoue N, Venema RC, Sayegh HS, Ohara Y, Murphy TJ, Harrison DG. Molecular regulation of the bovine endothelial cell nitric oxide synthase by transforming growth factor-beta 1. Arterioscler Thromb Vasc Biol 1995; 15:1255-61.

245. Tsukahara H, Ende H, Magazine HI, Bahou WF, Goligorsky MS. Molecular and functional characterization of the non-isopeptide-selective ETB receptor in endothelial cells. Receptor coupling to nitric oxide synthase. J Biol Chem 1994; 269:21778-85.

246. Dong Z, Qi X, Xie K, Fidler IJ. Protein tyrosine kinase inhibitors decrease induction of nitric oxide synthase activity in lipopolysaccharide-responsive and lipopolysaccharide-nonresponsive murine macrophages. J Immunol 1993; 151:2717-24.

247. Bugge E, Ytrehus K. Endothelin-1 can reduce infarct size through protein kinase C and KATP channels in the isolated rat heart. Cardiovasc Res 1996; 32:920-9.

248. Ray PS, Estrada-Hernandez T, Sasaki H, Zhu L, Maulik N. Early effects of hypoxia/reoxygenation on VEGF, ang-1, ang-2 and their receptors in the rat myocardium: implications for myocardial angiogenesis. Mol Cell Biochem 2000; 213:145-53.

249. McQuillan LP, Leung GK, Marsden PA, Kostyk SK, Kourembanas S. Hypoxia inhibits expression of eNOS via transcriptional and posttranscriptional mechanisms. Am J Physiol 1994; 267:H1921-7.

250. Zhang J, Patel JM, Li YD, Block ER. Proinflammatory cytokines downregulate gene expression and activity of constitutive nitric oxide synthase in porcine pulmonary artery endothelial cells. Res Commun Mol Pathol Pharmacol 1997; 96:71-87.

251. Boger RH, Bode-Boger SM. Asymmetric dimethylarginine, derangements of the endothelial nitric oxide synthase pathway, and cardiovascular diseases. Semin Thromb Hemost 2000; 26:539-45.

252. MacAllister RJ, Parry H, Kimoto M, et al. Regulation of nitric oxide synthesis by dimethylarginine dimethylaminohydrolase. Br J Pharmacol 1996; 119:1533-40.

253. Ito A, Tsao PS, Adimoolam S, Kimoto M, Ogawa T, Cooke JP. Novel mechanism for endothelial dysfunction: dysregulation of dimethylarginine dimethylaminohydrolase. Circulation 1999; 99:3092-5.

254. Brahmajothi MV, Campbell DL. Heterogeneous basal expression of nitric oxide synthase and superoxide dismutase isoforms in mammalian heart : implications for mechanisms governing indirect and direct nitric oxide-related effects. Circ Res 1999; 85:575-87.

255. Koning MM, Gho BC, van Klaarwater E, Duncker DJ, Verdouw PD. Endocardial and epicardial infarct size after preconditioning by a partial coronary artery occlusion without intervening reperfusion. Importance of the degree and duration of flow reduction. Cardiovasc Res 1995; 30:1017-27.

256. Kemper AJ, Force T, Perkins L, Gilfoil M, Parisi AF. In vivo prediction of the transmural extent of experimental acute myocardial infarction using contrast echocardiography. J Am Coll Cardiol 1986; 8:143-9.

257. Roberts CS, Maclean D, Braunwald E, Maroko PR, Kloner RA. Topographic changes in the left ventricle after experimentally induced myocardial infarction in the rat. Am J Cardiol 1983; 51:872-6.

258. Xu KY, Huso DL, Dawson TM, Bredt DS, Becker LC. Nitric oxide synthase in cardiac sarcoplasmic reticulum. Proc Natl Acad Sci U S A 1999; 96:657-62.

259. Marrero MB, Venema VJ, Ju H, et al. Endothelial nitric oxide synthase interactions with G-protein-coupled receptors. Biochem J 1999; 343 Pt 2:335-40.

260. Prabhakar P, Thatte HS, Goetz RM, Cho MR, Golan DE, Michel T. Receptor-regulated translocation of endothelial nitric-oxide synthase. J Biol Chem 1998; 273:27383-8.

261. Michell BJ, Griffiths JE, Mitchelhill KI, et al. The Akt kinase signals directly to endothelial nitric oxide synthase. Curr Biol 1999; 9:845-8.

262. Fulton D, Gratton JP, McCabe TJ, et al. Regulation of endothelium-derived nitric oxide production by the protein kinase Akt. Nature 1999; 399:597-601.

263. Woolfson RG, Patel VC, Neild GH, Yellon DM. Inhibition of nitric oxide synthesis reduces infarct size by an adenosine-dependent mechanism. Circulation 1995; 91:1545-51.

264. Weselcouch EO, Baird AJ, Sleph P, Grover GJ. Inhibition of nitric oxide synthesis does not affect ischemic preconditioning in isolated perfused rat hearts. Am J Physiol 1995; 268:H242-9.

265. Lu HR, Remeysen P, De Clerck F. Does the antiarrhythmic effect of ischemic preconditioning in rats involve the L-arginine nitric oxide pathway? J-Cardiovasc-Pharmacol 1995; 25:524-30.

266. Vegh A, Szekeres L, Parratt JR. Preconditioning of the ischaemic myocardium; involvement of the L-arginine nitric oxide pathway. Br J Pharmacol 1992; 107:648-52.

267. Lochner A, Marais E, Genade S, Moolman JA. Nitric oxide: a trigger for classic preconditioning? Am J Physiol Heart Circ Physiol 2000; 279:H2752-65.

268. Buxton IL, Cheek DJ, Eckman D, Westfall DP, Sanders KM, Keef KD. NG-nitro L-arginine methyl ester and other alkyl esters of arginine are muscarinic receptor antagonists. Circ Res 1993; 72:387-95.

269. Bolli R, Manchikalapudi S, Tang XL, et al. The protective effect of late preconditioning against myocardial stunning in conscious rabbits is mediated by nitric oxide synthase. Evidence that nitric oxide acts as both a trigger and as a mediator of the late phase of ischemic preconditioning. Circ res 1997; 81:1094-107.

270. Qiu Y, Rizvi A, Tang XL, et al. Nitric oxide triggers late preconditioning against myocardial infarction in conscious rabbits. Am J Physiol 1997; 273:H2931-6.

271. Takano H, Manchikalapudi S, Tang X, et al. Nitric oxide synthase is the mediator of late preconditioning against myocardial infarction in conscious rabbits. Circulation 1998; 98:441-9.

272. Xi L, Jarrett N, Hess M, Kukreja R. Essential role of inducible nitric oxide synthase in monophosphoryl lipid A-induced late cardioprotection: evidence from pharmacological inhibition and gene knockout mice. Circulation 1999; 99:2157-63.

273. Ping P, Takano H, Zhang J, et al. Isoform-selective activation of protein kinase C by nitric oxide in the heart of conscious rabbits: a signaling mechanism for both nitric oxide-induced and ischemia-induced preconditioning. Circ Res 1999; 84:587-604.

274. Baker CS, Rimoldi O, Camici PG, et al. Repetitive myocardial stunning in pigs is associated with the increased expression of inducible and constitutive nitric oxide synthases. Cardiovasc Res 1999; 43:685-97.

275. Bhagat K, Hingorani AD, Palacios M, Charles IG, Vallance P. Cytokine-induced venodilatation in humans in vivo: eNOS masquerading as iNOS. Cardiovasc Res 1999; 41:754-64.

276. Baines CP, Wang L, Cohen MV, Downey JM. Myocardial protection by insulin is dependent on phospatidylinositol 3-kinase but not protein kinase C or KATP channels in the isolated rabbit heart. Basic Res Cardiol 1999; 94:188-98.

277. Zeng G, Nystrom FH, Ravichandran LV, et al. Roles for insulin receptor, PI3-kinase, and Akt in insulin-signaling pathways related to production of nitric oxide in human vascular endothelial cells. Circulation 2000; 101:1539-45.

278. Zeng G, Quon MJ. Insulin-stimulated production of nitric oxide is inhibited by wortmannin. Direct measurement in vascular endothelial cells. J Clin Invest 1996; 98:894-8.

279. Borutaite V, Morkuniene R, Brown GC. Release of cytochrome c from heart mitochondria is induced by high Ca2+ and peroxynitrite and is responsible for Ca(2+)-induced inhibition of substrate oxidation. Biochim Biophys Acta 1999; 1453:41-8.

280. Brookes PS, Salinas EP, Darley-Usmar K, et al. Concentration-dependent Effects of Nitric Oxide on Mitochondrial Permeability Transition and Cytochrome c Release. J Biol Chem 2000; 275:20474-20479.

281. Rossig L, Haendeler J, Hermann C, et al. Nitric oxide down-regulates MKP-3 mRNA levels. Involvement in endothelial cell protection from apoptosis. J Biol Chem 2000; 275:25502-7.

282. Rossig L, Fichtlscherer B, Breitschopf K, et al. Nitric oxide inhibits caspase-3 by S-nitrosation in vivo. J Biol Chem 1999; 274:6823-6.

283. Gross GJ, Auchampach JA. Blockade of ATP-sensitive potassium channels prevents myocardial preconditioning in dogs. Circ Res 1992; 70:223-33.

284. Baxter GF, Yellon DM. ATP-sensitive K+ channels mediate the delayed cardioprotective effect of adenosine A1 receptor activation. J Mol Cell Cardiol 1999; 31:981-9.

285. Holmuhamedov EL, Wang L, Terzic A. ATP-sensitive K+ channel openers prevent Ca2+ overload in rat cardiac mitochondria. J Physiol (Lond) 1999; 519 Pt 2:347-60.

286. Sasaki N, Sato T, Ohler A, O'Rourke B, Marban E. Activation of mitochondrial ATP-dependent potassium channels by nitric oxide. Circulation 2000; 101:439-45.

287. Csont T, Szilvassy Z, Fulop F, et al. Direct myocardial anti-ischaemic effect of GTN in both nitrate-tolerant and nontolerant rats: a cyclic GMP-independent activation of KATP. Br J Pharmacol 1999; 128:1427-34.

288. Ishiyama S, Hiroe M, Nishikawa T, et al. Nitric oxide contributes to the progression of myocardial damage in experimental autoimmune myocarditis in rats. Circulation 1997; 95:489-96.

289. Takahashi W, Suzuki JI, Izawa A, Takayama K, Yamazaki S, Isobe M. Inducible nitric oxide-mediated myocardial apoptosis contributes to graft failure during acute cardiac allograft rejection in mice. Jpn Heart J 2000; 41:493-506.

290. Laubach VE, Shesely EG, Smithies O, Sherman PA. Mice lacking inducible nitric oxide synthase are not resistant to lipopolysaccharide-induced death. Proc Natl Acad Sci U S A 1995; 92:10688-92.

291. Huang PL, Huang Z, Mashimo H, et al. Hypertension in mice lacking the gene for endothelial nitric oxide synthase. Nature 1995; 377:239-42.

292. Lee TC, Zhao YD, Courtman DW, Stewart DJ. Abnormal aortic valve development in mice lacking endothelial nitric oxide synthase. Circulation 2000; 101:2345-8.

293. Speechly Dick ME, Baxter GF, Yellon DM. Ischaemic preconditioning protects hypertrophied myocardium. Cardiovasc-Res 1994; 28:1025-9 issn: 0008-6363.

294. Minhaz U, Koide S, Shohtsu A, Fujishima M, Nakazawa H. Perfusion delay causes unintentional ischemic preconditioning in isolated heart preparation. Basic-Res-Cardiol 1995; 90:418-23 issn: 0300-8428.

295. Awan M, Taunyane C, Aitchison K, Yellon D, Opie L. Normothermic transfer times up to 3 min will not precondition the isolated rat heart. J Mol Cell Cardiol 1999; 31:503-11.

296. Langendorff O. Unteruchungen am uberlebenden saugethierherzen. Pflugers Arch 1895; 61:291-332.

297. Wolfensohn S, Lloyd M. Handbook of laboratory animal management and welfare, 1995.

298. Hale SL, Kloner RA. Myocardial temperature in acute myocardial infarction: protection with mild regional hypothermia. Am J Physiol 1997; 273:H220-7.

299. Fishbein MC, Meerbaum S, Rit J, et al. Early phase acute myocardial infarct size quantification: validation of the triphenyl tetrazolium chloride tissue enzyme staining technique. Am Heart J 1981; 101:593-600.

300. Smith CC, Stanyer L, Cooper MB, Betteridge DJ. Platelet aggregation may not be a prerequisite for collagen-stimulated platelet generation of nitric oxide. Biochim Biophys Acta 1999; 1473:286-92.

301. Saiki RK, Bugawan TL, Horn GT, Mullis KB, Erlich HA. Analysis of enzymatically amplified beta-globin and HLA-DQ alpha DNA with allele-specific oligonucleotide probes. Nature 1986; 324:163-6.

302. Johnson N, Khan A, Virji S, Ward JM, Crompton M. Import and processing of heart mitochondrial cyclophilin D. Eur J Biochem 1999; 263:353-9.

303. Ehrenberg B, Montana V, Wei MD, Wuskell JP, Loew LM. Membrane potential can be determined in individual cells from the nernstian distribution of cationic dyes. Biophys J 1988; 53:785-94.

304. Loew LM, Tuft RA, Carrington W, Fay FS. Imaging in five dimensions: time-dependent membrane potentials in individual mitochondria. Biophys J 1993; 65:2396-407.

305. Scaduto RC, Grotyohann LW. Measurement of mitochondrial membrane potential using fluorescent rhodamine derivatives. Biophys J 1999; 76:469-77.

306. Kowaltowski AJ, Seetharaman S, Paucek P, Garlid KD. Bioenergetic consequences of opening the ATP-sensitive K(+) channel of heart mitochondria. Am J Physiol Heart Circ Physiol 2001; 280:H649-57.

307. Sumeray MS, Yellon DM. Characterisation and validation of a murine model of global ischaemia-reperfusion injury. Mol Cell Biochem 1998; 186:61-8.

308. Ytrehus K. The ischemic heart-experimental models. Pharmacol Res 2000; 42:193-203.

309. Tanaka M, Richard VJ, Murry CE, Jennings RB, Reimer KA. Superoxide dismutase plus catalase therapy delays neither cell death nor the loss of the TTC reaction in experimental myocardial infarction in dogs. J-Mol-Cell-Cardiol 1993; 25:367-78 issn: 0022-2828.

310. Sumeray MS, Yellon DM. Ischaemic preconditioning reduces infarct size following global ischaemia in the murine myocardium. Basic Res Cardiol 1998; 93:384-90.

311. Xi L, Hess ML, Kukreja RC. Ischemic preconditioning in isolated perfused mouse heart: reduction in infarct size without improvement of post-ischemic ventricular function. Mol Cell Biochem 1998; 186:69-77.

312. Walker DM, Walker JM, Yellon DM. Global myocardial ischemia protects the myocardium from subsequent regional ischemia. Cardioscience 1993; 4:263-6.

313. Guo Y, Wu WJ, Qiu Y, Tang XL, Yang Z, Bolli R. Demonstration of an early and a late phase of ischemic preconditioning in mice. Am J Physiol 1998; 275:H1375-87.

314. Dorn GW, 2nd, Souroujon MC, Liron T, et al. Sustained in vivo cardiac protection by a rationally designed peptide that causes epsilon protein kinase C translocation. Proc Natl Acad Sci U S A 1999; 96:12798-803.

315. Chen W, Wetsel W, Steenbergen C, Murphy E. Effect of ischemic preconditioning and PKC activation on acidification during ischemia in rat heart. J Mol Cell Cardiol 1996; 28:871-80.

316. Coccia EM, Stellacci E, Marziali G, Weiss G, Battistini A. IFN-gamma and IL-4 differently regulate inducible NO synthase gene expression through IRF-1 modulation. Int Immunol 2000; 12:977-85.

317. Baker JE, Konorev EA, Gross GJ, Chilian WM, Jacob HJ. Resistance to myocardial ischemia in five rat strains: is there a genetic component of cardioprotection? Am J Physiol Heart Circ Physiol 2000; 278:H1395-400.

318. Li Y, Kloner RA. Is There a Gender Difference in Infarct Size and Arrhythmias Following Experimental Coronary Occlusion and Reperfusion? J Thromb Thrombolysis 1995; 2:221-225.

319. Przyklenk K, Ovize M, Bauer B, Kloner RA. Gender does not influence acute myocardial infarction in adult dogs. Am-Heart-J 1995; 129:1108-13 issn: 0002-8703.

320. Thompson LP, Pinkas G, Weiner CP. Chronic 17beta-estradiol replacement increases nitric oxide-mediated vasodilation of guinea pig coronary microcirculation. Circulation 2000; 102:445-51.

321. Kim YD, Chen B, Beauregard J, et al. 17 beta-Estradiol prevents dysfunction of canine coronary endothelium and myocardium and reperfusion arrhythmias after brief ischemia/reperfusion. Circulation 1996; 94:2901-8.

322. Zhai P, Eurell TE, Cooke PS, Lubahn DB, Gross DR. Myocardial ischemia-reperfusion injury in estrogen receptor-alpha knockout and wild-type mice. Am J Physiol Heart Circ Physiol 2000; 278:H1640-7.

323. Stefano GB, Prevot V, Beauvillain JC, et al. Cell-surface estrogen receptors mediate calcium-dependent nitric oxide release in human endothelia. Circulation 2000; 101:1594-7.

324. Singh K, Balligand JL, Fischer TA, Smith TW, Kelly RA. Regulation of cytokine-inducible nitric oxide synthase in cardiac myocytes and microvascular endothelial cells. Role of extracellular signal-regulated kinases 1 and 2 (ERK1/ERK2) and STAT1 alpha. J Biol Chem 1996; 271:1111-7.

325. Jones WK, Flaherty MP, Tang XL, et al. Ischemic preconditioning increases iNOS transcript levels in conscious rabbits via a nitric oxide-dependent mechanism. J Mol Cell Cardiol 1999; 31:1469-81.

326. Lecour S, Maupoil V, Zeller M, Laubriet A, Briot T, Rochette L. Levels of nitric oxide in the heart after experimental myocardial ischemia. J Cardiovasc Pharmacol 2001; 37:55-63.

327. Nakano A, Liu GS, Heusch G, Downey JM, Cohen MV. Exogenous nitric oxide can trigger a preconditioned state through a free radical mechanism, but endogenous nitric oxide is not a trigger of classical ischemic preconditioning. J Mol Cell Cardiol 2000; 32:1159-67.

328. Post H, Schulz R, Behrends M, Gres P, Umschlag C, Heusch G. No involvement of endogenous nitric oxide in classical ischemic preconditioning in swine. J Mol Cell Cardiol 2000; 32:725-33.

329. Xia Y, Tsai AL, Berka V, Zweier JL. Superoxide generation from endothelial nitric-oxide synthase. A Ca2+/calmodulin-dependent and tetrahydrobiopterin regulatory process. J Biol Chem 1998; 273:25804-8.

330. Kerr S, Brosnan MJ, McIntyre M, Reid JL, Dominiczak AF, Hamilton CA. Superoxide anion production is increased in a model of genetic hypertension: role of the endothelium. Hypertension 1999; 33:1353-8.

331. Pernow J, Wang QD. The role of the L-arginine/nitric oxide pathway in myocardial ischaemic and reperfusion injury. Acta Physiol Scand 1999; 167:151-9.

332. Zhang JM, Orihashi K, Sueda T, Matsuura Y. Cardioprotective effects of FK409, a nitric oxide donor, after isolated rat heart preservation for 16 hours. Ann Thorac Surg 2000; 70:1601-6.

333. Lopez BL, Liu GL, Christopher TA, Ma XL. Peroxynitrite, the product of nitric oxide and superoxide, causes myocardial injury in the isolated perfused rat heart. Coron Artery Dis 1997; 8:149-53.

334. Weiland U, Haendeler J, Ihling C, et al. Inhibition of endogenous nitric oxide synthase potentiates ischemia-reperfusion-induced myocardial apoptosis via a caspase-3 dependent pathway. Cardiovasc Res 2000; 45:671-8.

335. Nossuli TO, Lakshminarayanan V, Baumgarten G, et al. A chronic mouse model of myocardial ischemia-reperfusion: essential in cytokine studies. Am J Physiol Heart Circ Physiol 2000; 278:H1049-55.

336. Baxter GF, Kerac M, Zaman MJ, Yellon DM. Protection against global ischemia in the rabbit isolated heart 24 hours after transient adenosine A1 receptor activation. Cardiovasc Drugs Ther 1997; 11:83-85.

337. Maldonado C, Qiu Y, Tang XL, Cohen MV, Auchampach J, Bolli R. Role of adenosine receptors in late preconditioning against myocardial stunning in conscious rabbits. Am J Physiol 1997; 273:H1324-32.

338. Feelisch M. The biochemical pathways of nitric oxide formation from nitrovasodilators: appropriate choice of exogenous NO donors and aspects of preparation and handling of aqueous solutions. J Cardiovasc Pharm 1991; 17(suppl 3):S25-S33.

339. Michel JB, Feron O, Sase K, Prabhakar P, Michel T. Caveolin versus calmodulin. Counterbalancing allosteric modulators of endothelial nitric oxide synthase. J Biol Chem 1997; 272:25907-12.

340. Sun JZ, Tang XL, Knowlton AA, Park SW, Qiu Y, Bolli R. Late preconditioning against myocardial stunning. An endogenous protective mechanism that confers resistance to postischemic dysfunction 24 h after brief ischemia in conscious pigs. J Clin Invest 1995; 95:388-403.

341. Zhao T, Xi L, Chelliah J, Levasseur JE, Kukreja RC. Inducible nitric oxide synthase mediates delayed myocardial protection induced by activation of adenosine A(1) receptors: evidence from gene-knockout mice. Circulation 2000; 102:902-7.

342. Johnson DA, Keegan DS, Sowell CG, et al. 3-O-Desacyl monophosphoryl lipid A derivatives: synthesis and immunostimulant activities. J Med Chem 1999; 42:4640-9.

343. Nathan C, Xie QW. Regulation of biosynthesis of nitric oxide. J Biol Chem 1994; 269:13725-8.

344. Yellon DM, Baxter GF. Reperfusion Injury revisited. Is there a role for growth factor signaling in limiting lethal reperfusion injury? Trends Cardiovasc Med 2000; 9:245-249.

345. Yellon DM, Baxter GF. Protecting the ischaemic and reperfused myocardium in acute myocardial infarction: distant dream or near reality? Heart 2000; 83:381-7.

346. Baxter GF, Mocanu MM, Brar BK, Latchman DS, Yellon DM. Transforming factor beta1 attenuates myocardial injury when given at reperfusion. Circulation 1999; 100:I-46 (Abstract).

347. Ritchie RH, Marsh JD, Schiebinger RJ. Bradykinin-stimulated protein synthesis by myocytes is dependent on the MAP kinase pathway and p70(S6K). Am J Physiol 1999; 276:H1393-8.

348. Yang XP, Liu YH, Shesely EG, Bulagannawar M, Liu F, Carretero OA. Endothelial nitric oxide gene knockout mice: cardiac phenotypes and the effect of angiotensin-converting enzyme inhibitor on myocardial ischemia/reperfusion injury. Hypertension 1999; 34:24-30.

349. Zahler S, Kupatt C, Becker BF. ACE-inhibition attenuates cardiac cell damage and preserves release of NO in the postischemic heart. Immunopharmacology 1999; 44:27-33.

350. Zhu P, Zaugg CE, Hornstein PS, Allegrini PR, Buser PT. Bradykinin-dependent cardioprotective effects of losartan against ischemia and reperfusion in rat hearts. J Cardiovasc Pharmacol 1999; 33:785-90.

351. Arstall MA, Sawyer DB, Fukazawa R, Kelly RA. Cytokine-mediated apoptosis in cardiac myocytes: the role of inducible nitric oxide synthase induction and peroxynitrite generation. Circ Res 1999; 85:829-40.

352. Suzuki H, Wildhirt SM, Dudek RR, Narayan KS, Bailey AH, Bing RJ. Induction of apoptosis in myocardial infarction and its possible relationship to nitric oxide synthase in macrophages. Tissue Cell 1996; 28:89-97.

353. GISSI-3: effects of lisinopril and transdermal glyceryl trinitrate singly and together on 6-week mortality and ventricular function after acute myocardial infarction. Gruppo Italiano per lo Studio della Sopravvivenza nell'infarto Miocardico. Lancet 1994; 343:1115-22.

354. ISIS-4: a randomised factorial trial assessing early oral captopril, oral mononitrate, and intravenous magnesium sulphate in 58,050 patients with suspected acute myocardial infarction. ISIS-4 (Fourth International Study of Infarct Survival) Collaborative Group. Lancet 1995; 345:669-85.

355. Jugdutt BI, Warnica JW. Intravenous nitroglycerin therapy to limit myocardial infarct size, expansion, and complications. Effect of timing, dosage, and infarct location. Circulation 1988; 78:906-19.

356. Yusuf S, Collins R, MacMahon S, Peto R. Effect of intravenous nitrates on mortality in acute myocardial infarction: an overview of the randomised trials. Lancet 1988; 1:1088-92.

357. Lis Y, Bennett D, Lambert G, Robson D. A preliminary double-blind study of intravenous nitroglycerin in acute myocardial infarction. Intensive Care Med 1984; 10:179-84.

358. Jaffe AS, Geltman EM, Tiefenbrunn AJ, et al. Reduction of infarct size in patients with inferior infarction with intravenous glyceryl trinitrate. A randomised study. Br Heart J 1983; 49:452-60.

359. Flaherty JT, Becker LC, Bulkley BH, et al. A randomized clinical trial of intravenous nitroglycerin in patients with acute myocardial infarction: benefits of early treatment. Z Kardiol 1983; 72:131-6.

360. Hingorani AD, Liang CF, Fatibene J, et al. A common variant of the endothelial nitric oxide synthase (Glu298-->Asp) is a major risk factor for coronary artery disease in the UK. Circulation 1999; 100:1515-20.

361. Schriefer JA, Broudy EP, Hassen AH. Endopeptidase inhibitors decrease myocardial ischemia/reperfusion injury in an in vivo rabbit model. J Pharmacol Exp Ther 1996; 278:1034-9.

362. Yang XP, Liu YH, Peterson E, Carretero OA. Effect of neutral endopeptidase 24.11 inhibition on myocardial ischemia/reperfusion injury: the role of kinins. J Cardiovasc Pharmacol 1997; 29:250-6.

363. Simons M. Molecular multitasking: statins lead to more arteries, less plaque. Nat Med 2000; 6:965-6.

364. Kureishi Y, Luo Z, Shiojima I, et al. The HMG-CoA reductase inhibitor simvastatin activates the protein kinase Akt and promotes angiogenesis in normocholesterolemic animals. Nat Med 2000; 6:1004-10.

365. Griffiths EJ, Halestrap AP. Mitochondrial non-specific pores remain closed during cardiac ischaemia, but open upon reperfusion. Biochem J 1995; 307:93-8.

366. Li P, Nijhawan D, Budihardjo I, et al. Cytochrome c and dATP-dependent formation of Apaf-1/caspase-9 complex initiates an apoptotic protease cascade. Cell 1997; 91:479-89.

367. Cleeter MW, Cooper JM, Darley-Usmar VM, Moncada S, Schapira AH. Reversible inhibition of cytochrome c oxidase, the terminal enzyme of the mitochondrial respiratory chain, by nitric oxide. Implications for neurodegenerative diseases. FEBS Lett 1994; 345:50-4.

368. Cassina A, Radi R. Differential inhibitory action of nitric oxide and peroxynitrite on mitochondrial electron transport. Arch Biochem Biophys 1996; 328:309-16.

369. Brown GC, Borutaite V. Nitric oxide, cytochrome c and mitochondria. Biochem Soc Symp 1999; 66:17-25.

370. Brookes PS, Zhang J, Dai L, et al. Increased Sensitivity of Mitochondrial Respiration to Inhibition by Nitric Oxide in Cardiac Hypertrophy. J Mol Cell Cardiol 2001; 33:69-82.

371. Loke KE, McConnell PI, Tuzman JM, et al. Endogenous endothelial nitric oxide synthase-derived nitric oxide is a physiological regulator of myocardial oxygen consumption. Circ Res 1999; 84:840-5.

372. Loke KE, Laycock SK, Mital S, et al. Nitric oxide modulates mitochondrial respiration in failing human heart. Circulation 1999; 100:1291-7.

373. Trochu JN, Bouhour JB, Kaley G, Hintze TH. Role of endothelium-derived nitric oxide in the regulation of cardiac oxygen metabolism : implications in health and disease. Circ Res 2000; 87:1108-17.

374. Hotta Y, Otsuka-Murakami H, Fujita M, et al. Protective role of nitric oxide synthase against ischemia-reperfusion injury in guinea pig myocardial mitochondria. Eur J Pharmacol 1999; 380:37-48.

375. Wang Y, Ashraf M. Role of protein kinase C in mitochondrial KATP channel-mediated protection against Ca2+ overload injury in rat myocardium. Circ Res 1999; 84:1156-65.

376. Holmuhamedov EL, Jovanovic S, Dzeja PP, Jovanovic A, Terzic A. Mitochondrial ATP-sensitive K+ channels modulate cardiac mitochondrial function. Am J Physiol 1998; 275:H1567-76.

377. Scarlett JL, Sheard PW, Hughes G, Ledgerwood EC, Ku HH, Murphy MP. Changes in mitochondrial membrane potential during staurosporine-induced apoptosis in Jurkat cells. FEBS Lett 2000; 475:267-72.

378. Mocanu MM, Maddock HL, Baxter GF, Lawrence CL, Standen NB, Yellon DY. Glimepiride, a novel sulfonylurea, does not abolish myocardial protection afforded by either ischemic preconditioning or diazoxide. Circulation 2001; In Press.

379. Borutaite V, Budriunaite A, Brown GC. Reversal of nitric oxide-, peroxynitrite- and S-nitrosothiol-induced inhibition of mitochondrial respiration or complex I activity by light and thiols. Biochim Biophys Acta 2000; 1459:405-12.

380. Garlid KD, Paucek P, Yarov-Yarovoy V, et al. Cardioprotective effect of diazoxide and its interaction with mitochondrial ATP-sensitive K+ channels. Possible mechanism of cardioprotection. Circ Res 1997; 81:1072-82.

381. Jaburek M, Yarov-Yarovoy V, Paucek P, Garlid KD. State-dependent inhibition of the mitochondrial KATP channel by glyburide and 5-hydroxydecanoate. J Biol Chem 1998; 273:13578-82.

Appendix 1. Infarct measurement macro programme.

{Infarct Area Calcuation Macro file:
Copyright (c) 1998 Rob Bell, Hatter Institute, UCL
Planimetry for the Mouse Myocardium version 1.2 (April)

1. Import the video image of the myocardial slice into NIH Image, and convert it to grayscale if imported as a colour picture.
2. Load the Infarct size Macro.
Select one of the planimetry tools from the special menu:
Standard mode: single pixel resolution
Auto-estimation mode
Variable resolution mode
In Variable resolution mode, select the pixel resolution; the areas with be calculated over a square with a edge length of n pixels where n = your pixel resolution. If 1/2 or more of the square is at or above threshold then the whole square is added to the area. If below threshold, the square will be ignored. For best results, use a pixel resolution of 2 to 3. If you want a pixel resolution of 1, use the standard mode, as it is more rapid.
Select a background filter threshold: this will ignor lighter shades in the background, but is advisable to manually 'clean' the image prior to running the macro for best results.
The image will then be replicated, and total area of the myocardial slice calculated excluding ventricular cavities, if present.
3. In autoestimate mode, the computer will make a first pass planimetry estimate. The area estimation is performed in 2x2 pixel resolution mode. This threshold can subsequently manually modified at the appropiate prompts.
4. In the other modes, from the replicated image use mouse cursor and click on a part of the image to select the density threshold from which area calculations will be made. Put the mouse pointer on the darker viable areas as on the replicated image, the area corresponding to viable (darker) tissue stained with tetrazolium will be shaded in a contrasting colour, and the area calculated. The area of infarction is derived from the subtraction of viable tissue from the total slice area.
5. If not satisfied of result of shading, the area can be recalculated.
6. Enter calibration: the number of pixels per square millimetre.
7. The calibration,total slice area, area infarcted and the slice's I/R ratio will then be displayed. A square at the bottom right hand corner of the image corresponds to one square millimetre to the appropiate scale. If in variable resolution mode, the resolution selected will also be displayed.

8. The macro has been completed.
}

```
procedure cleverthreshold;
var
 kounter,q:integer;
begin
 beginhistogram: = 255;
 endhistogram: = 255;
 gethistogram(0,0,320,240);
 for kounter: = 1 to 254 do begin
 q: = histogram[kounter];
 if q > 1 then begin
  endhistogram: = kounter;
  end;
 if beginhistogram = 255 then begin
  if q > 1 then beginhistogram: = kounter; end;
 end;
 threshold: = 1.3993*endhistogram-169.64;
 select: = true;
end;

procedure thresholdfromarea;
var
 kounter,q,harea,max:integer;
begin
 harea: = getnumber('Enter estimated infarct area:',1000);
 kounter: = endhistogram+1;
 repeat
 kounter: = kounter-1;
 q: = q+histogram[kounter];
  if q > max then begin
  max: = q;
  peakhistogram: = kounter;
  end;
 until q > harea;
 threshold: = kounter+1;
```

```
end;

procedure selectthreshold;
var
 x,y:integer;
begin
 select: = true;
 putmessage('Please move your mouse pointer and select threshold from image.');
 paste;
 wait(.25);
 repeat
 getmouse(x,y);
 threshold: = getpixel(x,y)-1;
 until button;
end;

procedure Area(x,y:integer);
begin
 karea: = 0;
 p: = getpixel(x,y);
 if select then begin
  if p > threshold then karea: = 1; end;
  end;
 if select = 0 then begin
  if p < threshold then karea: = 1; end;
  end;
 if p = threshold then karea: = 1; end;
end;

procedure shadearea;
var
 x,y:integer;
begin
 for x: = 1 to width do begin
  for y: = 1 to height do begin
  area(x,y);
  iarea: = iarea+karea;
  if karea = 1 then begin
```

```
   putpixel(x,y,(abs(180-p)));
   if x < px then px: = x; end;
   if x > pwidth then pwidth: = x; end;
   if y < py then py: = y; end;
   if y > pheight then pheight: = y; end;
   end;
  end;
 end;
 pheight: = pheight-py;
 pwidth: = pwidth-px;
end;

procedure blockarea(n);
var
 x,y,jarea,c,d:integer;
begin
 for x: = (px/n) to (pwidth/n+1) do begin
  for y: = (py/n) to (pheight/n+1) do begin
  jarea: = 0;
  for c: = 1 to n do begin
   for d: = 1 to n do begin
   area((x-1)*n+c-1,(y-1)*n+d-1);
   jarea: = jarea+karea;
   end;
   end;
   if jarea > (n*n/2-1) then begin
   jarea: = n*n;
    for c: = 1 to n do begin
    for d: = 1 to n do begin
    putpixel((x-1)*n+c-1,(y-1)*n+d-1,(abs(180-p)));
    end;
    end;
   end else begin
    jarea: = 0;
   end;
   iarea: = iarea+jarea;
  end;
 end;
```

```
end;

procedure calculateslicearea;
begin
 select: = true;
 threshold: = getnumber('Enter background threshold',50);
 shadearea;
end;

procedure results;
begin
moveto(0,10);
setfontsize(18);
setforegroundcolor(255);
settext('bold, underline');
writeln(title);
writeln('');
setfontsize(10);
settext('bold, no background');
writeln(' Calibration = ',calibration:8:0,' pixels/mm2');
writeln('');
writeln(' Area of slice = ',slicearea:8:0,' pixels or',(slicearea/calibration):8:2,'mm2');
writeln(' ');
writeln(' Area of Infarct = ',(slicearea-iarea):8:0,' pixels or',((slicearea-
iarea)/calibration):8:2,'mm2');
writeln(' ');
writeln(' Slice I/R ratio = ',(100*(1-iarea/slicearea)):8:2,'%');
moveto(0,180);
writeln(' Selected threshold = ',beginhistogram:4:0,' / ',threshold:4:0,' /
',endhistogram:4:0);
moveto(width-20,height-20);
lineto(width-20-sqrt(calibration),height-20);
lineto(width-20-sqrt(calibration),height-20-sqrt(calibration));
lineto(width-20,height-20-sqrt(calibration));
lineto(width-20,height-20);
end;

macro 'Planimeter {Auto-estimation mode}  [A]'
```

```
var

x,y,width,height,px,py,pwidth,pheight,calibration,threshold,karea,iarea,slicearea,p,pa
ss,beginhistogram,endhistogram:integer;
 select:boolean;
 title:string;
begin
 if npics < 1 then begin
 putmessage('Please open a window and import an image.');
 exit;
 end;
 GetPicSize(pwidth,pheight);
 makeroi(0,0,pwidth,pheight);
 getroi(x,y,width,height);
 width: = 320; height: = 240;
 title: = windowtitle;
 copy;
 setnewsize(width,height);
 makenewwindow('Infarct Size Analysis');
 tilewindows;
 paste;
 wait(0.25);
 iarea: = 0;
 px: = 0;
 py: = 0;
 pwidth: = 0;
 pheight: = 0;
 calculateslicearea;
 slicearea: = iarea;
 pass: = 0;
 repeat
 iarea: = 0;
 if pass = 1 then begin
  threshold: = getnumber('Enter new threshold :',threshold);
  end;
  paste;
  wait(.25);
```

```
  if pass = 0 then begin
  cleverthreshold;
  pass: = 1;
  end;
  blockarea(2);
 until getstring('Enter alternative threshold? (y/n)','n') = 'n';
 calibration: = getnumber('Number of pixels per square mm ?',1560);
 results;
end;
```